DYNAMIC RESPONSE OF THIN-WALLED COMPOSITE STRUCTURES WITH APPLICATION TO AIRCRAFT WINGS

by

Seyed Hamid Reza Eslimy-Isfahany

Thesis submitted for the Degree of Doctor of Philosophy

Centre for Aeronautics
Department of Mechanical Engineering and Aeronautics
The City University, London EC1V 0HB, UK.

November, 1998

To my grandmother, Talat, and my mother, Farideh,

for their love, support and patience.

The fact that they have always believed in me,

has been the main source of inspiration and strength in my life.

List of contents

List of tables

List of figures

Acknowledgements

I would first and foremost like to thank my supervisor, Dr JR Banerjee to whom I am greatly indebted for his invaluable guidance and strong support during the course of this research. He made substantial contributions to this work by actively participating and creating new ideas. The completion of this work would not have been possible without his detailed advice, constructive criticism and constant encouragement and patience.

I am also extremely grateful to Mr AJ Sobey who generously spent a great deal of time providing me with alternative viewpoints to my ideas through many helpful discussions. His invaluable knowledge, experience and moral support proved to be of inestimable value to the revision and completion of this thesis.

Special thanks are due to Professor ARD Thorley, Head of Department of Mechanical Engineering and Aeronautics, and his predecessor Professor GTS Done, for provision of laboratory and other facilities. Thanks are also due to Mr MC Smith and Mr MA Young for their time and effort in the preparation of specimens and redesigning the rig for buckling experiments. I am also grateful to Dr SJ Guo for his useful contributions.

My special thanks are extended to the members of staff and students in the Department of Mechanical Engineering and Aeronautics who have offered me intellectual stimulation and friendship, and my colleagues in Finsbury Halls of Residence for providing a warm and inspiring environment in which to reside.

I express my sincerest gratitude to my teachers, lecturers, tutors and advisors throughout my studies, from primary school to university, too numerous to mention, for teaching me the skills which have helped me to achieve so much. They have encouraged and inspired me, and presented me with the opportunity to broaden my horizons.

I am deeply grateful to my loving parents, members of my family and relatives, especially my uncle, Mr Hossein Akbaroff, who has always done his utmost to support me.

There are many other individuals too numerous to mention whom I would also like to thank for being understanding, caring and supportive, and hope that they forgive me for not mentioning them by name. I will always treasure their friendship. Among them my special thanks go to Dr SAM Mohammad-Hejazi who has been a great source of motivation and encouragement for me to undertake and continue this course, and also Dr AK Razavi for his invaluable support throughout my PhD.

Finally, I wish to thank The Ministry of Culture and Higher Education of The Islamic Republic of Iran for providing me with a scholarship, without which this research would not have been possible. I would also like to thank Dr H Salar-Amoli and Dr A Khodaie for their understanding and encouragement.

May God bless them all.

Declaration

I hereby grant powers of discretion to the University Librarian to allow this thesis to be copied in whole or in part without further reference to me. This permission covers only single copies made for study purposes, subject to normal conditions of acknowledgement.

Abstract

A general analytical method is developed to study first the buckling behaviour and then the dynamic characteristics of thin-walled composite structures with the presence of bending-torsion coupling. The dynamic response theory incorporates the dynamic stiffness matrix approach and generalised coordinates using the normal mode method. Structural components considered are thin-walled laminated composite beams with carbon-fibre, glass-fibre or other reinforced plastic lay-ups. The examples of such beams and their applications include aircraft wings, hulls of ships, helicopter and wind turbine blades. All assumptions made in this work are based on elastic linear small deflection beam theory so that the overall response of the beam is represented by the superposition of all individual responses in each mode.

Bending-torsion coupling effects arising from the anisotropic nature of fibrous composites, as well as due to non-coincident centroid and geometric shear centre of the beam cross-section, are the main contributory elements when developing the theory.

The beam is subjected to time dependent forces and/or torques which can be either concentrated or distributed over its length. Both deterministic and random loads are considered. An important example of a deterministic load is one that varies harmonically in time. The Duhamel integral is employed to calculate the response to any arbitrary time dependent deterministic load. The random load is assumed to be Gaussian, having both stationary and ergodic properties. The evaluation of the response to the random load is carried out in the frequency domain by relating the Power Spectral Density (PSD) of the output to that of the input using the complex frequency response function. A number of PSD distributions are considered as random input in order to determine the PSD of the dynamic response. Atmospheric turbulence, which is considered to be one of the forms of random excitation, is modelled using the von Karman spectra for composite aircraft wings.

In order to establish the methodology, bending-torsion coupled metallic beams are first investigated. The bending-torsion coupling in such beams occurs due to non-coincident centroid and geometric shear centre of the beam cross-section. The natural frequencies and mode shapes in undamped free vibration are obtained and the significance of generalised mass in each of the modes of vibration is evaluated. A normal mode method is then used to compute the frequency response function of the beam. The effects of shear deformation, rotatory inertia and axial load on the frequencies, mode shapes and dynamic response characteristics are demonstrated.

It was essential at an earlier stage of the investigation to validate the chosen composite beam modelling. Among all the different techniques used to determine the rigidities of a composite beam, the buckling load provides a reasonable estimate. The elastic critical buckling loads of thin-walled laminated composite columns for various end conditions are established theoretically using the exact stiffness method. The effect of shear deformation on the buckling characteristics of the column is demonstrated. Experiments are carried out to establish the elastic critical buckling load of metallic and laminated composite columns. Theoretical predictions of the buckling behaviour are corroborated by experimental results and other published results.

The investigation is then focused on composite beams, but the response analysis of such beams is significantly more complicated than that of their metallic counterparts. This is mainly due to anisotropic characteristics of laminated fibrous composites. A detailed parametric study with the variation of significant composite parameters, such as ply angle, is undertaken and the importance of the results are highlighted.

A suite of computer programs in FORTRAN is developed to predict the buckling behaviour, the free vibration and the response characteristics of thin-walled composite or metallic beams based on the theory proposed. Numerical results are presented, fully discussed and commented on.

Principal nomenclature

A	Cross-sectional area
b	Width of laminate
c_1, c_2, c_3	Damping coefficients
c_k^2	Material coupling parameter
c_x^2	Geometric coupling parameter
d	Beam depth
d_n	Frequency response function
E	Young's modulus
E_1, E_2, E_3	Young's modulus in the fibre and transverse directions
E_y^b, E_y	Equivalent elastic constants
EI	Bending rigidity
EA	Extensional rigidity
$f(y,t)$	Externally applied forces
$f_n^u, f_n^\psi, f_n^\theta$	Inertial forces
$F_n(t), \overline{F}_n(t)$	Generalised forces
$g(y,t)$	Externally applied torques
$G_n(t), \overline{G}_n(t)$	Generalised torques
G	Shear modulus
$G_{12}, G_{23}, G_{13},$	Shear moduli
G_{xy}^b	Equivalent Shear elastic constants
GJ	Torsional rigidity
H	Frequency response function
H_u, H_θ, H_ψ	The receptances for the bending displacement, the flexural rotations and torsional rotations
I, I_{xx}	Second moment of inertia
I_α	Mass moment of inertia per unit length
I_p	Second moment of area
k	Cross-sectional shape factor for shear
kAG	Shear rigidity
K	Bending-torsion coupling rigidity
K_{ij}	Stiffness elements of dynamic stiffness matrix of a bending-torsion coupled composite beam
L	Span-wise length
L_s	Scale length of a turbulence
M	Bending moment
m	Mass per unit length
N	Number of externally applied concentrated forces on the beam
NE	Number of layers (laminates)
N_x, N_y	Normal forces per unit length in x and y directions
N_{xy}	Shear force per unit length in x-y plane
p^2	Axial load parameter
P	Axial force

P_{cr}	Elastic critical buckling load
q_n	Generalised coordinates
q_s	Shear flow
R	GJ/EI
r^2	Rotatory inertia parameter
r_0	Radius of gyration
s^2	Shear deformation parameter
S_f, S_g	Spectral density of the excitation
S_u, S_θ, S_ψ	Spectral density of the response
S_{int}	Interlaminar ultimate shear strength
S_{shr}	In-plane ultimate shear strength
T	Internal torque
T_{ke}	The total kinetic energy
t	Time, Thickness
u	Flexural displacement
U	Mode shape for flexural displacement
V	Internal shear force
V_{pe}	The total potential energy
V_s	Speed of the flow, Flight speed
u, v, w	Displacement components in x, y, and z directions
x_α	Distance between shear centre and centroid of the cross-section
X_c	Longitudinal (fibre direction) ultimate compressive strength
X_t	Longitudinal (fibre direction) ultimate tensile strength
y	Variable of the space along the beam
Y_c	Transverse (matrix direction) ultimate compressive strength
Y_t	Transverse (matrix direction) ultimate tensile strength

Greek Symbols

β	Fibre angle
δ_{mn}	The Kronecker delta
$\chi_f(t)$, $\chi_g(t)$	Stochastic processes of the time dependent randomly varying excitation
ε	Normal strain
ϕ	Phase angle
μ_n	Generalised mass
ν, ν_{12}, ν_{23}, ν_{13}	Poisson's ratio
θ	Flexural rotation
Θ	Mode shape for flexural rotation
ρ	Density (air, material, etc.)
σ_1, σ_2	Normal stress in principal material direction
σ_x, σ_y	Normal stress
σ_g^2	Mean square value of gust velocity

τ_{12}	Shear stress in principal material direction
τ_{xy}	Shear stress
ω_n	Natural frequency
ω_c	The first coupled frequency
ω_b	The first uncoupled bending frequency
ω_t	The first uncoupled torsional frequency
Ω	Frequency of the exciting external force/torque
ξ	y/L
ψ	Torsional rotation
Ψ	Mode shape for torsional rotation
ζ_n	Damping ratio

Matrices

[D]	Displacement matrix
[F]	Force matrix
[K]	Stiffness matrix

Abbreviations

FSDT	First-order Shear Deformation Theory
CALFUN	CALculation of Flutter speed Using Normal modes
CAS	Circumferentially Asymmetric Stiffness
CFRP	Carbon-Fibre Reinforced Plastic
CRLP	Chord-wise Rigid Laminated Plate
CUS	Circumferentially Uniform Stiffness
C-C	Clamped-Clamped boundary condition
C-F	Clamped-Free boundary condition
C-S	Clamped-Simply supported boundary condition
DSM	Dynamic Stiffness Method
FEM	Finite Element Method
FI	Failure Index
HARP	High Aspect Ratio Plate model
HSDT	Higher-order Shear Deformation Theory
PSD	Power Spectral Density
RMS	Root Mean Square
S-S	Simply supported-Simply supported boundary condition

Chapter One

Introduction

1 Introduction

1.1. Overview and historical background

Flying machines have evolved remarkably during the present century from the Wright brothers Flyer at Kitty Hawk to Apollo on the moon, and a fighter ace of 1918 flew a very different aircraft from that flown by his successor today. Historically, all the divisions and subdivisions of aeronautics, which is made up of many branches of science and engineering, have advanced at different rates. The development usually consists of two or three great strides associated with new ideas, followed by many years of consolidation and expansion of those ideas.

In the early days of aircraft design, the most significant advances were made in the field of aerodynamics as speed increased, with the complications of compressibility. The structural aspect of design was a late developer and has a relatively shorter history than aerodynamics. Nevertheless, developments in the field of airframe structures have been especially vital, since the structure is a large fraction of the total cost and weight of an aircraft. The primary concern in the development of a good structural design is the provision of efficient "load paths" - the structural elements by which opposing forces are connected, using the least practical structural weight. The first major structural advance came with the introduction of the use of stressed skin and semi-monocoque construction, which became possible by the development of aluminium based light alloy in the 1930's. The second fundamental stride forward that aircraft structures have taken, was the application of fibrous composite materials following laboratory developments in the 1960's and 1970's. New and innovative structural design and fabrication techniques in composites promise to produce significant advancement towards exploiting fully all the advantageous characteristics of advanced composite structures.

An increasing attraction in the use of composite materials in the design of aircraft structures is evident in recent years. This is because fibrous composites offer numerous advantages over existing materials. Components made of anisotropic composite materials are ideal for structural applications due to their high strength-to-weight ratio, and their

ability to be tailored and designed to meet all the stiffness and strength requirements of the model. Recently, the advent of high modulus composites has led to its use in highly loaded, stiffness-critical wings and control surfaces, as well as in other structures. By taking advantage of the directional properties of fibre reinforced composite materials it has been possible to "tailor" the aeroelastic response, therefore aeroelastic tailoring and the capability of thereby achieving an improved design have advanced significantly. The use of composites is stimulated by the need for more efficient structures featuring higher strength-to-weight ratios, improved fatigue life, enhanced corrosion resistance, improving the aerodynamic smoothness (and thus reducing the aerodynamic drag), and a potential for optimal design. Generally, the use of composite materials offers a considerable potential for cost-effective design of aircraft structures. There are, however, a number of disadvantages, such as the sensitivity of the curing process, the necessity of special fasteners, vulnerability to impact with the possibility that certain types of damage may not be visible, high initial cost and more complex design engineering. Nevertheless, these disadvantages are mostly known and many have largely been overcome; those that have not can be endured.

Because of the growing interest in the application of composite materials in the design of aircraft structures, there is a need for the development of analytical and numerical methods to predict and optimise the behaviour of thin-walled composite structures in buckling, vibration and dynamic response. On the other hand, whilst a composite structure may be comparatively easy to model and analyse, it may behave less predictably than expected at the micro-level. Thus it is very important to plan for well-designed experiments to achieve a better understanding of behaviour of composite materials in airframe structures. These topics have constituted a major area of recent research in aeronautical and structural engineering, because of their novelty and, more importantly, due to the insufficiently understood behaviour of composite structures.

Various approximate and analytical techniques have been developed to address the problem, using one-dimensional theories for beams, since beam modelling for the analysis and design of different components in aircraft structures has become a common practice. Most of the investigations reported on the analytical solutions for vibration and response

analysis of composite beams have been limited to free vibration studies such as the determination of their natural frequencies and mode shapes. The analytical solutions for forced vibration problems, however, are only available for some very simple cases of limited practical interest. Likewise, literature on the effect of bending-torsion coupling on the dynamic response of composite beams is very scarce. Such coupling can be the consequence of an unsymmetrical cross-section and/or due to the stacking sequence of the laminates. In addition, incorporation of the secondary effects, such as transverse shear deformation and rotatory inertia, and the analysis of non-uniform beams further complicates the mathematical modelling of the structure, and its dynamic analysis.

1.2. A preliminary discussion of the topics developed in this study

This study is focused on an exact analytical method to address the buckling, the free vibration and dynamic response characteristics of a class of thin-walled laminated composite beams and provides a benchmark for other analysts who may use less rigorous methods. Such beams are the building blocks of many structural and mechanical systems including automobiles, space vehicles, aircraft wings and other major components such as control surfaces and undercarriage parts, together with helicopter and wind turbine blades. Among all the geometrical structural configurations, those with a cylindrical cross-section are most commonly used as parts of aerospace structure vehicles, and these form the main area of investigation in this work. Carbon fibre, glass fibre and Kevlar are the main types of fibrous composite materials considered in this investigation.

The finite element method is, of course, an alternative route to approach the problem. Although it is a universal numerical resource for structural analysis, it has its disadvantages too. In this method, stiffness and inertial properties of the structure are restricted by the number of elements used and the way the elements are defined. Unlike the dynamic stiffness matrix method, it generally provides much less accurate modal information when higher frequencies are involved, and better accuracy is needed in the analysis. Moreover, the computer time used for analysis can substantially be saved if explicit analytical expressions for the elements of the dynamic stiffness matrix are used instead of finite

element or other numerical methods. In this investigation, an exact analytical method has been developed and has clear advantages over the finite element method.

Progress in any field, particularly in aircraft design, is dependent on both experimental and theoretical investigations. There are always some aspects and characteristics of a mechanical system which do not behave quite as predicted by numerical and/or analytical methods. This is mainly because, in practice, there are many unknowns that we have not accounted for in theory. Therefore, it is very unlikely that progress can come from experiment alone, or from theory alone and thus to develop a realistic approach, experiment and theory need to go hand in hand. As a consequence, there is much emphasis on planning experimental investigations to ensure that the information needed to design high quality aircraft is obtained as effectively and with as much validity as possible. Planning and carrying out extensive experiments in order to evaluate the dynamic response behaviour of composite beams is beyond the scope of this investigation and can be a major advancement to further this research in future. However, to provide an awareness of the importance of experimental procedures in understanding the behaviour of composites, a number of experiments were carried out to evaluate the buckling characteristics of composite beams. A substantial part of the results obtained from the present approach have been compared with experimental results given in the literature.

In the course of this investigation, further insight is obtained into the buckling behaviour and the free vibration and dynamic response characteristics of thin-walled laminated composite beams. This is achieved by utilising the generalised mass and the modal interchange concepts. The importance of generalised mass in predicting the free vibration characteristics and dynamic response of a bending-torsion coupled beam has not featured significantly in the existing literature. This study establishes the interpretation of the behaviour of the overall dynamic response of bending-torsion coupled beams with the help of the generalised mass in each mode. Furthermore, modal interchanges between the flexural and the torsional modes also play very important roles in predicting the buckling load and the characteristics of dynamic response of bending-torsion coupled thin-walled composite beams. In such beams, a small alteration in the thickness and/or the length of

the beam; inclusion of secondary effects - such as shear deformation, rotatory inertia or warping stiffness; variation of ply angles or stacking sequences may push up the order of bending or torsional modes of vibration or may bring them down. Consequently, this will change the buckling load and/or the dynamic response of such beams. This distinctive feature which does not normally exist in Bernoulli-Euler beams (bending-torsion uncoupled), has not been addressed adequately in the existing literature.

Due to their anisotropy, laminated composite materials exhibit several interesting coupling phenomena, which can be used beneficially in engineering structures. For example, bending-torsion coupling can help to increase the divergence speed in a forward-swept wing and at the same time decrease its weight. The fact that there are not one or two types of composite materials, but an infinite variety of fibres, matrix, fibre orientations, and fibre contents, allows a new degree of freedom in structural design. This has a profound effect on the whole materials-design-fabrication process. Since the inherent properties of composite materials will vary with ply orientation and stacking sequences, the ground is thus set for structural optimisation. Because of the accuracy and conciseness of the methodology proposed in this study, it can be used in the design of airframe structures as part of an optimisation process to minimise the dynamic fibre stresses and/or to restrict the dynamic displacements in a laminated composite wing. Although the optimisation of laminated composite wings and aeroelastic tailoring are beyond the scope of this investigation, a parametric study is carried out to demonstrate the feasibility of using this method to minimise fibre stresses.

Finally, aircraft structures have been designed to meet specific requirements and some fundamental criteria, such as those of deformation, fatigue, allowable design materials, strength and load. Theory developed in this investigation sets a trend for dynamic response of laminated composite structure with particular reference to thin-walled composite beams such as composite wings, horizontal tails, vertical fins and elevators. This is a critical step towards analysis, design and optimisation of different components in aerospace structures with due attention to fundamental design criteria.

1.3. Definition of the problem

A general analytical method is developed to study the buckling behaviour and then to determine the dynamic response of thin-walled composite structures with bending-torsion coupling by using exact differential equations of motion. The dynamic response theory developed incorporates the dynamic stiffness matrix approach, generalised coordinates and the normal mode method for the beam element idealisation of the composite structures.

Due to the complexity of some physical systems, structural elements are often idealised as built up from several individual components. Their physical properties that govern the dynamic behaviour of the system are determined either theoretically or experimentally. These characteristics help in constructing, a mathematical model which represents an idealisation of the actual physical system. There are two main categories of mathematical models, namely the discrete parameter, or lumped, systems; and those with distributed parameters such as continuous systems. The former can be described by ordinary differential equations, whereas the latter are governed by partial differential equations, which are comparatively difficult to analyse. The latter is used in this investigation since it provides a more accurate model. Furthermore, the components of a structure can be idealised as a bar, beam, plate, or a shell element. It is generally an acceptable and common practice to choose beam elements to analyse certain types of airframe structures.

Once a suitable physical and mathematical model of the structural components is identified and the pattern for dynamic loads is known, the differential equations of motion follow and require no further simplification. It is in this sense that the word "exact" has been used in this study. Thus all the assumptions are within the limits of the governing differential equations of motion. A description of the physical and mathematical models considered in this investigation is given below.

The structural components considered are composite beams made of thin-walled laminated plates using lay-ups with plastic-reinforced carbon-fibre and/or glass-fibre. A typical example of such a beam may have a flat or box cross-section. The flat composite beam is assumed to have symmetric cross-ply (either balanced or unbalanced) and the box cross-section is assumed to have Circumferentially Asymmetric Stiffness (CAS) configuration. It

is well-known that these cross-sections exhibit the bending-torsion coupling effect.

The composite beam, which is the principal subject of study in this research, is assumed to be straight and its cross-section has at least one axis of symmetry. Although the theory is developed for beams with uniform cross-section, it can also cater for non-uniform beams either by defining a dynamic stiffness matrix for the non-uniform beam, or by dividing the beam into a number of elements with constant cross-section. The theory is valid for any beam, provided its end conditions are free, simply supported, or clamped, which cover most of the applications.

Bending-torsion coupling effects in composite beams occur due to material and/or geometric coupling. Material coupling arises from the anisotropic nature of fibrous composites, while geometric coupling arises from the non-coincident centroid and geometric shear centre of the beam cross-section. Both sources of coupling are taken into account when developing the theory. Effects such as shear deformation and rotatory inertia are included in the analysis, since they may significantly affect the response characteristic of composite laminates. A first-order shear theory is introduced to incorporate the effect of shear deformation. The importance of a constant axial load (compressive or tensile) on the dynamic response characteristics of such beams is also investigated. Warping stiffness is neglected when developing the theory, because it does not have a significant effect on the dynamic response of beams with closed cross-section.

Linear viscous damping in shear, flexure and torsion are the only sources of damping taken into account. It is assumed that each point of the cross-section moves with its own local velocity, so that the local damping force, bending moment and torque for each span-wise element are a product of the local velocity and damping terms.

During its varied motion through the atmosphere and in space, the structure of flight vehicles may be exposed to a variety of time-dependent loads induced by gust, sonic-boom, etc. In this way, the beam is subjected to vibrating flexural forces and/or torques which can be either deterministic or random in time. Concentrated and distributed loads for both these cases are considered when developing the theory.

The dynamic response of the beam is described by its transverse deflection, its flexural

slope and its torsional rotation and their associated accelerations; by its dynamic shear force, bending moment and torque at various point on the beam; and by the normal and shear stresses in the laminates. All the assumptions are based on the elastic, linear, small deflection theory for beams, so that the overall response of the beam can be represented by the superposition of all the individual responses in each mode.

1.4. Methodology and layout of the study

This research is based on the use of continuous analysis leading to exact differential equations, which describe the coupled flexural-torsional response of composite beams subjected to dynamic loading. A review of the available literature is given in ***Chapter Two***, to establish advancements in the dynamic response of composite beams and to identify the key areas of research.

The main areas of concern in dynamic analysis of any structural and mechanical system are modelling stiffnesses, inertial properties, methods of numerical analysis, and the loading. Therefore, to develop an exact method for dynamic analysis, uncertainties in any of those areas must be resolved, and the methodology must be established. In ***Chapter Three***, stiffness modelling of laminated composites is established using existing literature, so that the essential cross-sectional properties, namely the bending (EI), torsional (GJ), bending-torsion coupling (K) and shear (kAG) rigidities of the composite beam, are obtained using the variational-asymptotical method. Using this model, the variation of these rigidities with ply angle is investigated for each cross-section for some illustrative examples. These properties are subsequently used in the buckling and dynamic response analyses.

In order to validate the chosen composite beam modelling, and to resolve any uncertainty in the stiffnesses a series of experiments was conducted and a comparison between the experimental and numerical results of a static analysis has been carried out. Among all the different techniques to determine the stiffnesses, elastic critical buckling load of structural elements provides a reasonable estimate. Buckling analysis, therefore, is proposed to demonstrate the accuracy of the chosen composite beam modelling. In ***Chapter Four***, the

elastic critical buckling loads of thin-walled laminated composite columns with flat or box cross-sections having various end conditions are established. This theory is based on an exact static stiffness matrix for bending-torsion coupled composite columns, derived from solutions of the governing differential equations. The effect of shear deformation on the elastic buckling characteristics of a column is included in the theory. A series of experiments has been carried out on laminated composite flat columns (with classical boundary conditions) made of carbon-epoxy material with various ply angles to determine their elastic critical buckling load. Experimental and theoretical results are compared, good accuracy is observed, and the results are critically appraised.

The next step is to determine the free vibration characteristics of composite beams with particular reference to composite wings. For higher accuracy and greater computational efficiency, the dynamic stiffness matrix method has been used, allowing for both geometric and material coupling. The dynamic stiffness matrix of an element is frequency dependent and accounts for both stiffness and mass/inertia properties of the element. The method of Banerjee-Williams is presented in ***Chapter Five***, to establish the natural frequencies and mode shapes of the composite beams using the dynamic stiffness matrix method. This exact method provides a higher accuracy when compared with finite element and other approximate methods, especially for higher frequencies, because it is based on exact shape functions obtained from the solution of the element differential equations. Dynamic stiffness expression for a representative case is given in ***Appendix C***.

In ***Chapter Six*** a full account of the theory developed in this thesis is presented. Firstly, the governing differential equations of motion for important cases are given. The derivation of these equations of motion using Hamilton's principal for a representative case is shown in ***Appendix A***. A normal mode method, in conjunction with generalised coordinates, is then used to compute the forced vibration or dynamic response quantities. The orthogonality conditions for the normal modes are derived and generalised mass and non-dimensional damping coefficients in each mode are defined to uncouple the response equation in each mode. The derivation of these equations for a representative case is also shown in ***Appendix D***.

Before embarking on the analysis of the substantially complicated composite beams, the free vibration and the dynamic response of bending-torsion coupled metallic beams are investigated, first. In this case, the coupling exists due only to the geometry of the beam cross-section, where the centroid and geometric shear centre do not coincide. It is easier to demonstrate the appropriateness of the assumptions and methods of numerical analysis for metallic beams, since there has been more research carried out in that field, with associated published results. This is an important stepping stone in order to develop the methodology and achieve further insights in the behaviour of beams with bending-torsion coupling.

Aircraft and aerospace structures are subjected to loads with a high level of uncertainty; consequently, both deterministic and time-varying random loads are considered in this investigation. The Duhamel integral method is employed to calculate the dynamic transverse deflection, flexural rotation and torsional rotation in the deterministic case; a harmonically varying load is a typical example. In general, any periodic loading can be expressed in terms of harmonic loads using a Fourier series.

The random load is assumed to be Gaussian, having both stationary and ergodic properties. The evaluation of the dynamic transverse deflection, flexural rotation and torsional rotation due to the random load, is carried out in the frequency domain by relating the Power Spectral Density (PSD) of the output to that of the input via the modulus of the complex frequency response function. Three types of PSDs are used, namely white noise, and two well-known spectra due to von Karman and Dryden, to account for aerodynamic fluctuating gust and atmospheric turbulence, representative of wing loading.

Next, attention is focused on the dynamic response behaviour of composite beams. The response quantities together with the externally applied flexural and/or torsional loads are used to establish the time-dependent shear force, bending moment and torque. The dynamic normal and shear stresses in the laminate at any cross-section of a beam due to these loads are then computed using Engineer's theory of bending, Bredt-Batho and classical lamination theories.

Once the stresses are calculated, two main failure criteria are considered. The first, is a

non-interactive failure theory, where each stress component is looked at individually, and failure in any particular direction is caused independently of the stresses acting in other directions. As a result, ply failure occurs if any principal stresses or maximum shear stress exceeds their respective ultimate values. The second failure theory considers an interaction of the stresses in the material axes directions which is an estimate based on a weighted measure of the stresses and will only indicate whether ply failure has occurred or not; however, it will not indicate the mode of failure. For example, ply failure is said to occur when the failure index, given by the Tsai-Hill theory, exceeds unity. Similar expressions can be given for strain-based failure criteria.

Using the proposed methodology, a suite of computer programs in FORTRAN is developed to determine the rigidity properties, buckling analysis, free vibration characteristics and dynamic response behaviour of the structural components considered in this research. These programs have been validated using a series of carefully selected tests. A list of all the computer programs developed during this research and a description of their application is given in ***Appendix F***.

Numerical results are given in ***Chapter Seven*** for a number of metallic and composite beams. During the course of this investigation some of these results have been published in professional journals such as *Journal of Sound and Vibration* and *AIAA Journal of Aircraft*, and others have appeared in the proceedings of established international conferences such as *AIAA/ASME/ASCE/AHS/ASC Structures, Structural Dynamics and Materials Conference* and *Annual Conference of Aeronautical Engineers*. A list of published papers extracted from present work is given in ***Appendix G***.

Firstly, for metallic beams, results of the developed theory are compared with the classical Bernoulli-Euler theory and the effect of bending-torsion coupling on the free vibration characteristics and dynamic response is demonstrated. The effects of variation of damping ratio, axial load, shear deformation, rotatory inertia and slenderness ratio are also investigated. Modal interchange, which normally does not exist in uncoupled problems, plays an important rule in the dynamic response of bending-torsion coupled beams. Dynamic response results for metallic beams are given for both deterministic and random

loads.

Next for composite beams, results obtained using the proposed theory to calculate the dynamic response are again compared with classical Bernoulli-Euler theory (where bending-torsion coupling does not exist) and the effect of bending-torsion coupling on the free vibration characteristics and dynamic response is shown. Variation of frequencies and mode shapes of the beams with ply angle are illustrated. In a more comprehensive model, the effects of variation of damping ratio, axial load, shear deformation, rotatory inertia and slenderness ratio are also investigated. Modal interchange plays an important role in the dynamic response of bending-torsion coupled composite beams, in a much more significant way to that of metallic beams with bending-torsion coupling, mainly because of the ply orientations which results in material coupling. Dynamic response results for composite beams are given for both deterministic and random loads.

The significance of generalised mass in relation to the free vibration characteristics and dynamic response prediction of a bending-torsion coupled beam is investigated. This study confirms that examining mode shapes on the basis of displacements alone is not sufficient to identify the behaviour of one particular mode, that is, whether it is bending or torsion dominated, or is coupled, and the contribution of that mode to the overall response. Interpretation of the bending-torsion coupled mode using the concept of generalised mass is discussed and some conclusions are drawn.

For optimisation purposes, it is very important to investigate the effect of variation of ply angles and stacking sequences on rigidities, buckling loads, frequencies, mode shapes and ultimately on the dynamic response behaviour of composite beams. For this reason a parametric study is carried out and a model is proposed to optimise the design of composite beams taking into account buckling, vibration and dynamic response considerations.

Principal conclusions are drawn in ***Chapter Eight*** and recommendations are made for further work.

As mentioned earlier, the literature survey, which was carried out at the beginning and was sustained through out the course of research, is presented in the next chapter.

Chapter Two

Literature review

2 Literature review

In order to achieve a better understanding and to identify the key areas of research and the potential problems of analysing composite materials, a review of the relevant literature is presented throughout ***Chapters Two*** to ***Five***. The number of references surveyed for each topic is given in Table 2-1. The manifestation of the literature review in this thesis, for different subjects, is outlined as follows.

In this chapter, emphasis is given to the development of the dynamic response characteristics of bending-torsion coupled beams, both isotropic and composite, and stress analysis of laminated composite beams. These are the main focus areas of the present study.

Choosing a valid model for composite beams and subsequently realising an acceptably accurate solution for free vibration analysis of bending-torsion coupled beams, are the main stepping stones for the proposed methodology in this thesis. Thus, a strong background is needed on these two subjects. The most popular analytical stiffness models that have been developed for the modelling of laminated composite beams, such as, flat beams and thin-walled beams are discussed and compared in ***Chapter Three***. The buckling analysis of composite columns is investigated independently of the dynamic characteristics of laminated composites. A general background on this topic, along with the analytical and experimental result is presented in ***Chapter Four***. A literature review on the free vibration analysis and the use of dynamic stiffness method to calculate natural frequencies and mode shapes of composite beams, are given in ***Chapter Five***.

Table 2-1. Number of references to literature in each chapter

Topic	Chapter No.	No. of references
Dynamics of bending-torsion coupled beams	***Chapter 2***	118
Stress analysis of thin-walled composite structures	***Chapter 2***	19
Composite beam modelling	***Chapter 3***	23
Buckling analysis	***Chapter 4***	47
Dynamic stiffness method	***Chapter 5***	29

2.1. Introduction

Advances of composite materials for structural components : Application of fibrous composite materials is now being considered for aircraft primary structural components. At first glance, the weight, specific stiffness, and strength properties of the new generation fibres appear to be a phenomenal improvement over metals. However, when fibre properties are "averaged" by the presence of matrix materials, the advantages of composites over metals reduce considerably. Furthermore, off-axis ply orientations, joints and dropped plies also reduce the overall advantage of composite structures significantly. Added to this are material costs, labour intensive manual lay-up procedures (for prototypes) and costly curing, required for most composite material systems. For these reasons, at present the direct replacement of metals with composites in existing designs is marginally successful at best (Nagendra and Kapania, 1995).

In order to exploit fully the benefits of composite materials for primary aircraft structural components, advanced concepts are currently being studied. One of the main design features in fibrous composite materials is tailoring structural stiffness by changing fibre orientations or laminate stacking sequences, an idea which is difficult, if not impossible, to implement in metals. Laminated beams and plates are also finding an increasing use in mechanical, aerospace, marine, and other branches of engineering. Apart from the aircraft and aerospace industry, structural components made of laminated composite materials have a great potential for their utilisation in a wide variety of applications such as in automobile industry, sporting goods, offshore structures, and civil engineering type applications (Davies, 1987).

Composite materials are used for almost all parts of the Lear Fan 2100, different control surfaces of Boeing commercial aeroplanes, and X wings (Kapania and Raciti, 1989). The X wing consists of a symmetrical composite plastic envelope, fumed over a graphite I beam for support. A graphite fibre in a resin called bizmaldeimide together with adhesives that resist high temperature (up to 170 °C) is used.

Lancia, an Italian automobile manufacturer, has recently presented an "Experimental

Composite Vehicle" (ECV) designed for the world rally racing class. The ECV's load bearing centre section is made of carbon fibres and Kevlar impregnated in epoxy matrix, shaped into honeycomb sandwich panels that make the body's core. The estimated weight saving as compared to the tubular steel frame is about 20%, with no loss in torsional rigidity (Kapania and Raciti, 1989).

The most attractive properties of composite materials are the high strength-to-weight ratio and high stiffness-to-weight ratio. These, added to their excellent fatigue strength, ease of formability, wide range of operating temperatures (thermoplastic resins), negative or low coefficient of thermal expansion, high damping, resistance to corrosion, and their capability for being tailored according to a given requirement (Tsai, 1986) result in materials with almost unlimited potential.

Mechanics of fibrous composite materials : Before discussing the dynamic response of composite materials, it is necessary to introduce the relevant literature on the elementary behaviour of laminated composites. Many authors, such as Jones (1975), Tsai and Hahn (1980) and Datoo (1991), have widely covered the macro-mechanics (and micro-mechanics to some extent) of fibrous composite materials in their text books and while others, such as Vinson and Sierkowsaky (1986), discussed the characteristics of structures composed of composite materials.

It is also notable that a proper assessment of end or edge effects in any mechanical system, especially in laminated composite structures is of fundamental technological importance (Horgan and Simmonds, 1994). The extent to which local stresses, such as those produced by fasteners and at joints, can penetrate girders, beams, plates and shells must be understood by the designer. Thus a distinction must be made between global structural elements (where strength of materials or other classical or approximate theories may be used) and local elements which require more detailed analyses based on an exact theory of elasticity. Moreover, it must be recognised that it is impossible, in general, to refine global approximate theories without a simultaneous consideration of local effects. The neglect of end effects is usually justified by application of some form of Saint-Venant's principle. Also, years of experience with homogeneous isotropic elastic structures have served very

well to establish this standard procedure. Saint-Venant's principle is also the fundamental basis for static mechanical tests of material properties. Thus property measurements are made in a suitable gauge section where uniform stress and strain states are induced and local effects due to clamping of the specimen are neglected by an appeal to Saint-Venant's principle. Such traditional applications of Saint-Venant's principle require major modifications when strongly anisotropic and composite materials are considered. For such materials, local stress effects persist over distances far greater than are typical for isotropic materials, as shown in a comprehensive paper by Horgan and Simmonds (1994) who described some problems of static and dynamic elasticity where anisotropy induces such extended Saint-Venant end zones. They clearly pointed out that consideration of such extended end zones due to anisotropy is essential in the proper analysis and design of structures using advanced composite materials.

A significant amount of research has been conducted on the buckling, free and forced vibration analyses of laminated composite beams. A review of some of these developments is given here, and is restricted to studies published in the English language.

2.2. The development of free and forced vibration of beams

Use of beam theories to model laminated composite structures : All structures, no matter what their dimensions are, can be treated as three dimensional structures. It is well known that the solution of the three dimensional elasticity equations is generally very involved and in some cases is even unobtainable. To overcome this difficulty it is usual engineering practice, depending on the dimensions of the structure, to make some simplifying assumptions and reduce the structure to a two dimensional problem or even to a one dimensional problem.

For example, in the case of thin plates, thickness is much smaller than the length or width, and hence one can neglect the influence of strains and stresses in the thickness direction and model it as a two dimensional problem using Kirchoff's hypothesis. Similarly, beams are modelled as one dimensional structures using the Bernoulli-Euler hypothesis because their width and depth are much smaller when compared with the length. Obviously

because of the type of assumptions made, the solution of the reduced problem (in the present case, the beam problem) differs from the solution obtained from the three dimensional elasticity theory or that obtained from the two dimensional plate theory. The significance of the difference among the solutions depends on the initial assumptions and their order of severity. Beam approximation that gives comparable (as close as possible) results with those obtained from considering the same structure as a three and/or two dimensional problem, is the best approximation to be considered.

Many authors have used beam theory to model three dimensional structures. For example, a high aspect ratio composite wing has been modelled using beam idealisation to carry out aeroelastic calculations to reasonable accuracy (Weisshaar, 1981 and Green, 1987). More recently, Pedersen (1991) studied beam theories for bending-torsion coupled response of ship hulls. He presented a consistent one-dimensional finite element procedure for dynamic analysis of ship hulls. He included shear deformation and a higher order generalised warping deformation in his theory (Pedersen 1991).

Refined beam theories : The classical Bernoulli-Euler formulations for beams and plates that utilise the Kirchoff's assumption of straight lines perpendicular to the mid-plane before deformation remaining straight and perpendicular to the mid-plane after deformation have been used for a long time. The simple classical theory does not account for any shear deformation or rotatory inertia, and has been proven not to provide acceptable results for thick beams and plates and for structures made of materials that have high anisotropy ratio and low shear moduli as is quite often the case with composite materials (Kapania, and Raciti, 1989).

The theories that relaxed the Kirchoff's assumption came much later to account for shear deformation and rotatory inertia. A pioneering work in this field is due to Timoshenko (1921) who proposed a new beam theory that included the shear deformations and rotatory inertia effects. In this theory, straight lines perpendicular to the mid-plane before deformation still remain straight but not necessarily perpendicular to mid-plane after deformation. This is equivalent to assuming a constant value for the transverse shear strain (shear stress for isotropic beams) across the thickness of the beam.

This theory has been successfully used for many years to predict the behaviour of isotropic beams. In accordance with the standard terminology used by other research workers, this theory will be hereafter referred to as the Timoshenko beam theory. The theory was later generalised by Mindlin (1951) to include the effects of shear deformations and rotatory inertia in the static and dynamic analyses of plates. Several other researchers have studied the statics and dynamics of beams and plates modelled by this first order theory and its modifications and obtained satisfactory results.

The first order theory, although providing good results for the gross behaviour (natural frequencies and transverse displacements) of such structures, became inadequate for predicting the local behaviour (stresses and displacement across the thickness) of composite beams and plates (Kapania, and Raciti, 1989). In particular, the first order theory violated the condition of no shear stresses on the top and bottom free surfaces. This subsequently led to the assumption of deformation patterns, which ensure no shear condition on the free surfaces at the top and bottom of beams and plates. In the beginning, these assumed distributions were directly substituted in the equations of motions that were obtained from the first order theory (Levinson 1980, 1981). This led to inconsistent formulation and results, because interacting terms between normal and transverse shear stresses as well as some related inertia terms in both the equations of motion and boundary conditions were ignored.

A consistent higher order theory which utilised an assumed displacement field to assure zero shear on the free surfaces was, apparently, first proposed by Krishna Murty (1970, 1977) and Krishna Murty and Shimpi (1974). Later a similar third order theory was also used by Reddy (1984) and Bhimaraddi and Stevens (1984) in the analysis of composite beams and plates. The equations of motion and boundary conditions were obtained by a consistent variational principle. Other higher order shear deformation theories have arisen in the past two decades with the prime interest of having a simple model that can predict accurately the behaviour of beams and plates such as those of Librescu, Khdeir and Reddy (1987) and Dobyns (1981).

Bending-torsion coupling : The free vibration analysis of a bending-torsion coupled metallic beam, particularly when coupling occurs due to the geometry of the cross-section, has been attempted by a number of investigators in recent years (Hallauer and Liu 1982, Dokumaci 1987, Bishop, Cannon and Miao 1989, and Bishop and. Price 1977). In the case of composite beams, coupling between various modes of structural deformation, such as bending and torsion, can occur due to the anisotropic nature of fibrous composites as well as due to the geometry of the cross-section. Study of the influence of bending-torsion coupling on the performance of composites is by no means new. Many authors studied the effect of coupling and pointed out its importance (Chamis, 1969 and Grenestedt, 1992). However, the traditional finite element analysis based on plate or shell element idealisation does not give an insight into the coupling mechanism of the beam (Jensen and Crawley, 1982 and 1984). The use of beam theory often overcomes this difficulty by giving a better insight into the fundamental vibration characteristics. Rehfield and Atilgan (1987, 1988 and 1989) examined the concept of shear centre and elastic axis and their usefulness for composite thin-walled structures. They established that, generally, the real shear centre in composite beams is not the same as geometric shear centre for an isotropic material, because it is altered by the material bending-torsion coupling. Usually due to primary and accompanying elastic couplings there will be twisting even if transverse load is applied at the geometric shear centre. Therefore, use of the locus of shear centres for a reference axis does not simplify the analysis of bending-torsion coupled composite beams. They concluded that it is possible to define a new elastic axis, which uncouples bending and torsion (Rehfield and Atilgan; 1987; 1988 and 1989). Most of the works reported on the vibration of composite beam and plate structures have dealt with the free vibration analysis only, with the primary purpose of calculating natural frequencies.

Free vibration of laminated composite beams : Abarcar and Cunniff (1972), Teoh and Huang (1977), Teh and Huang (1979), Wu and Sun (1991), Banerjee and Williams (1995) and Teboub and Hajela (1995) have published notable works on the free vibration analysis of composite beams. Some investigators considered the effects of bending-torsion coupling on the free vibration of composite beams, which is applicable to aircraft wings,

wind turbine and helicopter blades; others examined the effect of extension-torsion coupling (Kosmatka, 1991 and Banerjee and Butler, 1994) which principally relates to wind turbine and helicopter blades.

Dudek (1970) used the results of Timoshenko beam theory to obtain the transverse shear modulus and studied the effect of the ratio of transverse shear and extensional moduli on beam frequencies. Abarcar and Cunniff (1972) were among the earliest investigators to study the effects of fibre orientation on the natural frequencies of composite beams and their results indicated the existence of bending-torsion interaction. They also showed the existence of coupling between bending and torsional modes in an orthotropic beam experimentally, and proposed a discrete model to analyse the free vibration characteristics of a cantilever beam (Abarcar and Cunniff 1972).

Neglecting shear deformation and rotatory inertia effects, Miller and Adams (1975) developed the equations of motion of a generally orthotropic beam with coupled bending and torsional vibrations, and obtained the free vibration characteristics of beams with several different boundary conditions. Later, Teoh and Huang (1977), and Teh and Huang (1979) further investigated the free vibration characteristics of composite beams, using respectively, an exact differential equation approach from which frequency equations were derived, and a finite element approach. They also included shear deformation and rotatory inertia according to the Timoshenko beam theory in a torsional-flexural vibration study of an orthotropic cantilever beam.

Krishna Murty (1970, 1979) and Krishna Murty and Shimpi (1974) appear to be the first authors to propose the use of a so-called third order theory to include the effect of shear deformation in the dynamic analysis of isotropic and laminated beams, respectively. More recently, Chandrashekhara et al (1990) have developed the equations of motion of composite beams using a first order shear deformation theory and have obtained the frequencies and mode shapes of composite beams with several different boundary conditions. Suresh et al. (1990) have studied the effect of assumed warping behaviour in the formulation, whilst studying on the free vibration characteristics of torsionally and flexurally coupled composite beams. More recently, Song and Wass (1997) examined

effects of shear deformation on the buckling and free vibration of laminated composite beams, having, stepped (unidirectionally) laminated cantilever beams. They compared different theories to assess the importance of shear deformation.

Jensen, Crawley and Dugundji (1982) used a Rayleigh Ritz type analysis to examine the effects of laminate unbalance on the natural frequencies and mode shapes of cantilever graphite/epoxy plates with bending torsion coupling. Their results were mainly centred on symmetric lay ups (laminates) and were validated both by comparison with a detailed finite element analysis (Crawley, 1979) using general anisotropic plate elements and by comparison with experimental results. Their results showed that, for the type of problems they investigated, five assumed modes (two bending, two torsional and one chordwise) were required for their Rayleigh Ritz formulation to determine the first three natural frequencies and mode shapes of the cantilever plate to adequate accuracy. They emphasised the importance of choosing a mode that involves chordwise deformation in order to calculate the natural frequencies accurately. Later on, Jensen and Crawley (1984) utilised the modes given by an earlier detailed finite element analysis (Crawley, 1979) to help the choice of which assumed modes to use in their formulation. Their results generally agreed well with both the finite element and experimental results.

Weisshaar and Foist (1985) used beam theory to understand the basic features of bending torsion coupling in vibrating composite wings of moderate to high aspect ratio. They adopted an aeroelastician's viewpoint and characterised a bending-torsion coupled composite beam/wing by its bending (EI), torsional (GJ) and bending-torsion coupling (K) rigidities. Their beam model used classical laminated plate theory to derive expressions for these parameters (Weisshaar and Foist, 1985). They showed the importance of including chordwise bending curvature in these derivations, consistently with the conclusions of Crawley and Dugundji (1980) and Jensen and Crawly (1984), reported above. Therefore, accurate determination of the natural frequencies of a composite beam requires an accurate determination of its rigidities. The need to determine these rigidities accurately, using both theoretical and experimental methods, has received considerable attention in recent years. Once the rigidity properties of a composite beam of any cross-section are accurately

known, the dynamic stiffness matrix method, which is often called an exact method, can be used to predict its natural frequencies. Different methods of composite beam modelling and the generality of the dynamic stiffness method are discussed in ***Chapters Three*** and ***Five***, respectively.

The above investigations yielded results primarily for flat composite beams of solid rectangular cross-section, for which the only form of coupling was between bending and torsion. The general conclusion drawn by the authors is that the extent of the bending torsion coupling present, and its subsequent effect on the free vibrational modes of a laminated composite beam, depend very much on the fibre orientation of the laminate, and on the wavelength of the vibrational mode.

Forced vibration : Exact solutions for forced vibration problems have been reported in the literature only for some very simple cases. For example, Sun and Whitney (1974, 1976), Sun and Chattopadhyay (1975), Whitney and Sun (1977), Dobyns (1981) and Reddy (1982) have studied the forced vibrations of simply supported plates or cylindrical bending problems formulated with the first order shear deformation theory. On the other hand, the third order theory has been used by Khdeir and Reddy (1988,1989), Bhimaraddi (1987) and Cederbaum (1988) but again for simple supported plates. Recently, Eslimy-Isfahany, Banerjee and Sobey (1996) investigated the dynamic response problem of a bending-torsion coupled beam using the dynamic stiffness method. The effect of an axial load on the free and forced vibration of the coupled beam was later included (Eslimy-Isfahany and Banerjee 1996b).

For composite beams and plates with arbitrary boundary conditions, forced vibration problems have generally been studied using the finite element analysis (Malikarjuna and Kant, 1988) and Galerkin method (Elishakoff, 1977). Other approximate methods have been used if transient or forced vibration problems are to be solved (Grenestedt, 1992).

Maiti and Sinha (1995) used both a Higher-order Shear Deformation Theory (HSDT) and the conventional First-order Shear Deformation Theory (FSDT) to develop a finite element method in order to analyse the impact behaviour of laminated composite beams. Their

higher-order theory assumes that all the displacement components contain variation up to cubic power of thickness. They studied the effects of various parameters, such as span-to-thickness ratios, support conditions and stacking sequence on the impact behaviour of laminated composite beams and observed that stresses computed using HST and FST exhibit wide variations (Maiti and Sinha, 1995).

Rao and Ganesan (1995) investigated harmonic response of tapered composite beams by using a finite element model based on a higher order shear deformation theory. Only uniaxial bending was considered and the inter-laminar shear stresses were neglected. The Poisson-ratio effect was incorporated in the formulation of beam constitutive equations. The effects of in-plane inertia and rotatory inertia were also considered in the formulation of the mass matrix. They carried out a parametric study to investigate the influence of taper profile and taper parameter. Two years later, they carried out a similar investigation, but this time the inter-laminar shear stresses were not neglected (Rao and Ganesan 1997).

Random vibration : The responses of (metallic) beams to random loads have been extensively investigated by many authors such as Eringen (1957), Bogdanoff and Goldberg (1960), Crandall and Yildiz (1962), Banerjee and Kennedy (1985) and Chang (1994). Some closed form solutions for random vibrations of both Bernoulli-Euler beams (Elishakoff and Livshits, 1984) and Bresse-Timoshenko beams (Elishakoff and Livshits, 1989) are available in the literature. The exact solution for the random vibrations of Timoshenko beams with generalised boundary conditions (Singh and Abdelnaser, 1990) and the solution to random vibration of externally damped viscoelastic Timoshenko beams with general boundary conditions (Singh and Abdelnaser, 1993) are also available.

However, it is significant to note that the random vibration analysis of beams reported in the literature is mainly for metallic beams and is mostly based on Bernoulli Euler assumptions and/or Timoshenko beam theory. Thus, when predicting the random response of a beam, it has been assumed that the beam deflects only in flexure (bending) which is uncoupled with torsion. Such an analysis is restrictive in the sense that it applies to beams with only doubly symmetric cross-sections. When bending-torsion coupling exists, Bernoulli Euler or Timoshenko theory is inadequate for the prediction of deterministic or

random response.

The dynamic response of composite structures has only recently been investigated. For instance, random vibrations of orthotropic or composite plates have been studied by Sundararajan and Reddy (1973), Kulkarni, Banerjee and Sinha (1975), Elishakoff (1977), and Mei and Wentz (1982) who have used different approximate methods to obtain the random response of orthotropic plates modelled by the classical theory. More recently, Cederbaum et al. (1988; 1992) discussed the theory of random vibration and reliability of composite structures. Singh and Abdelnaser (1992) investigated random response of symmetric cross-ply composite beams with arbitrary boundary conditions and Abdelnaser (1993) studied random vibrations of composite beams and plates. A full account of random vibration of bending-torsion coupled beams is given in ***Chapter Six***.

2.3. Dynamic Stress analysis

Stress analysis under static loads : Many investigators have studied the stress analysis of composite structures subjected to static loads. For example, Tripathy, Patel and Pang (1994) developed a finite element model based on the strain energy principle and carried out a bending analysis for the study of deflections and stresses for box beams of isotropic and laminated composite materials subjected to different kinds of loading conditions. Experiments using aluminium and composite laminates were conducted by them to verify the results and they also investigated the effect of transverse shear on the span-wise normal stress. However, no dynamic load was included in their investigations.

Jones (1975) and Datoo (1991) covered stress analysis of laminated composites , using the classical theory of elasticity and mechanics of fibrous composites and discussed different failure criteria of laminates and composite beams. Other authors used numerical methods for stress analysis of laminated composite beams. For example, Kant and Manjunatha (1992) studied accurate estimation of transverse stresses in multilayer laminates using numerical methods. They proposed numerical algorithms for the accurate evaluation of transverse stresses in general composite and sandwich laminates. One year later, Manjunatha and Kant (1993) compared different numerical techniques for the estimation

of multiaxial stresses in symmetric/unsymmetric composite and sandwich beams with a refined theory. They evaluated multiaxial stress behaviour in composites with a set of simple, efficient and accurate higher-order displacement models and compared their results with those of available closed form solutions for cross-ply and sandwich laminates.

Miravete (1990) studied strain and stress analysis in tapered laminated composite structures. He used a finite element model to evaluate longitudinal and interlaminar normal and shear strains and also carried out a failure analysis by means of a quadratic failure criterion. Then he carried out an experimental analysis to assess the accuracy of the theoretical model as well as to study the different failure mechanisms that appear in a variable thickness composite beam when subjected to a transverse load.

Ardic, Bolcan and Karan (1995) developed a method of (static) strain and stress analysis to predict the failure initiation in laminated composites containing two or more different kinds of laminae, calculating the principal strains and stresses both in the fibres and in the matrix. They checked their results with those obtained from the classical plate theory.

Failure criteria : The strength of composite material plies strongly depends on the orientation of the plies relative to the stress field. The longitudinal failure stress can be of the order of twenty times the transverse or shear failure stresses. The longitudinal failure strain is though usually of the same order as, for example, the transverse failure strain. A failure criterion based on strains is far less dependent on orientation of the plies than a failure criterion based on stresses. An approximate failure criterion can be based on the invariants of the strain tensor, thus the composite's strength would be independent of the rotation of the strain field. Tsai and Hahn (1980) laid emphasis on such criteria which can be used as a conservative first ply failure approximation.

Echaabi and Trochu (1996) proposed a methodology to derive an implicit equation of failure criteria for fibrous composite laminates. They implemented a systematic connection between parametric formulation and implicit formulation to describe the failure criteria of laminated composites.

Stress analysis under dynamic loads : There are not many published works about

dynamic stress analysis of laminated composite beams. Singh and Abdelnaser (1992) investigated random response of symmetric cross-ply composite beams with arbitrary boundary conditions. They presented a generalised modal approach to solve the equations of motion of a laminated composite flat beam using a third order shear deformation theory. They did not account for warping in their proposed theory. Presenting some numerical results for natural frequencies and mean square values of the deflections and normal stresses for different boundary conditions, they discussed the importance of shear deformation in the dynamic analysis of composite beams. They did not present any numerical results for the torsional rotation. However, one year later Abdelnaser and Singh (1993) examined the effects of bending-torsion coupling and warping on the random vibration of a cantilevered flat composite beam. They also reported on random vibrations of externally damped viscoelastic Timoshenko beams with general boundary conditions (Singh and Abdelnaser, 1993). Abdelnaser (1993) extensively studied the response of composite plates to spatially and temporally correlated random loads. However, none of the above mentioned publications deals with thin-walled composite box beams or composite beams with geometric bending-torsion coupling.

Maiti and Sinha (1995) examined bending and free vibration analysis of shear deformable laminated composite beams by the finite element method. They investigated the effects of fibre orientation, stacking sequence, span-to-thickness ratio and support condition on deflections, stresses and natural frequencies, and highlighted where only a higher order shear deformation theory is likely to yield accurate results.

2.4. Optimisation

Optimum design of composite structures means finding the most efficient composite structural design that meets the design specifications for a certain application. The advent of composites has been a challenge to the designer as laminated structures offer a wide range of parameters (e.g. stiffnesses, material properties, ply orientations and ply thicknesses) that can be varied both at the micro level as well as at the macro level. Furthermore, the designer has to account for a complex behaviour (e.g. both in-plane and

out-of-plane load interaction) and account for multiple failure modes and modal interaction. The inherent nature of composites as discrete laminated structures introduces a new dimension of using discrete variables (Nagendra and Kapania, 1995).

Composite plates and Composite thin-walled beams are often fabricated very thin and this is due to their high strength. Thin laminates result in low free vibration frequencies, low buckling loads and large deflection when subjected to a pressure normal to the plate. Lay-up optimisation to maximise natural frequencies, buckling loads and minimise deflections becomes important (Grenestedt, 1990). Although, optimisation is beyond the scope of the current research, a brief review of the literature is however, presented here for completeness.

Structural optimisation techniques have repeatedly proven to come to the designer's rescue with their ability to account simultaneously for all the design constraints posed by the designer, and to arrive at an optimum design of composite plates and shells under various loadings. Typical design variables are ply orientations or thickness of layers with prescribed ply orientations. In many practical applications the ply thicknesses are limited to integral multiples of the lamina thickness. An excellent source for various techniques used in structural optimisation is the text by Haftka and Gurdal (1992).

Optimisation of composite plates to maximise buckling loads has drawn considerable attention in recent years. Traditionally the design variables of the laminate stacking sequence are selected to be the number of plies of a given orientation. For example, Hirano (1980) considered the buckling load maximisation problem for unstiffened laminated plates.

Miki (1986) proposed a graphical method to determine the optimum fibre orientation angles using a flexural lamination parameter diagram assuming that the buckling wave number is known a priori for a plate of known aspect ratio. The lamination parameters are functions of the laminate in-plane and flexural stiffnesses, and hence of the stacking sequence. For unknown buckling wave numbers, the critical buckling mode method is proposed. The fibre orientation angles are determined so that the buckling strength does

not change when the buckling mode changes. The optimum design of laminates having any aspect ratio can be performed using this approach. This method can arrive at a multiple designs where various combinations of the lamination parameters can have the same buckling load. Later, Fukunaga and Vanderplatts (1991) used the lamination parameters suggested by Miki.

Adali and Duffy (1990) studied the buckling load maximisation problem for antisymmetric angle ply laminates using fibre orientations as design variables to maximise the buckling load subject to a minimum mass constraint. Different methods for finding minimum weight designs of stiffened panels has been of considerable interest and discussed by many authors. One of those, Manevich (1990), studied optimum design procedures for the minimum weight design of longitudinally compressed panels with 'T' shaped stiffeners. On the other hand, Shin (1991) used the homotopy method to arrive at optimum design of stiffened panels.

Grenestedt (1992) showed that the use of lamination parameters for the optimisation is efficient, because large non-linearities of the object function versus design parameters are avoided. This is due to the linearity of the stiffnesses in the lamination parameters (Grenestedt, 1992). Furthermore, the number of design parameters is kept to a minimum while maintaining more design freedom than discrete ply laminates (Grenestedt, 1992 and 1994). The main problem with lamination parameters is that the feasible region is not yet fully determined.

2.5. Summary

The literature review has shown that, as for any new technology, research activity on the use of composite materials for vibrating structures has proceeded at two levels, namely practical and academic levels. It is evident from these studies that the unique features of laminated composite materials make them prime candidates for aerospace applications and aeroelastic tailoring efforts.

However, the main bulk of available literature on vibrating composite beams concentrates

either on a simple Bernoulli-Euler beam or on a Timoshenko beam or on an axially loaded Timoshenko beam, in all of which only flexural displacement of the beam is considered with torsion absent. Thus, the beam theory reported assumes that there is no coupling between the bending displacement and any torsional rotation. Such an assumption is valid only for simple beams with coincident mass centre and shear centre. Naturally, the assumption imposes a severe restriction on the dynamic response analysis of beams for which the mass centre and shear centre are not coincident. Furthermore, it should be recognised that composite beams exhibit material coupling between various modes of deformation (specifically bending-torsion coupling) unlike their metallic counterparts and hence, the response analysis of composite beams is significantly more complicated than that of metallic beams.

It has also been shown that despite extensive numerical and experimental analysis by others in this field, an exact analytical approach to the dynamic response of thin-walled laminated composite beams with substantial coupling between the bending and torsional modes of deformation, has not yet been fully understood or well documented. To make good this deficiency, the present investigation uses an exact differential equation approach and addresses the bending-torsion-coupled response of composite/metallic beams to deterministic and random loads.

The next chapter deals with stiffness modelling of composite beams, which is an essential prerequisite for any dynamic response investigation. In particular, the various methods associated with published work that have been developed for modelling thin-walled laminated composite beams are introduced and examined and, wherever possible, comparisons are made.

Chapter Three

Composite beam modelling

3 Composite beam modelling

3.1. Introduction

A successful prediction of the static and dynamic behaviour of any structure depends on an accurate evaluation of the mechanical properties of its components, such as flexural, torsional and coupling rigidities, the mass and the shear centre locations, the polar mass moment of inertia and the mass per unit length. For an accurate prediction of rigidity properties of isotropic materials, theoretical models and experimental procedures have already been established. The mechanical properties of structural elements made of isotropic materials, such as, Young's modulus and Shear modulus, are independent of the cross-section of the component and the loading conditions, and thus the rigidity properties only depend on the geometrical properties of the cross-section.

However, for composite materials, due to the fibrous nature of their make up, the eventual material characteristics will vary with the orientation of the fibres and the stacking sequence of the plies. The cross-section of the structure and the loading conditions will also affect the mode of deformation and eventually the stress-strain conditions in the structure. Thus an altogether different set of equations to calculate the mechanical properties of composite structures is required. Once the material properties are evaluated, the sectional characteristics can be investigated, for example the location of shear centre for a given cross-section. In the case of isotropic materials, this is purely a sectional property depending on the geometry of the section only, but in the case of composite materials, the location of shear centre is a totally different concept. It is influenced by the laminate material properties, which again depend on the laminate stacking sequence and ply angles, as well as the shape of the cross-section.

In order to obtain experimental, analytical and numerical estimates of structural properties of composite structures, considerable efforts have been made in the past two decades. Some investigations have considered simple beam theory, whereas others used more refined theories. Each investigator has developed the approach for a particular cross-section and its ply configurations, and accounted for certain secondary effects and ignored

others. Some of the methods have not been fully developed and most of them have not been thoroughly validated experimentally for general composite designs. Even today, the structural behaviour of composite beams does not appear to be thoroughly understood. A summary of studies on composite beam modelling is given in this chapter. The main objective here is to discuss and compare the most popular stiffness models that have been developed for the modelling of laminated composite beams, such as, flat beams (plates) and thin-walled beams (box beams), single cell or multi-cell. Applications of different methods are also examined and some conclusions are drawn on the best choice of composite beam modelling.

3.2. Essential rigidities

Stiffness of a structure is its resistance to deformation as the structure comes in contact with an unbalanced system of forces and moments. It primarily depends on the material property and the geometry of the cross-section. Therefore, a given value of stiffness can be achieved by selecting from a range of materials and varying the geometrical parameters such as size and shape of the cross-section. In the case of composite materials the fibre orientation and laminate overall sequence gives a wide number of possibilities to achieve a certain values of stiffness.

For thin-walled beams made of isotropic materials, bending or flexural rigidity EI, torsional rigidity GJ, extensional rigidity EA and transverse shear rigidity kAG are often considered. The concept of shear centre can be dated back as early as 1926 when Eggensschwyler and Maillart (1926) for the first time coined the concept of shear centre and advocated the idea that the centroid is not the only important point in the cross-section. In the case of thin-walled beams made of isotropic materials, a single point called the shear centre can be located, such that a cross-sectional shear force passing through that point will not produce any twist. Alternatively, a torque about this point will not produce any bending displacement. The shear centre is also known as the centre of twist of the cross-section. This point which gives torsion free bending and bending free torsion, is a geometric property of the cross-section and is independent of the loading. On the other

hand, in composite materials the general concept and physical role of shear centre remains the same, but its location depends in addition on the material properties, such as coupling effects, and loading conditions. For composite materials, therefore, bending-torsional coupling rigidity K for symmetric laminates and extensional-torsional coupling rigidity K_a for antisymmetric laminates are further added to the above list of stiffnesses. The accurate determination of these stiffnesses ensures a correct prediction of natural frequencies and other dynamic characteristics of the structure.

In the case of conventional isotropic materials the task of calculating the stiffnesses mainly involves the computation of the geometrical properties, such as the area of the cross-section, the second area moment, etc. Once these properties are computed the stiffnesses are then found as the product of the elastic moduli of the material and the geometric property of the section. However, in the case of anisotropic composite materials, the task is not so straightforward and is generally twofold. Firstly, the laminate equivalent elastic constants are evaluated and, secondly, the sectional properties are determined. Another approach which can be followed is that of the macro-mechanics of the composites, where the overall stiffness estimation can be obtained by developing the stiffness matrix that will relate the stresses to the strains. In the latter approach material and sectional details both go into the analysis together.

3.3. Existing models

The material moduli of isotropic materials are independent of the cross-sectional details and the boundary conditions of the structure. The cross-sectional area, second moment of area, warping inertia, and Saint-Venant torsion constant for various shapes are well known quantities. By way of illustration, Blevins (1979) has provided a comprehensive list of these properties. The product of appropriate quantities such as Young's modulus of elasticity multiplied with the second area moment will give the bending or flexural rigidity, and similarly, the Saint Venant torsion constant times the shear modulus of elasticity will give the measure of torsional rigidity of the structure, etc.

The geometry, along with the loading conditions, will influence the procedures through

which the material moduli of the composite structures are to be obtained. Thus, for example, on occasions, the laminate equivalent elastic constants based on a membrane mode may be required, while at other times the bending mode will be desired (Datoo, 1991). For some geometries it may be possible to compute the laminate equivalent elastic constants and sectional properties separately and the product of both will give the stiffness but in other cases it will be desirable to approach the problem in a unified manner so that the stiffnesses are computed directly (Datoo, 1991).

The introduction of composite materials into aircraft structures has added the material coupling rigidity terms to the complexity of the problem. Two separate approaches associated with published work have been developed for the modelling of composite beams. One is a numerical method using the well-known finite element based approach, and the other is usually termed as the analytical approach. The main advantage that the finite element method offers is the modelling flexibility and versatility, which no analytical method can provide so that almost any structural analysis can be reduced to an automatic process. With this method one can determine the shear centre, and elastic properties for any cross-sectional configuration that can be modelled with two dimensional finite elements, no matter how complicated its geometry is. However, its disadvantage is the loss of physical insight. Analytical methods are the main concern in this investigation, so that, numerical methods will only be briefly summarised.

Among those who used numerical methods, Worndle (1982) developed a method for the determination of the position of shear centre and warping functions based on a two dimensional finite element analysis. Bauchau (1985) developed an anisotropic beam theory in which out-of-plane cross-section warping is expanded in terms of so called eigenwarpings. Kosmatka (1986) used Worndle's analysis but included blades made of orthotropic materials with arbitrary fibre orientation instead of transversely isotropic materials. Stemple and Lee (1988, 1989) developed a finite element based approach in which the warping behaviour is determined through specification of warping nodes over the cross-section. It considers only thin-walled cross-sections, and out-of-plane warping. Suresh and Malhotra (1997) recently studied effects of material and lay-up sequence on

the structural behaviour of a rectangular cross-section thin-walled composite box beam under a uniformly distributed load on the top face, with end supports, using the finite element method and taking shear deformation of the beam into consideration.

Many researchers have investigated analytically the mechanical properties of composite beams. Housner and Stein (1974) provided the model for balanced ply of symmetrical laminates. The bending and torsional stiffnesses were assumed to arise solely from thin laminated composite cover sheets forming the upper and lower surfaces of the wing. The equivalent bending and torsional stiffnesses of the resulting box beam were computed by using classical Euler Bernoulli beam deformation assumptions. The same structural idealisation was used by Weisshaar (1980, 1982) when he investigated the divergence behaviour of forward-swept composite wings. He also conducted a systematic study of bending-torsion and extension-torsion coupling rigidity terms for linear displacements (Weisshaar 1982, 1985).

Mansfield and Sobey (1979), dealt with the composite thin cylindrical tube (beam) composed of an arbitrary lay up of fibre composite plies. Expressions were derived for the coupled torsional, extensional and flexural stiffnesses for linear displacements. Mansfield (1981) subsequently extended the theory to two-celled beams. Libove (1988) presented more or less the same theory in the later years and admitted that at the time of his investigations he was not aware of Mansfield and Sobey's contributions to the subject (1979). He also stated that, due to the effects of coupling terms, the local rate of twist not only depend on the torque and the shear forces but also varies with the axial load applied and moments about chordwise and span-wise axes.

Rehfield (1985) pointed out that the above theoretical developments were rather difficult to follow, and a single variationally consistent theory was not clearly emerging. He performed a similar contour analysis to Mansfield and Sobey (1979) in which a general rotor blade cross-section is idealised as a single celled box beam subjected to axial, bending, torsional, transverse shear, and warping loads. Nixon (1987) compared the theory of Rehfield (1985) with experimental data and showed that transverse shear is very important for an accurate modelling of extension-torsion coupled circular tubes. Hodges,

Nixon and Rehfield (1987) further demonstrated the accuracy and effectiveness of Rehfield's (1985) approach by showing favourable correlation between this relatively simple theory and a NASTRAN finite element model for a single cell closed beam.

Hong and Chopra (1985, 1986) developed a non-linear analysis for thin-walled composite beams, under going transverse bending (flap and lag), torsion and axial deflections based on non-linear strain displacement relations of Hodges and Dowell (1974). A simple analytical expression was given for the cross-sectional warping, while effects of transverse shear were neglected. Later extensive investigations in the behaviour of structural coupling terms due to ply orientations were made by Chandra, Stemple, and Chopra (1990) and Smith and Chopra (1991). A direct analytical method for the prediction of the effective elastic stiffnesses and corresponding load deformation behaviour of composite symmetric and antisymmetric box beam structures was developed.

Berdichevsky, Armanios, and Badir (1992) developed a variationally and asymptotically consistent theory in order to derive the governing equations of anisotropic thin-walled beams with closed cross-sections subjected to axial, bending and torsional loads. This theory is based on an asymptotic analysis of two dimensional shell theory. Closed form expressions for the beam stiffness coefficients, stress and displacement fields are provided. It is assumed that the in-plane deformation of the cross-section is zero, but the out-of-plane warping is included. In addition to the classical out-of-plane torsional warping, two new contributions are identified by the authors; these are the axial strain and bending warping. The theory correlated very well with both experimental data and other theories in the literature.

Recently, Song and Librescu (1997) presented a refined theory of a rotating blade modelled as a thin-walled composite beam of arbitrary closed cross-sections to study its free vibration behaviour. The structural model encompasses a number of non-classical features such as the anisotropy and heterogeneity of constituent materials, transverse shear, primary and secondary warpings. In their study the influence of the ply orientation on the flap-lag-transverse shear and twist-extension coupled free vibration eigencharacteristics are presented and the benefits of exploiting the induced elastic

couplings are highlighted.

Among those researchers who recently suggested experimental methods to verify a composite beam modelling, are Qian, Hoa and Xiao (1997). They proposed a vibration experiment for measuring mechanical properties of composites. They established an analysis based on a finite element model that considers the effect of transverse shear deformation and hysteretic damping. Qian et al. (1997) also used vibration test data for identifying elastic and damping properties of composite laminates. Their numerical study showed that satisfactory results including transverse shear moduli can be obtained by designing a suitable plate specimen. They demonstrated the efficiency of their proposed method by experimental results. In principle, their method allows all elastic constants and damping factors to be determined simultaneously (Qian et al., 1997).

3.4. Choosing a suitable model

Three different methods have been mainly used to analyse a thin-walled composite beam. Two of these are the contour analysis (Mansfield, and Sobey, 1979 , Libove, 1988 and Rehfield 1985) and the variational-asymptotical analysis (Berdichevsky, Armanios, and Badir, 1992) where the displacements and stresses are integrated around the cross-section and as a consequence the cross-section is analysed as a unit regardless of its shape. The third is the simplified linear analysis used by Chandra, Stemple and Chopra (1990) and Smith and Chopra (1991) where the four sides of the thin-walled beam are modelled as general composite laminated plates. An important advantage of the contour and variational-asymptotical analyses is that the cross-sectional warping can be more accurately predicted as it is taken around the cross-section. However, in the simplified theory where each side of the beam is modelled as a plate, the torsion related warping is expressed in an approximate manner.

In the case of infinitely long beams made of conventional materials with a closed cross-section, the effects of transverse shear deformation and warping inertia are small enough to be neglected. However, these effects cannot always be ignored for thin-walled composite beams. In a comprehensive model of composites, the effect of transverse shear

deformation on the bending deformation and the effect of the warping inertia term on open sections, both need to be considered because they may cause substantial differences between the predicted and experimental results. The inclusion of the cross-sectional warping allows three-dimensional contributions to be recovered from a one-dimensional beam formulation. The major difference between the various theories generally lies in the methodology used to analyse the box beam and particularly in the methodology used to derive the warping of the cross-section and to include its contributions into a one-dimensional theory.

In order to compare different approaches, loading conditions and secondary effects considered in the various analytical theories for stiffness predictions of thin-walled composite beams are summarised in Table 3-1. Thorough examination is needed when choosing a model for the prediction of stiffnesses of a laminated composite beam. Generally the choice of model depends on the size and the shape of cross-section (box or flat beam), loadings considered, accuracy required and nature of secondary effects that are taken into account. Recently, many researchers have discussed the choice of composite beam modelling and some investigators have even carried out comparative studies on different existing models (Khan, 1993 and Georghiades, 1997) in order to demonstrate their differences numerically. To summarise, a Chordwise-Rigid-Laminated-Plate (CRLP) model can give satisfactory results only when the wing has such a high torsional rigidity for the chordwise rigidity to be assumed. Chordwise rigidity is often assumed in wing design when stiff, closely spaced ribs are present within a wing of moderate to high aspect ratio. If this is not the case, a High-Aspect-Ratio-Plate (HARP) model is definitely a better choice. When a thin-walled beam cross-section is present within a wing, such as a torque box of small width-to-depth ratio, a box beam model like the ones given by Berdichevsky et al. (1992) and by Rehfield (1985) is a better choice. However, if the width-to-depth ratio of the thin-walled beam is large, the HARP model appears to be a better choice since the use of axial rigidity terms (instead of the bending rigidity terms) in box beam models to estimate the rigidity properties is not valid for high width-to-depth ratios resulting in an overestimation of stiffnesses.

3.5. Effect of ply orientation on the stiffnesses: case studies

In this section the effect of ply orientation on the stiffnesses of three composite beams are shown. The chosen composite beams are (i) a flat plate (Jensen, Crawley, and Dugundji, 1982), (ii) a rectangular box (Cesnik, Hodges, and Patil, 1996) and (iii) a bi-convex shape (Librescu, Meirovitch, and Song 1996). Cross-sectional and other properties are all given in Figures 3-1a to 3-3a. Variations of stiffnesses for each case are calculated according to Berdichevsky et al. (1992) and plotted against ply orientation and are shown in Figures 3-1b to 3-3b. The flexural, torsional, and bending-torsional coupling rigidities are grouped together to obtain a non-dimensional quantity given by

$$\frac{K^2}{EI\ GJ} \tag{3-1}$$

and this is also plotted against the ply orientation as shown in Figures 3-1b to 3-3b.

The variation of stiffnesses in all the cases show a similar trend. For example, as can be seen in Figure 3-1b, for the flat plate, the flexural rigidity decreases when the ply angle increases. The torsional rigidity increases for ply angles between zero to thirty degrees and then decreases when ply angle is further increased. A similar trend is evident for the bending-torsion coupling rigidity and the non-dimensional coupling rigidity parameter when plotted against the ply orientation. The only difference is in the occurrence of the peak for each plot. The peak of bending-torsion coupling rigidity occurs at twenty degrees whereas the maximum for non-dimensional coupling rigidity occurs at twenty five degrees. The other two graphs (see Figures 3-2b and 3-3b) show similar behaviour but peaks do not occur at exactly the same ply angles.

The presence of bending-torsion coupling has a significant effect on both static and dynamic characteristics of composite beams. Since studying the static behaviour is a stepping stone before embarking on the dynamic behaviour of structures, the next chapter sets out to investigate the elastic buckling behaviour of composite columns, mainly when coupling rigidity is present. The buckling load is calculated theoretically, and is measured experimentally and finally, the associated results are compared.

Table 3-1. Loadings and non-classical effects considered in the various analytical theories for rigidity predictions of thin-walled composite beams

		Loadings considered					Non-classical effects included			
Authors	**Date**	**Axial**	**Torsional**	**Bending**	**Shear**	**Warping**	**Transverse shear**	**Warping due to torsion**	**Warping due to bending**	**Warping axial strain**
Reissner and Tsai	1972	✓	✓	✓	-	-	-	-	-	-
Mansfield and Sobey	1979	✓	✓	✓	-	-	-	-	-	-
Hong and Chopra	1985	✓	✓	✓	-	-	-	✓	-	-
Rehfield	1985	✓	✓	✓	✓	✓	✓	✓	-	-
Libove	1988	✓	✓	✓	-	-	-	-	-	-
Rehfield and Atilgan	1989	✓	✓	✓	✓	✓	✓	✓	-	-
Chandra et al.	1990	✓	✓	✓	-	-	-	✓	-	-
Smith and Chopra	1991	✓	✓	✓	✓	-	✓	✓	-	-
Berdichevsky et al.	1992	✓	✓	✓	-	-	-	✓	✓	✓

$E_1 = 98.0\ GPa$

$E_2 = 7.9\ GPa$

$G_{12} = G_{13} = G_{23} = 5.6\ GPa$

$\nu_{12} = 0.28$

Ply thickness $= 0.134\ mm\ \ [\beta_2/0]_s$

Density $= 1520\ kg/m^3$

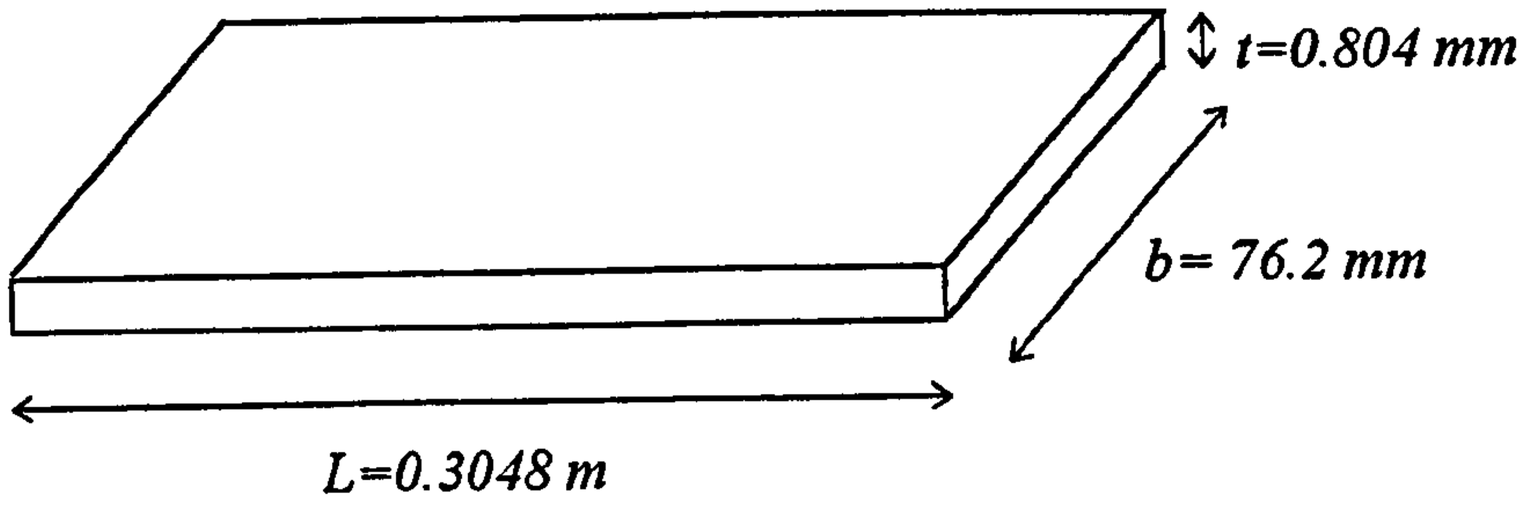

Figure 3-1(a) Configuration of the laminated flat beam.

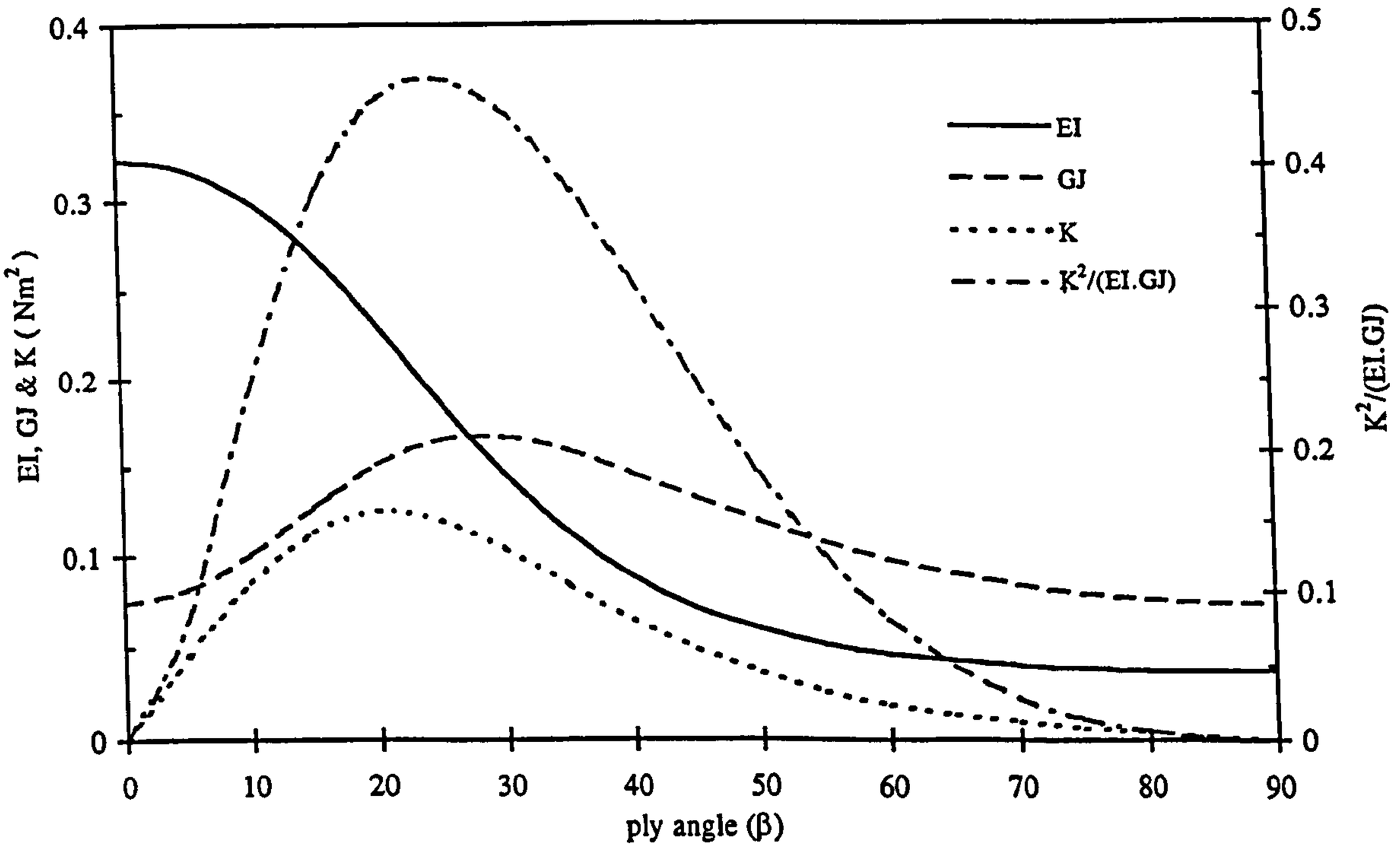

Figure 3-1(b) Variation of flexural rigidity (EI), torsional rigidity (GJ), coupling rigidity (K) and coupling parameter with ply angle for the flat beam.

$E_1 = 206.92 \times 10^9\ Nm^{-2}$

$E_2 = E_3 = 5.17 \times 10^9\ Nm^{-2}$

$G_{12} = 3.10 \times 10^9\ Nm^{-2}$

$G_{13} = G_{23} = 2.55 \times 10^9\ Nm^{-2}$

$\nu_{12} = \nu_{23} = \nu_{13} = 0.25$

$\rho = 1529.48\ kgm^{-3}$

Thickness=1.016 cm

Length = 203.2 cm

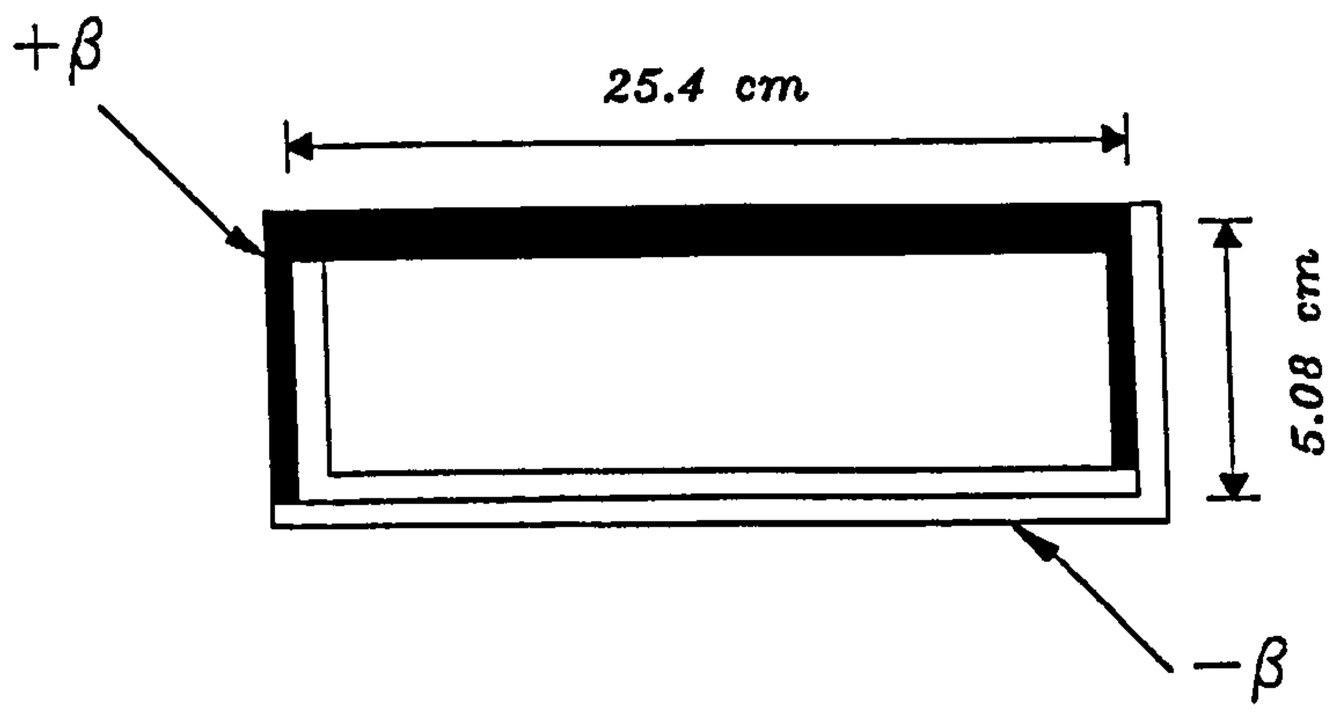

Figure 3-2(a) Configuration of the laminated wing box section.

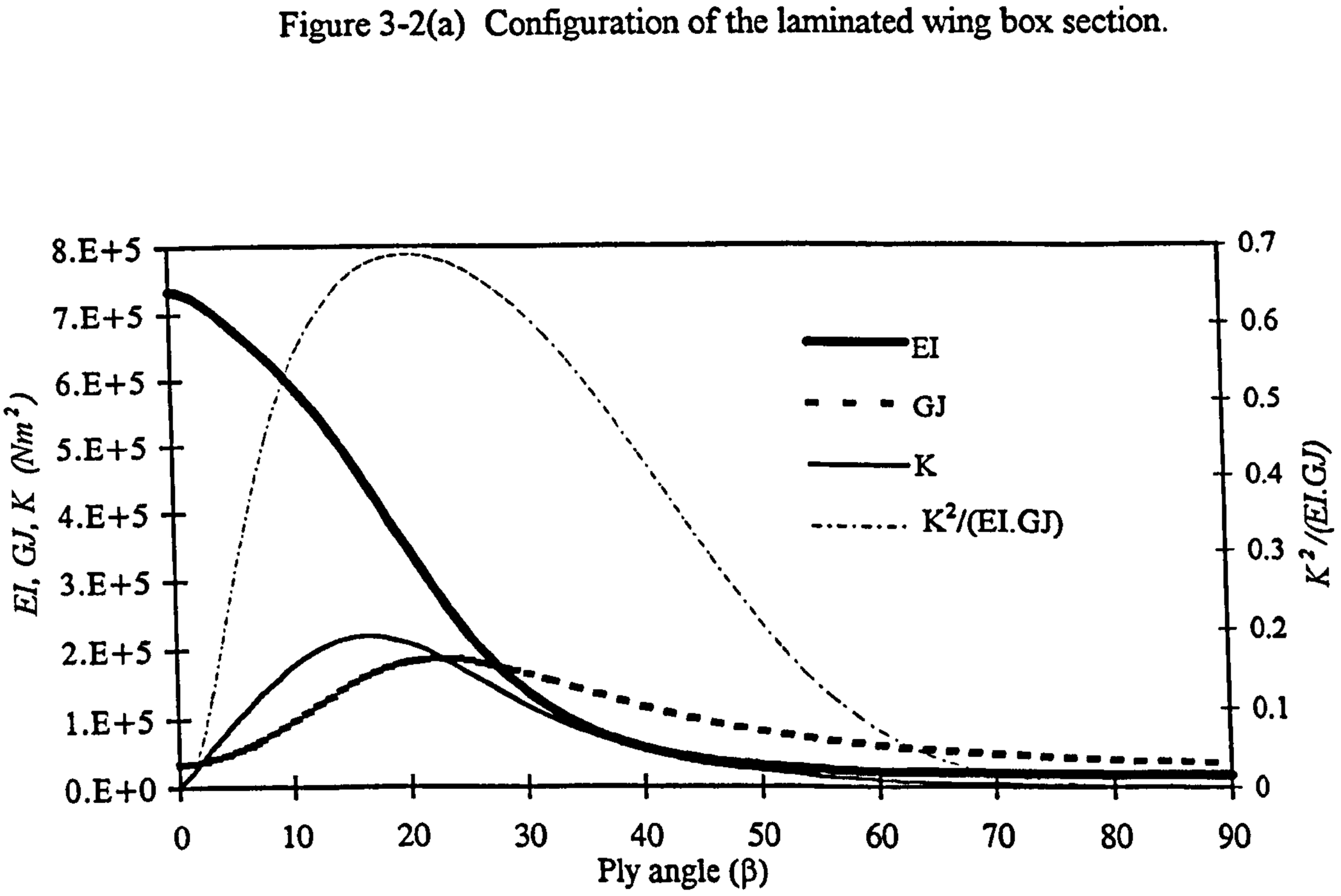

Figure 3-2(b) Variation of flexural (EI), torsional (GJ), bending-torsion coupling (K) rigidities and coupling parameter against ply angle for the rectagular box.

$E_1 = 30 \times 10^6\ psi$

$E_2 = E_3 = 0.75 \times 10^6\ psi$

$G_{12} = 0.45 \times 10^6\ psi$

$G_{23} = G_{31} = 0.37 \times 10^6\ psi$

$\nu = 0.25$

All plies are unidirectional.

$\rho = 14.3 \times 10^{-5}\ lb\text{-}sec^2 / in^4$

$L = 2.032\ m$

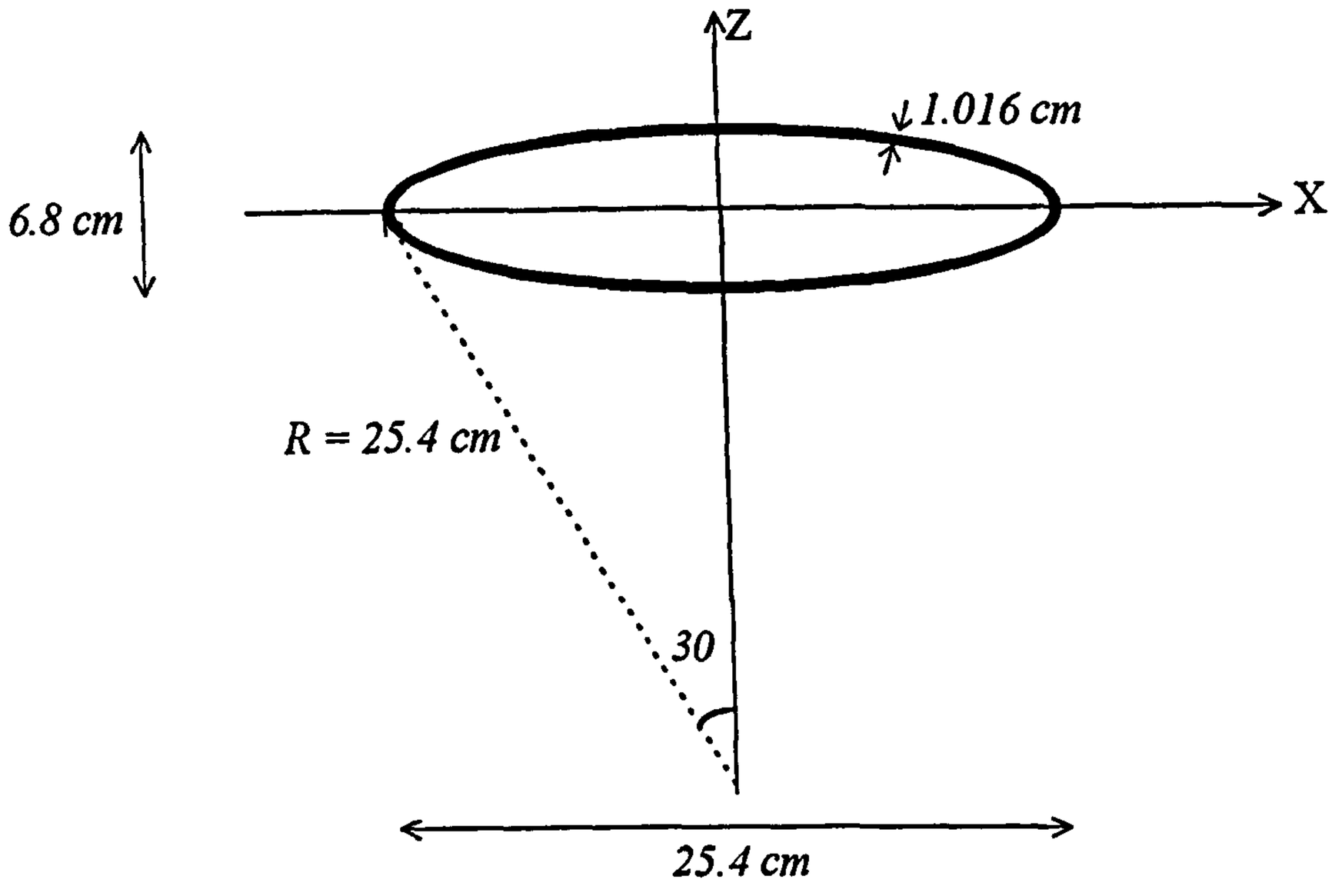

Figure 3-3(a) Configuration of the laminated bi-convex beam.

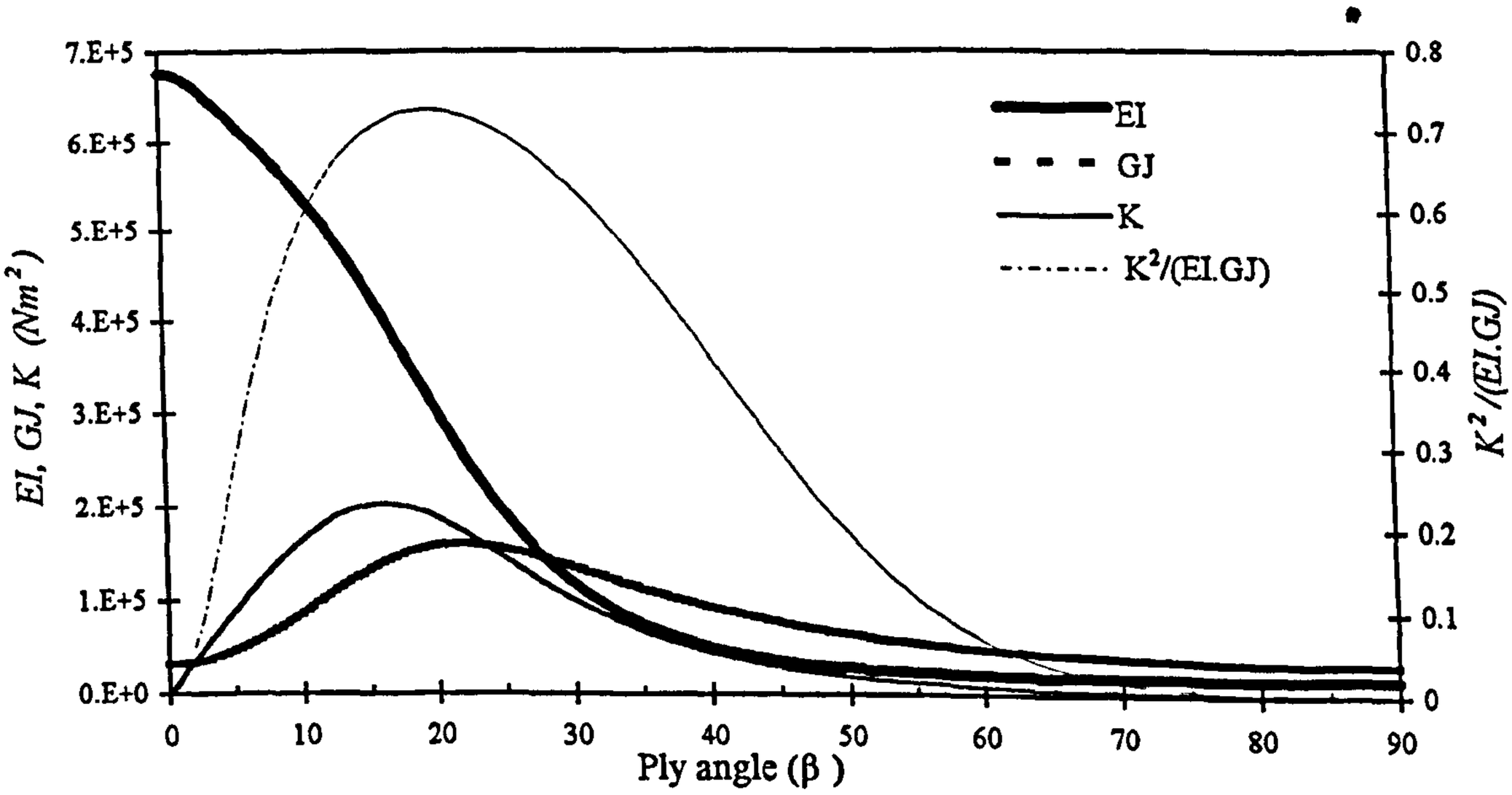

Figure 3-3(b) Variation of bending (EI), torsional (GJ) and bending-torsion coupling (K) rigidities and coupling parameter against ply angle for the bi-convex beam.

Chapter Four

Buckling of composite columns

4 Buckling of composite columns

4.1. Introduction

Among all the different techniques to determine the stiffnesses of a composite beam, the elastic buckling load provides a reasonable estimate. As was mentioned in ***Chapter One***, it is essential to validate the chosen composite beam modelling, and to resolve any uncertainty in the stiffnesses. Therefore, determination of the buckling load was chosen, a series of experiments was conducted and a comparison between the experimental and numerical results has been carried out. In the present chapter reports are given on this comparison.

The elastic critical buckling loads of thin-walled laminated composite columns with flat or box cross-sections having various end conditions are established, following a brief review of the literature. The theory is based on an exact stiffness matrix for bending-torsion coupled composite columns, derived from a rigorous formulation of the basic bending-torsion buckling theory. The stiffness expressions are based upon the closed form solution of the governing differential equations.

Simultaneous bending and torsion in a composite column, caused by both geometric and material couplings, are considered. The effect of shear deformation on the buckling characteristics of the composite column is also included in the theory. The stiffness matrix for the degenerate case of the composite column which reduces to a metallic column (for which geometric coupling exists but there is no material coupling) is deducible from the original matrix.

The importance of experimental procedures in understanding the structural behaviour of composites is emphasised. Experiments are carried out to establish the elastic critical buckling load of laminated composite flat columns made of carbon-epoxy material. Other objectives are to gain further insights into the buckling characteristics of bending-torsion coupled composites columns. Classical boundary conditions are applied. These are simply supported-simply supported (S-S), clamped-simply supported (C-S) and clamped-

clamped (C-C). Southwell's method (1932) has been used in this investigation to determine the critical elastic buckling load (P_{cr}) from the experimental data. The experimentally determined buckling load is compared with theoretical predictions. A number of observations about testing methodology are also presented.

Using the proposed method, some numerical results are presented for both metallic and composite columns and compared with published results. The significance of the results is discussed and some conclusions are drawn.

4.2. An overview on the bending-torsion coupled buckling of composite columns

Geometric bending-torsion coupling : The problem of the bending-torsion (elastic) buckling analysis of metallic columns has been extensively researched for well over half a century and is well documented. Hoff and Goodier (1943), Timoshenko (1945), Renton (1960) and Pekoz and Winter (1969) are among many pioneering researchers in this field. However, only a very few investigators have used the stiffness matrix method to solve such problems using coupled flexural torsional column theory. One of the advantages of stiffness matrix based solutions is of course, that it covers frameworks as well as individual members.

Barsoum and Gallagher (1970) formulated the finite element stiffness matrix of a bending-torsion coupled column using an approximate displacement field. Renton (1960, 1962) used a method that derived the exact stiffness matrix from the classical differential equations of the coupled column. Renton's work is very important because it used exact classical theory as opposed to the more usual approximate finite element theory. However, his work was not followed up and has often been overlooked by later investigators. It may be significant that Renton developed his exact stiffness matrix before a well known algorithm (Wittrick and Williams, 1971), which uses exact member theory to solve buckling (and vibration) eigenvalue problems, was available. Wittrick and Williams (1971) developed this algorithm to ensure the prediction of any eigenvalue with certainty, when using exact theory. This algorithm is explained in ***Chapter Five***.

Chamis (1969) and Ashton and Whitney (1970) used Galerkin's method and observed in their theoretical and experimental results that significant non-conservative estimations of buckling loads can occur if bending-torsion coupling is not taken into account. Noor and Mathers (1976) and Noor et.al. (1977) proposed an energy measure to indicate the influence of bending-torsion coupling, whereas Nemeth (1986) used finite element solution to show how different parameters affect buckling loads.

Williams and Anderson (1983) and Al Shareedah and Seirig (1986) used a Lagrangian multiplier approach to include strain and displacement constraints as boundary conditions in the formulation of the potential energy functional. Their method accounts for additional constraints in addition to the natural boundary conditions derived as part of the variational formulation. The resultant problem is solved using techniques for the minimisation of the Lagrangian functional of the system.

Sridharan and Peng (1989) questioned the validity of the classical assumption in modelling prismatic plate assemblies, namely that out-of-plane displacements vanish at points where two plate elements meet at an angle as does the normal stress resultant N_y for each plate element at a corner. Sheinman (1987) modelled a stiffened panel using a plate and beam combination and derived exact non-linear equations by a variational approach. The equations are exact in terms of the von Karman relations. The panel is modelled by plate elements for which the non-linear equations are resolved into eigenfunctions and then solved using a finite difference approach.

Composite columns : Investigation into the buckling behaviour of thin-walled composite structures is a relatively recent phenomenon and is mostly confined to laminated plates or structures assembled from them. Kapania and Raciti (1989) and Nagendra and Kapania (1995) gave an extensive bibliography on the subject. In the case of composite elements bending-torsion coupling can occur both because of the geometry of the cross-section and also because of the anisotropic, or directional, nature of the fibrous composites.

Hajela and Shih (1989) proposed a modified branch-and-bound approach to include non-linear optimisation problems involving continuous, integer and discrete design variables

for the optimum design of a laminated composite beam. The methodology was based on a piece-wise linear representation of the non-linear problem. A modified branch-and-bound method was used to solve the problem. The approach consisted of a systematic search of continuous solutions in which the discrete and integer variables are successively forced to assume specific values. The approach was used for the solution of structural design problems that are described in terms of continuous and discrete variables. Shin et al (1990) used an extension of the penalty-function approach for solving a non-linear optimisation problem with discrete variables. The extension was based on the introduction of additional penalty terms into the augmented objective function to reflect the requirement that the design variables take discrete values.

Analysis of elastic buckling using plate and shell theories : Grenestedt (1989a) is among the first of those who have examined the effects of bending-torsion coupling on the buckling strength of composite plates. He investigated the buckling behaviour of rectangular plates and showed that neglecting bending-torsion coupling will result in non-conservative approximations for the buckling load. Sheinman (1989) threw some light on this by arriving at the correct generalised force and generalised strain relations, but by ignoring the forces in the y direction. This operation involves inversion of certain matrices and is restricted to limited types of beams (Sheinman 1989).

Bhimaraddi and Chandrashekhara (1991) published their observations on the modelling of laminated composite beams with general lay-ups. They considered the modelling of laminated beams by systematic reduction of the constitutive relations of the three dimensional anisotropic body. The basic equations of the beam theory that they used are those of the parabolic shear deformation theory. All the results and the correctness of their model were verified by modelling the same beam as a plate (Bhimaraddi et al. 1989). Results obtained from the theory presented in this thesis are compared with those from Bhimaraddi and Chandrashekhara (1991) for a flat beam with different ply angles and shown later in this chapter.

Gerhard, Gurdal, and Kapania (1994) used a finite element method based on Reddy's layer-wise theory to study buckling and post buckling of geodesically stiffened laminated

cylindrical shells. The beam was also examined using the Ritz approach. The method used the Lagrange multiplier approach to attach the stiffeners to the shell. The buckling results from the Ritz discrete analytical method are compared with smeared buckling results and with NASA tested finite element results. The report also presented a development of layer-wise shell and beam finite elements. The layer-wise beam element was directly attached to the layer-wise shell model. These developments were used to obtain displacements, stresses and compressive loads for first ply failures using the Tsai-Wu failure criterion. Postbuckling behaviour of stiffened cross-ply cylindrical shells using the layer-wise shell theory of Reddy and the smeared stiffener approach was studied by Savoia and Reddy (1994) and postbuckling analysis of laminated stiffeners was performed by Shen and Williams (1993).

Jaunky et al. (1995a) solved the problem of buckling of arbitrary quadrilateral anisotropic plates. They also considered general triangular anisotropic plates (1995b) subjected to combined in-plane loads and having different boundary conditions. They obtained solutions for plate buckling by using Rayleigh-Ritz method combined with a variational formulation using both classical laminated plate theory and first-order shear-deformation theory. In their study the Ritz functions consist of polynomials that include circulation functions which are used to impose various boundary conditions. Later in this chapter, some numerical results are presented using the method of Jaunky et al. (1995a, 1995b and 1997).

Refined one-dimensional theories : Other investigators on the buckling behaviour of composite structures include Abramovich (1994), who studied analytically the thermal buckling of a cross-ply composite laminate using a first order shear deformation theory. He presented and discussed some results for various boundary conditions, lay-up sequences, slenderness ratios and transverse shear moduli. Bhaskar and Librescu (1995) investigated the buckling behaviour of single-cell thin-walled composite beams exhibiting extension-twist coupling. They also investigated the effects of direct transverse shear and the bending-transverse shear coupling as well as those of different boundary conditions and ply angles.

Abramovich et al. (1995) studied the vibration and buckling of non-symmetric laminated composite beams using the exact element method, which they applied to calculate the natural frequencies, buckling loads and the influence of the axial load on the natural frequencies and mode shapes of non-symmetric laminated composite beams. In their investigation the theoretical model uses a first order shear deformation theory and includes the effects of rotatory inertia, shear deformation and coupling between the longitudinal and transverse displacements. They also carried out a parametric study to investigate the influence of boundary conditions, materials and lay-up sequence on the buckling loads and natural frequencies of laminated composite beams with a rectangular cross-section. However, they did not discuss the effect of bending-torsion coupling on the buckling load or on the natural frequencies of composite structures.

More recently, Khadeir and Reddy (1997) studied the buckling of rectangular cross-ply laminated beams with arbitrary boundary conditions. They used a state space concept in conjunction with a Jordan canonical form to solve the governing equations of the buckling problem and present analytical solutions of refined beam theories. Song and Waas (1997) investigated the effects of shear deformation on the buckling and free vibration of stepped laminated composite beams with rectangular cross-section. They used a simple higher-order theory that assumes a displacement field varying cubically through the thickness. Neither Khadeir and Reddy (1997) nor Song and Waas (1997) produced any results to show the effects of bending-torsion coupling on the buckling load.

Shield and Morey (1997) developed a new theory for the buckling analysis of composite beams of open and closed cross-section by taking into account deformation in the plane of the cross-section due to anticlastic curvature. They investigated the effects of anticlastic curvature and the ply angle on buckling load, and showed that inclusion of the anticlastic curvature substantially reduces the predicted buckling load, and that the effect is most pronounced when the ply angle is around *45* degrees. For comparative reasons they also studied previous works of Rehfield and Atilgan (1989). Some of the Shield and Morey (1997) and Rehfield and Atilgan (1989) results are reproduced and presented later in this chapter.

Comparison of experimental and theoretical results : Since there are always some aspects and characteristics of a mechanical system which do not behave quite as predicted by numerical and/or analytical methods, many researchers have put a great deal of emphasis on planning experimental investigations to ensure that the information needed to design high quality aircraft is obtained as accurately and as effectively as possible. For example, Barbero and Tomblin (1993) investigated the Euler buckling characteristics of thin-walled composite columns. They investigated the global buckling phenomenon and experimentally determined the critical buckling loads for various fibre reinforced composite **I** beams . They used Southwell's method to determine the critical buckling load about strong and weak axes. Theoretical predictions were subsequently compared with experimental results.

Ishikawa et al. (1993) and Davalos et al. (1997) are among others who performed analytical/numerical and experimental studies of the buckling characteristics of thin-walled fibrous composite beams. Ishikawa et al. (1993) conducted experimental and numerical investigations for the rigorous correlation of initial buckling properties of stiffened panels made of carbon fibre composites. They also developed a conventional analytical Rayleigh-Ritz approach considering only a local buckling mode of skin. They achieved very good agreement between numerical, analytical and experimental results. Davalos et al. (1997) carried out a combined analytical/numerical and experimental investigation on flexural-torsional buckling of pultruded fibre reinforced plastic (FRP) composite I-beams. They obtained good agreement between the experimental results, proposed analytical solutions and finite element analyses. Through the combined experimental and analytical evaluations, they showed that the testing set-up used can be efficiently implemented in the characterisation of flexural-torsional buckling of FRP shapes and their proposed analytical design equations can be adopted to predict flexural-torsional buckling loads (Davalos et al. 1997).

4.3. An exact stiffness matrix of a bending-torsion coupled column

A straight uniform composite column of length L is shown in Figure 4-1, with x_α being the separation between the centroidal axis and the elastic axis, i.e. between the loci of respectively the centroid and the shear centre of the cross-section. In the right handed coordinate system of Figure 4-1, the Y axis coincides with the elastic axis, which is permitted flexural translation $u(y)$ and torsional rotation $\psi(y)$ as indicated, where y is measured from the origin. The constant compressive axial load (P) is assumed to act through the centroid of the cross section. P can be negative, so that tension is included. Characterisation of bending-torsion coupled composite columns by the use of three important parameters, namely the flexural rigidity (EI), the torsional rigidity (GJ) and the bending-torsion material coupling rigidity (K), is essential in the derivations which follows.

Using coupled flexural torsional beam theory for thin-walled composites with shear deformation and warping stiffness neglected, the governing differential equations for static behaviour are given by Mansfield and Sobey (1979)

$$EI\ u'''' + K\psi''' + P(u'' - x_\alpha \psi'') = 0 \tag{4-1}$$

$$GJ\ \psi'' + Ku''' - P(r_0^2 \psi'' - x_\alpha\ u'') = 0 \tag{4-2}$$

where: primes denotes differentiation with respect to y; EI, GJ and K have already been defined above; and r_0 is the radius of gyration of the beam cross section about the Y axis, i.e. the elastic axis, so that the polar second moment of area of the cross section is Ar_0^2, A being the cross sectional area.

Substituting

$$\xi = y/L \quad \text{and} \quad D = d/d\xi \tag{4-3}$$

into equations (4-1)-(4-2) gives

$$D^4 u + (KL/EI)D^3 \psi + (PL^2/EI)\{D^2 u - x_\alpha D^2 \psi\} = 0 \tag{4-4}$$

$$L D^2 \psi + (K/GJ) D^3 u - (PL/GJ)\{ r_0^2 D^2 \psi - x_\alpha D^2 u \} = 0 \qquad (4\text{-}5)$$

Equations (4-4) and (4-5) can be combined into one equation by eliminating either u or ψ to give

$$D^2 (D^2 + \overline{\alpha}^2) W = 0 \qquad (4\text{-}6)$$

where

$$W = u \text{ or } \psi \quad \text{and} \quad \overline{\alpha}^2 = b(1 + c)/(1 - a) \qquad (4\text{-}7)$$

with

$$a = K^2 / EI\ (GJ - P r_0^2)$$

$$b = PL^2 / EI \qquad (4\text{-}8)$$

$$c = P x_\alpha^2 / (GJ - P r_0^2)$$

The solution of the differential equation (4-6) is

$$W(\xi) = \overline{C}_1 + \overline{C}_2 \xi + \overline{C}_3 S(\alpha, \xi) + \overline{C}_4 C(\alpha, \xi) \qquad (4\text{-}9)$$

where $\overline{C}_1$-$\overline{C}_4$ are constants, and

$$\alpha = \sqrt{j\overline{\alpha}^2} \qquad (4\text{-}10)$$

$j = 1$ when $\overline{\alpha}^2$ is positive, $j = -1$ when $\overline{\alpha}^2$ is negative and

$$j = 1 \ ; \ S(\alpha, \xi) = \sin \alpha\xi \ ; \ C(\alpha, \xi) = \cos \alpha\xi \ \text{ for } \overline{\alpha}^2 > 0 \qquad (4\text{-}11a)$$

$$j = -1 \ ; \ S(\alpha, \xi) = \sinh \alpha\xi \ ; \ C(\alpha, \xi) = \cosh \alpha\xi \ \text{ for } \overline{\alpha}^2 < 0 \qquad (4\text{-}11b)$$

W(ξ) in equation (4-9) represents the solution for both the flexural displacement u and the torsional rotation ψ, but with different constants. Thus

$$u(\xi) = C_1 + C_2 \xi + C_3 S(\alpha, \xi) + C_4 C(\alpha, \xi) \qquad (4\text{-}12)$$

$$\psi(\xi) = C_5 + C_6 \xi + C_7 S(\alpha, \xi) + C_8 C(\alpha, \xi) \qquad (4\text{-}13)$$

It can be readily verified by substituting equations (4-12) and (4-13) into equation (4-4), that the constants C_7 and C_8 are related to the constants C_3 and C_4 by

$$C_7 = -(\nu/L)\, C_3 + (j\mu\alpha/L)\, C_4 \qquad (4\text{-}14a)$$

$$C_8 = -(\mu\alpha/L)\, C_3 - (\nu/L)\, C_4 \qquad (4\text{-}14b)$$

where

$$\mu = K/(GJ - P r_0^2) \;\; ; \;\; \nu = P L x_\alpha/(GJ - P r_0^2) \qquad (4\text{-}15)$$

The anticlockwise rotation $\theta(\xi)$, the bending moment $M(\xi)$, the shear force $V(\xi)$ and the torque $T(\xi)$ can be obtained by substituting equations (4-12) and (4-13) into the following equations

$$\theta(\xi) = (1/L)\, du/d\xi \qquad (4\text{-}16)$$

$$M(\xi) = -(EI/L^2)\, d^2u/d\xi^2 - (K/L)\, d\psi/d\xi \qquad (4\text{-}17)$$

$$V(\xi) = (EI/L^3)\, d^3u/d\xi^3 + (K/L^2)\, d^2\psi/d\xi^2 + (P/L)\,(du/d\xi - x_\alpha\, d\psi/d\xi) \qquad (4\text{-}18)$$

$$T(\xi) = (GJ/L)\, d\psi/d\xi + (K/L^2)\, d^2u/d\xi^2 - (Pr_0^2/L) d\psi/d\xi + (Px_\alpha/L)\, du/d\xi \qquad (4\text{-}19)$$

The end conditions for displacements and forces are respectively,

$$\text{at end 1 } (\xi = 0) : u = u_1 \;;\; \theta = \theta_1 \text{ and } \psi = \psi_1 \qquad (4\text{-}20a)$$

$$\text{at end 2 } (\xi = 1) : u = u_2 \;;\; \theta = \theta_2 \text{ and } \psi = \psi_2 \qquad (4\text{-}20b)$$

and

$$\text{at end 1 } (\xi = 0) : V = V_1 \;;\; M = M_1 \text{ and } T = -T_1 \qquad (4\text{-}21a)$$

$$\text{at end 2 } (\xi = 1) : V = -V_2 \;;\; M = -M_2 \text{ and } T = T_2 \qquad (4\text{-}21b)$$

Substituting equations (4-20) into equations (4-12), (4-13) and (4-16) and making use of equations (4-14), the end displacements of the column can be related to the constants C_1-C_6 by

$$\begin{bmatrix} u_1 \\ \theta_1 \\ \psi_1 \\ u_2 \\ \theta_2 \\ \psi_2 \end{bmatrix} = \begin{bmatrix} 1 & 0 & 0 & 1 & 0 & 0 \\ 0 & 1/L & \alpha/L & 0 & 0 & 0 \\ 0 & 0 & -\alpha\mu/L & -\nu/L & 1 & 0 \\ 1 & 1 & S_\alpha & C_\alpha & 0 & 0 \\ 0 & 1/L & \alpha C_\alpha/L & -j\alpha S_\alpha/L & 0 & 0 \\ 0 & 0 & h_\alpha/L & k_\alpha/L & 1 & 1 \end{bmatrix} \begin{bmatrix} C_1 \\ C_2 \\ C_3 \\ C_4 \\ C_5 \\ C_6 \end{bmatrix} \quad (4\text{-}22)$$

or

$$U = A\,C \quad (4\text{-}23)$$

where

$$S_\alpha = \sin\alpha \;\; ; \;\; C_\alpha = \cos\alpha \quad for\ \bar{\alpha}^2 > 0 \quad (4\text{-}24a)$$

$$S_\alpha = \sinh\alpha \;\; ; \;\; C_\alpha = \cosh\alpha \quad for\ \bar{\alpha}^2 < 0 \quad (4\text{-}24b)$$

and

$$h_\alpha = -\nu S_\alpha - \alpha\mu C_\alpha \;\; ; \;\; k_\alpha = j\alpha\mu S_\alpha - \nu C_\alpha \quad (4\text{-}25)$$

Substituting the end conditions for forces given by equations (4-21) into equations (4-17)-(4-19) and making use of equations (4-12)-(4-15), the end forces can be related to the unknown constants by

$$\begin{bmatrix} V_1 \\ M_1 \\ T_1 \\ V_2 \\ M_2 \\ T_2 \end{bmatrix} = \begin{bmatrix} 0 & P/L & 0 & 0 & 0 & -Px_\alpha/L \\ 0 & 0 & \alpha\nu K/L^2 & j\alpha^2(EI-\mu K)/L^2 & 0 & -K/L \\ 0 & -Px_\alpha/L & 0 & 0 & 0 & -(GJ-Pr_0^2)/L \\ 0 & -P/L & 0 & 0 & 0 & -Px_\alpha/L \\ 0 & 0 & -f_\alpha/L^2 & -g_\alpha/L^2 & 0 & K/L \\ 0 & Px_\alpha/L & 0 & 0 & 0 & (GJ-Pr_0^2)/L \end{bmatrix} \begin{bmatrix} C_1 \\ C_2 \\ C_3 \\ C_4 \\ C_5 \\ C_6 \end{bmatrix} \quad (4\text{-}26)$$

or

$$F = B\,C \quad (4\text{-}27)$$

where

$$f_\alpha = \alpha\nu K C_\alpha + j\alpha^2 (EI - \mu K) S_\alpha \quad (4\text{-}28a)$$

$$g_\alpha = j\alpha^2 (EI - \mu K) C_\alpha - j\alpha\nu K S_\alpha \quad (4\text{-}28b)$$

Eliminating C from equation (4-27) with the help of equation (4-23) gives

$$F = K\,U \quad (4\text{-}29)$$

or

$$\begin{bmatrix} V_1 \\ M_1 \\ T_1 \\ V_2 \\ M_2 \\ T_2 \end{bmatrix} = \begin{bmatrix} K_{1,1} & K_{1,2} & K_{1,3} & K_{1,4} & K_{1,5} & K_{1,6} \\ & K_{2,2} & K_{2,3} & K_{2,4} & K_{2,5} & K_{2,6} \\ & & K_{3,3} & K_{3,4} & K_{3,5} & K_{3,6} \\ & & & K_{4,4} & K_{4,5} & K_{4,6} \\ & Sym. & & & K_{5,5} & K_{5,6} \\ & & & & & K_{6,6} \end{bmatrix} \begin{bmatrix} u_1 \\ \theta_1 \\ \psi_1 \\ u_2 \\ \theta_2 \\ \psi_2 \end{bmatrix} \qquad (4\text{-}30)$$

where

$$K = B A^{-1} \qquad (4\text{-}31)$$

is the required stiffness matrix.

The stiffness matrix of equation (4-31) is obtained by inverting the A matrix of equations (4-22) and (4-23) and premultiplying by the matrix B of equations (4-26) and (4-27). This can be done numerically or algebraically. However, if explicit analytical expressions for each of the stiffness elements of equation (4-30) are generated by performing the matrix inversion and matrix multiplication steps of equation (4-31) algebraically (or symbolically), a significant saving in computational time can be achieved, as demonstrated by Banerjee and Williams (1992) in their investigation of a related problem. Explicit expressions are particularly useful when some, but not all, of the stiffnesses are needed. So the tedious task of inverting the A matrix algebraically and premultiplying the resulting matrix by the B matrix was undertaken, using the symbolic computing package REDUCE (Fitch, 1985 and Rayna, 1986). The derived expressions are presented in concise form in equations (4-32), as follows

$$\begin{aligned}
K_{1,1} = K_{4,4} = -K_{1,4} &= (EI/L^3)\ \Phi_1/\Delta \\
K_{1,2} = -K_{2,4} &= (EI/L^2)\ \Phi_2/\Delta \\
K_{1,3} = K_{4,6} = -K_{1,6} = -K_{3,4} &= (EI/L^2)\ \Phi_3/\Delta \\
K_{1,5} = -K_{4,5} &= (EI/L^2)\ \Phi_4/\Delta \\
K_{2,2} &= (EI/L)\ \Phi_5/\Delta \\
K_{2,3} = K_{5,6} = -K_{2,6} = -K_{3,5} &= (EI/L)\ \Phi_6/\Delta \\
K_{2,5} &= (EI/L)\ \Phi_7/\Delta \\
K_{3,3} = K_{6,6} = -K_{3,6} &= (GJ/L)\ \Phi_8/\Delta \\
K_{5,5} &= (EI/L)\ \Phi_9/\Delta
\end{aligned} \qquad (4\text{-}32)$$

where

$$\eta = K/EI \quad ; \quad \zeta = 1 - Pr_0^2/GJ \quad ; \quad \varepsilon = x_\alpha/L \tag{4-33}$$

$$\delta = 1 + \varepsilon\nu \quad ; \quad \gamma = \mu + \nu \quad ; \quad \lambda = 1 - \eta\mu \tag{4-34}$$

$$\Delta = \alpha S_\alpha - 2j(1-C_\alpha) \tag{4-35}$$

and

$$\Phi_1 = -b[\alpha S_\alpha + 2j\varepsilon\nu(1-C_\alpha)]$$

$$\Phi_2 = b[\varepsilon\mu\Delta - j\delta(1-C_\alpha)]$$

$$\Phi_3 = b\varepsilon\Delta$$

$$\Phi_4 = b\Delta + \Phi_1 - \Phi_2$$

$$\Phi_5 = \eta\gamma\Delta + \alpha\lambda(\alpha C_\alpha - S_\alpha) \tag{4-36}$$

$$\Phi_6 = \eta\Delta$$

$$\Phi_7 = -\eta\mu\Delta - \alpha\lambda(\alpha - S_\alpha)$$

$$\Phi_8 = \zeta\Delta$$

$$\Phi_9 = \Phi_5 - 2\eta\nu\Delta$$

The geometric coupling term x_α, and/or the material coupling term K, can optionally be substituted by zero in the above stiffness expressions without causing any overflow or under-flow, but the axial load P must not be substituted by zero. If x_α is put to zero in equations (4-32) to (4-36) the remaining matrix represents the exact stiffness matrix of a composite column with no geometric coupling. Similarly, if K is put to zero in equations (4-32) to (4-36) the resulting matrix represents the exact stiffness matrix of a metallic column with geometric coupling only. Nevertheless, separate sets of stiffness expressions for $P = 0$, $K = 0$ and $x_\alpha = 0$ are given by Banerjee, Eslimy-Isfahany and Williams (in progress).

The determination of the elastic critical buckling load of a single composite column, or of a structure assembled from such columns, follows from the application of the Wittrick-Williams algorithm (1971), either to the single exact stiffness matrix of the column or to the overall stiffness matrix assembled from such columns, respectively. The same principle applies when calculating the elastic critical buckling load of metallic columns. The Wittrick-Williams algorithm is briefly explained in ***Chapter Five***, and, a more detailed description of the application of this algorithm for the determination of the buckling loads of composite or metallic columns is given by Banerjee, Eslimy-Isfahany and Williams (in progress).

4.4. Experiment

An experimental programme consisting of several specimens has been undertaken. The main purpose is to observe the buckling behaviour of laminated flat composite columns and then to verify it with the theoretical predictions. Special attention has been focused on the bending-torsion coupling effect, which plays a dominant role in the buckling behaviour of composite columns.

Instrumentation : The Euler or long column tests are performed using the INSTRON-2000 testing machine. Rigs are specifically designed and developed, and the set up of the testing machine is altered for this investigation. The altered testing frame can easily accommodate all the required end conditions. Figures 4-2(a) to 4-2(g) show a schematic diagram of the testing frame and six photos of the experimental set up in various test conditions.

Calibration : Before every set of tests, calibration checks were performed carefully according to the INSTRON manufacturer's manual. Moreover, some of the experimental results of the INSTRON-2000 were compared with the results measured from the INSTRON-1112. An excellent agreement was found.

Specimens : Rectangular specimens are cut from a unidirectional plate made of carbon-epoxy material of which the mechanical and other properties are given in Figure 4-3. Altogether fourteen specimens are tested, each of which is *0.27 (m)* long, *0.035 (m)* wide and *0.002 (m)* thick. Ply angles chosen are respectively *0*, *5*, *10*, *15*, *20*, *30*, *40*, *45*, *60*, *75* and *90* deg. There are more specimens made in the range of *0* to *45* deg because of the nature and magnitude of rigidities of the column within that range. For example, there are two specimens cut at *0* deg due to the appearance of an unexpected peak around *5* deg in the preliminary test. There are also three specimens cut at *20* deg because the bending-torsion coupling rigidity is at its maximum around this ply angle. Testing more than one specimen at *0* and *20* deg is expected to rectify some uncertainties in the measurement procedure, ensuring reproducibility of the experimental results.

Testing procedure : Each specimen is set on the INSTRON-2000 testing machine. The specimen is very carefully set in the testing machine so that the centroidal axis of the specimen coincided with the applied loading axis. The centres of the two compressive

heads are selected as references to determine the loading axis. The geometric centre axis of the specimen is calculated by using the nominal dimensions of the specimen. Adjustments are made so that the two axes meet together for various boundary conditions.

The loading process is conducted using stroke control. The stroke rates are set to be 1 mm/min. Unidirectional compression is applied monotonically on the specimen until the ultimate load is reached. This is reached when the mid-span of the column deflects horizontally whilst the top-end deflects vertically with no further increase in the externally applied axial load. For each specimen, the horizontal deflection of the mid-span and the vertical deflection of the top-end are measured against the applied load. To eliminate random errors, the same procedure is carried out for the specimen turned up side down and the average of the two results is recorded. The procedure is repeated for different end conditions with the same specimen.

In order to validate the test technique the above procedure was followed to measure the buckling load of a metallic specimen made of Duralumin. The procedure produced satisfactory results. It is notable that, although this was a case for a torsion free buckling, to some extent it can provide reasonable certainty in the results.

Southwell's technique : Euler's theory assumes an initially straight column with no eccentricity or imperfections such as initial crookedness, as does the Timoshenko theory for bending-torsion coupled columns (Timoshenko and Gere, 1961; Popov, 1976). Agreement between the critical load obtained in laboratory experiments and the critical load determined by Euler's analysis is a somewhat fortuitous occurrence and is expected only in the case of perfect columns (Barbero and Tomblin, 1993).

Southwell (1932 and 1941) accounted for both manufacturing irregularities and unavoidable loading eccentricities by using a data reduction technique on the hyperbolic experimental data. In Southwell's method, the critical load is determined by using the asymptote of the experimental measurements. The method is attractive because it does not require that the critical load be reached. It is, thus, non destructive, and also it properly accounts for imperfections in the column or the testing fixture. Southwell's method was extended to account for transverse lateral loads (Fisher, 1934) and extreme eccentricities

(Tsai, 1986). The method works well when there is no modal interaction and the imperfections have a strong component of the form of the buckling mode. Therefore, the method is ideal for composite materials that remain linear for large values of strains. Thus experimental results can be expected to behave in a manner similar to Southwell's tests.

Load versus lateral deflection of the mid-span is recorded, and if the buckling mode is isolated, the data show a hyperbolic shape. The raw data are transformed in order to obtain the asymptote of the hyperbola from a linear regression of the transformed data. Firstly, the load versus lateral deflection graph (P-δ) is plotted. This plot is subsequently converted into a graph showing variation of the ratio of lateral deflection to axial load against lateral deflection (δ/P-δ). This transforms a rectangular hyperbola in the former into a straight line in the latter with a slope $1/P_{cr}$, where P_{cr} is the critical buckling load (Gregory, 1967).

All measurements are taken from a central point with respect to the column length. However, as shown by Tomblin (1991), any point along the length can be used to measure the deflections. Furthermore, Tsai (1986) noted that enough data points must be collected in the linear range of the material to obtain good regression, thus limiting the applicability of the method for the case of almost perfect metal columns. As was mentioned earlier, Barbero and Tomblin (1993) are among those who recently used Southwell's technique to determine elastic buckling load in composite columns.

Errors in experimentation : Every measurement involves an error. The nature of these errors may vary, as may their magnitudes, but total elimination of errors for experimentation and testing remains beyond human power (Penny 1974). Because errors cannot be completely avoided, one must learn to assess their magnitudes so as to be able to control them according to justified needs. In order to achieve accurate and precise experimental results, all the potential sources of errors have been considered in designing and planning the experiment. Generally, in error analysis, the word accuracy is reserved for systematic errors, whereas the word precision is related to all incidental random errors (Penny 1974). Systematic errors, such as method errors, instrument errors, calibration errors, can be detected and prevented. Random errors, such as variation of condition, can also be accounted for by using statistical methods.

Experimental observations : In relation to the particular specimen tested, the following points are relevant :

(i) As the load approaches P_{cr} , the lateral deflection is found to be around *L/40* (L being the column length). If any extra load is applied, the centre deflection is observed to be very large, leading to a complete column failure.

(ii) If all centre deflections are kept at or below L/100, it is evident that the tests are entirely non-destructive. Note also that after each test, the central deflection of the column returned to its unloaded position.

(iii) For all the boundary conditions imposed, bending-torsion coupling is evident, especially when the coupling rigidity is high. The buckling mode is a combination of flexural and torsional modes, except for the ply angles *0* and *90* deg for which the buckling is purely flexural.

4.5. Results and discussions

Metallic columns : The first two examples given are for metallic columns of singly-symmetric cross-section (Goland, 1945 and Banerjee and Fisher, 1992), whose mechanical properties are given in Table 4-1. The critical elastic buckling loads were calculated for all sets of standard classical end conditions for both columns and are presented in Table 4-2.

These results were then compared with those given by Akesson (1980). He proposed the following equation which represents the non-dimensionalised exact expression of the critical elastic buckling load of an individual column with classical end conditions, when coupling exists between bending and torsional deformations (Akesson, 1980)

$$P_{y\theta} = \frac{P_y + P_\theta}{2\left(1-\frac{x_\alpha^2}{r_0^2}\right)}\left[1-\left\{1-\frac{4P_y\,P_\theta}{(P_y+P_\theta)^2}\left(1-\frac{x_\alpha^2}{r_0^2}\right)\right\}^{0.5}\right] \qquad (4\text{-}37)$$

where

$$P_y = \frac{\pi^2 EI}{\lambda^2 L^2} \quad \text{and} \quad P_\theta = \frac{GJ}{r_o^2} \tag{4-38}$$

with λ = 2, 1, 0.6992 and 0.5 for clamped-free (C-F), (S-S), (C-S) and (C-C) end conditions, respectively. The results for both columns are shown in Table 4-2. These results agree completely with the results obtained using Akesson's (1980) theory.

Composite columns : There are three illustrative examples of composite columns presented in this section. In the first illustrative example, the critical elastic buckling load is determined experimentally and then compared with those obtained from the present method. The other two, are based on theoretical investigation and are taken from existing literature.

(i) The composite column shown in Figure 4-3 and described in ***Section 4-4***, is studied here. (S-S), (C-S) and (C-C) end conditions are considered. For this composite column, two sets of material properties are given by Jensen et al. (1982), namely, flexural and axial values (see Figure 4-3). The present theory was used to calculate the buckling loads using both sets of material properties. Obviously, values for material properties obtained from tensile test, give higher sets of buckling load than the ones obtained when using results of flexural tests. As was explained in ***Section 4-4***, experiments were carried out to determine the buckling load of the composite column for different ply angles.

Experimental and theoretical results for the buckling load of the composite column with three different end conditions are given in Figure 4-4. Testing two specimens at *0* deg and three at *20* deg were intended to rectify some of the uncertainties in the measurement procedure. For *0* deg ply angle, the maximum difference between results from the two specimens is around 5 percent, and the difference between results from the three specimens at *20* deg is less than 6 percent, ensuring reproducibility of the experimental results.

Generally, experimental results show a trend similar to that predicted by theory. Apart from a very small range of ply angles, the experimental results are usually between the two sets of theoretical results, namely, flexural and axial values. When the ply angle is around five degrees there is an unexpected peak in the results. This may be because the

experimental set up did not match exactly what is assumed in the theoretical model particularly in relation to the end conditions. In the experiment both ends were restrained from any lateral movement, whereas this was not taken into account in the theory. Furthermore, the Poisson's ratio effect is not considered in the theory, whereas it will affect experimental results.

(ii) A flat rectangular composite column examined by Jensen et al. (1982) is further investigated here. Structural properties of this column are given in Figure 3-1a and the variation of the flexural, torsional and coupling rigidities against ply angle is shown in Figure 3-1b.

Using the present method the buckling load is calculated for the composite column for four different classical boundary conditions, namely with (C-F), (S-S), (C-S) and (C-C) end conditions. Figure 4-5 shows the variation of the buckling load of the column against ply angle for different end condition.

In all cases, the buckling load decreases when the ply angle increases as expected. Among the different boundary conditions, for any given ply angle, the buckling load is progressively higher for (C-F), (S-S), (C-S) and (C-C) case, respectively. The fifth curve in Figure 4-5, gives the results for (S-S) case, obtained from an established computer program VICONOPT (Williams et al., 1990). The results show a similar trend and agree very well with the present theory.

For the same composite column with (S-S) end conditions, the buckling load is calculated and compared, using three different methods in order to gain further insights. The three methods are : (i) the present theory, (ii) the laminated plate theory (Jaunky et al., 1995a and 1995b) and the use of an established computer program VICONOPT (Williams et al., 1990). Results given in Table 4-3, show very good agreement among the three different methods for different ply angle, but, the present theory provides a more conservative estimate than other methods, providing a greater margin of safety in design.

Similar observations were made when the effect of the bending-torsion coupling parameter (see equation 3-1) on the buckling load of the composite column was studied. Figure 4-6

shows the effect of the bending-torsion coupling parameter on the non-dimensional buckling load of the composite column for different end conditions.

(iii) The third example is a rectangular box column made of Carbon Fibre Reinforced Plastic (CFRP) which was previously investigated by Shield and Morey (1997). Material and cross-sectional properties of the rectangular box column are given in Figure 4-7.

The buckling load is calculated using three different methods : those given by Shield and Morey (1997) [*S-M*], Rehfield and Atilgan (1989) [*R-A*] and the well-known Bernoulli-Euler theory (uncoupled theory) [*B-E*] for the composite column with (S-S) end conditions. The results are shown in Figure 4-8. For the same boundary condition, the critical elastic buckling load of the composite beam is also calculated using the present theory and shown in Figure 4-8. Rigidity properties of the column are calculated from both Rehfield simplified formula (1990) [*P-R*], and Armanios general formula (1995) [*P-A*], when applying the present theory. As can be seen in Figure 4-8, the present theory generally provides a more conservative estimate of the elastic buckling load.

4.6. Summary

The theoretical and experimental results show the same trend. However, there are certain small discrepancies in the results. This can be either because of the presence of the bending-torsion coupling or due to an incompatibility between theoretical and experimental modelling, especially around the boundary of the specimen. Further investigation is needed to revise the experimental model.

The method of Berdichevsky, Armanios, and Badir (1992) for composite beam modelling was examined. They used the variational-asymptotical analysis where the displacements and stresses are integrated around the cross-section and as a consequence the cross-section is analysed as a unit regardless of its shape. All in all, the present study shows that the chosen composite beam modelling is a satisfactory model and can be used for buckling and vibration analysis of laminate composites.

Table 4-1. Mechanical properties of bending-torsion coupled columns.

	Goland (1945)	Banerjee and Fisher (1992)
EI (Nm^2)	9.75×10^6	6380
GJ (Nm^2)	9.88×10^5	43.46
r_0^2 (m^2)	0.242	0.0245
L (m)	6.0	0.0155
x_α (m)	0.18	0.82

Table 4-2. Critical elastic buckling load of bending-torsion coupled columns.

		Pcr (N)	
		Goland wing (1945)	Banerjee and Fisher beam (1992)
		Akesson (1980) & Present theory	Akesson (1980) & Present theory
λ=2	C-F	6.5168×10^5	20261
λ=1	S-S	2.2845×10^6	49786
λ=0.7	C-S	3.3631×10^6	60999
λ=0.5	C-C	3.8018×10^6	66632

Table 4-3. Critical buckling load of a bending-torsion coupled composite column.

	Pcr (N)		
β (deg)	Present theory	VICONOPT	Jaunky et al.(1995, 1997)
0	34.36	34.39	34.38
10	29.79	31.58	31.11
20	20.92	23.78	23.14
25	16.82	19.25	18.77
30	13.35	15.17	14.87
45	7.104	7.586	7.526

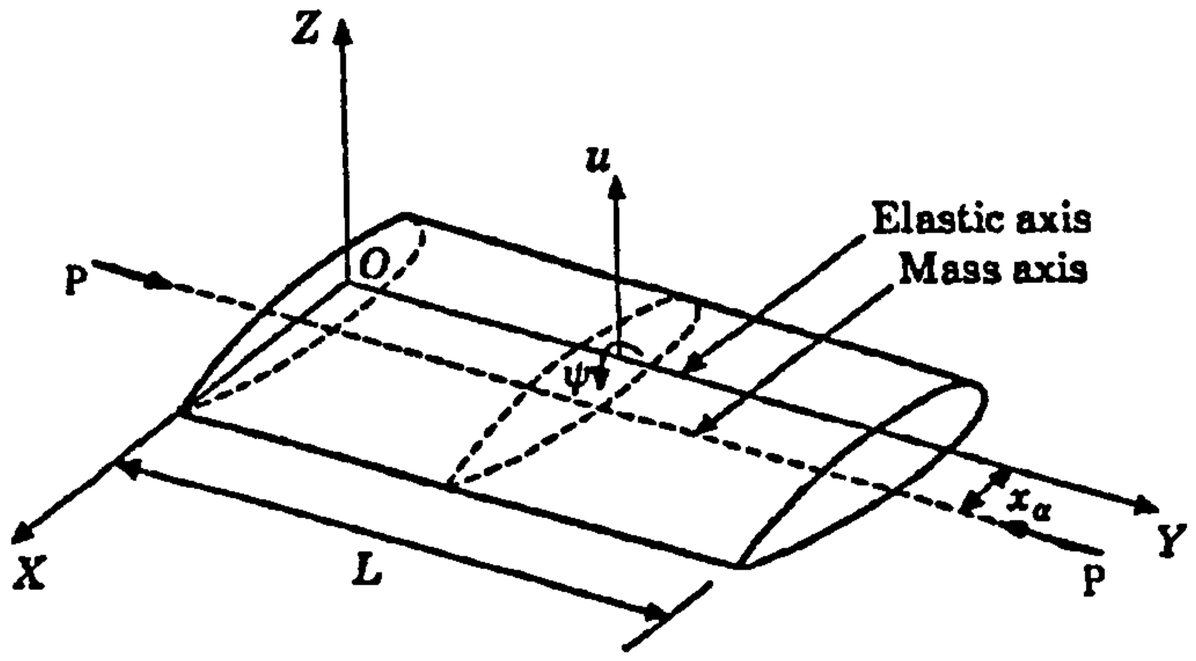

Figure 4-1. Coordinate system and notation for bending-torsion coupled buckling of composite columns.

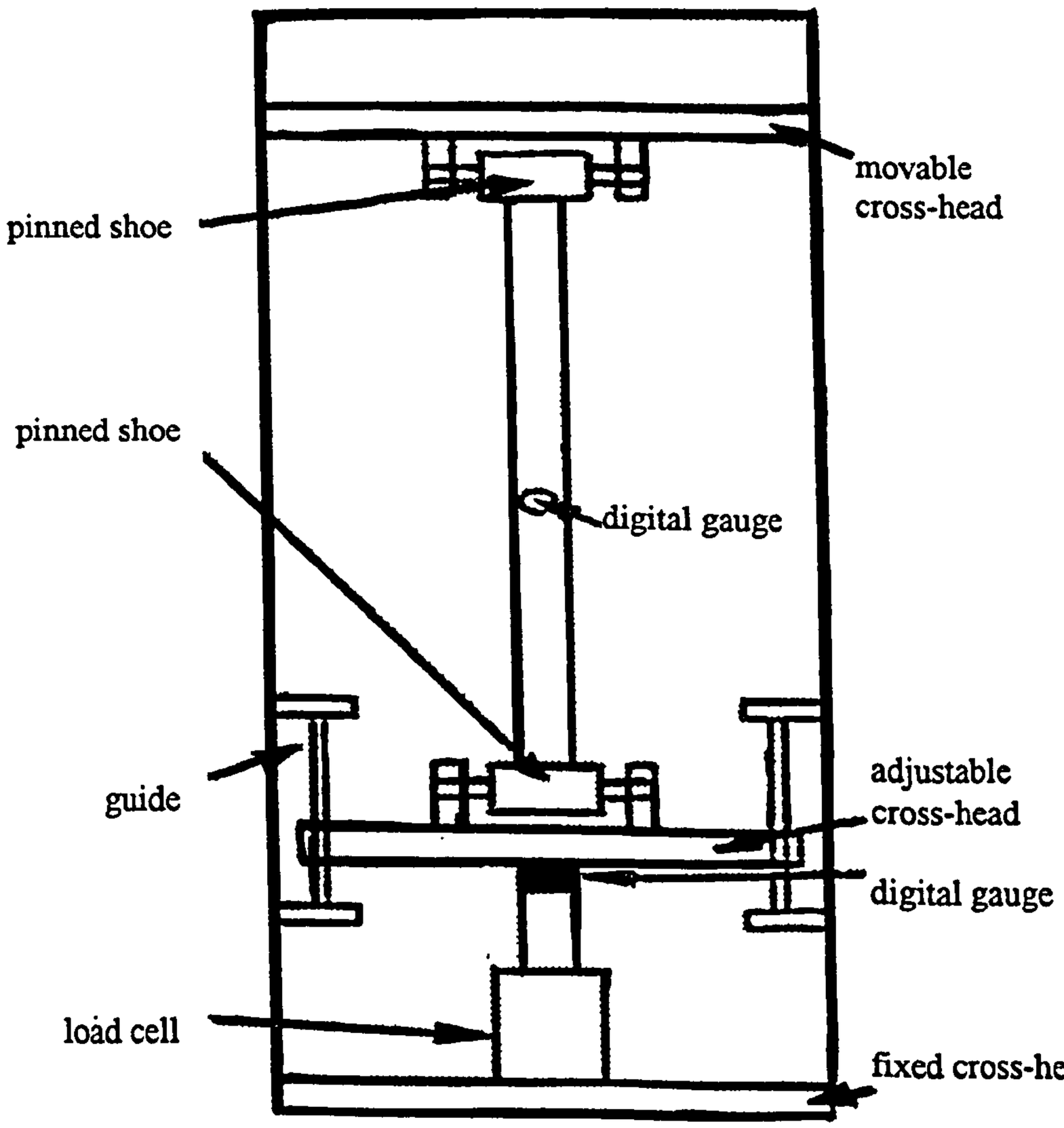

Figure 4-2(a). Schematic diagram of the testing frame with specimen mounted.

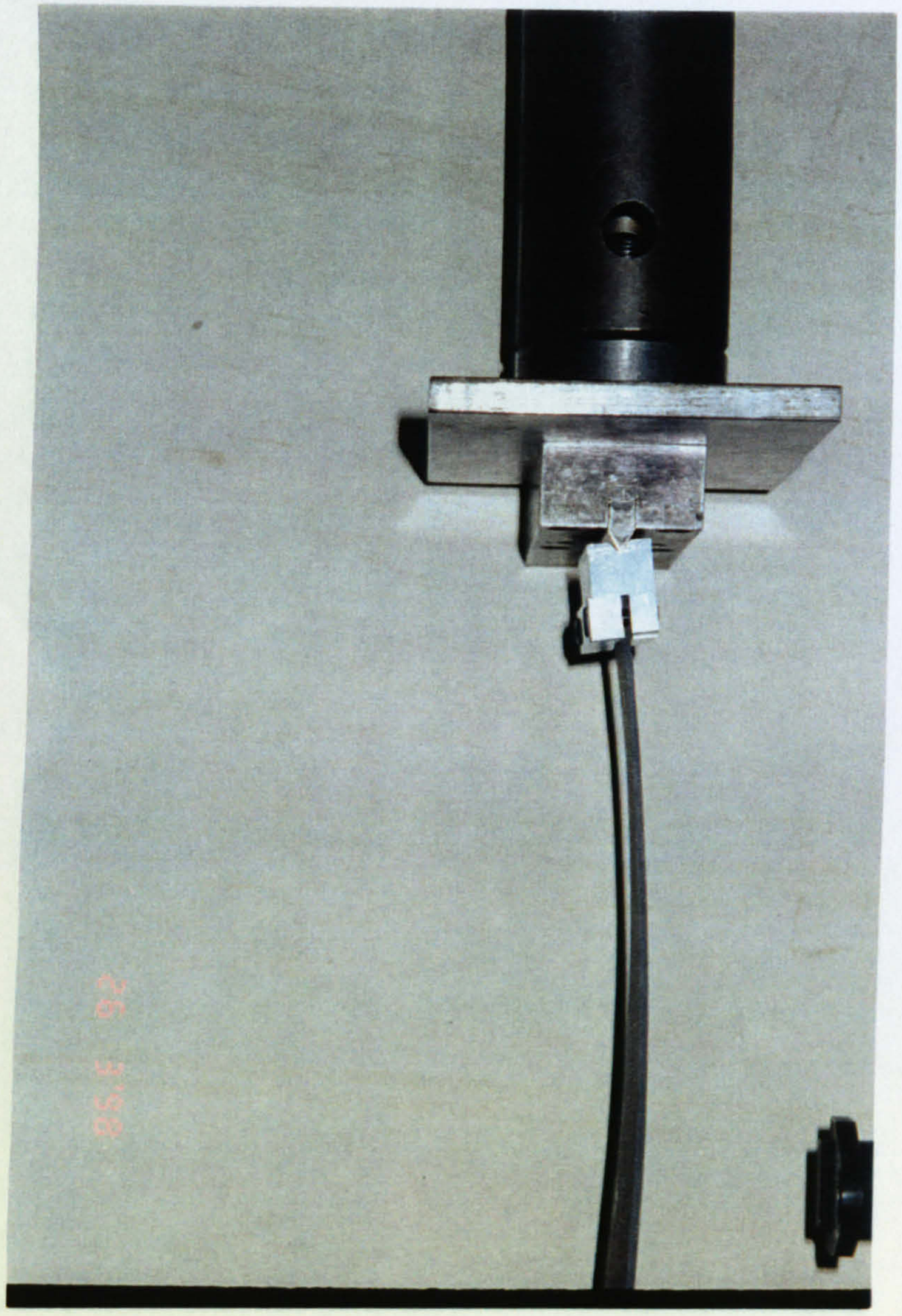

Figure 4-2(b) Experimental set-up showing Simple support (S) end condition.

Figure 4-2(c) Experimental set-up showing Clamped (C) end condition.

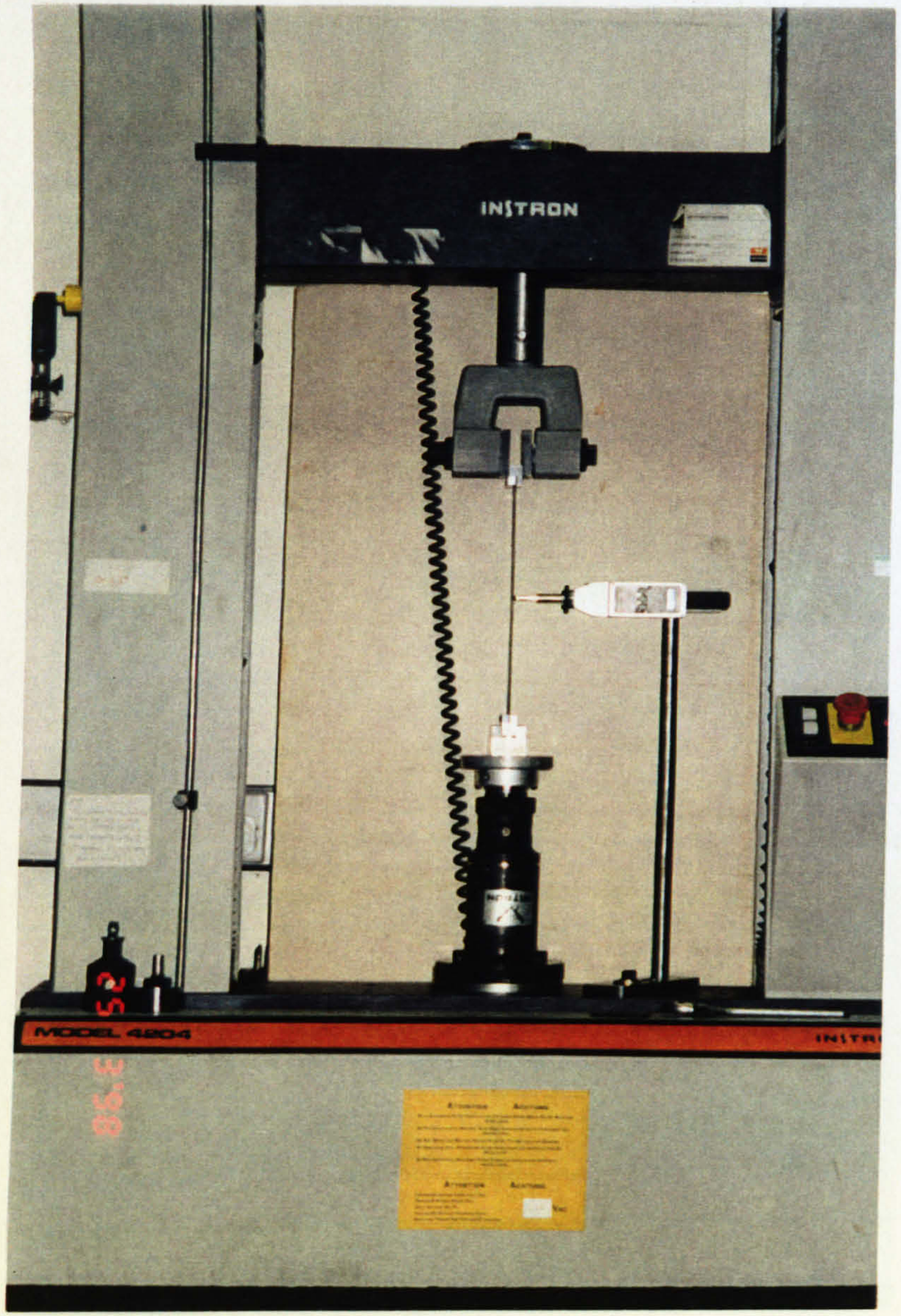

Figure 4-2(d) C-C set up: unloaded case for β = 10 deg.

Figure 4-2(e) C-C set up during loading for β = 10 deg.

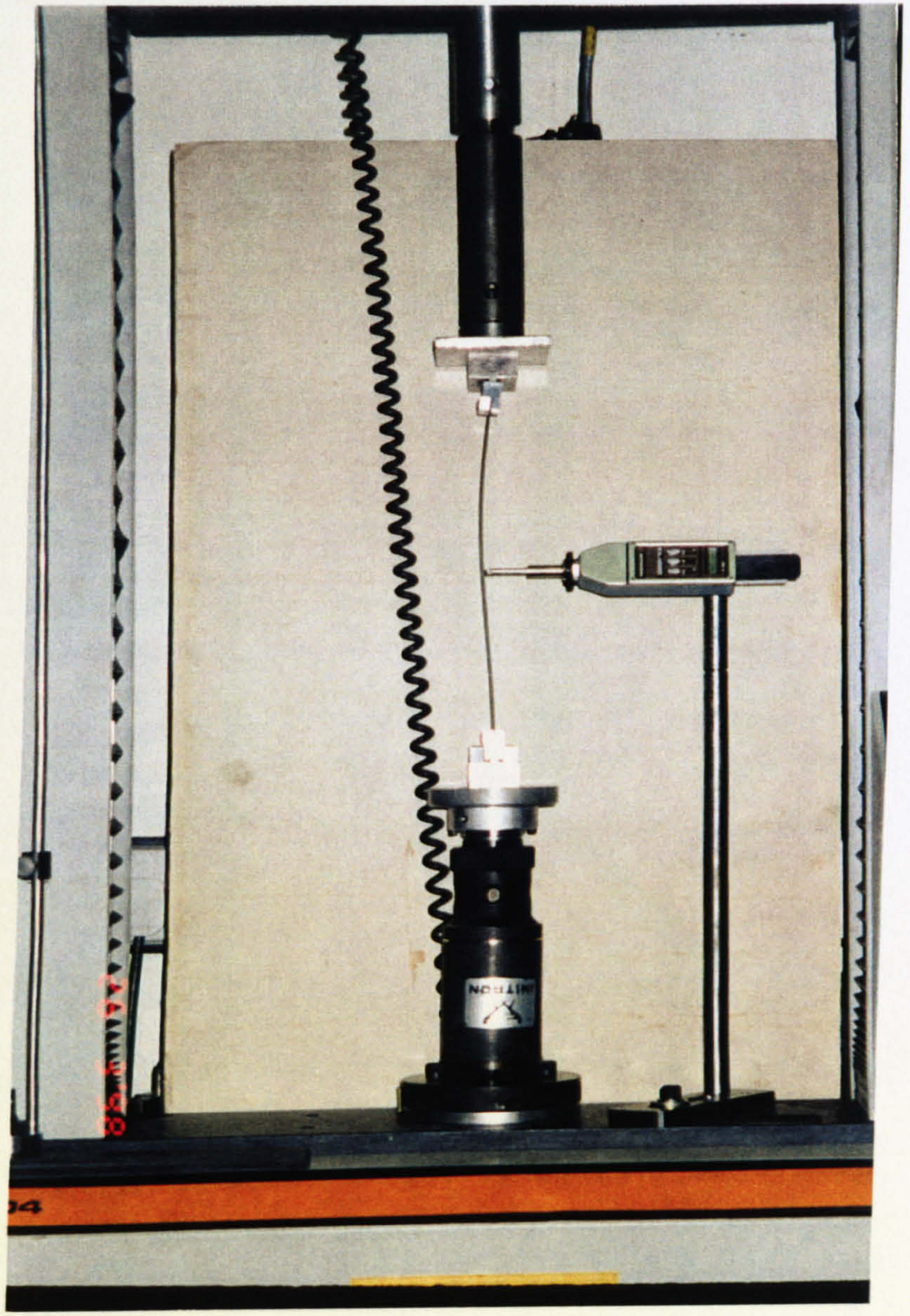

Figure 4-2(f) C-S set up during loading for $\beta = 0$ deg.

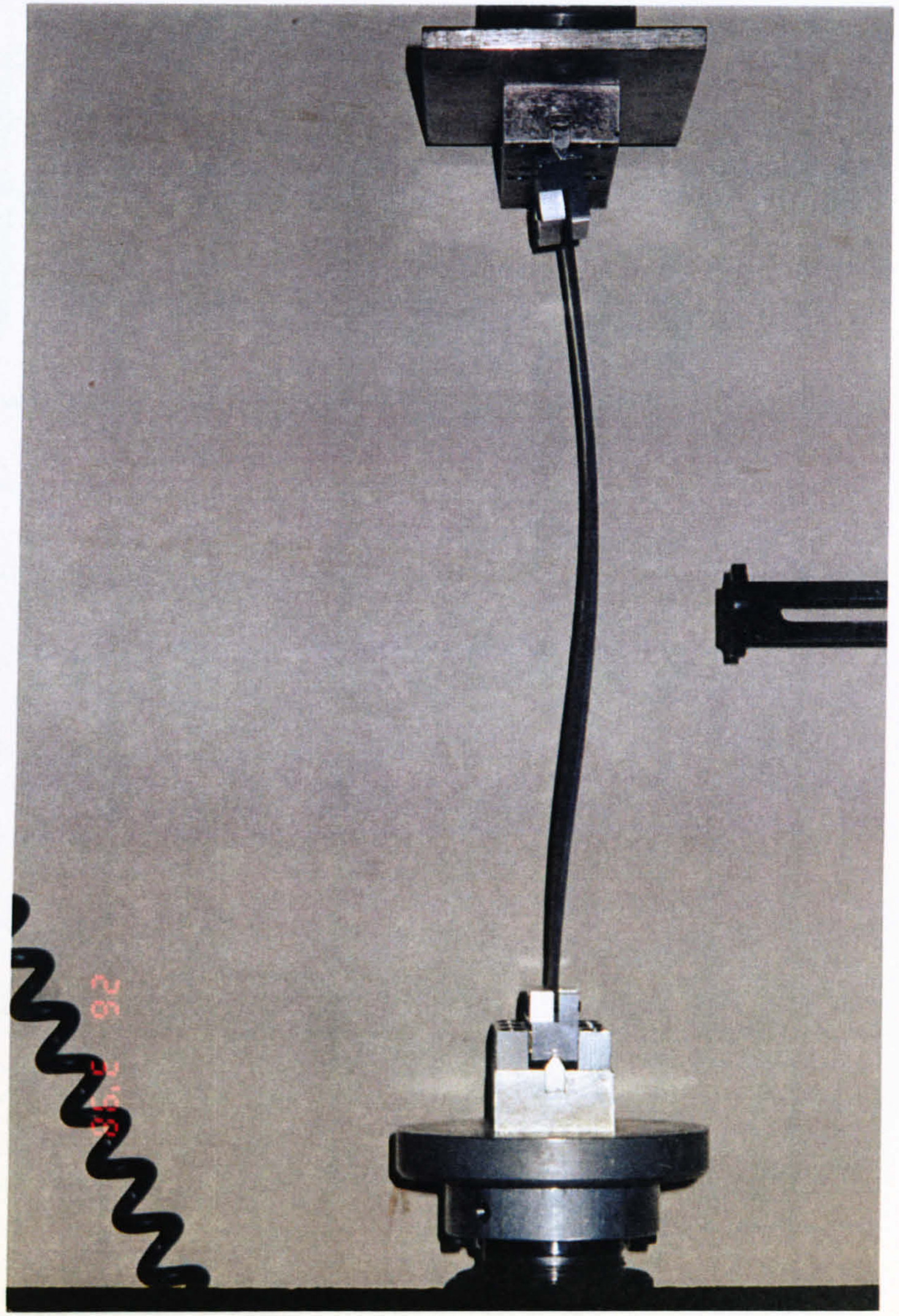

Figure 4-2(g) C-S set up during loading for $\beta = 20$ deg.

	flexural values	extentional values
E_1 (GPa)	98.0	130
E_2 (GPa)	7.9	10.5
$G_{12} = G_{13} = G_{23}$ (GPa)	5.6	6.0
ν_{12}	0.28	0.28
Density (kg/m^3)	1520	1520

ply angle β (deg)	0	5	10	15	20	30	40	45	60	75	90
Number of specimen	2	1	1	1	3	1	1	1	1	1	1

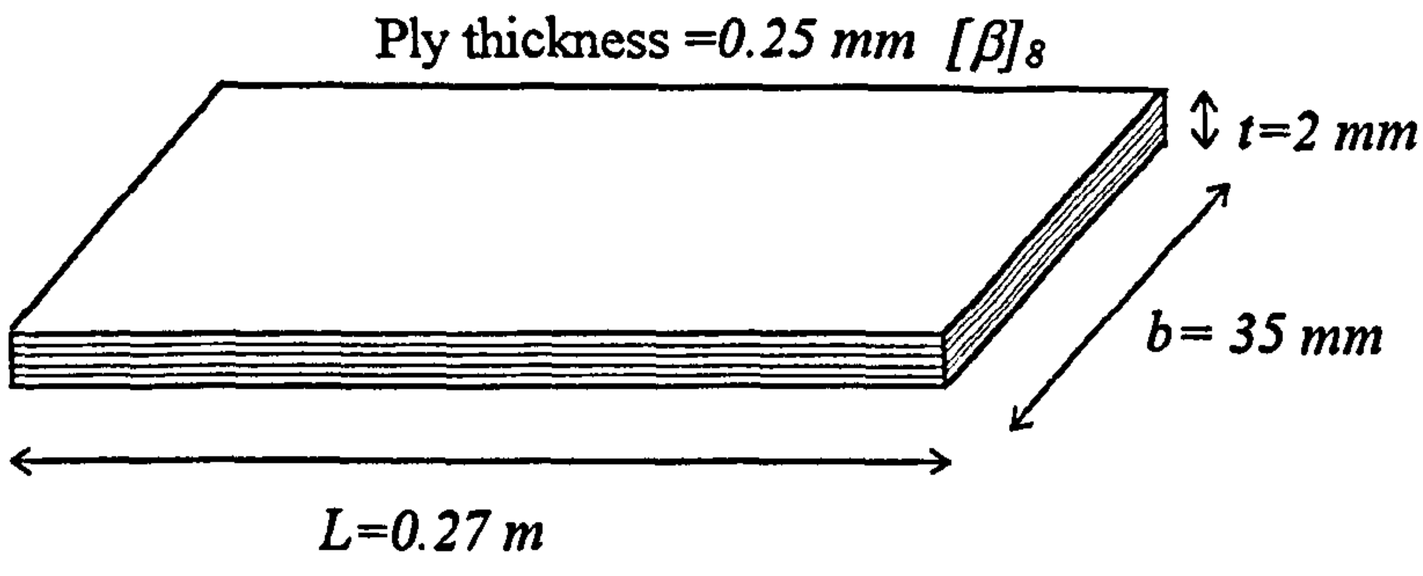

Figure 4-3. Mechanical properties (Jensen et. al., 1982) and configuration of the laminated flat composite column used in the experiment.

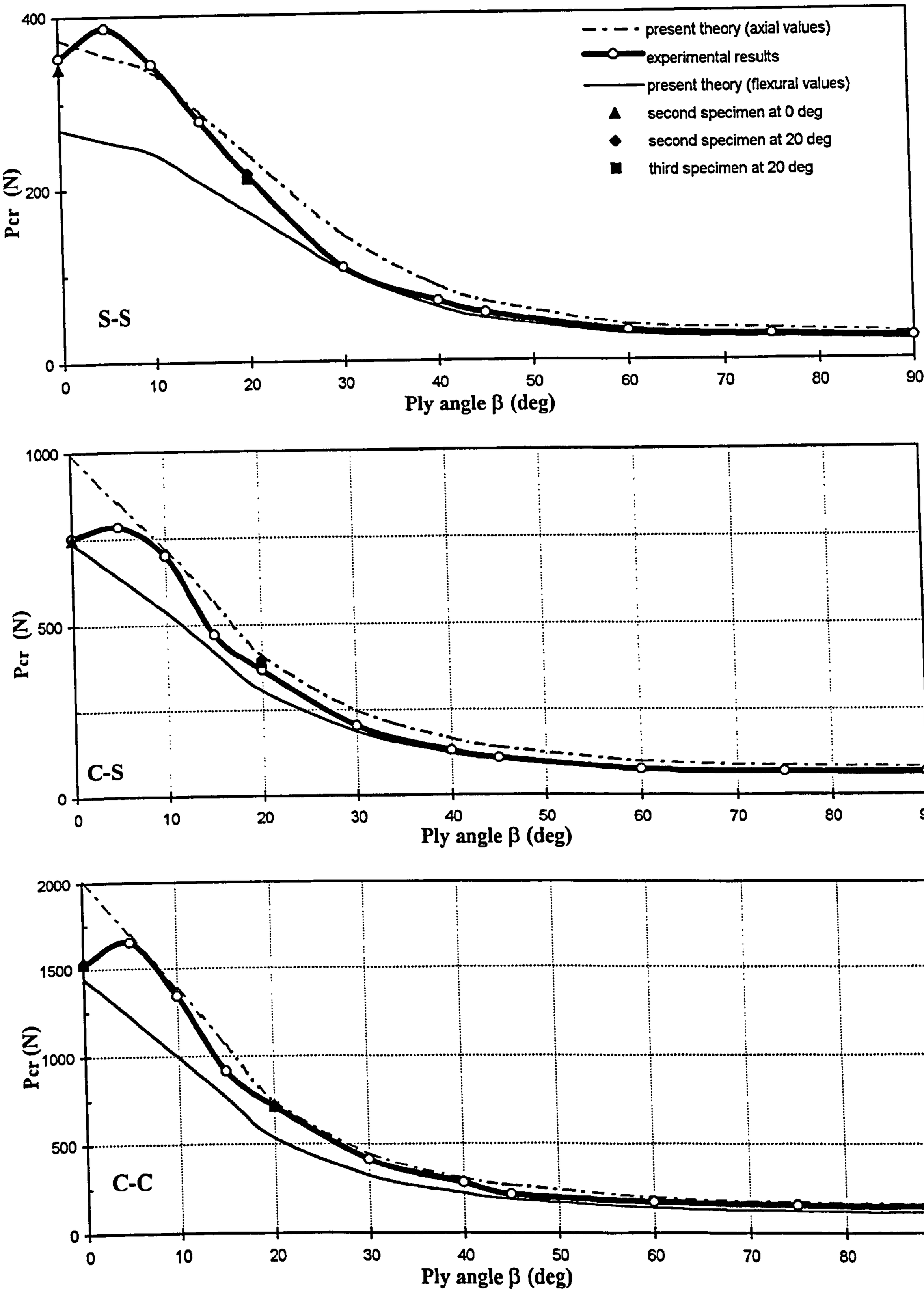

Figure 4-4. Variation of the buckling load against ply angle for the composite column shown in Figure 4-3 a comparison between experimental results and the present theory.

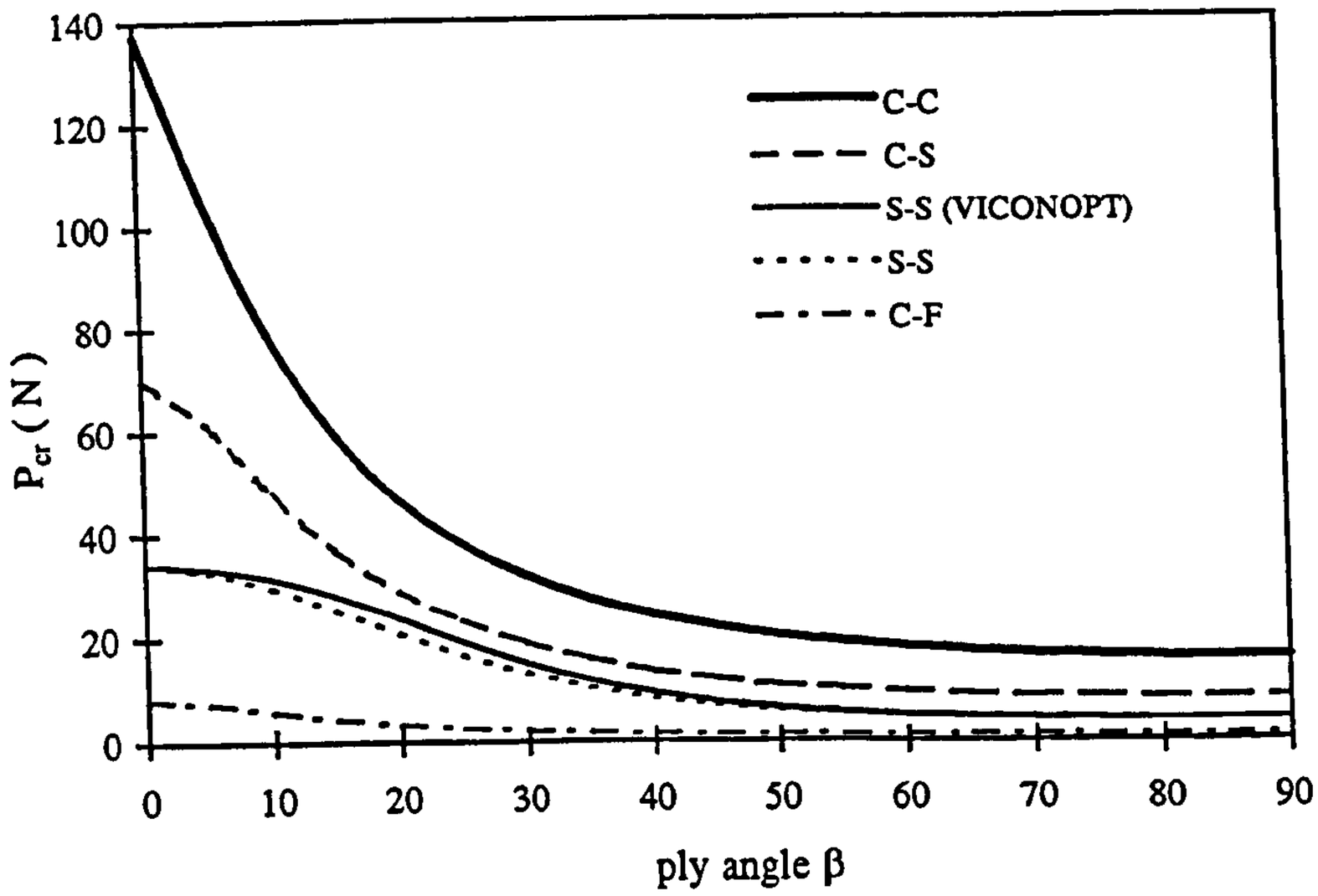

Figure 4-5. Effect of ply angles on the buckling load of a composite column (Jensen et al., 1982) with different end conditions.

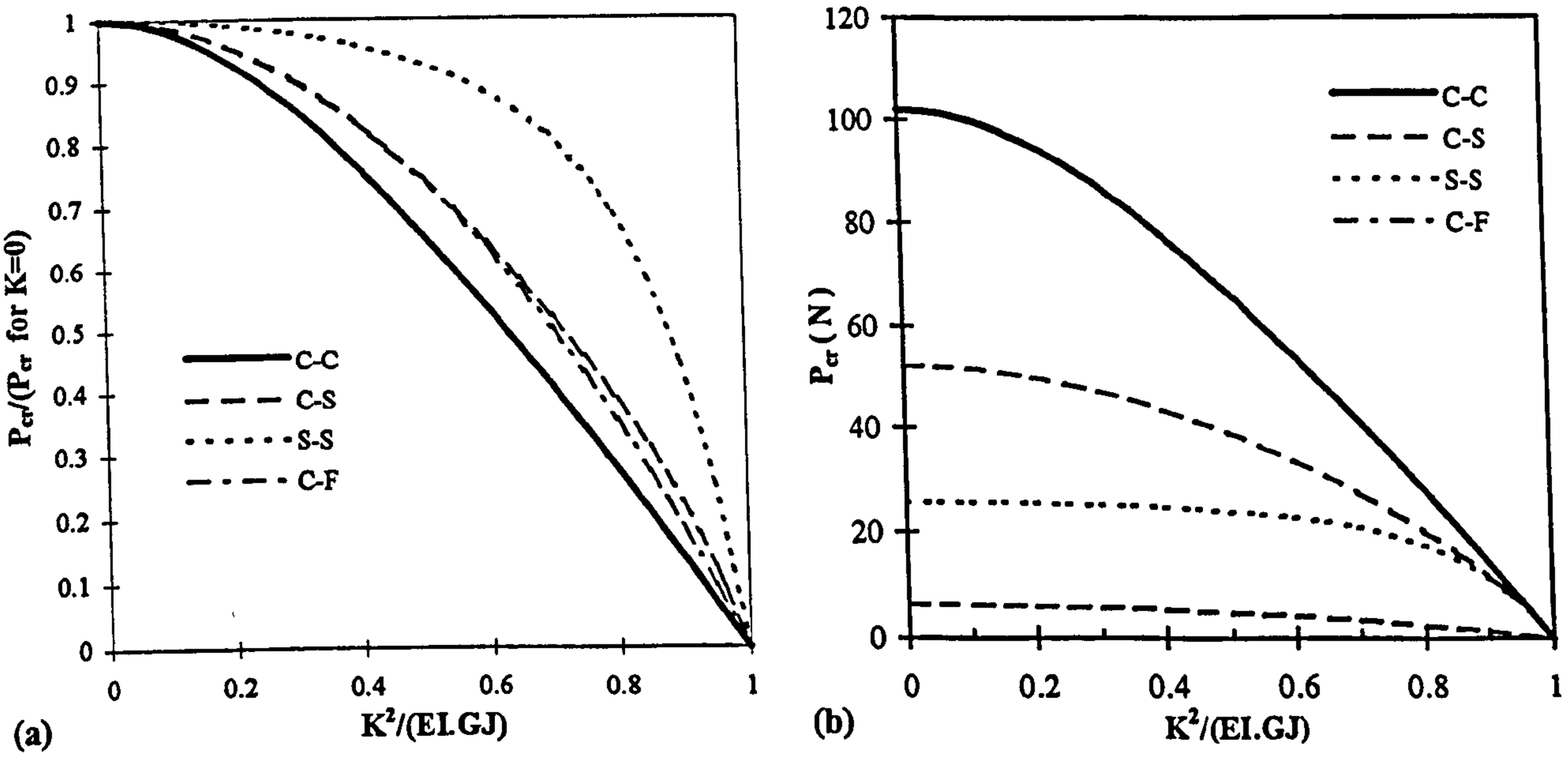

Figure 4-6. Effect of bending-torsion coupling parameter on
(a) the non-dimensional buckling load, (b) elastic critical buckling load
of a composite column (Jensen et al., 1982) with different end conditions.

$E_1 = 138\ GPa$
$E_2 = 8.96\ GPa$
$G_{12} = 7.10\ GPa$
$G_{13} = G_{23} = 2.37\ GPa$

$\nu_{tl} = 0.3$
$Ply\ thickness = 0.003125\ m\ \ [\beta]_8$
$L = 5.0\ m$

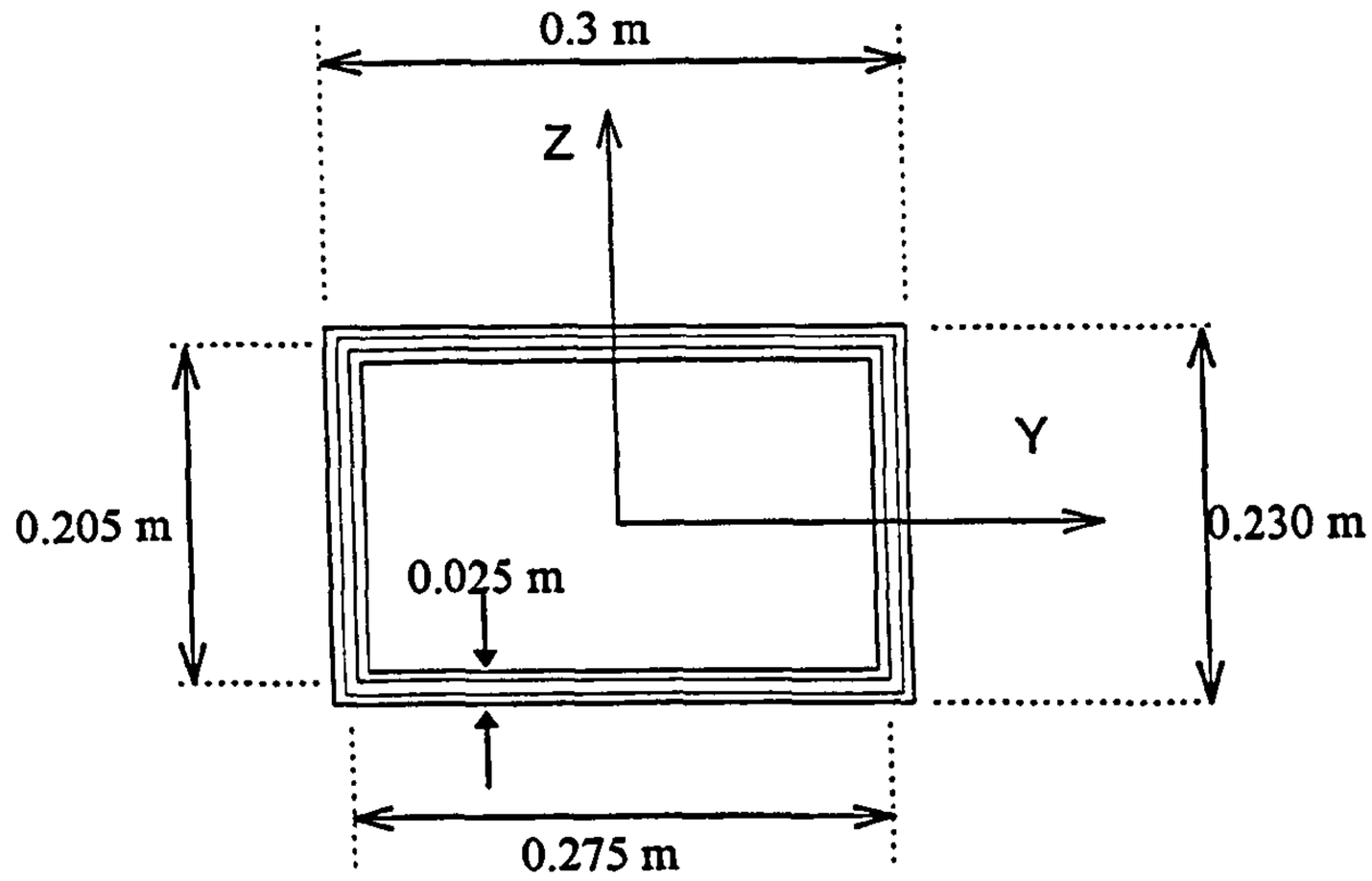

Figure 4-7 Configuration of the laminated box column (Shield and Morey, 1997).

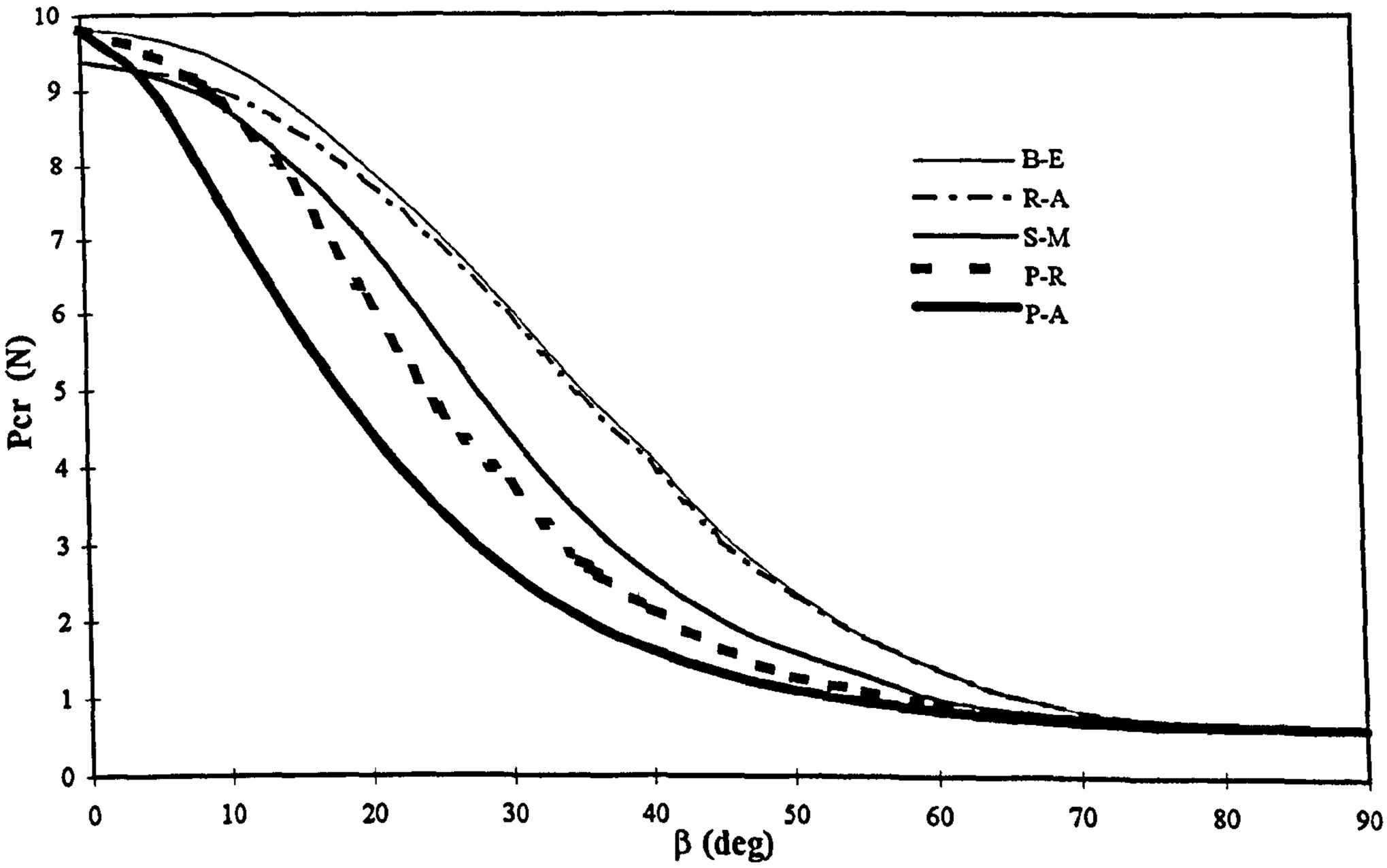

Figure 4-8. Variation of elastic buckling load of a composite box column (Shield and Morey, 19
with ply angle; a comparison between different buckling theories for composite c

Chapter Five

Dynamic stiffness method

5 Dynamic stiffness method

5.1. Introduction

Prediction of the dynamic behaviour of physical systems plays an important role in modern day engineering and analysis of free vibratory motion of a mechanical system is a stepping stone in structural dynamics. In this chapter, after a brief description of various discrete and approximate methods, the choice of the dynamic stiffness matrix method is made for the determination of bending-torsion coupled natural frequencies and mode shapes of thin-walled composite beams, with particular reference to the Wittrick-Williams algorithm. Spatial discretisation errors are eliminated in this method, to give an exact solution in a classical sense. This technique is fairly general and widely used in various dynamic problems.

5.2. A review of solution techniques for free vibration problems

Approximate methods (Rayleigh, 1945) and exact modal solutions for free vibration problems have been produced by many authors (Goland, 1945 and Timoshenko and Young, 1955), for simple boundary conditions. Approximate solutions have also been tried, making use of discretisation by either the lumped mass method (Hurty and Rubinstein, 1964) or by assumed deformation shapes, such as the Rayleigh Ritz method (Bisplinghoff, Ashley, and Halfman, 1955), the Galerkin method (Fung, 1969 and Rao, and Carnegie 1970) and of course, the finite element method (Mei, 1970) have been investigated. Additional works based on approximate methods are, amongst others, by Engelbrecht (1951) and Stacey (1976). Most of the aforementioned methods are applicable to single span beams (i.e. beams supported only at the ends), except the lumped mass method (Hurty and Rubinstein, 1964).

The finite element method is widely used for the vibration and stability analyses of structures including thin-walled beams and columns. In a free vibration analysis, the finite element method results in a set of algebraic equations whose solutions have become standard. However, since the vibrating shape of a structural member varies with the frequency of vibration, the finite element method which is based on frequency independent

shape functions requires subdivision of a thin-walled beam into many elements for reasonably accurate solutions. Alternatively, if the shape functions are frequency dependent, then the subdivision becomes unnecessary. One may use the Kantorovich method and obtain a set of ordinary differential equations (when the time variable is eliminated for harmonic oscillation). In conjunction with the natural boundary conditions, the solutions of the ordinary differential equations give the dynamic stiffness matrix. The major advantage of this method is that it can be used for the determination of an unlimited number of frequencies, and a single element can successfully determine any number of natural frequencies for a structure without any loss of accuracy. Naturally, the dynamic stiffness method involves fewer assumptions and therefore is more accurate.

The dynamic stiffness matrix method used to solve free or forced vibration problems of structures (or structural elements) has received wide attention in recent years and is often referred to as an exact method. A dynamic stiffness matrix is made by frequency dependent shape functions, which are exact solutions of the governing differential equations, and it accounts for both mass/inertia and stiffness properties. Predictably the method provides the analyst with much better model accuracy when compared to finite element or other approximate methods. The usefulness of the method becomes apparent when higher frequencies and better accuracy of results are required. Generally, the dynamic stiffness matrix method enables one to model an infinite number of natural modes by means of a small number of unknowns and it eliminates spatial discretisation errors too. Substantial saving in computer time can be achieved if explicit analytical expressions for the elements of the dynamic stiffness matrix are used instead of numerical methods. Such expressions can be derived with the help of symbolic computation. This method has been applied with success to many dynamic problems including natural vibration and response analysis.

Friberg (1985) solved the Vlasov equations (1959) analytically and formed the exact dynamic stiffness matrix for metallic beams without the assumption of cross-sectional symmetry of the beam. He presented a procedure in FORTRAN to generate the dynamic stiffness of a thin-walled beam using complex arithmetics. Leung (1992a, 1992b) extended the application to lateral buckling. The essential differences from Friberg's study

were as follows: (i) the characteristic polynomial was expanded explicitly; (ii) the characteristic roots were proved to be either real or purely imaginary: (iii) there were only six distinct characteristic vectors associated with the differential equations; (iv) all characteristic vectors were real; and (v) the in-plane moment was included.

Banerjee and Williams (1985, 1992, 1994a and 1994c), Banerjee (1989), Leung and Zhou (1995a, 1995b) and Banerjee and Fisher (1992) have developed dynamic stiffness matrices of different types of beam elements, starting from the basic governing differential equations of motion and has applied them to free vibration analysis of space structures (Banerjee and Williams, 1983; 1984). The method has been successfully used for coupled flexural-torsional vibration of beams (Banerjee and Williams, 1995) as well as flutter analysis of aircraft wings (Banerjee, 1984 and 1988).

The dynamic stiffness method has been extended to skeletal structures with uniform members (Kolousek, 1973) or non-uniform members (Leung and Zhou, 1995a and 1995b), straight (Howson, Banerjee and Williams, 1983) or curved members (Henrych, 1981 and Pearson and Wittrick, 1986), damped (Lundon and Akesson, 1983) or undamped beam members exactly. For two dimensional structures, if one of the dimensions can be eliminated by means of the Kantorovich method (Leung and Zeng, 1994), the method still applies. However, for more complicated systems, analytical formulation of the dynamic stiffness is tedious.

Banerjee and Williams (1995) recently derived the dynamic stiffness matrix of a bending-torsion coupled composite beam. They have taken material coupling into account when developing the dynamic stiffness matrix. As discussed in ***Chapter Three***, structures made of orthotropic materials such as laminated composite beams, may display coupling between bending and torsional modes of vibration, depending on the ply orientation. Material coupling is independent of the geometric coupling. Rigidity properties of composite beams are assumed to be known either theoretically or experimentally (see ***Chapter Three***).

For many beam theories, if the coefficients of the governing differential equations are constants, then closed form solutions can be found. When the coefficients are variables of

spatial coordinates, closed form solutions are available only for some special cases, for example, beams with thickness and width varying according to two arbitrary powers of the longitudinal coordinate (Lee and Lin, 1992). Using these power series solutions, the shape functions and dynamic stiffness matrix of a Timoshenko beam element can he constructed without difficulty. Non-uniform beams have considerable technological importance in many situations of engineering practice (Leung and Zhou, 1995a and 1995b). The existing literature (Leung, 1993a and 1993b) reveals that the problem of transverse vibrations of non-uniform beams has been historically treated on the basis of classical Bernoulli-Euler beam theory. However, if the effects of shear deformation and rotatory inertia are considered, Timoshenko beam theory is required (Rossi, Laura and Maurizi, 1992). If the beams are under axial force, then the governing equations should include the effect of initial stresses. The natural frequencies of the non-uniform beams under axial force can be found by equating to zero the determinant of the dynamic stiffness matrix of the system.

5.3. Dynamic stiffness formulation

The first step towards developing the dynamic stiffness matrix of a structural element is to derive its governing differential equations of motion in free vibration. This can be accomplished using various techniques such as by applying Newton's laws, D'Alembert's principle, principle of virtual work, Lagrange's equations or Hamilton's principle which have all been extensively covered in the literature.

The governing differential equation of motion of a structural element undergoing free undamped vibration can be symbolically written as

$$\mathcal{L}(u) = 0 \tag{5-1}$$

where $\mathcal{L}$ is a differential operator and u is the corresponding generalised displacement vector.

The next step is to solve the above differential equation analytically for harmonically varying u. (The dynamic stiffness matrix relates harmonically varying forces to harmonically varying displacements at the nodes of a structural element.) So, the displacement u is expressed as

$$u = \mathcal{U} e^{i\omega t} \tag{5-2}$$

where $\mathcal{U}$ represents amplitudes of displacements, ω is frequency (rad/s), t is time and $i = \sqrt{-1}$.

Substitution of equation (5-2) into equation (5-1) eliminates the time dependent terms in the differential equation to give

$$\mathcal{L}_l(\mathcal{U}, \omega) = 0 \tag{5-3}$$

where $\mathcal{L}_l$ is a differential operator. The general solution of the differential equation (5-3) is sought in the form

$$\mathcal{U} = A\,C \tag{5-4}$$

where C is a constant vector and A is a frequency dependent square matrix. Now, the boundary (end) conditions for displacements and forces are applied to eliminate the constant vector C in equation (5-4) in order to obtain the force displacement relationship via the dynamic stiffness matrix. Firstly, the boundary conditions for the displacements (i.e. displacements at nodes) are applied to equation (5-4) to give

$$\Delta = B\,C \tag{5-5}$$

where Δ is the displacement vector which corresponds to the nodal displacements, and B is a square matrix obtained from matrix A when boundary conditions for displacements are substituted. Next, the boundary conditions for forces are applied. The forces at the nodes of the structural element can be related to the constant vector C in a similar manner to that of equation (5-5) to give

$$\mathcal{F} = D\,C \tag{5-6}$$

where $\mathcal{F}$ is the force vector which corresponds to the nodal forces and D is a frequency dependent square matrix. The constant vector C can now be eliminated from equations (5-5) and (5-6) to give

$$\mathcal{F} = D\,B^{1}\,\Delta = K\,\Delta \tag{5-7}$$

where in equation (5-7)

$$K = D\,B^{-1} \tag{5-8}$$

is the required dynamic stiffness matrix.

In equation (5-8), the two steps involved to obtain the dynamic stiffness matrix are: (i) to invert the B matrix to give B^{-1}; and then (ii) to premultiply the inverted matrix by the D matrix to give K. Computer implementation of these steps can be accomplished either numerically or algebraically. Banerjee and Williams (1994a, 1994c, 1995) have shown that there are substantial savings in computer time if explicit analytical expressions for the elements of the dynamic stiffness matrix are used to compute K, as opposed to the use of numerical methods to obtain K (i.e. the matrix inversion and matrix multiplication steps of equation (5-8)). However, the task of inverting the B matrix algebraically and then premultiplying by the D matrix, again algebraically, to obtain explicit expressions for the elements of the dynamic stiffness matrix K, can be quite formidable. This has only become possible due to recent advances in symbolic computing (Fitch, 1985). Moreover, explicit expressions are particularly useful when some, but not all, of the stiffness coefficients are needed (Banerjee, 1997).

5.4. Application

The application of the dynamic stiffness matrix to solve free vibration problems of structures (or structural elements) is quite simple. Firstly, the dynamic stiffness matrices of all the individual elements in a structure are assembled in the usual way, as is done in the finite element method (except that there is only one matrix for each element to assemble, i.e., there are no separate mass/inertia and stiffness matrices). Then a suitable eigensolution procedure can be adopted to obtain the natural frequencies. It should be noted that the solution procedure using the dynamic stiffness method leads to a non-linear eigenvalue problem. The natural frequency of the structures can be determined by two independent methods. Firstly, by using a frequency-determinant plot, which is an old, easy and quick way to establish the natural frequencies of a structure. However, this technique involves certain difficulties in determining the mode shapes of the structure. Secondly, a

safe and reliable way to solve the problem is to use the Wittrick-Williams algorithm (1971), which gives all required natural frequencies with certainty and to any desired accuracy. The main features of the algorithm are discussed by many authors such as Banerjee (1989) and Leung (1992a, 1992b).

To use the algorithm, the overall dynamic stiffness matrix of the final structure and information about the clamped-clamped natural frequencies of the constituent members of the structure are needed (Banerjee and Williams, 1994b and Banerjee, Guo and Howson, 1996). The Wittrick-Williams algorithm gives the number of natural frequencies of a structure that lie below an arbitrarily chosen trial frequency ω^*. It is briefly described as follows.

If j is the number of eigenvalues present in a range of frequencies from zero to ω^*, then

$$j = j_0 + s\{K^+\} \tag{5-9}$$

where

j = number of natural frequencies of the structure exceeded by the trial frequency ω^*;

j_0 = number of natural frequencies which will still be exceeded if constraints were imposed upon the structure so as to suppress all the nodal displacements so that

$j_0 = \Sigma j_m$;

j_m = number of natural frequencies of a component member with its ends clamped, which have been exceeded by ω^* ;

K^+ = the overall dynamic stiffness matrix evaluated at $\omega = \omega^*$;

$s\{K^+\}$ = number of negative elements on the leading diagonal of K^* ;

K^* = upper triangular matrix obtained by the application of Gauss elimination to K^+ .

Therefore, with the knowledge of the above mentioned parameters, natural frequencies of a structure to any order of accuracy can be found. An important feature of the algorithm is that it guarantees that no natural frequency of the structure is missed, even in the exceptional cases where two modes have the same natural frequency.

The identification of the number of clamped-clamped natural frequencies of all individual members in a structure, under a specified trial frequency is an important part of the

algorithm, see j_0 in equation (5-9), to ensure that no natural frequency of the structure is missed. In the particular case of a bending-torsion coupled beam such as an aircraft wing Banerjee and Williams (1994b) have ingeniously given an exact method to determine the number of clamped-clamped natural frequencies of such beams which exists below a given trial frequency. The procedure put forward by Banerjee and Williams (1994b) has been used in implementing the Wittrick-Williams algorithm in this thesis.

5.5. Summary

A systematic procedure is given for the derivation of the dynamic stiffness matrix of a structural element. Generating explicit analytical expressions for the elements of the dynamic stiffness matrix gives significant savings in computer time. Such expressions can be derived by using symbolic computing. The method presented is fairly general and can be extended to cover any structural members, the governing differential equations of which are expressible in matrix polynomials in one spatial coordinate when the other spatial coordinates are eliminated by the Kantorovich method (Leung and Zeng, 1994).

An important difference between the dynamic stiffness method and finite element method is that the dynamic stiffness matrix method uses a single transcendentally frequency dependent matrix of an element, which accounts for both mass/inertia and stiffness properties, whereas the finite element method uses separate mass and stiffness matrices which are both generally independent of frequency and may be modelled to different orders of accuracy. Another related and significant difference is that, unlike the finite element method, the dynamic stiffness method accounts for the infinite number of natural frequencies of a vibrating structure and so can be used to find higher natural frequencies exactly, without the discretisation errors of the finite element method.

In the subsequent work, the dynamic stiffness method is used to solve the free vibration problem of bending-torsion coupled beams. In order to implement this technique a computer program is developed to calculate the dynamic stiffness matrix of a bending-torsion coupled beam. Dynamic stiffness matrix for a representative case is given in *Appendix C* (Banerjee, 1998).

Chapter Six

Dynamics of composite beams : Theory

6 Dynamics of composite beams : Theory

6.1. Introduction

In this chapter, an analytical method is developed to predict the flexural and torsional response of a beam coupled in bending and torsion when acted upon by deterministic or random loads. Normal modes are used and both geometric and material coupling are considered when developing the theory. The effects of shear deformation, rotatory inertia and axial load are also taken into account. An example of a bending-torsion coupled beam, which is an aircraft wing, is shown in Figure 6-1. The mass and the elastic axes of the beam (the loci of the mass centres and the geometric shear centres of the cross-section) are separated by a distance x_α as shown. The beam is uniform and subjected to time dependent bending and/or torsional loads which can be either deterministic or random. A harmonically varying load is considered for the deterministic case whilst in the case of random loading, the input is considered to have stationary and ergodic properties. Both concentrated and distributed loads are taken into account. The theory presented covers both metallic and composite beams, unless otherwise stated.

The following steps are taken when presenting the theory. Firstly, the basic governing differential equations of motion for the bending-torsion coupled beam are derived using Hamilton's principle. The governing differential equations of motion are presented for a variety of cases, starting from the elementary case where only geometric coupling exists (metallic beam), to the most complicated case considered where both geometric and material coupling exist and the effects of shear deformation, rotatory inertia and axial load are taken into account.

Secondly, the natural frequencies and mode shapes of the beam in undamped free vibration are established using the calculus of ordinary and partial differential equations. For every case of a bending-torsion coupled beam, the orthogonality condition of the beam and the damping ratio in each mode are derived to decouple the equations of motion of the beam, using analytical mechanics and variational analysis.

The derivation and solution procedure for each set of equations given in the next section are similar, therefore for brevity, the derivations of the governing differential equations of motion and details of the solution for the undamped free vibration for a representative case are given in ***Appendices A*** and ***B***, respectively. The derivation of the orthogonality condition is also given in ***Appendix D*** for a representative case.

Since linear small deflection theory has been used, the overall response of the beam is represented by the superposition of all individual responses in each mode.

Next, Duhamel's integral is employed to calculate the response of the beam to deterministic loads. The evaluation of the response for the random load is, however, carried out in the frequency domain using the theories of random vibration and spectral analysis. This is accomplished by relating the power spectral density (PSD) of the output to that of the input using the modulus of the complex frequency response function.

For composite beams, dynamic displacements together with the externally applied loads are used to calculate the time dependent shear force, bending moment and torque acting on the beam. The dynamic stresses at a cross-section of the thin-walled laminated composite beam due to these loads are then computed using the Engineer's bending theory, Saint-Venant's torsion theory and classical mechanics of laminated fibrous composites. Finally, a failure criterion for stresses is established, based on a detailed examination of the fibre and its surrounding matrix.

6.2. Governing differential equations of motion

In this section the differential equations of motion are given, for a number of viscously damped metallic and composite beams with bending-torsion coupling present in their modes of deformation (see ***Appendix A*** for derivation of these equations).

In the following partial differential equations; $u=u(y,t)$, $\theta=\theta(y,t)$ and $\psi=\psi(y,t)$ are the transverse displacement and the flexural and the torsional rotation of the elastic axis of the beam, respectively. Also $f(y,t)$ and $g(y,t)$ are the external force and torque acting on, and

about, the flexural axis of the beam, m is the mass per unit length, ρ is the density of the material, I is the second moment of inertia about the X-axis, EI, kAG, GJ and K are the bending, shear, torsional and bending-torsion coupling (material) rigidities of the beam, I_α is the mass moment of inertia per unit length, P is a compressive axial load (Note that P can be negative so that, tension is included). An over-dot represents differentiation with respect to time and a dash represents differentiation with respect to space. It is notable that the geometric and material bending-torsion coupling are characterised by x_α (see Figure 6-1) and K, respectively.

The coefficients c_1, c_2 and c_3 are linear viscous damping terms per unit length in flexure, torsion and shear, respectively. It is assumed that each point of the cross section moves with a different local velocity, so that the local damping force sums over the section to the given expression containing the c_1 term. Similarly, the expression containing the c_2 term is a torque about the elastic axis brought about by elemental damping forces. The expression containing c_3 is associated with the bending moment about the X-axis. No other sources of damping are taken into account.

It should be noted that in the following derivation flexural rotation (θ) is of importance only when the effect of transverse shear deformation and rotatory inertia are included (Timoshenko beams); otherwise, the flexural rotation is simply the first differentiation of the flexural displacement (u) with respect to the space variable (y). Furthermore, c_3, which derives from linear viscous damping in shear, appears in the equations of motion only in the case of Timoshenko beams.

The governing differential equations of motion for different cases of bending-torsion coupled beams are as follows

Bending-torsion coupled metallic beams :

(i) Bending-torsion coupled (Bernoulli-Euler) beam

$$EIu'''' - c_1(\dot{u} - x_\alpha\dot{\psi}) - m(\ddot{u} - x_\alpha\ddot{\psi}) = f(y,t) \tag{6-1}$$

$$GJ\psi'' - c_2\dot{\psi} + c_1x_\alpha\dot{u} - I_\alpha\ddot{\psi} + mx_\alpha\ddot{u} = g(y,t) \tag{6-2}$$

(ii) Axially loaded bending-torsion coupled (Bernoulli-Euler) beam

$$EIu''''' - P(u'' - x_\alpha \psi'') - c_1(\dot{u} - x_\alpha \dot{\psi}) - m(\ddot{u} - x_\alpha \ddot{\psi}) = f(y,t) \quad (6\text{-}3)$$

$$GJ\psi'' - P\{(I_\alpha / m)\psi'' - x_\alpha u''\} - c_2\dot{\psi} + c_1 x_\alpha \dot{u} - I_\alpha \ddot{\psi} + m x_\alpha \ddot{u} = g(y,t) \quad (6\text{-}4)$$

(iii) Bending-torsion coupled Timoshenko beam

$$kAG(u'' - \theta') - c_1(\dot{u} - x_\alpha \dot{\psi}) - m(\ddot{u} - x_\alpha \ddot{\psi}) = f(y,t) \quad (6\text{-}5)$$

$$GJ\psi'' - c_2\dot{\psi} + c_1 x_\alpha \dot{u} - I_\alpha \ddot{\psi} + m x_\alpha \ddot{u} = g(y,t) \quad (6\text{-}6)$$

$$EI\theta'' + kAG(u' - \theta) - c_3\dot{\theta} - \rho I\ddot{\theta} = 0 \quad (6\text{-}7)$$

(iv) Axially loaded bending-torsion coupled Timoshenko beam

$$kAG(u'' - \theta') - P(u'' - x_\alpha \psi'') - c_1(\dot{u} - x_\alpha \dot{\psi}) - m(\ddot{u} - x_\alpha \ddot{\psi}) = f(y,t) \quad (6\text{-}8)$$

$$GJ\psi'' - P\{(I_\alpha / m)\psi'' - x_\alpha u''\} - c_2\dot{\psi} + c_1 x_\alpha \dot{u} - I_\alpha \ddot{\psi} + m x_\alpha \ddot{u} = g(y,t) \quad (6\text{-}9)$$

$$EI\theta'' + kAG(u' - \theta) - c_3\dot{\theta} - \rho I\ddot{\theta} = 0 \quad (6\text{-}10)$$

Bending-torsion coupled composite beams :

(a) Composite beams when in every cross-section along the beam geometric shear centre is coincident with centroid ($x_\alpha = 0$ & $K \neq 0$)

(i) Materially bending-torsion coupled composite (Bernoulli-Euler) beam

$$EIu''''' + K\psi''' - c_1\dot{u} - m\ddot{u} = f(y,t) \quad (6\text{-}11)$$

$$Ku''' + GJ\psi'' - c_2\dot{\psi} - I_\alpha \ddot{\psi} = g(y,t) \quad (6\text{-}12)$$

(ii) Axially loaded materially bending-torsion coupled composite (Bernoulli-Euler) beam

$$EIu''''' + K\psi''' - P\ u'' - c_1\dot{u} - m\ddot{u} = f(y,t) \quad (6\text{-}13)$$

$$Ku''' + GJ\psi'' - P(I_\alpha / m)\psi'' - c_2\dot{\psi} - I_\alpha \ddot{\psi} = g(y,t) \quad (6\text{-}14)$$

(iii) Materially bending-torsion coupled composite Timoshenko beam

$$kAG(u'' - \theta') - c_1\dot{u} - m\ddot{u} = f(y,t) \quad (6\text{-}15)$$

$$K\theta'' + GJ\psi'' - c_2\dot{\psi} - I_\alpha\ddot{\psi} = g(y,t) \quad (6\text{-}16)$$

$$EI\theta'' + kAG(u' - \theta) + K\psi'' - c_3\dot{\theta} - \rho I\ddot{\theta} = 0 \quad (6\text{-}17)$$

(iv) Axially loaded materially bending-torsion coupled composite Timoshenko beam

$$kAG(u'' - \theta') - P\ u'' - c_1\dot{u} - m\ddot{u} = f(y,t) \quad (6\text{-}18)$$

$$K\theta'' + GJ\psi'' - P(I_\alpha / m)\psi'' - c_2\dot{\psi} - I_\alpha\ddot{\psi} = g(y,t) \quad (6\text{-}19)$$

$$EI\theta'' + kAG(u' - \theta) + K\psi'' - c_3\dot{\theta} - \rho I\ddot{\theta} = 0 \quad (6\text{-}20)$$

(b) Composite beams with both geometric and material coupling ($x_\alpha \neq 0$ & $K \neq 0$)

(i) Bending-torsion coupled composite (Bernoulli-Euler) beam

$$EIu'''' + K\psi''' - c_1(\dot{u} - x_\alpha\dot{\psi}) - m(\ddot{u} - x_\alpha\ddot{\psi}) = f(y,t) \quad (6\text{-}21)$$

$$Ku''' + GJ\psi'' - c_2\dot{\psi} + c_1x_\alpha\dot{u} - I_\alpha\ddot{\psi} + mx_\alpha\ddot{u} = g(y,t) \quad (6\text{-}22)$$

(ii) Axially loaded bending-torsion coupled composite (Bernoulli-Euler) beam

$$EIu'''' + K\psi''' - P(u'' - x_\alpha\psi'') - c_1(\dot{u} - x_\alpha\dot{\psi}) - m(\ddot{u} - x_\alpha\ddot{\psi}) = f(y,t) \quad (6\text{-}23)$$

$$Ku''' + GJ\psi'' - P\{(I_\alpha / m)\psi'' - x_\alpha u''\} - c_2\dot{\psi} + c_1x_\alpha\dot{u} - I_\alpha\ddot{\psi} + mx_\alpha\ddot{u} = g(y,t) \quad (6\text{-}24)$$

(iii) Bending-torsion coupled composite Timoshenko beam

$$kAG(u'' - \theta') - c_1(\dot{u} - x_\alpha\dot{\psi}) - m(\ddot{u} - x_\alpha\ddot{\psi}) = f(y,t) \quad (6\text{-}25)$$

$$K\theta'' + GJ\psi'' - c_2\dot{\psi} + c_1x_\alpha\dot{u} - I_\alpha\ddot{\psi} + mx_\alpha\ddot{u} = g(y,t) \quad (6\text{-}26)$$

$$EI\theta'' + kAG(u' - \theta) + K\psi'' - c_3\dot{\theta} - \rho I\ddot{\theta} = 0 \quad (6\text{-}27)$$

(iv) Axially loaded bending-torsion coupled composite Timoshenko beam

$$kAG(u'' - \theta') - P(u'' - x_\alpha\psi'') - c_1(\dot{u} - x_\alpha\dot{\psi}) - m(\ddot{u} - x_\alpha\ddot{\psi}) = f(y,t) \quad (6\text{-}28)$$

$$K\theta'' + GJ\psi'' - P\{(I_\alpha / m)\psi'' - x_\alpha u''\} - c_2\dot{\psi} + c_1x_\alpha\dot{u} - I_\alpha\ddot{\psi} + mx_\alpha\ddot{u} = g(y,t) \quad (6\text{-}29)$$

$$EI\theta'' + kAG(u' - \theta) + K\psi'' - c_3\dot{\theta} - \rho I\ddot{\theta} = 0 \quad (6\text{-}30)$$

6.3. Free vibration analysis

For each of the cases of bending-torsion coupled beams described above, the normal modes of the beam in free undamped vibration are established by setting to zero the damping coefficients, the external force $f(y,t)$ and torque $g(y,t)$, in the differential equations of motion. Solutions for $u=u(y,t)$, $\theta=\theta(y,t)$ and $\psi=\psi(y,t)$ are then sought in the form

$$u(y,t) = U(y)e^{i\omega_n t}$$

$$\theta(y,t) = \Theta(y)e^{i\omega_n t} \tag{6-31}$$

$$\psi(y,t) = \Psi(y)e^{i\omega_n t}$$

where ω_n is the natural frequency of the system and, $U(y)$, $\Theta(y)$ and $\Psi(y)$ are the eigenfunctions (mode shapes) for flexural deformation, flexural rotation and torsional rotation, respectively. By extensive algebraic manipulation, for each of the cases, the solutions are obtained in the following general form

$$U(\xi) = A_1 \cosh\alpha\xi + A_2 \sinh\alpha\xi + A_3 \cos\beta\xi + A_4 \sin\beta\xi + A_5 \cos\gamma\xi + A_6 \sin\gamma\xi \quad (6\text{-}32)$$

$$\Theta(\xi) = B_1 \cosh\alpha\xi + B_2 \sinh\alpha\xi + B_3 \cos\beta\xi + B_4 \sin\beta\xi + B_5 \cos\gamma\xi + B_6 \sin\gamma\xi \quad (6\text{-}33)$$

$$\Psi(\xi) = C_1 \cosh\alpha\xi + C_2 \sinh\alpha\xi + C_3 \cos\beta\xi + C_4 \sin\beta\xi + C_5 \cos\gamma\xi + C_6 \sin\gamma\xi \quad (6\text{-}34)$$

where A_1–A_6 , B_1–B_6 and C_1–C_6 are the three different sets of constants, α, β, γ are dependent on the type of beam model considered (see ***Appendix B***) and are functions of mechanical properties of the beam; $\xi=y/L$ and L is the length of the beam. Equations (6-32) to (6-34) in conjunction with the boundary conditions, yield the eigenvalues (natural frequencies) and eigenfunctions (mode shapes) of the bending-torsion coupled beam. Arriving from equation (6-31) to equations (6-32)-(6-34) is given in ***Appendix B***.

6.4. Orthogonality condition and damping representation

Following the procedure described by Clough and Penzien (1975), Bishop and Price (1977) and Banerjee and Williams (1995), the orthogonality condition of the principal

modes of undamped free vibration of the bending-torsion coupled beam can be derived. In this section, the generalised mass, μ_n, and the non-dimensional damping ratio, ζ_n of the beam in each mode of vibration are given, for a number of metallic and composite beams exhibiting bending-torsion coupling behaviour.

The orthogonality condition is essential for application of the separation of variable method and is valid, provided the end conditions of the beam (at $\xi=0$ and/or $\xi=1$) are free, simply supported, or clamped. Introduction of the non-dimensional damping ratio is also important for application of the separation of variable method. Besides, it is impractical to work with original damping coefficients (c_1 , c_2 and c_3), therefore, the damping is reinterpreted in its modal form. For brevity, derivation of these equations is not presented here (***Appendix D***). Note that, in the following equations δ_{mn} is the Kronecker delta.

The orthogonality condition and modal damping for different cases of bending-torsion coupled beams are as follows

Bending-torsion coupled metallic beams :

Bending-torsion coupled Bernoulli-Euler beam (elementary case)

Axially loaded bending-torsion coupled Bernoulli-Euler beam

$$\begin{aligned}&\int_0^1 [mU_mU_n + I_\alpha \Psi_m\Psi_n - mx_\alpha(U_m\Psi_n + U_n\Psi_m)]d\xi = \mu_n\delta_{mn}\\ &\int_0^1 [c_1U_mU_n + c_2\Psi_m\Psi_n - c_1x_\alpha(U_m\Psi_n + U_n\Psi_m)]d\xi = 2\zeta_n\omega_n\mu_n\delta_{mn}\end{aligned} \qquad (6\text{-}35)$$

Bending-torsion coupled Timoshenko beam

Axially loaded bending-torsion coupled Timoshenko beam

$$\begin{aligned}&\int_0^1 [mU_mU_n + I_\alpha \Psi_m\Psi_n + \rho I\Theta_m\Theta_n - mx_\alpha(U_m\Psi_n + U_n\Psi_m)]d\xi = \mu_n\delta_{mn}\\ &\int_0^1 [c_1U_mU_n + c_2\Psi_m\Psi_n + c_3\Theta_m\Theta_n - c_1x_\alpha(U_m\Psi_n + U_n\Psi_m)]d\xi = 2\zeta_n\omega_n\mu_n\delta_{mn}\end{aligned} \qquad (6\text{-}36)$$

Bending-torsion coupled composite beams :

(a) Composite beams when in every cross-section along the beam geometric shear centre is coincident with centroid ($x_\alpha = 0 \;\&\; K \neq 0$)

Bending-torsion coupled Bernoulli-Euler composite beam (elementary case)

Axially loaded bending-torsion coupled Bernoulli-Euler composite beam

$$\int_0^1 [mU_m U_n + I_\alpha \Psi_m \Psi_n] d\xi = \mu_n \delta_{mn}$$

$$\int_0^1 [c_1 U_m U_n + c_2 \Psi_m \Psi_n] d\xi = 2\zeta_n \omega_n \mu_n \delta_{mn} \qquad (6\text{-}37)$$

Bending-torsion coupled Timoshenko composite beam

Axially loaded bending-torsion coupled Timoshenko composite beam

$$\int_0^1 [mU_m U_n + I_\alpha \Psi_m \Psi_n + \rho I \Theta_m \Theta_n] d\xi = \mu_n \delta_{mn}$$

$$\int_0^1 [c_1 U_m U_n + c_2 \Psi_m \Psi_n + c_3 \Theta_m \Theta_n] d\xi = 2\zeta_n \omega_n \mu_n \delta_{mn} \qquad (6\text{-}38)$$

(b) Composite beams with both geometric and material coupling ($x_\alpha \neq 0 \;\&\; K \neq 0$)

Bending-torsion coupled Bernoulli-Euler composite beam (elementary case)

Axially loaded bending-torsion coupled Bernoulli-Euler composite beam

$$\int_0^1 [mU_m U_n + I_\alpha \Psi_m \Psi_n - mx_\alpha (U_m \Psi_n + U_n \Psi_m)] d\xi = \mu_n \delta_{mn}$$

$$\int_0^1 [c_1 U_m U_n + c_2 \Psi_m \Psi_n - c_1 x_\alpha (U_m \Psi_n + U_n \Psi_m)] d\xi = 2\zeta_n \omega_n \mu_n \delta_{mn} \qquad (6\text{-}39)$$

Bending-torsion coupled Timoshenko composite beam

Axially loaded bending-torsion coupled Timoshenko composite beam

$$\int_0^1 [mU_m U_n + I_\alpha \Psi_m \Psi_n + \rho I \Theta_m \Theta_n - mx_\alpha (U_m \Psi_n + U_n \Psi_m)] d\xi = \mu_n \delta_{mn}$$

$$\int_0^1 [c_1 U_m U_n + c_2 \Psi_m \Psi_n + c_3 \Theta_m \Theta_n - c_1 x_\alpha (U_m \Psi_n + U_n \Psi_m)] d\xi = 2\zeta_n \omega_n \mu_n \delta_{mn} \qquad (6\text{-}40)$$

With the free vibration modes, natural frequencies and orthogonality condition described above, it is now possible to return to the general forced vibration problem of the damped bending-torsion coupled beams.

6.5. Forced vibration analysis

The solutions for the general forced vibration problem, specified by differential equations of motion given in ***Section 6.1***, in terms of eigenfunctions are sought as follows

$$\begin{aligned} u(y,t) &= u(\xi L,t) = \sum_{n=1}^{\infty} q_n(t) U_n(y) \\ \theta(y,t) &= \theta(\xi L,t) = \sum_{n=1}^{\infty} q_n(t) \Theta_n(y) \\ \psi(y,t) &= \psi(\xi L,t) = \sum_{n=1}^{\infty} q_n(t) \Psi_n(y) \end{aligned} \tag{6-41}$$

where $q_n(t)$ is a time dependent generalised coordinate for each mode. Substituting equations (6-41) into the differential equations of motion, using the orthogonality condition expressed in ***Section 6.4*** and by algebraic manipulation, the following equations are derived

$$\ddot{q}_n(t) + 2\zeta_n \omega_n \dot{q}_n(t) + \omega_n^2 q_n(t) = [F_n(t) + G_n(t)] \tag{6-42}$$

where $F_n(t)$ and $G_n(t)$ can be expressed as

$$\begin{aligned} F_n(t) &= -\frac{1}{\mu_n} \int_0^L U_n(y) f(y,t) dy = \frac{1}{\mu_n} \overline{F}_n(t) \\ G_n(t) &= -\frac{1}{\mu_n} \int_0^L \Psi_n(y) g(y,t) dy = \frac{1}{\mu_n} \overline{G}_n(t) \end{aligned} \tag{6-43}$$

$\overline{F}_n(t)$ and $\overline{G}_n(t)$ are the generalised forces.

6.6. Response to deterministic loads

Using Duhamel's integral, the general solution for equation (6-42) can be found as follows

$$q_n(t) = e^{-\zeta_n \omega_{n} t}\{A_n^* cos(\omega_{nd} t) + B_n^* sin(\omega_{nd} t)\}$$
$$+\frac{1}{\omega_{nd}}\int_0^t \{F_n(\tau) + G_n(\tau)\} e^{-\zeta_n \omega_n (t-\tau)} sin\{\omega_{nd}(t-\tau)\} d\tau \quad (6\text{-}44)$$

where $\omega_{nd} = \omega_n (1-\zeta_n^2)^{1/2}$ is the damped natural frequency and A^*_n and B^*_n are coefficients related to initial conditions. Substitution of equation (6-44) into equations (6-41) gives the general solution for bending displacement, flexural and torsional rotations of the beam in the following form

$$u(\xi,t) = \sum_{n=1}^{\infty} U_n(\xi) \left[e^{-\zeta_n \omega_{n} t}\{A_n^* \cos(\omega_{nd} t) + B_n^* \sin(\omega_{nd} t)\} \right.$$
$$\left. +\frac{1}{\omega_{nd}}\int_0^t \{F_n(\tau) + G_n(\tau)\} e^{-\zeta_n \omega_n (t-\tau)} \sin\{\omega_{nd}(t-\tau)\} d\tau \right] \quad (6\text{-}45)$$

$$\theta(\xi,t) = \sum_{n=1}^{\infty} \Theta_n(\xi) \left[e^{-\zeta_n \omega_{n} t}\{A_n^* \cos(\omega_{nd} t) + B_n^* \sin(\omega_{nd} t)\} \right.$$
$$\left. +\frac{1}{\omega_{nd}}\int_0^t \{F_n(\tau) + G_n(\tau)\} e^{-\zeta_n \omega_n (t-\tau)} \sin\{\omega_{nd}(t-\tau)\} d\tau \right] \quad (6\text{-}46)$$

$$\psi(\xi,t) = \sum_{n=1}^{\infty} \Psi_n(\xi) \left[e^{-\zeta_n \omega_{n} t}\{A_n^* \cos(\omega_{nd} t) + B_n^* \sin(\omega_{nd} t)\} \right.$$
$$\left. +\frac{1}{\omega_{nd}}\int_0^t \{F_n(\tau) + G_n(\tau)\} e^{-\zeta_n \omega_n (t-\tau)} \sin\{\omega_{nd}(t-\tau)\} d\tau \right] \quad (6\text{-}47)$$

Equations (6-45) to (6-47) represent the general solutions due to arbitrary deterministic forces $f(y,t)$ and torques $g(y,t)$, respectively.

Multi-point force and torque excitation : To cover the solution for a series of externally applied isolated forces and torques, the loading is assumed to be in the form

$$f(y,t) = \delta(y-a_i) F_i \sin\Omega_i t$$
$$g(y,t) = \delta(y-b_i) G_i \sin\Omega_i t \quad (6\text{-}48)$$

which represent a system of harmonically applied concentrated forces and torques with

circular frequency Ω_i at points a_i and b_i respectively, with $i = 1, 2, 3, \ldots, N$, and $\delta(y)$ is the Dirac delta function. Then the dynamic response for bending displacement, flexural and torsional rotations of the beam follows from equations (6-45) to (6-47) as

$$u(\xi,t) = \sum_{n=1}^{\infty} U_n(\xi)\left[e^{-\zeta_n \omega_n t}\{A_n^* \cos(\omega_{nd} t) + B_n^* \sin(\omega_{nd} t)\}\right]$$

$$+ \sum_{n=1}^{\infty} U_n(\xi) \sum_{i=1}^{N} \frac{\{U_n(a_i)\ F_i + \Psi_n(b_i)\ G_i\}}{\mu_n\{(\omega_n^2 - \Omega_i^2)^2 + (2\zeta_n \omega_n \Omega_i)^2\}} \tag{6-49}$$

$$\times \{(\omega_n^2 - \Omega_i^2)\sin\Omega_i t - (2\zeta_n \omega_n \Omega_i)\cos\Omega_i t\}$$

$$\theta(\xi,t) = \sum_{n=1}^{\infty} \Theta_n(\xi)\left[e^{-\zeta_n \omega_n t}\{A_n^* \cos(\omega_{nd} t) + B_n^* \sin(\omega_{nd} t)\}\right]$$

$$+ \sum_{n=1}^{\infty} \Theta_n(\xi) \sum_{i=1}^{N} \frac{\{U_n(a_i)\ F_i + \Psi_n(b_i)\ G_i\}}{\mu_n\{(\omega_n^2 - \Omega_i^2)^2 + (2\zeta_n \omega_n \Omega_i)^2\}} \tag{6-50}$$

$$\times \{(\omega_n^2 - \Omega_i^2)\sin\Omega_i t - (2\zeta_n \omega_n \Omega_i)\cos\Omega_i t\}$$

$$\psi(\xi,t) = \sum_{n=1}^{\infty} \Psi_n(\xi)\left[e^{-\zeta_n \omega_n t}\{A_n^* \cos(\omega_{nd} t) + B_n^* \sin(\omega_{nd} t)\}\right]$$

$$+ \sum_{n=1}^{\infty} \Psi_n(\xi) \sum_{i=1}^{N} \frac{\{U_n(a_i)\ F_i + \Psi_n(b_i)\ G_i\}}{\mu_n\{(\omega_n^2 - \Omega_i^2)^2 + (2\zeta_n \omega_n \Omega_i)^2\}} \tag{6-51}$$

$$\times \{(\omega_n^2 - \Omega_i^2)\sin\Omega_i t - (2\zeta_n \omega_n \Omega_i)\cos\Omega_i t\}$$

Equations (6-49) to (6-51) provide the general solutions for harmonically varying multi-point force and torque loading at given locations.

Single-point force and torque excitation : If there is only one external force and only one external torque acting on the beam at $y = a_1$, and $y = b_1$, respectively, then $N = 1$ and $f(y,t) = \delta(y-a_1)\, F \sin \Omega t$ and $g(y,t) = \delta(y-b_1)\, G \sin \Omega t$, and the steady state bending displacement, flexural and torsional rotations of the beam, for zero initial conditions, can easily be obtained from equations (6-49) to (6-51) which reduce to :

$$u(\xi,t)=\sum_{n=1}^{\infty}U_n(\xi)\{U_n(a_1)F+\Psi_n(b_1)G\}\frac{(\omega_n^2-\Omega^2)\sin\Omega t-(2\zeta_n\omega_n\Omega)\cos\Omega t}{\mu_n\{(\omega_n^2-\Omega^2)^2+(2\zeta_n\omega_n\Omega)^2\}} \quad (6\text{-}52)$$

$$\theta(\xi,t)=\sum_{n=1}^{\infty}\Theta_n(\xi)\{U_n(a_1)F+\Psi_n(b_1)G\}\frac{(\omega_n^2-\Omega^2)\sin\Omega t-(2\zeta_n\omega_n\Omega)\cos\Omega t}{\mu_n\{(\omega_n^2-\Omega^2)^2+(2\zeta_n\omega_n\Omega)^2\}} \quad (6\text{-}53)$$

$$\psi(\xi,t)=\sum_{n=1}^{\infty}\Psi_n(\xi)\{U_n(a_1)F+\Psi_n(b_1)G\}\frac{(\omega_n^2-\Omega^2)\sin\Omega t-(2\zeta_n\omega_n\Omega)\cos\Omega t}{\mu_n\{(\omega_n^2-\Omega^2)^2+(2\zeta_n\omega_n\Omega)^2\}} \quad (6\text{-}54)$$

Equations (6-52) to (6-54) can be expressed in simplified form as

$$u(\xi,t)=\sum_{n=1}^{\infty}U_n(\xi)\{U_n(a_1)F+\Psi_n(b_1)G\}\left[A_n/\left(\mu_n\omega_n^2\right)\right]\sin(\Omega t-\phi) \quad (6\text{-}55)$$

$$\theta(\xi,t)=\sum_{n=1}^{\infty}\Theta_n(\xi)\{U_n(a_1)F+\Psi_n(b_1)G\}\left[A_n/\left(\mu_n\omega_n^2\right)\right]\sin(\Omega t-\phi) \quad (6\text{-}56)$$

$$\psi(\xi,t)=\sum_{n=1}^{\infty}\Psi_n(\xi)\{U_n(a_1)F+\Psi_n(b_1)G\}\left[A_n/\left(\mu_n\omega_n^2\right)\right]\sin(\Omega t-\phi) \quad (6\text{-}57)$$

where

$$\tan\phi=2\zeta_n(\Omega/\omega_n)/\left\{1-(\Omega^2/\omega_n^2)\right\} \quad (6\text{-}58)$$

$$A_n=\left[\left\{1-(\Omega^2/\omega_n^2)\right\}^2+\left\{2\zeta_n(\Omega/\omega_n)\right\}^2\right]^{-1/2} \quad (6\text{-}59)$$

Equations (6-55) to (6-57) constitute the general solution for a single force and/or torque varying harmonically at given locations.

The equations for u, θ and ψ presented in this section are based on well established principles which have been applied to simpler problems before. These equations represent an original contribution and were first presented by Eslimy-Isfahany, Banerjee and Sobey (1996) and, in the present form, for the first time here.

6.7. Response to Random Loads

The response of a bending-torsion coupled beam to stationary ergodic random excitation with zero initial conditions is now considered. The derivations that follow are made in the frequency domain, using the receptance method which is also known as the complex frequency response function method. As in the case of free vibration analysis, both material and geometric coupling is included in the theory.

Externally applied force and torque are assumed to be uncorrelated. The cross-spectral densities of the input excitation, $S_f(\xi_1, \xi_2, \Omega)$ and $S_g(\xi_1, \xi_2, \Omega)$, are assumed to be known. They are related (Robson, 1963) to the cross-correlation functions $R_f(\xi_1, \xi_2, \tau)$ and $R_g(\xi_1, \xi_2, \tau)$ of the input excitation, by the following Fourier transform pair (the suffices f and g denotes external force and torque, respectively)

$$S_f(\xi_1,\xi_2,\Omega) = \frac{1}{2\pi}\int_{-\infty}^{\infty} R_f(\xi_1,\xi_2,\tau)e^{-i\Omega t}d\tau$$
$$S_g(\xi_1,\xi_2,\Omega) = \frac{1}{2\pi}\int_{-\infty}^{\infty} R_g(\xi_1,\xi_2,\tau)e^{-i\Omega t}d\tau \qquad (6\text{-}60a)$$

or

$$R_f(\xi_1,\xi_2,\tau) = \int_{-\infty}^{\infty} S_f(\xi_1,\xi_2,\Omega)e^{i\Omega t}d\Omega$$
$$R_g(\xi_1,\xi_2,\tau) = \int_{-\infty}^{\infty} S_g(\xi_1,\xi_2,\Omega)e^{i\Omega t}d\Omega \qquad (6\text{-}60b)$$

The cross-correlation functions $R_f(\xi_1, \xi_2, \tau)$ & $R_g(\xi_1, \xi_2, \tau)$ of the excitation are given by

$$R_f(\xi_1,\xi_2,\tau) = \langle f(\xi_1,t)f(\xi_2,t+\tau)\rangle$$
$$R_g(\xi_1,\xi_2,\tau) = \langle g(\xi_1,t)g(\xi_2,t+\tau)\rangle \qquad (6\text{-}61)$$

where < > denotes the ensemble average of the stochastic process (Robson, 1963).

Cross-spectral density of the unknown response is related to cross-spectral density of the excitation via the receptance. Once the receptances are known, the mean square value of the response can be found by following the standard procedure. Crandall (1958), Robson (1963), Lin (1967), Elishakoff (1983), Newland (1984) and Piszczek and Niziol (1986)

have published excellent text books which cover the basic concepts, as well as some advanced aspects of the theory of random vibration and spectral analysis for continuous linear systems. More recently, Cederbaum et al. (1992) discussed the theory of random vibration and reliability of composite structures.

Some authors modified the classical procedure of the spectral analysis to arrive at the dynamic response of beam like structures, such as an axially loaded Timoshenko beam (Banerjee and Kennedy, 1985), an axially loaded Timoshenko beam resting on an elastic foundation (Chang, 1994) and a metallic bending-torsion coupled beam (Eslimy-Isfahany, Banerjee and Sobey, 1996), subjected to random vibration. The following derivations are based on the earlier work of Eslimy-Isfahany, Banerjee and Sobey (1996) and represent an original contribution, in the present form.

The receptances $H_u(\xi, \xi_1, \Omega)$, $H_\theta(\xi, \xi_1, \Omega)$ and $H_\psi(\xi, \xi_1, \Omega)$ for the bending displacement (u), the flexural rotations (θ), and torsional rotations (ψ), respectively are defined by their amplitudes at the point ξ when a harmonically varying force and/or torque with amplitude 1 and circular frequency Ω is applied at the point ξ_1. Thus for the purpose of computing receptances, the externally applied loading $f(\xi, t)$ and $g(\xi, t)$ are represented by

$$f(\xi,t) = \delta(\xi - \xi_1)e^{i\Omega t}$$
$$g(\xi,t) = \delta(\xi - \xi_1)e^{i\Omega t} \qquad (6\text{-}62)$$

Substituting from equations (6-62) into equations (6-43) gives

$$F_n(t) = -(1/\mu_n)U_n(\xi_1)e^{i\Omega t}$$
$$G_n(t) = -(1/\mu_n)\Psi_n(\xi_1)e^{i\Omega t} \qquad (6\text{-}63)$$

The solution of equation (6-42) for the above loading is taken in the form

$$q_n(t) = q_{0n}(\xi_1, \Omega)e^{i\Omega t} \qquad (6\text{-}64)$$

and on substituting into equation (6-42) and using equations (6-63), leads to

$$q_{0n}(\xi_1, \Omega) = d_n(\Omega).V_n(\xi_1) \qquad (6\text{-}65)$$

in which

$$d_n(\Omega) = 1/\mu_n\left(\omega_n^2 - \Omega^2 + 2i\zeta_n\Omega\omega_n\right) \tag{6-66}$$

and

$$V_n(\xi) = -a_F U_n(\xi_1) - a_G \Psi_n(\xi_1) \tag{6–67}$$

where a_F is equal to 1 if applied transverse force is present and is equal to 0 if otherwise. Similarly, a_G is equal to 1 if applied torque is present and is equal to 0 if otherwise. The receptances for u, θ and ψ can now be obtained from equations (6-41) with the help of equation (6-65) in the form

$$\begin{aligned} H_u(\xi,\xi_1,\Omega) &= \sum_{n=1}^{\infty} q_{0n}(\xi_1,\Omega)U_n(\xi) \\ H_\theta(\xi,\xi_1,\Omega) &= \sum_{n=1}^{\infty} q_{0n}(\xi_1,\Omega)\Theta_n(\xi) \\ H_\psi(\xi,\xi_1,\Omega) &= \sum_{n=1}^{\infty} q_{0n}(\xi_1,\Omega)\Psi_n(\xi) \end{aligned} \tag{6-68}$$

The time dependent randomly varying excitation can be represented by

$$\begin{aligned} f(\xi,t) &= f(\xi).\chi_f(t) \\ g(\xi,t) &= g(\xi).\chi_g(t) \end{aligned} \tag{6-69}$$

where $\chi_f(t)$ and $\chi_g(t)$ are stochastic processes and their spectral densities are $S_f^{\chi}(\Omega)$ and $S_g^{\chi}(\Omega)$, respectively. Note that the excitation considered here is random with respect to time only, as the loading is not spatially varying. However, the method could readily be extended to cover spatially varying random loads but this is not further discussed as it goes beyond the scope of the present study. The cross-spectral density for the above loading is

$$\begin{aligned} S_f(\xi_1,\xi_2,\Omega) &= f(\xi_1)f(\xi_2)S_f^{\chi}(\Omega) \\ S_g(\xi_1,\xi_2,\Omega) &= g(\xi_1)g(\xi_2)S_g^{\chi}(\Omega) \end{aligned} \tag{6-70}$$

For distributed loading, the spectral density functions of the bending displacement and flexural and torsional rotations (i.e. $S_u(\xi,\Omega)$, $S_\theta(\xi,\Omega)$ and $S_\psi(\xi,\Omega)$) are related to the cross-spectral densities of the force $S_f(\xi_1,\xi_2,\Omega)$ and torque $S_g(\xi_1,\xi_2,\Omega)$ by the following relationships

$$S_u(\xi,\Omega)=\int_0^1\int_0^1 H_u^*(\xi,\xi_1,\Omega)H_u(\xi,\xi_2,\Omega)\left\{S_f(\xi_1,\xi_2,\Omega)+S_g(\xi_1,\xi_2,\Omega)\right\}d\xi_1 d\xi_2$$

$$S_\theta(\xi,\Omega)=\int_0^1\int_0^1 H_\theta^*(\xi,\xi_1,\Omega)H_\theta(\xi,\xi_2,\Omega)\left\{S_f(\xi_1,\xi_2,\Omega)+S_g(\xi_1,\xi_2,\Omega)\right\}d\xi_1 d\xi_2 \quad (6\text{-}71)$$

$$S_\psi(\xi,\Omega)=\int_0^1\int_0^1 H_\psi^*(\xi,\xi_1,\Omega)H_\psi(\xi,\xi_2,\Omega)\left\{S_f(\xi_1,\xi_2,\Omega)+S_g(\xi_1,\xi_2,\Omega)\right\}d\xi_1 d\xi_2$$

where * denote the complex conjugate. Substituting the expressions for receptances from equations (6-68) into equations (6-71) gives

$$S_u(\xi,\Omega)=\sum_{m=1}^{\infty}\sum_{n=1}^{\infty} d_m^*(\Omega)d_n^*(\Omega)\eta_{mn}(\Omega)U_m(\xi)U_n(\xi)$$

$$S_\theta(\xi,\Omega)=\sum_{m=1}^{\infty}\sum_{n=1}^{\infty} d_m^*(\Omega)d_n^*(\Omega)\eta_{mn}(\Omega)\Theta_m(\xi)\Theta_n(\xi) \quad (6\text{-}72)$$

$$S_\psi(\xi,\Omega)=\sum_{m=1}^{\infty}\sum_{n=1}^{\infty} d_m^*(\Omega)d_n^*(\Omega)\eta_{mn}(\Omega)\Psi_m(\xi)\Psi_n(\xi)$$

where

$$\eta_{mn}(\Omega)=\int_0^1\int_0^1 V_m(\xi_1)V_n(\xi_2)\left\{S_f(\xi_1,\xi_2,\Omega)+S_g(\xi_1,\xi_2,\Omega)\right\}d\xi_1 d\xi_2 \quad (6\text{-}73)$$

Substituting equations (6-70) into equation (6-73) leads to

$$\eta_{mn}(\Omega)=f_m f_n S_f^x+g_m g_n S_g^x \quad (6\text{-}74)$$

where

$$f_n=\int_0^1 V_n(\xi)f(\xi)d\xi \quad \text{and} \quad g_n=\int_0^1 V_n(\xi)g(\xi)d\xi \quad (6\text{-}75)$$

Substituting equation (6-74) into equations (6-72) gives

$$S_u(\xi,\Omega)=\left|\sum_{n=1}^{\infty} f_n d_n(\Omega)U_n(\xi)\right|^2 S_f^x(\Omega)+\left|\sum_{n=1}^{\infty} g_n d_n(\Omega)U_n(\xi)\right|^2 S_g^x(\Omega)$$

$$S_\theta(\xi,\Omega)=\left|\sum_{n=1}^{\infty} f_n d_n(\Omega)\Theta_n(\xi)\right|^2 S_f^x(\Omega)+\left|\sum_{n=1}^{\infty} g_n d_n(\Omega)\Theta_n(\xi)\right|^2 S_g^x(\Omega) \quad (6\text{-}76)$$

$$S_\psi(\xi,\Omega)=\left|\sum_{n=1}^{\infty} f_n d_n(\Omega)\Psi_n(\xi)\right|^2 S_f^x(\Omega)+\left|\sum_{n=1}^{\infty} g_n d_n(\Omega)\Psi_n(\xi)\right|^2 S_g^x(\Omega)$$

If damping is small and the natural frequencies are well separated, equations (6-76) can be approximated by (Robson, 1963 and Chang, 1994)

$$S_u(\xi,\Omega)=\sum_{n=1}^{\infty}\left|f_n d_n(\Omega)U_n(\xi)\right|^2 S_f^x(\Omega)+\sum_{n=1}^{\infty}\left|g_n d_n(\Omega)U_n(\xi)\right|^2 S_g^x(\Omega)$$

$$S_\theta(\xi,\Omega)=\sum_{n=1}^{\infty}\left|f_n d_n(\Omega)\Theta_n(\xi)\right|^2 S_f^x(\Omega)+\sum_{n=1}^{\infty}\left|g_n d_n(\Omega)\Theta_n(\xi)\right|^2 S_g^x(\Omega) \qquad (6\text{-}77)$$

$$S_\psi(\xi,\Omega)=\sum_{n=1}^{\infty}\left|f_n d_n(\Omega)\Psi_n(\xi)\right|^2 S_f^x(\Omega)+\sum_{n=1}^{\infty}\left|g_n d_n(\Omega)\Psi_n(\xi)\right|^2 S_g^x(\Omega)$$

When the beam is acted upon by a finite number, N, of concentrated, randomly varying forces and torques, integrals over the beam length in equations (6-71), (6-73) and (6-75) are replaced by the summations over N.

Finally, the mean square value of the response can be found by integrating the spectral density functions over all frequencies, so that

$$\left\langle u^2(\xi,t)\right\rangle=\int_{-\infty}^{\infty}S_u(\xi,\Omega)d\Omega$$

$$\left\langle \theta^2(\xi,t)\right\rangle=\int_{-\infty}^{\infty}S_\theta(\xi,\Omega)d\Omega \qquad (6\text{-}78)$$

$$\left\langle \psi^2(\xi,t)\right\rangle=\int_{-\infty}^{\infty}S_\psi(\xi,\Omega)d\Omega$$

If the input random excitation follows a Gaussian probability distribution, the response probability will also be Gaussian and therefore, the response can be fully described by its spectral density function. The solution enables us to construct the response for any external forces with given power spectral density (PSD) distribution (Robson, 1963 and Newland, 1984).

Response to atmospheric turbulence : The experimental data on turbulence in clear air and in thunderstorms, and from altitudes below *5000* up to *40000* (*ft*) have been reviewed by Houbolt et al. (1964). The authors have examined it from the standpoint of scale, intensity, shape of one-dimensional spectra, homogeneity, isotropy, and normality. Their general conclusion is that an adequate model for analysis purposes is the simplest one, that

is one which is isotropic, homogeneous, Gaussian and frozen. Etkin (1972) also studied the spectral component of isotropic turbulence. In most of the available literature, the one dimensional spectrum that best fits the data for the vertical component of turbulence is the von Karman spectrum. In this research power spectral density of atmospheric turbulence is modelled using the well-known von Karman spectrum given, amongst others, by Houbolt et al. (1964) and Perry et al. (1990) as follows

$$S^x(\Omega) = \frac{\sigma_g^2 L_s}{\pi V_s} \frac{[1+(8/3)\{1.339(L_s/V_s)\Omega\}^2]}{[1+\{1.339(L_s/V_s)\Omega\}^2]^{11/6}} \tag{6-79}$$

where σ_g^2 is the mean square value of the gust (turbulence) velocity, L_s is the scale length of the turbulence and V_s is the airspeed.

Others have suggested using the well-known Dryden spectra (Bisplingoff et al., 1955) which closely resemble the von Karman spectra and assume the turbulence in the gust field is isotropic. The PSD of Dryden spectra is given by

$$S^x(\Omega) = \frac{\sigma_g^2 L_s}{\pi V_s} \frac{[1+3(\Omega \frac{L_s}{V_s})^2]}{[1+(\Omega \frac{L_s}{V_s})^2]^2} \tag{6-80}$$

For scientific purposes, it is interesting to investigate the random vibration of a structure when it is excited over a wide range of frequencies. The white-noise power spectra (equation 6-81) are preferred by many researchers because they cover the whole range of frequencies and thus give a conservative estimate of the response. The PSD of white-noise spectra is constant over all frequencies as shown below

$$S^x(\Omega) = constant \tag{6-81}$$

This completes the analytical analysis of the dynamic response of the bending-torsion coupled beams to deterministic and random forces.

6.8. Stress analysis of thin-walled laminated composite beams

In order to determine dynamic stresses in the laminates, there are two main choices, namely the stiffness method and the displacement method. In the stiffness method, strains in any cross-section are derived directly from the dynamic displacement field and stresses are determined using stress-strain relationship. The most appropriate manner in which one should treat the problem is to arrive at the correct stress and strain relations at the beginning, rather than correcting the generalised force and generalised strain relations, whose definition varies from one beam theory to another. In the displacement method, however, internal forces along the beam are calculated first, using the dynamic displacement field and stresses are determined using internal forces-stresses relationship in any cross-section. The displacement method has been chosen here and the following steps are used in this investigation to find and assess the dynamic stresses in fibres :

(i) dynamic internal forces in each cross-section are calculated using the equilibrium of forces acting on an infinitesimal segment of the beam; (ii) normal and shearing stresses induced by axial load, bending moment, shear force and torque are found in the cross-section; (iii) stresses are found in the principal material direction; (iv) failure criteria is specified and examined.

6.8.1. Internal forces : Obtaining the internal forces is the first step in order to find the stresses in fibres. For a thin-walled laminated composite beam, internal forces are defined as follow:

$$V = \int_L^y \frac{\partial V}{\partial y} dy + V_L$$

$$M = \int_L^y \frac{\partial M}{\partial y} dy + M_L \qquad (6\text{-}82)$$

$$T = \int_L^y \frac{\partial T}{\partial y} dy + T_L$$

where

$$\frac{\partial V}{\partial y} = f(y,t) + m(\ddot{u} - x_a\ddot{\psi})$$
$$\frac{\partial M}{\partial y} = V + \rho I\ddot{\theta} + P(u' - x_a\psi') \qquad (6\text{-}83)$$
$$\frac{\partial T}{\partial y} = g(y,t) - (mx_a\ddot{u} - I_a\ddot{\psi})$$

and V_L , M_L and T_L are, respectively, the values of concentrated external flexural force, bending moment and torque at the far end, i.e. $y=L$ (or $\xi=1$). P will be zero when there is no applied axial load and ρI is ignored (set to zero) when the effect of rotatory inertia is neglected.

The equilibrium of forces acting on the element is considered at a particular instant, when the beam is at maximum displacement, so the acceleration is at its maximum and the speed at that instant is zero. As a result, damping forces, which are assumed to be proportional to speed, are not present in the equilibrium. It is also important to be noted that damping forces acting on a structure are not in phase with the external and inertia forces and they are usually much smaller than these forces.

In equations (6-83), to determine $\ddot{u}$, θ and $\ddot{\psi}$, dynamic displacement and rotations (see equations 6-31) are differentiated with respect to time to give

$$u(y,t) = U(y)e^{i\omega t} \quad ; \quad \ddot{u}(y,t) = -\omega^2 U(y)e^{i\omega t} = -\omega^2 u(y,t)$$
$$\psi(y,t) = \Psi(y)e^{i\omega t} \quad ; \quad \ddot{\psi}(y,t) = -\omega^2 \Psi(y)e^{i\omega t} = -\omega^2 \psi(y,t) \qquad (6\text{-}84)$$
$$\theta(y,t) = \Theta(y)e^{i\omega t} \quad ; \quad \ddot{\theta}(y,t) = -\omega^2 \Theta(y)e^{i\omega t} = -\omega^2 \theta(y,t)$$

and there is no need to calculate u' and ψ' , because when equations (6-83) are used together with equations (6-82), they give

$$\int_L^y P(u' - x_a\psi')dy = P[(u_y - u_L) - x_a(\psi_y - \psi_L)] \qquad (6\text{-}85)$$

*6.8.2. **Stress analysis in composite beams** :* Based on the mechanics of fibrous composites (Datoo, 1991), stress analysis of composite beams is presented in this section. Stresses in each ply are a combination of normal and shear stresses induced by axial load *(P)*, bending moment *(M)*, shear force *(V)* and torque *(T)* in each cross-section. Usually there are differences in stress calculations for flat composite plates and thin-walled composite cross-sections.

6.8.2.1. Normal and shear stresses in thin-walled composite cross-sections

The common axial strain in the cross-section (ε) is

$$\varepsilon = \frac{P}{\sum_{j=1}^{NE} (E_y tb)_j} \tag{6-86}$$

where NE is the number of laminate parts which constitute the circumference of the cross-section, t is the thickness of each laminate part, b is the width of each laminate part, E_y is the membrane equivalent Young's modulus value of the laminate with reference to the y direction for each individual laminate part in the cross-section. Therefore the proportion of the axial load carried by an individual element in the cross-section is

$$P_j = (E_y tb)_j \ \varepsilon \tag{6-87}$$

Thus the individual element axial load is

$$P_j = \frac{(E_y)_j A_j}{A'} P \tag{6-88}$$

where

$$A_j = (tb)_j \tag{6-89a}$$

$$A' = \sum_{j=1}^{NE} (E_y tb)_j \tag{6-89b}$$

and the force intensity in the y direction is

$$(N_y)_j = {}^{P_j}\!/_{b} \tag{6-90}$$

Therefore, normal stresses due to the axial load (P) is given by

$$\sigma_y = \frac{(E_y)_j P}{\sum_{j=1}^{NE} (E_y tb)_j} \tag{6-91}$$

Normal stresses due to symmetrical bending are given by

$$(\sigma_y)_j = \frac{(E_y)_j Mz}{I'_{xx}} \tag{6-92}$$

where

$$I'_{xx} = \sum_{j=1}^{NE} (E_y I_{xx})_j \tag{6-93}$$

and z is the ordinate from the neutral plane of the cross-section to the point of the element under consideration.

Shear stresses due to shear forces are given by

$$\tau_{xy} = \frac{q_s}{t} \tag{6-94}$$

where

$$N_{xy} = q_s = -E_y \left(\frac{V}{I'_{xx}} \int_0^s tzds \right) + q_{s=0} \tag{6-95}$$

and

for open cross-section $$q_{s=0} = 0 \tag{6-96a}$$

for closed cross-section $$q_{s=0} = \frac{-\oint r q_{open} ds}{2\oint dA} \tag{6-96b}$$

Where r is the distance from shear centre and $\oint dA$ is the area enclosed by the closed cross-section profile. It is to be noted that for cross-sections with at least one axis of symmetry $q_{s=0}$ is always zero.

Shear stresses in closed cross-sections due to torsion are given by

$$\tau_{xy} = \frac{q_s}{t} \tag{6-97}$$

where

$$N_{xy} = q_s = \frac{T}{2\oint dA} \tag{6-98}$$

Shear stresses in open cross-sections due to torsion (T) are given by

$$\tau_{xy} = G_{xy}^{b}(2d)\frac{T}{\sum_{j=1}^{NE}\frac{1}{3}(G_{xy}^{b}bt^{3})_{j}} \tag{6-99}$$

where b is width of the element, t is thickness of the element, G_{xy}^{b} is bending equivalent shear modulus and d is the distance from the mid-plane of the element $(-t/2 \le d \le +t/2)$. τ_{xy} is a maximum where $d=t/2$.

6.8.2.2. Normal and shear stresses in flat composite cross-sections

The common axial strain in the cross-section (ε) is

$$\varepsilon = \frac{P}{E_{y}tb} \tag{6-100}$$

Therefore, normal stresses due to axial load are given by

$$\sigma_{y} = \frac{(E_{y})_{k}P}{E_{y}tb} \tag{6-101}$$

where $(E_y)_k$ is the Young's modulus value of the kth layer of the laminate in reference to the y direction.

Normal stresses due to symmetrical bending

$$\sigma_{y} = \frac{(E_{y})_{k}Mz}{I'_{xx}} \tag{6-102}$$

where

$$I'_{xx} = E_{y}^{b}I_{xx} \tag{6-103}$$

where z is the ordinate from the neutral plane of the cross-section to the point of the element in equation and E_y^b is the bending equivalent Young's modulus value of the laminate in reference to the y direction.

Shear stresses due to shear force

$$\tau_{xy} = 0 \tag{6-104a}$$

$$(\tau_{xz})_{\max} = \frac{V}{kbtG_{xy}^{b}} \tag{6-104b}$$

where k is the cross-sectional shape factor for shear.

Shear stresses due to torsion

$$\tau_{xy} = (G_{xy}^{b})_{k}(2d)\frac{T}{\frac{1}{3}(G_{xy}^{b}bt^{3})} \tag{6-105}$$

where $(G_{xy}^{b})_{k}$ is shear modulus of the *kth* layer, d is the distance from the mid-plane of the element ($-t/2 \le d \le +t/2$). τ_{xy} is maximum where $d=t/2$.

6.8.2.3. *Stresses in principal material direction:* The stress transformation from the reference axes to material axes is given below

$$\begin{bmatrix} \sigma_1 \\ \sigma_2 \\ \tau_{12} \end{bmatrix} = \begin{bmatrix} \sin^2\beta & \cos^2\beta & -2\sin\beta\cos\beta \\ \cos^2\beta & \sin^2\beta & +2\sin\beta\cos\beta \\ +\sin\beta\cos\beta & -\sin\beta\cos\beta & \sin^2\beta-\cos^2\beta \end{bmatrix} \begin{bmatrix} \sigma_x = 0 \\ \sigma_y \\ \tau_{xy} \end{bmatrix} \tag{6-106}$$

where σ_1, σ_2 and τ_{12} are the stresses in the principal material direction and β is the ply angle.

6.8.3. ***Failure criteria :*** The basic types of damage in composites are matrix cracking, fibre breakage, debonding of interface and delamination (Zhang and Zhu, 1996). Macroscopically, such damage will lead to stiffness reduction but not necessarily to structural failure. In this investigation excessive stress is used as the failure criteria of fibrous composite laminates. It is assumed that X_t, X_c, Y_t, Y_c, S_{shr} and S_{int} are the six

basic ultimate strengths of the composite material, where

X_t is the longitudinal (fibre direction) ultimate tensile strength.

X_c is the longitudinal (fibre direction) ultimate compressive strength.

Y_t is the transverse (matrix direction) ultimate tensile strength.

Y_c is the transverse (matrix direction) ultimate compressive strength.

S_{shr} is the in-plane ultimate shear strength.

S_{int} is the interlaminar ultimate shear strength.

Maximum stress theory : Ply failure occurs if any stress value in the material axes direction exceeds their respective ultimate strengths:

for tensile stresses: $\sigma_1 < X_t$ and $\sigma_2 < X_t$

for compressive stresses $|\sigma_1| < |X_c|$ and $|\sigma_2| < |X_c|$ (6-107)

for shear stresses $|\tau_{12}| < S_{shr}$ and $|\tau_{xz}| < S_{int}$

where τ_{xz} is interlaminar shear stress, σ_{12}, σ_{12} and τ_{12} are principal stresses in material direction, respectively.

The above failure criteria is a non-interactive theory, in that each stress component is looked at individually and failure in any particular direction is caused independently of the stresses acting in other directions.

Tsai-Hill theory : This theory considers an interaction of the stresses in the material axes directions. Ply failure is said to occur when the failure index, given by Tsai-Hill theory, exceeds 1. The following inequality must be satisfied for no ply failure:

$$F.I. = (\sigma_1 / X)^2 + (\sigma_2 / Y)^2 + (\tau_{12} / S_{shr})^2 - (\sigma_1 / X)(\sigma_2 / X) < 1 \qquad (6\text{-}108)$$

where $X = X_t$ or X_c and $Y = Y_t$ or Y_c. This theory will only indicate whether ply failure has occurred or not; it will not indicate the mode of failure.

This completes the dynamic stress analysis of the bending-torsion coupled composite beams.

6.9. Summary

An exact analytical method has been developed to perform the dynamic response analysis of bending-torsion coupled beams when subjected to deterministic or random loads. The theory covers both geometric and material bending-torsion coupling effects and includes effects of shear deformation, rotatory inertia and axial load in a unitary manner.

The theory developed is based on the normal mode method with generalised coordinates so that the overall response of the beam is computed by the superposition of all individual responses in each mode. The coupled bending and torsional displacements and accelerations of the beam due to the externally applied dynamic loads are first calculated. These data are then used in the expressions for the time-dependent internal shear force, bending moment and torque at a cross-section of the beam. Finally, dynamic stresses in the fibres are determined using the classical lamination theory. Failure analysis of thin-walled laminated composite beams is also incorporated.

Developing the methodology has involved a significant amount of original work using analytical mechanics, calculus of partial differential equations, symbolic computing, variational analysis, structural dynamics of continuous systems, random vibration and spectral analysis, and mechanics of fibrous composites.

In the next chapter, the theory developed here is applied to a number of bending-torsion coupled metallic and composite beams and numerical results are presented, commented on and discussed.

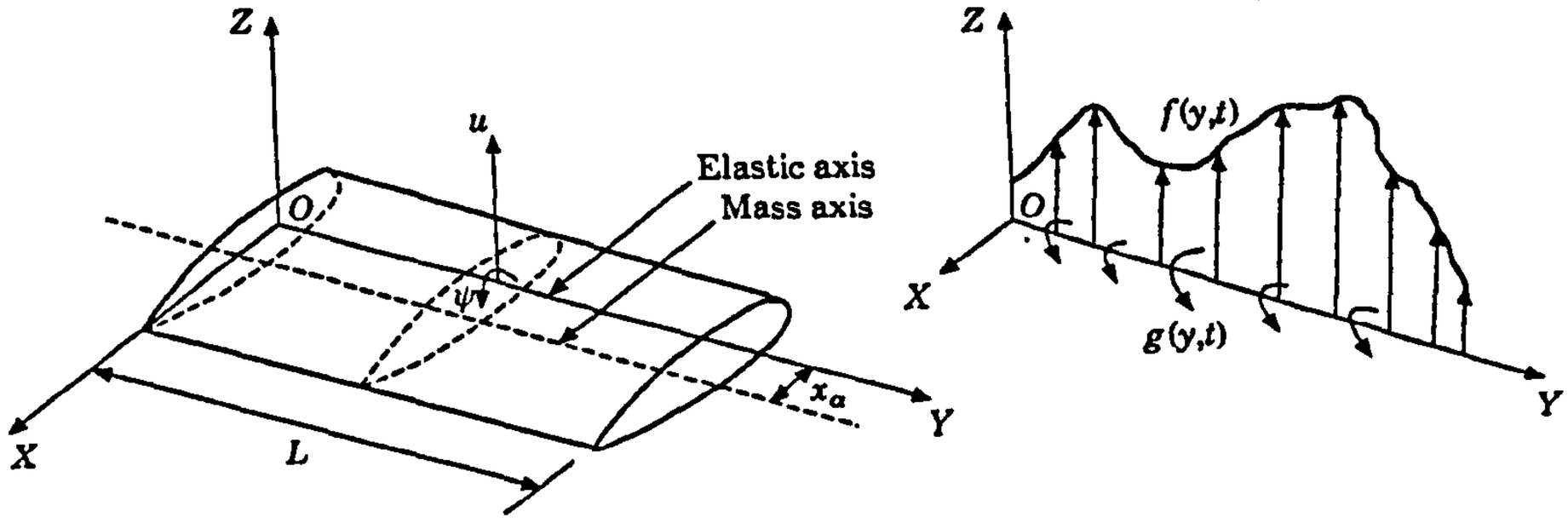

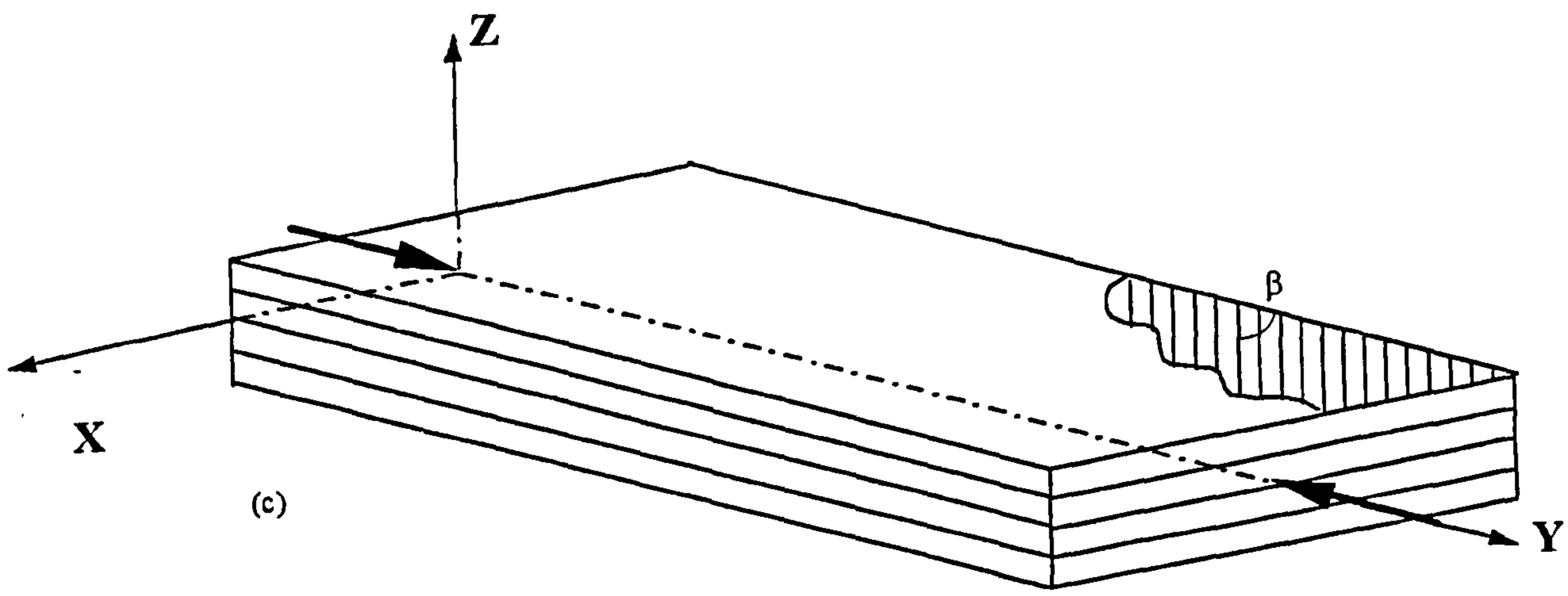

$$c_x^2 = 1 - mx_\alpha^2 / I_\alpha = (I_\alpha - mx_\alpha^2) / I_\alpha$$

$$I_\alpha = \rho I_p \quad ; \quad I_p = I_G + Ax_\alpha^2 \quad ; \quad I_G = I_{xx} + I_{zz}$$

$$c_x^2 = I_G / I_p = I_G / (I_G + Ax_\alpha^2)$$

$$a^2 = I_\alpha \omega^2 L^2 / GJ$$

$$b^2 = m\omega^2 L^4 / EI_{xx}$$

$$p^2 = PL^2 / EI_{xx}$$

$$r^2 = I_{xx} / AL^2$$

$$s^2 = EI_{xx} / kAGL^2$$

$$c_k^2 = 1 - K^2 / EI_{xx}.GJ$$

I_α = Polar mass moment of inertia about shear centre
I_P = Polar moment of inertia about shear centre
I_G = Polar moment of inertia about mass centre
I_{XX} = Moment of inertia of the cross-sectional area about X-axis
I_{ZZ} = Moment of inertia of the cross-sectional area about Z-axis
J = Torsion constant
A = Area of cross-section

Figure 6-1. (a) The coordinate system and notation for coupled bending-torsional vibration of a beam; —— elastic axis, - - - - mass axis; (b) The distribution of bending and torsional loads; (c) Composite laminates and fibre angle.

Chapter Seven

Dynamics of composite beams :

Results and discussions

7 Dynamics of composite beams : Results and discussions

7.1. Introduction

Based on the theories developed in ***Chapter Six***, illustrative results for free and forced vibration of several bending-torsion coupled metallic and composite beams are obtained and presented in this chapter. A suite of computer programs in FORTRAN was developed for this purpose. The programs have been written, debugged and validated during the course of this investigation, to determine the free vibration characteristics and dynamic response behaviour of bending-torsion coupled beams. A list of these computer programs and a brief description of their application are given in ***Appendix F***.

Results presented in this chapter are given in two separate sections. Firstly, numerical results are given for metallic beams for which only geometric coupling exists. By way of illustration, seven different types of metallic beams with geometric (bending-torsion) coupling have been selected from published literature to show every possible case of important primary as well as secondary effects. Mechanical properties of these beams are given in Table 7-1.

Results are then presented for seven selected composite beams in all of which significant material coupling exists between bending and torsional modes of deformation. Flexural, torsional and coupling rigidities of three composite beams , namely, a flat beam (Jensen, et al., 1982), a box beam (Cesnik, et al., 1996) and a bi-convex beam (Librescu, et al., 1996), have been given in ***Chapter Three*** (see Figure 3-1 to 3-3). The mechanical properties of the composite materials used for these three beams and two other composite beams (Teboub and Hajela, 1995; Dancila and Armanios, 1995) are given in Table 7-2. Numerical results are also given for two more composite beams. One was examined by Eslimy-Isfahany and Banerjee (1996a) and the other by Teoh and Huang (1977) and Banerjee and Williams (1996).

In order to examine fully and to understand the free vibration and dynamic response

characteristics of bending-torsion coupled composite beams, very many numerical results were obtained during the course of this research, for many metallic and composite illustrative examples. However, only a carefully selected set of representative results are given in this chapter, in order to present a comprehensive account of observations made in this investigation, in a concise form. Thus, when presenting the results, similar or repetitive results are -wherever possible- avoided in different cases.

In ***Sections 7.2*** and ***7.3***, firstly, the effects of bending-torsion coupling, axial load, shear deformation and rotatory inertia on free vibration analysis of coupled beams, with different boundary conditions, are investigated. Numerical results are then presented giving the dynamic response of bending-torsion coupled beams subjected to a time dependent harmonic varying force. The contribution from each mode to the dynamic response of bending-torsion coupled beams is of particular interest.

Next, results are presented to demonstrate the behaviour of bending-torsion coupled beams when subjected to random excitation, using both concentrated and uniformly distributed forces. The effects of damping ratio, bending-torsion coupling, axial load, shear deformation and rotatory inertia in these studies are investigated. Several classical boundary conditions (S-S, C-F, C-S and C-C) are considered. For composite beams, the effects of material (bending-torsion) coupling and ply orientation on the free and forced vibration analysis are investigated and results are given for dynamic stresses in bending-torsion coupled composite beams.

The accuracy of the dynamic stiffness method in predicting the natural frequencies is demonstrated by comparing the results for a range of metallic and composite beams with those available in the literature. For example, explicit analytical solutions are available in the literature for the free vibration analysis of bending-torsion coupled metallic beams with simply supported end conditions. Thus, at the beginning of ***Section 7.2***, results obtained from the present theory are given for such beams and compared with the existing literature.

Two important concepts are further discussed here. One is the interpretation of normal modes using the concept of generalised mass in each mode of vibration. The other one is the significance of modal interchanges between flexural and torsional modes of vibration, which may occur due to the effects of axial load, shear deformation and/or rotatory inertia. Variation in ply orientation is an important cause of modal interchange in composite beams.

When composite aircraft wings are in an air stream, there will be a significant amount of aerodynamic damping (provided there is wing flexure), and structural damping is a small fraction of the total damping in the structure. However, in the present investigation the bending-torsion coupled beam is not considered to be in forward motion, hence the beam is not assumed to be subjected to oscillatory aerodynamic forces. Thus, in the absence of aerodynamic damping, only arbitrary values of structural damping has been taken in to account. This optional value of damping ratio is assumed to be a constant value in all the modes.

All the results presented are fully discussed and commented on. A schematic check list of presented results is given in Table 7-3 where secondary effects are symbolised by the following non-dimensional parameters, namely, effects of shear deformation by ($s^2=EI/kAG\ L^2$), rotatory inertia by ($r^2=I\ /\ AL^2$ or L/r), axial load by ($p^2=PL^2\ /\ EI$), geometric coupling by ($c_x^2=\ 1-\ mx_\alpha^2/I_\alpha$) and material coupling by ($c_k^2=\ K^2/EI\ GJ$). In Table 7-3, ζ indicates that the effect of damping ratio on the dynamic response is demonstrated. Figure 7-1 shows a schematic flow-chart of all the results presented in this chapter.

7.2. Bending-torsion coupled beams with geometric coupling only

7.2.1. Free vibration characteristics : Free vibration analysis of geometrically bending-torsion coupled beams is investigated and the accuracy of the dynamic stiffness method in predicting the natural frequencies and mode shapes is demonstrated by comparing these frequencies with results for a range of bending-torsion coupled beams having different

cross-sections which are available in the literature. In all the Figures in this chapter where mode shapes are shown a solid line is used for flexural displacements and a broken line is for torsional ones.

7.2.1.1. Natural frequencies and mode shapes of a bending-torsion coupled beam with simply supported end conditions : The natural frequencies and mode shapes of undamped free vibration of the Goland wing (Goland, 1945) are computed using the method proposed by Timoshenko and Young (1955) and compared with the results obtained from the theory presented in this thesis. The Timoshenko and Young (1955) method is an exact solution, but valid for bending-torsion coupled metallic beams with simply supported end conditions only. Therefore, for validation purposes the wing is assumed to have (S-S) boundary conditions. Mechanical properties of the wing are given in Table 7-1.

The two methods produced precisely the same results for free vibration analysis of the wing with (S-S) boundary conditions. The first five mode shapes and corresponding frequencies are shown in Figure 7-2. All the modes show substantial coupling between bending displacements and torsional rotations. A convergence study has been performed to find the optimum number of modes that is required in the response analysis to produce accurate results. It is found that in most cases, the first four modes have the most significant contribution in the response.

Once the natural frequencies and mode shapes of the beam are obtained, modal analysis is then used to compute the dynamic response of the structure, namely the flexural displacement and torsional rotation, and some statistical response such as mean square values of the dynamic flexural and torsional displacements. These dynamic responses are useful in structural design, while the statistical dynamic response plays an important role in structural reliability analysis.

The dynamic flexural displacements and torsional rotations at the mid-span of the beam due to a harmonically varying concentrated flexural force of unit amplitude at the mid-span, versus the forcing frequency are plotted in Figures 7-3 and 7-4, respectively. The

response of the beam becomes larger whenever the forcing frequency is near one of the natural frequencies. Note that there is no peak close to the third frequency, because load is applied in the middle of the beam, which is a node for the third mode of vibration, so that the third mode does not have any contribution to the response. Damping ratio is considered to be $\zeta=0.02$ in all modes.

For random vibration analysis, the externally applied flexural force is a uniformly distributed load for which the cross-spectral density function $S_f(\Omega)$ is assumed to be an ideal white noise, where $S_f(\Omega) = S_f$ with S_f being a constant. The results of the analysis showing the mean square values of the flexural displacement and the torsional rotation along the beam for different damping ratios are illustrated in Figures 7-5 and 7-6, respectively. These show that the mean square values of the flexural displacement and torsional rotation decrease when damping ratio increases.

Figures 7-3 to 7-6 show a torsional response for both deterministic and random response, although the beam is subjected only to a flexural force. This has occurred due to the presence of geometric bending-torsion coupling.

7.2.1.2. *Natural frequencies of bending-torsion coupled beams* : In this section the first five coupled natural frequencies of three different bending-torsion coupled beams with cantilever end conditions are calculated and compared with those of published by other authors (see Tables 7-4 to 7-6). Friberg (1985), Banerjee and Fisher (1992), Leung and Zeng (1994) and Bercin and Tanaka (1997) have determined coupled natural frequencies of a bending-torsion coupled beam with a semi-circular cross-section (see beam no.4 Table 7-1). Bercin and Tanaka (1997) have calculated coupled natural frequencies of a concrete channel beam (see beam no.5 Table 7-1) and a box beam with axial slit (see beam no.7 Table 7-1). It is evident from Tables 7-4 to 7-6 that the agreement between the results calculated by the present method and those obtained by Friberg (Tables 7-4) and Bercin and Tanaka (Tables 7-4 to 7-6) is very close, which proves the validity of the present method. Note that warping effects were neglected when using Friberg's method.

7.2.2. Response of Goland wing to deterministic and random loads : The Goland wing (Goland, 1945) is actually a typical cantilever aircraft wing, for which flexural and torsional motions are inertially coupled (see Table 7-1). This wing is not subjected to an axial load, and the effects of shear deformation and rotatory inertia are ignored. The undamped free vibration natural frequencies and mode shapes of the wing are computed by setting the damping coefficients c_1, c_2 and the external forces $f(y,t)$ and $g(y,t)$ in equations (6-1) and (6-2) to zero. The natural frequencies of the wing are plotted against the frequency number n, and shown in Figure 7-7, and the corresponding mode shapes of the first five normal modes are illustrated in Figure 7-8. The natural frequencies are quite well separated and the modes generated show substantial coupling between flexural displacements and torsional rotations. Note that these first five normal modes were subsequently found to be sufficient to describe the response of the wing quite accurately (i.e., the contribution from the modes higher than the fifth was not found to be significant).

Two types of loading are considered next. In the first, the flexural and torsional responses due to a harmonically varying concentrated flexural force, with constant amplitude F, are calculated. Figures 7-9 and 7-10, respectively, show the dynamic flexural and torsional displacements at mid-span and tip of the wing when a harmonic flexural force of unit amplitude is applied at the tip. The value of the damping ratio(ζ) has been taken to be *0.01* for these results. Peak responses in these figures correspond to wing natural frequencies as expected.

To compare results obtained from the present theory with those given by the simple Bernoulli-Euler beam theory, the dynamic flexural displacement at a distance $y = 4\ m$ from the wing root (which is about *0.67* of the span) is calculated using both theories. The beam is subjected to a unit harmonically varying concentrated force acting at the tip. The two sets of results are obtained, using the present theory and also simple Bernoulli-Euler beam theory, and are shown in Figure 7-11. Although the response of the wing in the fundamental mode is very little altered, the response behaviour in higher modes predicted by the present theory is significantly different from that predicted by the simple Bernoulli-

Euler beam theory (see Figure 7-11). The present theory has predicted a substantial response of the wing in torsion due to the bending-torsion coupling effect. Clearly the simple Bernoulli-Euler beam theory would not predict such a response. Results for the torsional response at this *67%* span are not presented, but they are similar to those obtained for at the tip and mid-span as shown in Figure 7-10.

The second loading is considered to be a uniformly distributed random atmospheric turbulence acting in the flexural direction only. Atmospheric turbulence is modelled by the well known von Karman spectrum which is illustrated in Figure 7-12 for $L_s/V_s = 1$, together with the first five natural frequencies of the wing.

The mean square values of the output responses in flexure and in torsion are presented in Figures 7-13 and 7-14, respectively, in which three representative values of the ratio of scale length to air speed (L_s/V_s) are used for a fixed value of the damping ratio $\zeta = 0.05$. The corresponding effects of the variation of ζ on the output responses are shown in Figures 7-15 and 7-16, for one fixed value of $L_s/V_s = 10$.

To compare once again results obtained from the present theory with those given by the simple Bernoulli-Euler beam theory, the mean square values of the flexural and torsional responses at the tip of the wing were calculated for $\zeta = 0.01$ and $L_s/V_s = 1$ using both theories. The results are shown in Table 7-7. The difference in results in flexure is noticeable but, more importantly, in the simple Bernoulli-Euler beam theory the torsional response of the wing is neglected completely.

7.2.3. Effect of axial load on the dynamic response of a wind turbine blade : Results are obtained for an axially loaded bending-torsion coupled beam which is, in fact, a wind turbine blade (Petersen, 1979) with cantilever end conditions (see Table 7-1). In the analysis the damping ratio ζ is taken to be *0.01* for all modes.

Three load levels are considered : $P = 190000\ N$ (which is about *50%* of the elastic critical buckling load of the cantilever) $P = 0$ and $P = -190000\ N$ (tension). The first ten natural

frequencies of the blade are shown in Table 7-8. The effect of axial load on the natural frequencies is quite noticeable. The presence of the compressive load has reduced the natural frequencies as expected. For instance, the difference in results when compared with the unloaded (P=0) case is 28% in the first natural frequency and 3% in the second natural frequency. In contrast, the presence of the tensile load has predictably increased the natural frequencies by 20% in the first mode and 2% in the second mode.

The corresponding mode shapes of the first five natural frequencies for those three levels of axial load are shown in Figure 7-17. For all loading cases, substantial coupling exists between bending displacements and torsional rotations in the free vibrational modes of the blade, except for the fundamental one. The corresponding natural frequencies and mode shapes for the degenerate case of the simple Bernoulli-Euler beam theory and Saint-Venant's torsion theory in which the bending-torsion coupling effect is ignored (when $x_\alpha=0$ in the present theory) for $P=0$, are shown and compared with the coupled case in Figure 7-18. For the degenerate case this clearly indicates torsion-free bending and bending-free torsion as expected. The difference between the two sets of results in Figures 7-18a and 7-18b is quite noticeable, particularly for higher modes.

To compare results obtained from the present theory with those given by the simple Bernoulli-Euler beam theory, the dynamic flexural displacement at the tip of the blade due to a unit harmonically varying concentrated force acting at the same point, was calculated using the modes shown in Figures 7-18, respectively. The difference between the two sets of results obtained from the two theories is illustrated in Figure 7-19, showing that the response of the blade in the fundamental mode is very little altered whereas the response behaviour in higher modes has significantly changed. This may be attributed to the fact that the fundamental mode of the blade is predominantly a bending mode with torsional coupling (deformation) almost non-existent in Figure 7-18a whereas for all other modes there is significant coupling between bending displacement and torsional rotation.

The dynamic flexural and torsional displacements at the mid-span and at the tip of the blade due to a harmonically varying concentrated flexural force of unit amplitude applied

at the tip, for three different levels of axial load are shown respectively in Figures 7-20.

In the case of random loading, the externally applied force is assumed to be uniformly distributed as an ideal white noise over the blade length and is assumed to act only in the flexural direction. The mean square values of the flexural displacement and torsional rotation from root to tip of the blade, for three different levels of axial load are shown in Figures 7-21a and 7-21b. A compressive axial load increases the mean square values of the flexural and torsional response and a tensile axial load decreases them.

For both sets of deterministic and random loadings, it was found that the first five normal modes were sufficient to describe the response of this particular problem adequately.

7.2.4. Non-dimensional bending-torsion coupled natural frequency graphs : A graph showing non-dimensional coupled natural frequencies of a bending-torsion coupled beam with cantilever boundary conditions is illustrated in Figure 7-22. It relates the first uncoupled flexural frequency (ω_b) and the first uncoupled torsional frequency (ω_t) of the beam to the first coupled frequency (ω_c) of the bending-torsion coupled beam. Figure 7-22 shows the non-dimensional coupled frequencies for various values of the geometric coupling parameter (c_x^2).

This is a universal graph and the fundamental natural frequencies of a series of bending-torsion coupled beams can be extracted from it. The geometric coupling parameter (c_x^2) varies between zero (heavily coupled) to 1 (uncoupled). Effects of shear deformation and rotatory inertia are neglected in Figure 7-22. Similar graphs can be produced for higher modes, other boundary conditions, beams with axial load and/or with effects of shear deformation and rotatory inertia. It is also possible to produce graphs to show the non-dimensional coupled frequencies for various values of the material coupling parameter (c_k^2) for composite beams.

7.2.5. Significance of generalised mass in the free and forced vibration characteristics of bending-torsion coupled beams: An investigation has been carried out on the

significance of generalised mass in order to gain further insight into the dynamic characteristics of bending-torsion coupled beams in each mode. The investigation confirms that appearance of a mode shape in the form of displacements only, may not be sufficient to identify whether that particular mode is bending or torsion dominated, or whether that mode is coupled. By looking at the mode shape one is not comparing like with like (i.e. a linear displacement with angle of twist).

From the orthogonality condition of the principal modes of free vibration of the bending-torsion coupled beams, it can be shown that the generalised mass of such beams is given by (see equation 6-35)

$$\int_0^1 \{mU_n^2 + I_\alpha \Psi_n^2 - 2mx_\alpha (U_n \Psi_n)\} d\xi = \mu_n \qquad (7\text{-}1)$$

where m is the mass per unit length, I_α is the mass moment of inertia per unit length about the Y-axis, U_n and Ψ_n are the *nth* flexural and torsional mode shapes respectively, x_α is the distance between the mass and the elastic axes and μ_n is the generalised mass in the *nth* mode. The generalised mass μ_n is comprised of three parts : mU_n^2 which is due to flexure alone, $I_\alpha \Psi_n^2$ which is due to torsion alone and $2mx_\alpha(U_n \Psi_n)$ which is due to bending-torsion coupling. In each of the modes of vibration, the contribution of each term in equation (7-1) is a measure of the importance of that term to generalised mass and hence to the response characteristics of that mode.

Results are given for five bending-torsion coupled (metallic) beams with cantilever end conditions (see Table 7-1). For simplicity these beams have been numbered from ① to ⑤ as follows; ① is the Goland wing (Goland, 1945), ② is the Loaring wing, ③ is the box beam with axial slit (Banerjee, 1989), ④ is the thin-walled semi-circle (Friberg, 1985) and ⑤ the concrete channel (Bercin and Tanaka, 1997). Each beam is subjected in turn to a unit transverse force or to a unit torque at the tip. The externally applied force and torque are random in nature with an ideal white noise power spectral density. Generalised masses for flexural ($mL/4$ kgm^2) and torsional ($I_\alpha L/2$ kgm^2) uncoupled vibration of these beams

are given in Table 7-9. In undamped uncoupled free vibration of beams, generalised masses for each of the flexural and torsional modes are constant in all the modes. Figures 7-23 to 7-27 show the results of this investigation for beams ① to ⑤, respectively. The following results are given for each beam; *(a)* the first six frequencies and mode shapes, *(b)* comparison of generalised mass in each bending-torsion coupled mode with generalised mass in purely flexural or torsional modes, *(c)* contribution of each term (bending, torsion and coupling) to the generalised mass in different modes, *(d)* percentage of modal contribution in the response of the beam at the tip due to a flexural load at the tip and *(e)* percentage of modal contribution in the response of the beam at the tip due to a torque at the tip. The following observations were made when analysing the results

(i) Beam subjected to transverse load : The following comments are relevant;

The first few bending dominated modes have made the largest contribution to the dynamic flexural displacement for all the beams. See beam ① first mode, beam ② first mode, beam ③ first, second and third modes, beam ④ first and second modes and beam ⑤ fifth mode.

The first few coupled modes have made the largest contribution to the dynamic torsional rotation for all the beams. See beam ① first and second modes, beam ② first and third modes, beam ③ first, second and third modes, beam ④ first and second modes and beam ⑤ fifth mode.

Torsion dominated modes with little or no coupling have little contribution to the dynamic flexural displacement or the torsional rotation (see beam ⑤ first, second, third and fourth modes).

(ii) Beam subjected to torque : The following comments are relevant;

The first few torsion dominated modes have made the largest contribution to the dynamic torsional rotation for all the beams. See beam ① second mode, beam ② third mode, beam ③ first, and third modes, beam ④ second mode and beam ⑤ first mode.

Although the exciting loads contain all frequencies in equal proportions, the contribution of

each mode in the overall response falls with increasing mode number, because the complex impedance increases with mode number. As a consequence of that, the first few coupled modes have the largest contribution to the dynamic flexural displacement. See beam ① first and second modes, beam ② first and third modes, beam ③ first, second and third modes, beam ④ first and second modes and beam ⑤ fifth mode.

Coupled (bending or torsion dominated) modes have some contribution to the dynamic torsional rotations. See beam ④ first and third modes.

Bending dominated modes with little or no coupling have no significant contribution to the dynamic flexural displacement or the torsional rotation (see beam ② second mode and beam ⑤ second, third and fourth modes).

Beam ③; the first three modes look like torsion dominated modes, but the second mode is a bending dominated mode and all of them are heavily coupled.

Beam ④; the first, second and sixth modes look like torsion dominated modes, whilst the, first and sixth modes are bending dominated modes and all of them are heavily coupled. This is mostly due to a relatively small moment of inertia per unit length (I_α).

Beam ⑤; the fifth mode looks like a torsion dominated mode, whereas, it is in fact a heavily coupled bending dominated mode.

*7.2.6. **Effects of shear deformation and rotatory inertia on bending-torsion coupled frequencies** :* The effects of shear deformation and rotatory inertia on the natural frequencies and mode shapes of simple uncoupled Bernoulli-Euler or Timoshenko beams have been well-documented in the literature. They usually reduce the flexural natural frequencies of beams, but do not affect the torsional modes of vibration. The effect can be more significant on short beams and those with high thickness/length ratio. Also, higher frequencies and mode shapes are relatively more sensitive to these effects than the lower modes, because the inter-nodal distance decreases with mode number.

In the case of bending-torsion coupled beams, these effects can be very different and the use of general statements similar to those of uncoupled case may not apply. To investigate the effects of shear deformation and rotatory inertia on the free vibration characteristics of bending-torsion coupled beams, an independent study has been carried out on a number of metallic beams. The cantilever turbine blade (Petersen, 1979), which was used in ***Section 7.2.3***, here has been chosen with a different length as a representative illustrative example. Results are shown in Figures 7-28 to 7-31 and are explained in the following paragraphs.

The first six natural frequencies and mode shapes of the turbine blade ($L = 2.6\ m$), with and without effects of shear deformation and rotatory inertia, are given in Figures 7-28a and 7-28b, respectively. Natural frequencies are lower when the effects of shear deformation and rotatory inertia are included. The first two mode shapes are virtually identical in both cases. Changes appear from the third mode onwards and more interestingly, a modal interchange takes place between the fourth and the fifth modes.

Figure 7-29 shows the variation of the first six natural frequencies of the turbine blade against slenderness ratio (L/r). It also indicates whether the frequency pertains to a bending (B) or a torsional (T) dominated mode. For each mode of vibration, the variation of non-dimensional frequencies for different values of s^2 against slenderness ratio (L/r) is given in Figure 7-30, whilst Figure 7-31 show the corresponding cross-plot of frequency against s^2 for different values of slenderness ratio (L/r).

Shear deformation and rotatory inertia will affect natural frequencies and mode shapes in all modes since the modes are all coupled in bending and torsion. Obviously, the effect will be relatively more significant on bending dominated modes by decreasing the natural frequencies. Lower frequencies in short bending-torsion coupled beams and those with high thickness/length ratio, are usually torsion dominated modes. Generally, the effects of shear deformation and rotatory inertia will be more pronounced on higher modes, whereas for beams with relatively higher (L/r) ratio, these effects will be more pronounced on lower modes. Effects of shear deformation and rotatory inertia may cause the very important phenomenon of modal interchange as shown in Figures 7-28 and 7-29.

7.3. Composite beams

7.3.1. Free vibration characteristics : In this section free vibration analysis of bending-torsion coupled composite beams is investigated and the accuracy of the dynamic stiffness method in predicting the natural frequencies and mode shapes is demonstrated by comparing with results for a range of composite beams with varying lay-ups and different cross-sections that are available in the literature.

First, bending torsion coupled composite beams made of flat graphite (carbon)/epoxy laminates with lay up $[\beta_2 /0°]_s$ are considered, because the free vibration characteristics of such composite beams have been quite extensively investigated (Crawley, 1979; Jensen, et al., 1982; Jensen, and Crawley, 1984; Georghiades, 1997). The natural frequencies of these beams, with cantilever end conditions, were calculated by using the dynamic stiffness matrix method. Table 7-10 shows these results (eighth and ninth columns), along with those of Jensen and Crawley (1984). The results show that the natural frequencies given by the Rayleigh Ritz and partial Ritz (beam) methods are consistently higher than those from the dynamic stiffness formulation, and that the Rayleigh Ritz solutions with four modes and the partial Ritz solutions with two modes are less accurate when compared with detailed finite element analysis and experimental results. Interestingly, Rayleigh Ritz with five modes and partial Ritz with three modes gave better accuracy than the dynamic stiffness method. However, this conclusion is specific to the range of problems of Table 7-10 and so cannot be taken as a general rule. Another important difference is that the choice of assumed modes is very problem dependent and hence subjective judgement often has to be made in deciding the approximate shapes, whereas the dynamic stiffness matrix method has no such limitation and hence gives consistently good results for any type of composite beam problem. Note that, because of the fragile nature of unidirectional laminates, Jensen, and Crawley (1984) have given numerical and experimental results for $[0_2/90]_s$ instead of $[0_2/0]_s$.

The second example is the cantilever rectangular box beam (Dancila, and Armanios, 1995) with lay up: $[\beta]_6$ in the top wall, $[-\beta]_6$ in the bottom wall and $[\beta/-\beta]_3$ in the

vertical walls. This CAS box beam configuration exhibits bending-torsion coupling. The cross-section of the above box beam has the following specifications: exterior width = *24.21 (mm)* and exterior height = *13.46 (mm)* with $L = 0.84455$ *(m)*, $m = 0.0882$ *(kg/m)* , $I_\alpha = 9.61725x10^6$ *(kgm)* and the total thickness = *0.762 (mm)*. Using the material properties given in Table 7-2, the rigidity properties were calculated for a wide range of the values of the ply orientation. Then using the dynamic stiffness matrix method, the free vibration natural frequencies of the beam are computed for different fibre angles. Table 7-11 shows the first ten natural frequencies calculated by the present dynamic stiffness matrix method alongside the theoretical results of Dancila and Armanios (1995). The agreement between the two sets of results is well within *1.5%*. The symbols *T* denotes torsion dominated modes, whereas *B* denotes bending dominated modes.

The third example is a bending torsion coupled graphite/epoxy laminated cantilever beam of solid rectangular cross-section and with all its plies at either 15° or 30°, for which Teboub. and Hajela (1995) recently gave theoretical and experimental results. The beam has $L = 0.1905$ *m*, width = *0.0127 m*, thickness = *0.003175 m* and its material properties are given in Table 7-2. The bending, torsional and bending torsion coupling rigidities were calculated using the HARP model as $EI = 3.568\ Nm^2$, $GJ = 1.553\ Nm^2$ and $K = 1.668\ Nm^2$ for the $\beta=15°$ lay up case, and $EI = 1.596\ Nm^2$, $GJ = 2.158\ Nm^2$ and $K = 1.369\ Nm^2$ for the $\beta=30°$ lay up case. For both cases $m = 0.0625\ kg/m$ and $I_\alpha = 0.8926x10^6\ kgm$ were used. Table 7-12 shows the first six natural frequencies calculated by the present dynamic stiffness matrix method alongside the theoretical and experimental results given by Teboub. and Hajela (1995). It should be noted that the theoretical model used by them to obtain the above results did not predict the torsional modes. The agreement of the results from the dynamic stiffness method with those of experimental and theoretical results is very good. The disagreement is usually within 1.5% except for the 4th natural frequency for the 15° lay up and the 5th natural frequency for the 30° lay up, which are both torsional frequencies and where the differences are 14% and 12%, respectively.

7.3.2. Effects of material bending- torsion coupling on the free and forced vibration of a composite beam: Material bending-torsion coupling, which usually exists in composite beams, is considered in this section. Using computer programs based on the theory developed in ***Chapter Six***, the response of a bending-torsion coupled composite beam due to both deterministic and random loads is computed. The data used for a flat composite beam (Eslimy-Isfahany and Banerjee, 1996a) are as follows : (i) bending rigidity $EI = 9.75x10^6\ Nm^2$, (ii) torsional rigidity $GJ = 9.88x10^5\ Nm^2$, (iii) bending-torsion coupling rigidity $K = 2.19x10^6\ Nm^2$, (iv) mass per unit length $m=35.75\ kg/m$, (v) mass moment of inertia per unit length $I_\alpha = 8.65\ kgm$ and (vi) length of the beam $L = 6\ m$.

The first five natural frequencies and mode shapes of the above beam with cantilever end conditions are shown in Figure 7-32. The modes generated are clearly all coupled. Using these normal modes, the response of the beam to a harmonically varying concentrated flexural force of amplitude F applied at the tip is evaluated. Figures 7-33 shows both the flexural and torsional response at mid-span and tip respectively against the frequency of the forcing function. The non-dimensional damping ratio in each mode (ζ_n) was set to 0.05. There is significant amount of torsional response at both the tip (Figure 7-33b) and mid-span (Figure 7-33a) of the beam, even though there is only flexural load applied at the tip. This response is clearly induced by modal coupling.

The next set of results was obtained when the beam was excited by a uniformly distributed flexural random load over its length. Ideal white noise of constant power spectral density S_f was used to represent the random load. The mean square values of both the flexural displacement and the torsional rotation along the length of the beam were computed and are shown in Figure 7-34, using a non-dimensional damping ratio of 0.05. Torsional response is again evident even though the random load is entirely flexural, for the reason given above. A convergence test of results (based on modal elimination technique) showed that the first five normal modes of the beam shown in Figure 7-32 were sufficient to describe both the deterministic and random response of the beam sufficiently accurately.

In order to illustrate the effects of bending-torsion coupling on the response, the three main rigidities, *EI*, *GJ* and *K*, are combined to give two non-dimensional parameters. One is the bending-torsion cross-coupling parameter defined as $K^2/(EI\ GJ)$, the other is the ratio between the torsional and bending rigidity defined as *GJ/EI*. The value of $K^2/(EI\ GJ)$ was varied by changing *K* while *GJ/EI* was kept constant at *0.101*. Note that $K^2/(EI\ GJ)$ is always between zero and one (Weisshaar and Foist, 1985). The mass and inertial properties of the beam were not changed. The computed mean square values of the flexural displacement and torsional rotation at mid-span and tip due to the same random loading acting in the flexural direction are shown in Figures 7-35a and 7-35b, respectively. The cross-coupling parameter has a dominant effect on both flexural and torsional response when it is above *0.7*. For most practical cases, however, the value the cross-coupling parameter is expected to be less than *0.7* (see ***Chapter Three***). The torsional response in the absence of any torsional load is again quite pronounced both at mid-span and at the tip of the beam (see Figures 7-35).

*7.3.3. **Dynamic response of composite box wing :*** A graphite/epoxy composite wing with a thin-walled rectangular box cross-section, as shown in Figure 3-2a, is considered and for which flexural and torsional motions are coupled as a result of the intrinsic nature of laminated fibrous composites. This Circumferentially Asymmetric Stiffness (CAS) configuration exhibits bending-torsional coupling because it has [+β/+β] lay-up on the top wall, [-β/-β] on the bottom wall and [+β/-β] on the side walls. Firstly, the effects of ply orientation on rigidity properties and their subsequent effects on response characteristics are demonstrated. The variations of the bending (*EI*), torsional (*GJ*) and bending-torsional coupling (*K*) rigidities with ply angles are established using the theory of Armanios and Badir and have already been shown in Figure 3-2b.

Using these rigidities and the dynamic stiffness method, the free vibration characteristics of the wing with cantilever end conditions are investigated for various ply angles. The variation of the first five natural frequencies of the wing against ply angles is shown in

Figure 7-36. The effect of ply orientation on natural frequencies is quite pronounced as can be seen. The essential purpose of Figure 7-36 is, however, to show trends and modal interchanges as a result of ply orientations which can be interpreted as follows. The first mode is basically a fundamental bending mode (with a small amount of torsion in it) and remains so for all ply angles. The second mode starts as a torsional mode in the region $0<\beta<10$, and then becomes a bending dominated mode as β is increased. The variation of the third natural frequency reveals a different picture. It is predominantly a bending mode in the region $0<\beta<10$; however, it becomes a predominantly torsional mode in the region $10<\beta<25$, and predominantly bending again in the region $25<\beta<70$, before finally becoming a predominantly torsional mode again. In contrast, the fourth natural frequency first starts as a torsional mode within the range $0<\beta<10$, then it becomes a bending dominated mode within the range $10<\beta<25$. Subsequently, it becomes torsion dominated again within the range $25<\beta<70$, before finally becoming a bending mode. The modal interchange (flip-over) between modes 3 and 4 around $\beta = 70$ deg is noticeable, i.e. the third bending mode becomes the first torsion whereas the first torsion becomes the third bending mode. Finally the fifth mode starts as a torsional mode and remains so until $\beta = 15$ deg and then it becomes a bending mode within the range $15<\beta<90$.

Representative results for the first five natural frequencies and mode shapes of the wing for different fibre angles ($\beta = 10, 15, 20, 25, 30, 60, 70, 80$ deg) are shown in Figure 7-37. When $\beta = 10$ deg, apart from the first mode (which has significant coupling between bending and torsion), the wing exhibits predominantly torsional deformation as can be seen, see Figures 7-36 and 7-37. It is evident form Figure 7-36 that a modal interchange has occurred between the third and the fourth mode of vibration around 70 deg. This can also be seen in Figure 7-37, where mode shapes clearly show a modal flip over.

Note that the first five modes of the wing were used in the response analysis for both deterministic and random loads and were subsequently found to be adequate. Damping was assumed to be 3% in all modes, i.e. $\zeta_n = 0.03$.

The amplitudes of the dynamic flexural and torsional displacements at the tip of the wing under the action of a harmonically varying concentrated flexural force of unit amplitude applied at the same point (tip), are computed using the present theory. The results for $\beta =$ *10* deg are shown in Figure 7-38 where the absolute values of the response are shown. The peaks in Figure 7-38 correspond to the natural frequencies of the wing as expected. For instance, the first peak occurs around the first natural frequency, i.e. *149 rad/s*, whereas the second and third peaks occur around second and third natural frequencies, i.e. *811, 1089 rad/s*, see Figures 7-37 and 7-38. Note that the results shown in Figure 7-38 are obtained under the action of flexural load only, but a dynamic torsional rotation is again evident as a consequence of the (material) coupling effect. Because of the intrinsic nature of the material coupling present in laminated (fibrous) composites, the two displacements (bending and torsion), must not be considered in isolation. At the tip where there is a concentrated flexural load (but no torsional load), the amplitude of the flexural response (unlike the torsional one) is always in the same direction as the applied load. However, for certain forcing frequencies, sudden drops in the torsional response occur as shown (in the logarithmic scale) in Figure 7-38. This indicates a change in sign for the torsional rotation induced by flexural displacement.

Next, the flexural and torsional response of the wing due to a uniformly distributed atmospheric turbulence modelled by the von Karman spectra, defined by equation (6-79), is investigated. The spectrum is shown in Figure 7-39 for three different values of L/V. The excitation is again assumed to be flexural only. The mean square values of the bending displacements and torsional rotations against ply angle (β) are shown in Figure 7-40a and 7-40b respectively, for two different values of L/V ratio. These figures show that the torsional response arises solely due to material bending-torsion coupling. Because the bending rigidity reduces with the increase in ply angle (see Figure 3-2b), the flexural response increases as a consequence. However, no such predictable pattern can be observed for the flexure induced torsional response that has been computed in the absence of any externally applied torsional load. This investigation shows that the flexure induced

torsional response is quite a complex phenomenon, which is primarily dependent upon the bending-torsion coupling rigidity. Finally, the flexural and torsional responses were computed at various points on the wing. The mean square values of the flexural displacement and torsional rotation along the length of the wing for $\beta=10$ deg are shown in Figure 7-41a and 7-41b respectively for two values of the damping ratio. Both flexural and torsional responses are at their maximum at the tip as expected. The investigation has shown that for both deterministic and random excitation, response induced by material coupling as a consequence of ply orientation can be significant.

7.3.4. Effects of shear deformation, rotatory inertia and axial load on the free vibration of a composite beam with rectangular cross-section: A cantilever glass-epoxy composite beam (Teoh and Huang, 1977 and Banerjee and Williams, 1996) is chosen here to demonstrate the effects of shear deformation, rotatory inertia and axial load on the free vibration of composite beams. The beam is of rectangular cross-section with *width = 12.7 mm* and *thickness = 3.18 mm*. It is made up of unidirectional plies with fibre angles in each ply set to $\beta = +15$ *deg*. (From a computational point of view, the beam is equivalent to a single thick ply.) Following the models described in ***Chapter Three***, the rigidity properties of the beam were calculated as follows ; (i) bending rigidity *(EI) = 0.2865* Nm^2; (ii) torsional rigidity *(GJ)=0.1891* Nm^2;(iii) bending torsion coupling rigidity *(K)=0.1143* Nm^2; (iv) shear rigidity *(kAG) = 6343.3 N*; whilst other properties are : (v) mass per unit length *(m) = 0.0544 kg/m*; (vi) mass moment of inertia per unit length $(I_\alpha) = 0.7770 \times 10^{-6}$ *kgm*; (vii) length of the beam *(L) = 0.1905 m*.

The first sets of results were obtained to show the variation of the first six natural frequencies with the slenderness ratio (L/r) of the beam for different boundary conditions when the axial load is set to zero (see Figures 7-42a to 7-42d). Bending-torsion coupled natural frequencies are plotted with and without the inclusion of shear deformation and rotatory inertia effects. For all cases, natural frequencies decrease when L/r increases, as expected. Unlike the simple Bernoulli-Euler metallic beam, the effects of shear

deformation and rotatory inertia are not necessarily at their maximum when the slenderness ratio is at a minimum. The reason for this can be attributed to the fact that the modes generated are all bending-torsion coupled modes. Also, changing the *L/r* ratio can alter a bending dominated mode to a torsion dominated one and vice-versa. Of course, for a torsion dominated mode, the effects of shear deformation and rotatory inertia are expected to be relatively small. For a given *L/r* ratio, the effects of shear deformation and rotatory inertia are more pronounced in higher natural frequencies, particularly when the mode is dominated by bending deformation. This accords with the well known trends observed in simple Bernoulli-Euler or Timoshenko beam theory.

Another intriguing feature of the results shown in Figures 7-42a to 7-42d is that for certain *L/r* ratios, modal interchanges are seen to have taken place, particularly between higher modes. For instance, in Figures 7-42a which gives results for the C-C case, modal couplings between modes 2 and 3 around $L/r = 80$, and between 5 and 6 around $L/r = 130$ are apparent. The modal coupling is also evident for the C-S, S-S and C-F cases. Due recognition to modal coupling must, therefore, be given when studying the free vibration characteristics of composite beams.

Representative results are shown in Table 7-13 for the first six natural frequencies of the cantilever (C-F) beam with and without the effects of shear deformation, rotatory inertia and axial load, noting that these effects can be uniquely described by the parameters r^2, s^2 and p^2 (see Figure 6-1). The natural frequencies shown in columns 2 and 3 agreed completely with those given by Banerjee and Williams (1996). The shear deformation and rotatory inertia are seen to have a relatively marginal effect on the natural frequencies of this particular composite beam, as was observed by Banerjee and Williams (1996). The axial load is taken to be about *50%* of the critical buckling load of the cantilever ($P=0.5P_{cr}$ where $P_{cr}=14.8N$) which corresponds to the non-dimensional values of $p^2=-0.95$ and $p^2=0.95$ for the tensile and compressive loads, respectively. The axial load has made quite a significant difference to the fundamental natural frequency of the beam as can be seen in Table 7-13. Similar to previous examples of geometric bending-torsion coupled beams

presented in ***Section 7.2***, a compressive axial load has reduced the natural frequencies whereas a tensile one has increased them. The fourth and fifth natural frequencies are virtually unaltered because these frequencies, unlike the first three, represent torsion dominated modes for which the axial load does not have any major effect.

The next set of results was obtained to illustrate the sole effect of the axial load on the fundamental natural frequency of the beam by ignoring the effects of shear deformation and rotatory inertia (i.e. s^2 =0 and r^2 =0). Figure 7-43 shows the variation of the first natural frequency of the beam with the non-dimensional axial load P/P_{cr} for different boundary conditions. The change in the natural frequency due to axial load is noticeable. The natural frequency diminishes when the axial load changes from tensile to compressive as expected. Finally, for all cases, at $P/P_{cr}=1$, the natural frequency becomes zero which implies that, at this load level, buckling of the composite column occurs as a degenerate case of natural vibration at zero frequency which is a case of the duality between buckling and natural vibration problems (Wittrick, 1968).

This investigation on the effects of shear deformation, rotatory inertia and axial load on free vibration of composite beam has shown that significant changes in natural frequencies can occur as a result of changing these parameters.

7.3.5. Effects of shear deformation, rotatory inertia and axial load on the free and forced vibration of a bi-convex composite wing : A cantilever composite wing with bi-convex cross-section (Librescu et. al., 1996) is considered now. Attention here is confined to the effect of bending-torsion material coupling only. This effect is prevalent in composite wings but non-existent in metallic ones. The cross-section of the wing is shown in Figure 3-3a. This bi-convex cross-section has Circumferentially Asymmetric Stiffness (CAS) configuration so that it exhibits bending-torsional coupling while undergoing free vibration. The rigidity properties of the wing for different ply angles are independently established using the theory of Armanios and Badir and have already been shown in Figure 3-3b. Note that the elastic constants and other properties used to obtain these

results, are those of Carbon-Fibre Reinforced Plastic (CFRP) taken from (Librescu et. al., 1996). In this section, the effects of shear deformation, rotatory inertia and axial load on the free and forced vibration of the composite wing are investigated, in the order given.

Next, the free vibration characteristics of this composite wing are investigated using the dynamic stiffness method. The variation of the first six natural frequencies against ply angles is shown in Figure 7-44, both with and without the effect of shear deformation. Although, the effect of shear deformation is not so pronounced on the first two frequencies, higher frequencies have significantly altered as can be seen. Figure 7-44 shows that the variation of natural frequencies due to ply orientation is quite noticeable. The effect of rotatory inertia was also investigated but it did not have any significant influence on the natural frequencies of this particular wing. Representative results for natural frequencies and mode shapes corresponding to the fibre angle $\beta=10\ deg$ are shown in Figure 7-45, both with and without the inclusion of the shear deformation effect. The bending deformation in the fundamental mode is quite evident whereas the rest of the modes are dominated by torsional displacements only. The inclusion of shear deformation has made hardly any difference to the mode shapes except to the sixth one.

Representative results for free vibration and response behaviour to deterministic and random loads, corresponding to the fibre angle $\beta = 10$ deg. are given next. Three axial load levels are considered in the analysis. These are : (i) $P=70000\ N$ (which is almost 50% of the lowest critical buckling load of the beam), (ii) $P=0$ and (iii) $P=-140000\ N$ (tension). Damping is assumed to be 3% in all modes.

Table 7-14 shows the effect of axial load on the first five natural frequencies of the beam. The presence of the compressive load has reduced the natural frequencies; for instance, the difference in results when compared with the unloaded case ($P=0$) is 29% in the first natural frequency. In contrast, the presence of the tensile load has predictably increased the natural frequencies by 37% in the first mode. For all loading cases, substantial coupling exists between bending displacement and torsional rotations in the free vibrational modes

of the beam. The effect of axial load on the sixth natural frequency of the beam is less than *1%* and is not given here.

The amplitude of dynamic flexural and torsional displacements at the tip of the beam under a harmonically varying concentrated flexural force of unit amplitude applied at the tip, for the above three levels of axial load, are computed using the present theory and are shown in Figures 7-46a and 7-46b, respectively. The peaks in Figures 7-46 correspond to the natural frequencies of the beam as expected. Note that the results shown in these figures are obtained under the action of flexural load only, but a dynamic torsional rotation is evident as a consequence of the material bending-torsion coupling effect.

In the case of random loading, two types of power spectra are considered. Firstly, the wing is assumed to be subjected to an atmospheric turbulence, modelled using the von Karman spectra (see equation 6-79). The excitation is assumed to be entirely flexural, so that any torsional response arises solely due to bending-torsion (material) coupling. The mean square values of the dynamic response of the bending displacements and torsional rotations against ply orientation are shown in Figures 7-47a and 7-47b respectively, both with and without the inclusion of shear deformation. The results show that shear deformation has a relatively small effect on the torsional response of the beam, whereas for small ply angles it has made about *10%* difference to the bending response.

Next, the externally applied flexural force is assumed to be uniformly distributed as an ideal white noise over the beam's length. The mean square values of the flexural displacement and torsional rotation for three different axial loads, are shown in Figures 7-48a and 7-48b, from root to tip of the beam. As in the case of deterministic load, the torsional response is induced by modal coupling only. The use of the Bernoulli-Euler or Timoshenko beam theory would not predict such a response.

The first six modes of the beam were used in the response analysis (and were subsequently found to be adequate) for both deterministic and random response analysis.

7.3.6. Dynamic stress analysis : Dynamic stresses in the laminated carbon/epoxy composite box wing (Figure 3-2) are considered now, for which the (material) coupling between bending and torsional deformations can be significant. The composite beam has cantilever end conditions. The variations of these natural frequencies with ply angle are shown in Figure 7-36. The modal interchanges from bending to torsional mode and vice-versa, which are due to changes in ply orientations, were observed in all natural frequencies except the fundamental. This particular feature of modal interchanges in thin-walled composite beams was discussed in details earlier in this chapter (see ***Section 7.3.2***).

The theory on the dynamic response given in ***Chapter Six*** accounts for both deterministic and random loads as inputs, but numerical results for illustrative purposes are given only for the random case when the wing is subjected to atmospheric turbulence as modelled by the von Karman spectra. It was assumed that this externally applied random load was purely flexural. The first five normal modes were used in the response analysis which were subsequently found to be adequate.

The variation of the mean-square value of the flexural and torsional displacements of the mid-plane of the box, along the wing-span, is shown in Figure 7-49. These results were obtained for a ply angle $\beta=10$ *deg*. Note that an inspection of the first five normal modes used in the analysis, for this particular ply orientation revealed that they were all dominated by torsional deformation (see Figure 7-37). The maximum response (both flexural and torsional) occurs at the tip of the cantilever as expected but, more importantly, the torsional response in the absence of any externally applied torsional load is significantly pronounced in Figure 7-49. Clearly such a torsional response is a direct consequence of material coupling induced by the fibre orientations in the laminate. The variations of the flexural and torsional accelerations along the wing-span are shown in Figure 7-50 where the flexure induced torsional acceleration is also pronounced.

The mean-square values of the bending moment (M), shear force (V) and torque (T) were computed based on the above results (see Figures 7-49 and 7-50). The variation of the

mean square values of the bending moment and shear force along the span is shown in Figure 7-51a, and that of torque is shown in Figure 7-51b. The maximum of bending moment, shear force and torque occurs at the root of the cantilever as expected. The results show that the a significant amount of torsional load is experienced by the wing even though the externally applied load is entirely flexural. The bending-torsion coupling effect due to the directional nature of fibrous composites is again a contributory factor to explain this phenomenon.

Next, a dynamic stress analysis is carried out. For illustrative purposes, attention is focused at the mid-span cross-section of the wing. The variations of mean-square values of both displacements and accelerations for bending and torsional motions at mid-plane of this cross-section against ply angles are shown in Figures 7-52 and 7-53, respectively. The maximum flexural displacement occurs when the fibre angle β=*90 deg* (see Figure 7-52). This is expected because the bending rigidity is at its minimum for this ply angle (see Figure 3-2). However, the reason for the maximum torsional displacement around β=*35 deg* (see Figure 7-52) is not so obvious although it could be argued that the strong bending-torsion coupling present for this fibre orientation (see Figure 3-2) might have caused this large torsional displacement at mid-span. The results on accelerations (see Figure 7-53) indicate that the flexural acceleration is at its maximum when β is *90 deg* (which is expected) whereas the maximum torsional acceleration occurs when β is around *10 deg*. The normal modes of the wing for this fibre angle showed that it deforms primarily in torsion, which might have attributed to this large torsional acceleration.

In order to determine the stresses, the dynamic internal forces (i.e. bending moment, shear force and torque) were calculated at the mid-span for various ply angles. The variation of the mean-square values of the bending moment and shear force with ply angle at the mid-span are shown in Figure 7-54a and for torque in Figure 7-54b. The results of Figures 7-54 are subsequently used to calculate the stresses σ_1 , σ_2 and τ_{12}. The variation of the mean-square value of these stresses at the mid-span of the wing against ply angle is shown

in Figure 7-55. It is quite apparent from this figure that σ_1 , σ_2 and τ_{12} reach their maximum values when the fibre angles are *0 deg*, *90 deg* and *45 deg* respectively.

Representative results are given to demonstrate the effect of axial load on dynamic response and stresses of the composite wing to random loads, corresponding to the fibre angle $\beta = 10\ deg$. Three axial load levels are considered in the analysis. These are : (i) *P=80 kN* (compressive load which is almost *50%* of the lowest critical buckling load of the wing), (ii) *P=0* and (iii) *P=-160 kN* (tensile load). For all loading cases, substantial coupling exists between bending displacement and torsional rotations in the free vibrational modes of the wing. Damping was assumed to be *3%* in all modes.

Axial load has a pronounced effect on the first five natural frequencies of the wing, as shown in Table 7-15 for the three load cases. The presence of the compressive load has reduced the natural frequencies; for instance, the difference in results when compared with the unloaded case (*P=0*) is *27 %* in the first natural frequency. In contrast, the presence of the tensile load has predictably increased the natural frequencies by *36 %* in the first mode.

Numerical results are given when the wing is subjected to atmospheric turbulence as modelled by the von Karman spectra. It is assumed that this externally applied random load is entirely flexural with no torsional component present. The mean square values of the flexural displacement and torsional rotation from root to tip of the wing, for three different axial loads, are respectively shown in Figures 7-56a and 7-56b. A dynamic torsional rotation is evident as a direct consequence of the bending-torsion coupling induced by the fibre orientations in the laminate. The variations of the flexural and torsional accelerations along the wing-span are shown in Figures 7-57a and 7-57b, where the flexure induced torsional acceleration is even more pronounced. The maximum response (both flexural and torsional) occurs at the tip of the cantilever.

Next, the mean-square values of the bending moment (M), shear force (V) and torque (T) for the ply angle, $\beta = 10\ deg$, were computed using a normal distribution. The variation of shear force, bending moment and torque along the span are shown in Figures 7-58. The

maximum of each of the bending moment, shear force and torque occurs at the root of the cantilever.

Finally, the effects of variation of the non-dimensional axial load (P/P_{cr}) on dynamic response are shown in Figures 7-59. A detailed stress analysis for the above loading conditions is carried out by varying the axial load. For illustrative purposes, stresses are calculated at the middle of the top wall on the mid-span of the wing. The variations of stresses in the principal material direction (σ_1 , σ_2 and τ_{12}) against the non-dimensional axial load (P/P_{cr}) for the fibre angle $\beta = 10\ deg$, are shown in Figure 7-59d. The results of Figures 7-59 show that flexural and torsional displacement and their respective acceleration, shear force, bending moment, torque and stresses increase with the increase in (P/P_{cr}), as expected. The investigation has shown that the dynamic stresses in composite wings are heavily influenced by fibre angle and axial load (β, P).

7.4. Summary

The general exact analytical method developed in ***Chapter Six***, has been applied to a number of bending-torsion coupled beams, representative of aircraft wings, wind turbine blades, composite beams and composite wings, for which a substantial amount of coupling between the bending and torsional modes of deformation was prevalent. Numerical results are given and discussed for these beams when subjected to time dependent deterministic or random loads. Significant conclusions are drawn from these results.

Both free and forced vibration characteristics of bending-torsion coupled beams have been investigated. The accuracy of the method in predicting the natural frequencies has been demonstrated by comparing results obtained from the analysis of a range of metallic and composite beams having different cross-section and varying lay-ups with those available in the literature.

In some of the illustrative examples given, attention is mainly confined to the effect of bending-torsion coupling on the free and forced vibration of the coupled beams. This

affects the natural frequencies and the mode shapes of different beams differently. Although the coupling effect on the natural frequencies is sometimes relatively small, the corresponding effect on the mode shapes of the beam may be significant. Generally it was observed that both geometric and material bending-torsion coupling reduce the fundamental natural frequency of the beam. With regard to dynamic response, when a bending-torsion coupled beam is subjected to a purely transverse force, usually there is a significant difference in flexural response of the beam when compared to Bernoulli-Euler theory but, more importantly, a torsional (that is rotational) response is evident. The latter is due to geometric and/or material bending-torsion coupling effect. Simple Bernoulli-Euler or Timoshenko beam theory cannot predict such response, because such theories assume torsion free bending and bending free torsion. It has been shown that due recognition to modal coupling must be given when studying the free and forced vibration characteristics of bending-torsion coupled metallic or composite beams.

Ideally an infinite number of modes is needed to calculate exactly the dynamic response of a continuous system. However, in practice, depending on the type of the loading, only a few carefully chosen modes are needed to predict the response with reasonable accuracy. In most of the cases, for both sets of deterministic and random loadings, it has been found that the first four to six normal modes were sufficient to describe the response of the particular problem investigated. The number of modes considered in the analysis is indicated for each illustrative example.

Numerical results are given for all standard classical boundary conditions, showing the effects of shear deformation, rotatory inertia, axial load and slenderness ratio on natural frequencies. The investigation has shown that significant changes in natural frequencies can occur as a result of changing these parameters and mode shapes can vary considerably as result of changes in natural frequencies.

The effect of a constant axial load on the free vibration and dynamic response of the beam is also noticeable. Effects of a compressive axial load are opposite to those of a tensile

load. A compressive axial load reduces the natural frequencies and increases the dynamic response of the beam whereas the tensile load has a stabilising effect, increasing the natural frequencies and reducing the dynamic response.

Shear deformation and rotatory inertia will affect natural frequencies and mode shapes in almost all modes since most of the modes are coupled in bending and torsion. Obviously, the effect will be relatively more significant on bending dominated modes, decreasing the natural frequencies. Lower frequencies in short bending-torsion coupled beams and those with high thickness/length ratio, are usually torsion dominated modes. Generally, the effects of shear deformation and rotatory inertia are much more pronounced on higher modes, whereas for beams with relatively higher (L/r) ratio, these effects will be more pronounced on lower modes. Effects of shear deformation and rotatory inertia may also cause the very important phenomenon of modal interchange. They always increase the dynamic response of the coupled beams.

The effects of ply orientation on rigidity properties and their subsequent effects on natural frequencies, mode shapes and dynamic response characteristics of composite beams are demonstrated. The investigation has shown that response induced by material coupling as a consequence of ply orientation can be significant. The investigation has shown that the dynamic stresses in composite wings are heavily influenced by fibre angle, axial load and the effects of shear deformation and rotatory inertia.

Table 7-1 Mechanical properties of six chosen isotropic bending-torsion coupled beams.

	EI ($N m^2$)	**GJ** ($N m^2$)	**m** (kg/m)	$\mathbf{I_\alpha}$ (kg-m)	$\mathbf{x_\alpha}$ (m)	**L** (m)
1.Goland wing (Goland, 1945)	9.7567×10^6	9.88×10^5	35.75	8.65	0.183	6.096
2.Loaring Wing (Loaring, 1944)	677.6	1019	8.06	0.0585	0.038	2.06
3.Box beam with axial slit (Banerjee, 1989)	5.8×10^4	78.3	2.45	0.02	0.08	5
4.Thin-walled semi-circle (Friberg, 1985)	6380.14	43.46	0.835	0.000501	0.0155	0.82
5.Concrete channel beam (Bercin and Tanaka, 1997)	30.43×10^7	97.83×10^4	225	56.87	0.336	3.2
6.Wind turbine blade (Petersen, 1979)	2.2101×10^7	5.1483×10^6	112	21.8	0.153	12
7.Box beam with axial slit (Bercin and Tanaka, 1997)	14.36×10^4	346.71	4.256	0.0317	0.0735	2.7

Table 7-2 Material properties of three chosen composite beams.

	$\mathbf{E_1}$ (GPa)	$\mathbf{E_2=E_3}$ (GPa)	$\mathbf{G_{12}}$ (GPa)	$\mathbf{G_{23}}$ (GPa)	$\mathbf{G_{13}}$ (GPa)	$\nu_{12}=\nu_{13}$	ν_{23}	ρ (kg/m^3)
Flat beam (Jensen, et al., 1982)	98.0	7.9	5.6	5.6	5.6	0.28		1520
Flat beam (Teboub and Hajela, 1995	129.11	9.408	5.1568	2.541	4.304	0.3		1550.1
Box beam (Cesnik, et al., 1996)	206.92	5.17	3.10	2.55	2.55	0.25		1529
Box beam (Dancila and Armanios, 1995)	142.0	9.8	6.0	4.83	6.0	0.42	0.5	1604.1
Bi-convex beam (Librescu, et al., 1996)	206.8	5.17	3.1	2.55	2.55	0.25		1400

Table 7-3. A schematic check list of results presented in this chapter.

	Metallic beams						Composite beams					
	7.2.1	7.2.2	7.2.3	7.2.4	7.2.5	7.2.6	7.3.1	7.3.2	7.3.3	7.3.4	7.3.5	7.3.6
cross-section	*DMB*	*Goland wing*	*WTB*	-	*DMB*	*WTB*	*DCB*	*flat beam*	*wing box*	*flat beam*	*bi-convex*	*wing box*
Secondary effects discussed in details	ζ	c_x^2 ζ	p^2 c_x^2 ζ	c_x^2	c_x^2	s^2 & r^2		c_k^2	ζ	s^2 & r^2 p^2	s^2 & r^2 β p^2	β p^2
frequencies	*T 7-4* *T 7-5* *T 7-6*	F7-7 F7-12	*T 7-8*	F7-22		F7-29 F7-30 F7-31	*T 7-10* *T 7-11* *T 7-12*		F7-36	F7-42 F7-43 *T 7-13*	F7-44 *T 7-14*	*T 7-15*
mode shapes and generalised mass	F7-2	F7-8	F7-17 F7-18		F7-23 F7-24 F7-25 F7-26 F7-27 *T 7-9*	F7-28		F7-32	F7-37		F7-45	
deterministic response	F7-3 F7-4	F7-9 F7-10 F7-11	F7-19 F7-20					F7-33	F7-38		F7-46	
Random response (white noise spectra)	F7-5 F7-6		F7-21		F7-23 F7-24 F7-25 F7-26 F7-27			F7-34 F7-35	F7-39 F7-40 F7-41		F7-48	
Random response (von Karman spectra)		F7-12 F7-13 F7-14 F7-15 F7-16 *T 7-7*									F7-47	F7-49 F7-50 F7-52 F7-53 F7-56 F7-57
Dynamic forces and stresses when beam is subjected to random loads												F7-51 F7-54 F7-55 F7-58 F7-59

WTB : wind turbine blade; F: Figure; T: Table; DMB: different metallic beams; DCB: different composite beams.

Table 7-4. Natural frequencies (Hz) of a cantilever semi-circular beam.

Frequency No.	Friberg (1985) and Bercin and Tanaka (1997)	Present method
1	63.39	62.34
2	129.34	129.88
3	259.22	259.21
4	415.72	418.91
5	607.29	605.20

Table 7-5. Natural frequencies (Hz) of a cantilever channel beam.

Frequency No.	Bercin and Tanaka (1997)	Present method
1	10.19	10.19
2	30.34	30.57
3	50.99	51.17
4	69.68	71.60
5	91.60	86.34

Table 7-6. Natural frequencies (Hz) of a cantilever box beam with an axial slit. (Bercin and Tanaka, 1997)

Frequency No.	Bercin and Tanaka (1997)	Present method
1	8.30	8.31
2	23.79	23.81
3	36.63	36.56
4	47.21	47.26
5	67.15	67.18

Table 7-7 Mean square values of the flexural and torsional responses at the wing tip obtained by using the present theory and Bernoulli-Euler theory (ζ=0.01 and L_e/V=1)

		Present theory	Bernoulli-Euler theory
Flexural	$\langle u^2\rangle/\sigma_f^2 \times 10^{10}$ (s^2)	20.13	22.09
Torsional	$\langle \psi^2\rangle/\sigma_f^2 \times 10^{11}$ (rad s/m)^2	13.18	-

Table 7-8 Natural frequencies of an axially loaded cantilever turbine blade with different axial loads.

Frequency number	Frequency (rad/s)		
	P=190 kN	P=0	P=-190 kN
1	7.8	10.8	13.0
2	62.4	64.4	65.8
3	70.1	71.2	72.8
4	177.3	179.5	181.6
5	211.4	212.3	213.2
6	319.9	321.8	323.7
7	374.9	376.4	377.9
8	470.7	472.8	474.9
9	554.3	556.1	557.8
10	636.1	638.7	641.4

Table 7-9 Generalised mass for flexural and torsional uncoupled vibration of bending-torsion coupled beams, given in Table 7-1.

	$mL/4$ (kgm^2)	$I_\alpha L/2$ (kgm^2)
Goland Wing	54.483	23.365
Loaring Wing	4.1509	0.060255
Box Beam with an axial slit	3.0625	0.05
Semi-circle, thin-walled	0.171175	2.0541×10^{-4}
Concrete Channel Beam	180.0	90.992

Table 7-10 Comparison of natural frequencies (Hz) of $[\beta_2/0]_s$ lay-up composite beam using various methods with B and T respectively indicating predominantly bending or torsional modes (Jensen, Crawley, 1984).

Ply angle β(deg)	Mode	Finite element (365 DoF)	Rayleigh-Ritz (4modes)	Rayleigh-Ritz (5modes)	Partial-Ritz (2 modes)	Partial-Ritz (3 modes)	DSM (HARP)	DSM (CRLP)	Exp. Results
0	B1	11.1	11.1	11.1	11.1	11.1	11.1	11.1	11.2
	T1	39.5	39.6	39.6	39.7	39.7	33.2	31.4	42.4
	B2	69.5	69.4	69.3	72.1	72.0	69.2	69.3	70.5
15	B1	8.9	8.8	8.7	9.0	9.0	8.1	8.1	9.4
	T1	42.9	48.8	48.2	44.5	43.5	41.0	40.4	45.8
	B2	62.7	60.5	59.9	66.9	65.0	52.6	52.5	66.2
30	B1	6.3	6.2	6.2	6.4	6.3	5.6	5.6	6.6
	B2	37.3	42.0	42.0	39.4	38.9	33.9	33.9	40.0
	T1	56.9	69.0	60.7	70.9	58.5	51.4	60.9	59.1
45	B1	4.9	4.9	4.8	4.9	4.9	4.6	4.6	4.8
	B2	30.1	32.7	32.6	31.6	31.5	28.2	28.3	29.8
	T1	49 4	73.9	56.3	74.1	51.2	45.0	66.2	51.3
60	B1	4.2	4.2	4.2	4.2	4.2	4.1	4.1	4.3
	B2	26.1	27.0	26.8	27.2	27.2	25.4	25.6	27.1
	T1	41.7	65.4	47.1	65.4	42.7	38.4	59.4	47.7
75	B1	3.9	3.9	3.9	3.9	3.9	3.8	3.9	3.8
	B2	24.3	24.5	24.4	25.3	25.3	24.2	24.3	25.1
	T1	36.7	47.2	39.2	47.4	37.0	34.5	42.7	38.9
90	B1	3.8	3.8	3.8	3.8	3.8	3.8	3.8	3.7
	B2	23.9	23.9	23.9	23.8	23.8	23.8	23.8	24.3
	T1	35.1	35.1	35.1	35.2	35.2	33.2	31.4	38.2

Dof : Degree of Freedom

Table 7-11 Natural frequencies (Hz) for the Circumferentially Asymmetric Stiffness (CAS) cantilever box-beam with lay-up: $[\beta]_6$ in the top wall, $[-\beta]_6$ in the bottom wall and $[\beta/-\beta]_3$ in the vertical walls. T indicates pure torsional mode (Dancila and Armanios, 1995).

	β= 0°		β=15°		β=30°		β=45°		β= 60°		β=75°		β=9 0°	
Mode No	D/A	Present	D/A	Present	D/A	Present	D/A	Present	D/A	Present	D/A	Present	D/A	Present
1	43.757	44.307	30.568	30.800	19.920	20.031	14.688	14.766	12.516	12.619	11.697	11.832	11.491	11.639
2	274.22	277.67	191.10	192.55	124.74	125.42	92.025	92.512	78.432	79.075	73.304	74.149	72.014	72.938
3	483.17T1	484.58T1	532.73	536.76	348.74	350.65	257.56	258.92	219.59	221.39	205.25	207.62	201.64	204.23
4	767.83	777.47	701.76T1	709.69T1	681.56	685.35	504.35	507.03	430.23	433.76	402.20	406.83	395.14	400.21
5	1449.5T2	1453.7T2	1040.1	1047.9	862.68T1	875.48T1	782.42T1	792.72T1	660.07T1	666.50T1	557.98T1	561.55T1	483.17T1	484.58T1
6	1504.6	1523.5	1700.7	1713.4	1124.5	1130.8	833.49	837.99	711.14	716.98	664.85	672.51	653.19	661.57
7		2422.9	2113.6T2	2137.5T2	1673.7	1683.1	1243.3	1250.0	1062.0	1070.7	993.12	1004.6	975.75	988.27
8	2487.3	2518.5	2520.0	2538.7	2323.8	2337.4	1733.9	1743.4	1482.7	1495.0	1387.0	1403.0		1380.3
9		3392.1		3485.8	2593.6T2	2631.7T2	2302.4	2315.9	1970.9	1987.8	1674.0T2	1684.7T2	1449.5T2	1453.7T2
10		3762.3		3587.5		3101.5	2352.0T2	2382.2T2	1983.0T2	2001.7T2	1846.5	1867.9	1837.7	

Table 7-12.Natural frequencies (Hz) for the unidirectional graphite/epoxy cantilever beam (Teboub and Hajela, 1995).

	15°			30°		
Mode No	T/H	expt	present	T/H	expt	present
1	85.4	82.5	82.1	52.7	52.7	52.6
2	531.5	511.3	511.3	329.8	331.8	328.8
3	1472.2	1423.4	1413.8	921.7	924.7	917.4
4	-	1526.9	1741.4	1801.4	1766.9	1783.9
5	2839.1	2783.6	2743.6	-	1827.5	2050.0

Table 7-13. Natural frequencies of a cantilever composite beam with and without the effects of shear deformation (s^2), rotatory inertia (r^2) and axial load (p^2).

Frequency No	Natural frequency (rad/sec)			
	$r^2 = s^2 = 0$	$r^2 = 0.00002322$ and $s^2 = 0.001245$		
	$p^2 = 0$	$p^2 = 0$	$p^2 = 0.95$	$p^2 = -0.95$
1	193.6	193.2	138.2	233.1
2	1211	1192	1140	1242
3	3376	3260	3216	3303
4	4076	4073	4070	4076
5	6596	6196	6155	6238
6	10780	9832	9791	9872

Table 7-14 Natural frequencies of an axially loaded cantilever beam with different axial loads

	Frequency (rad/s)		
Frequency no.	*P=70 kN*	*P=0*	*P=-140kN*
1	99.4	139.3	191.3
2	707.0	740.4	801.4
3	1061.4	1077.8	1111.3
4	1791.5	1824.9	1890.5
5	2991.5	3022.7	3083.3

Table 7-15 Natural frequencies of an axially loaded composite wing with different axial loads

Frequency No.	Frequency, rad/s		
	P = 80 kN	P = 0	P = -160 kN
1	109.2	149.0	202.7
2	785.8	810.9	853.1
3	1075	1089	1121
4	2075	2100	2147
5	3296	3309	3336

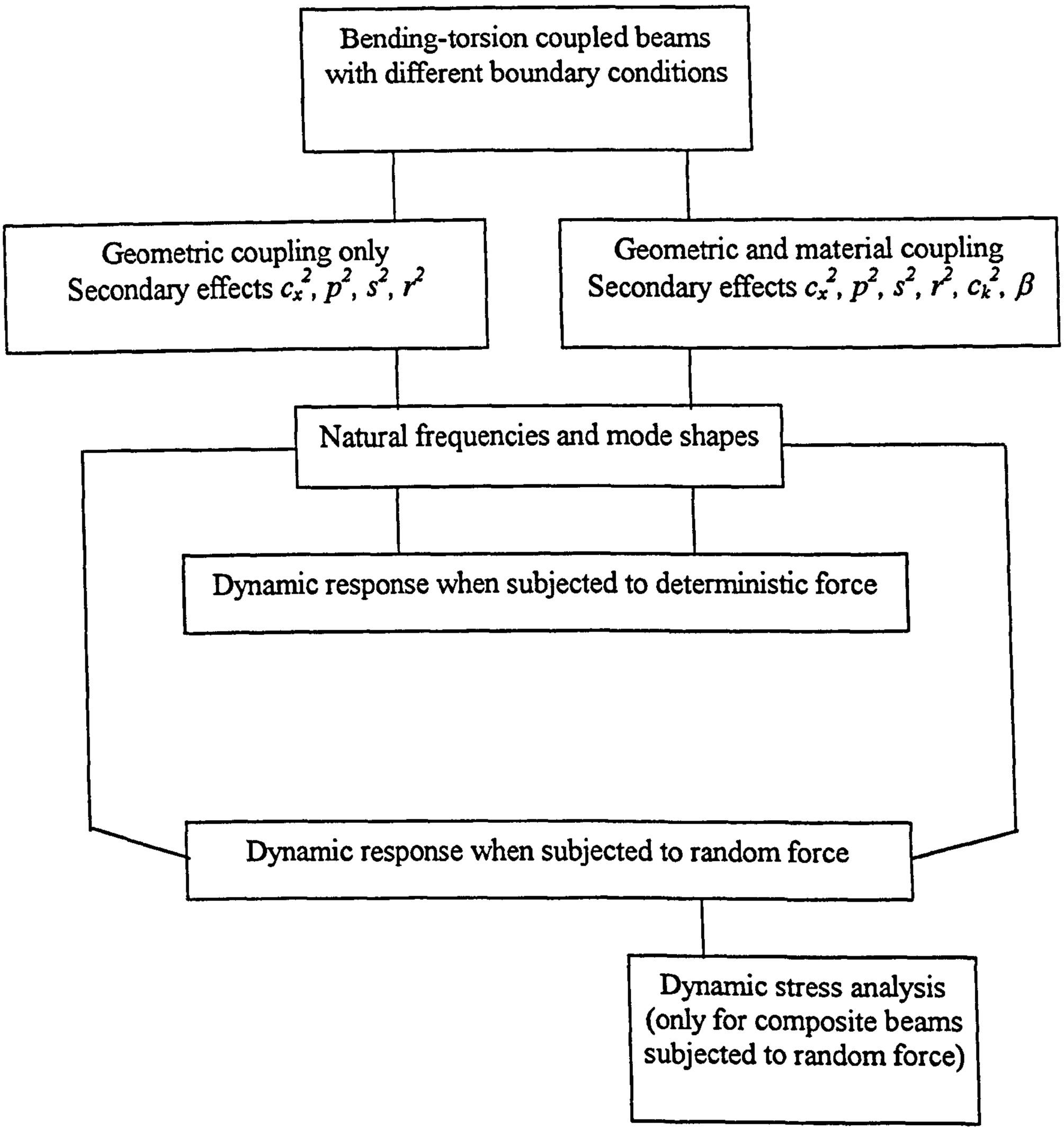

Figure 7-1. A schematic flow-chart of results presented in this chapter.

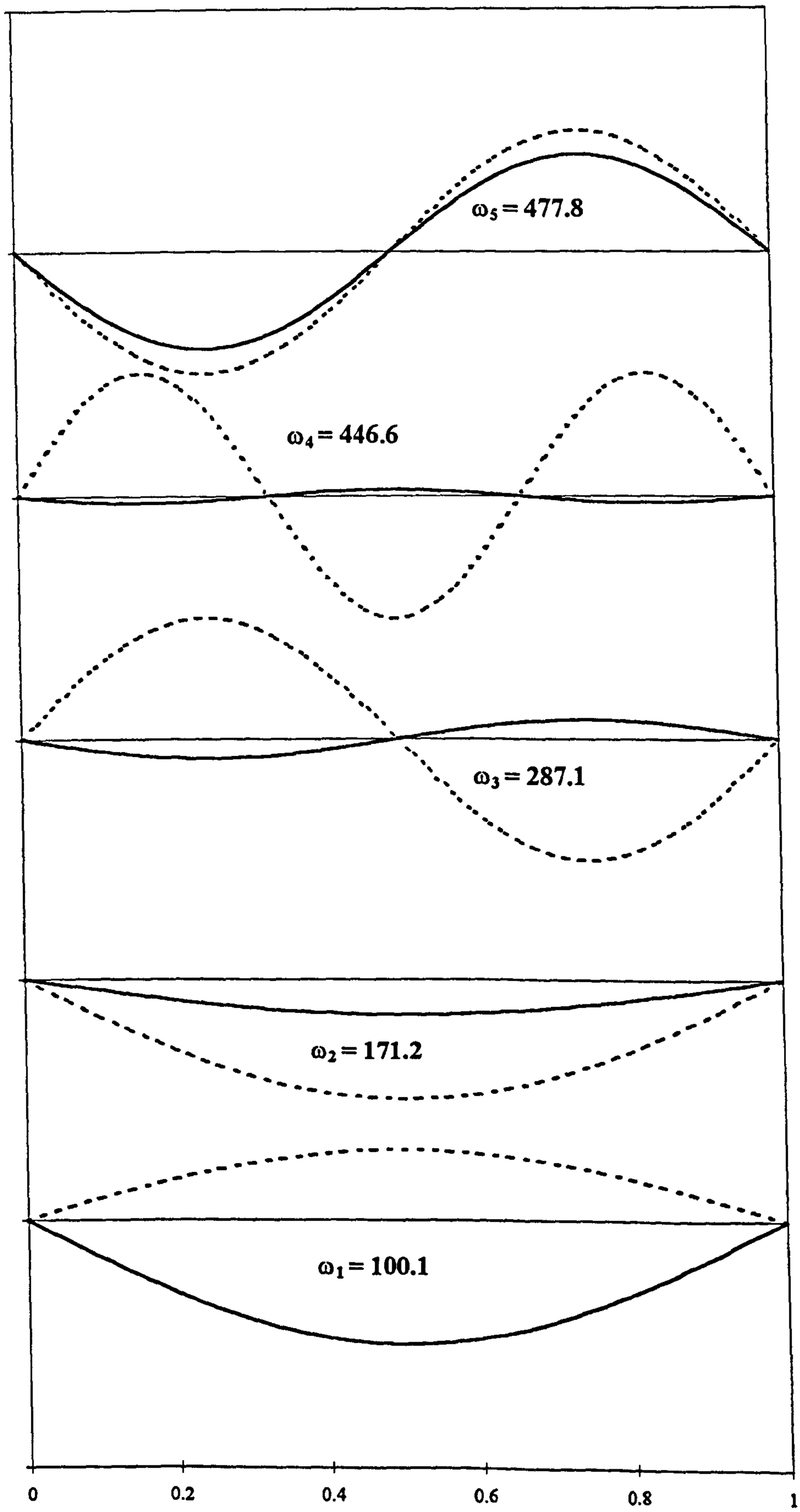

Figure 7-2. Bending-torsion coupled natural frequencies (rad/s) and mode shapes of the Goland wing with S-S end conditions.

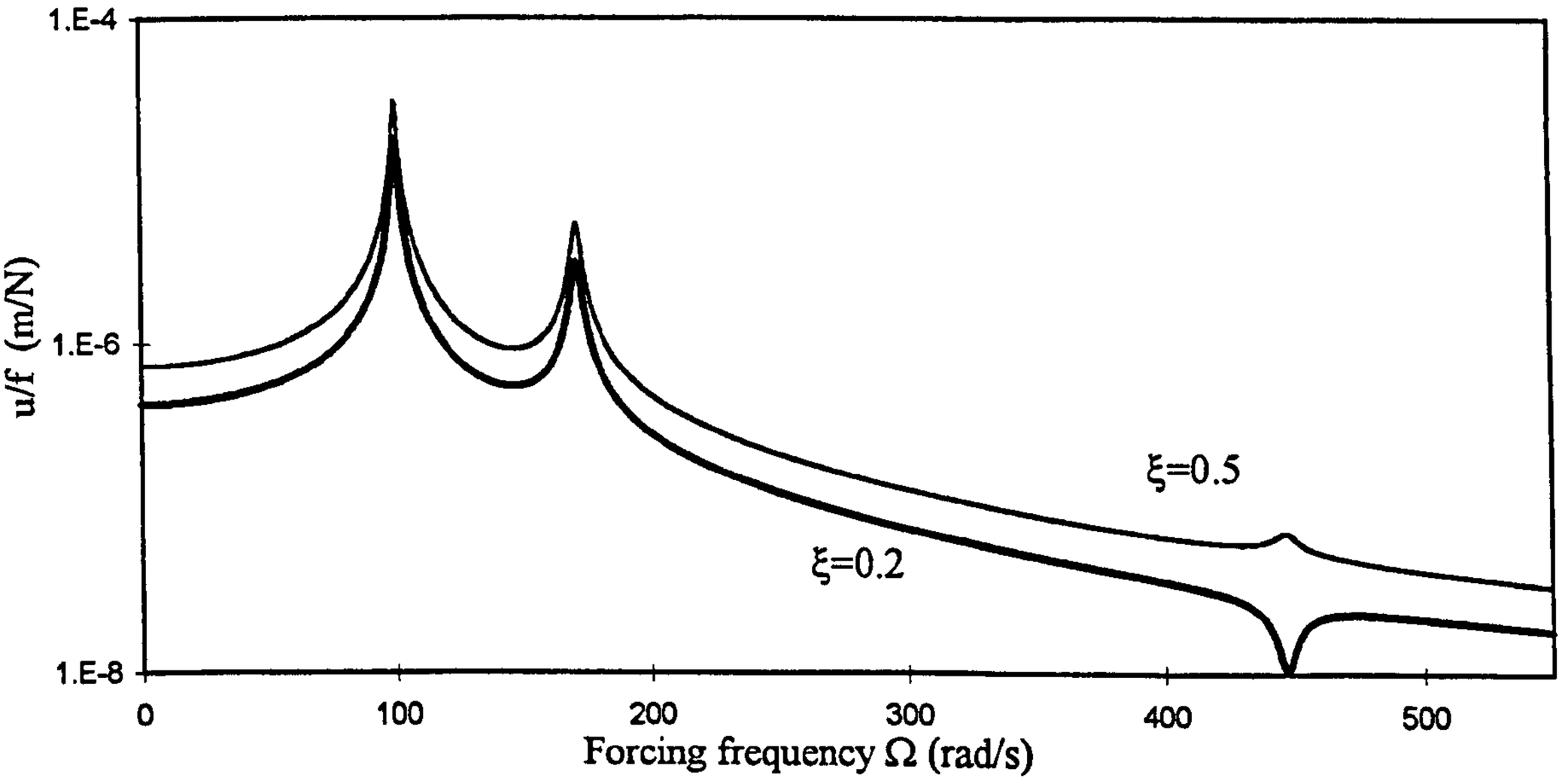

Figure 7-3. Dynamic flexural displacement of the Goland wing with (S-S) end conditions due to a unit harmonically varying force at the mid-span, response at ξ=0.2 and ξ=0.5.

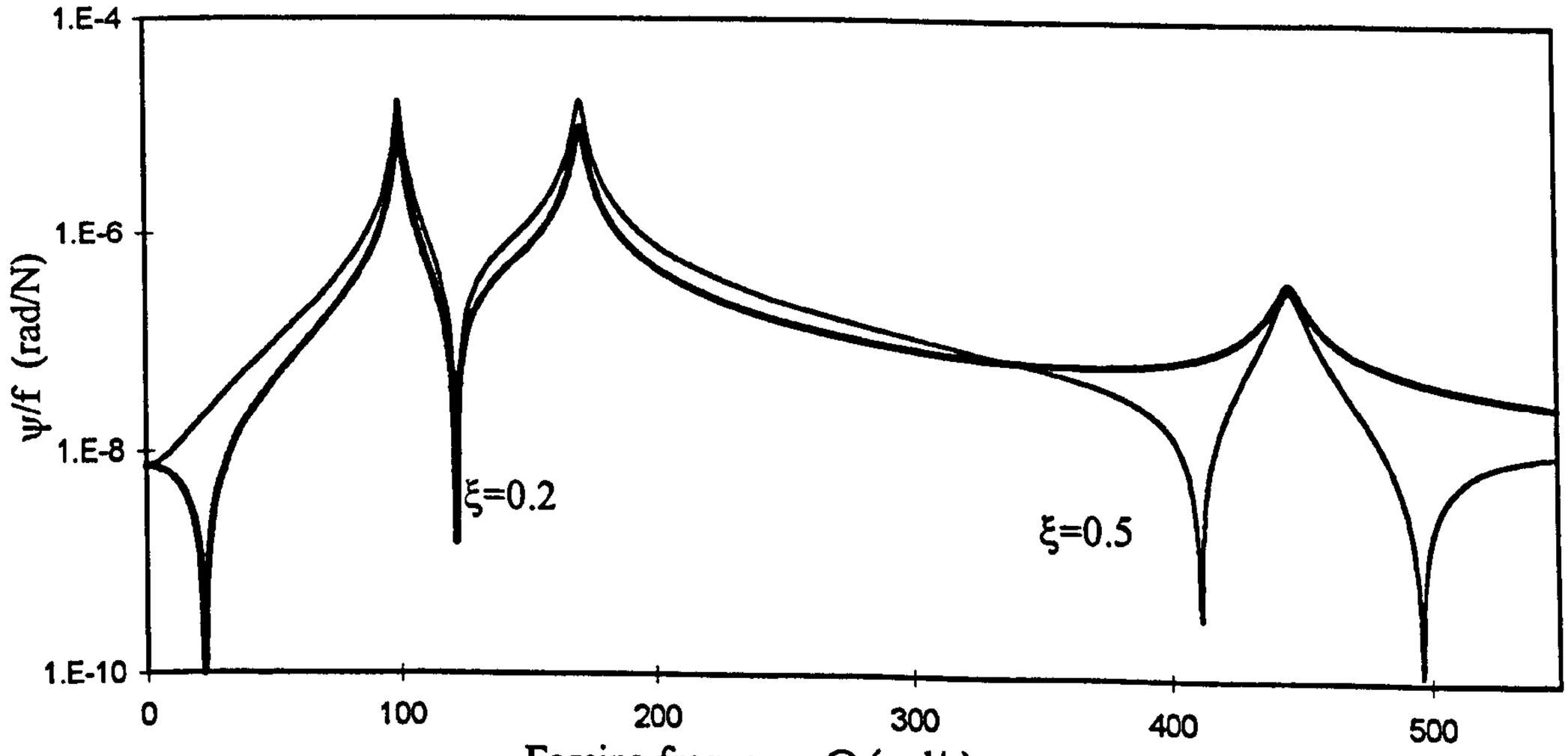

Figure 7-4. Dynamic torsional rotation of the Goland wing with (S-S) end conditions due to a unit harmonically varying force at the mid-span, response at ξ=0.2 and ξ=0.5.

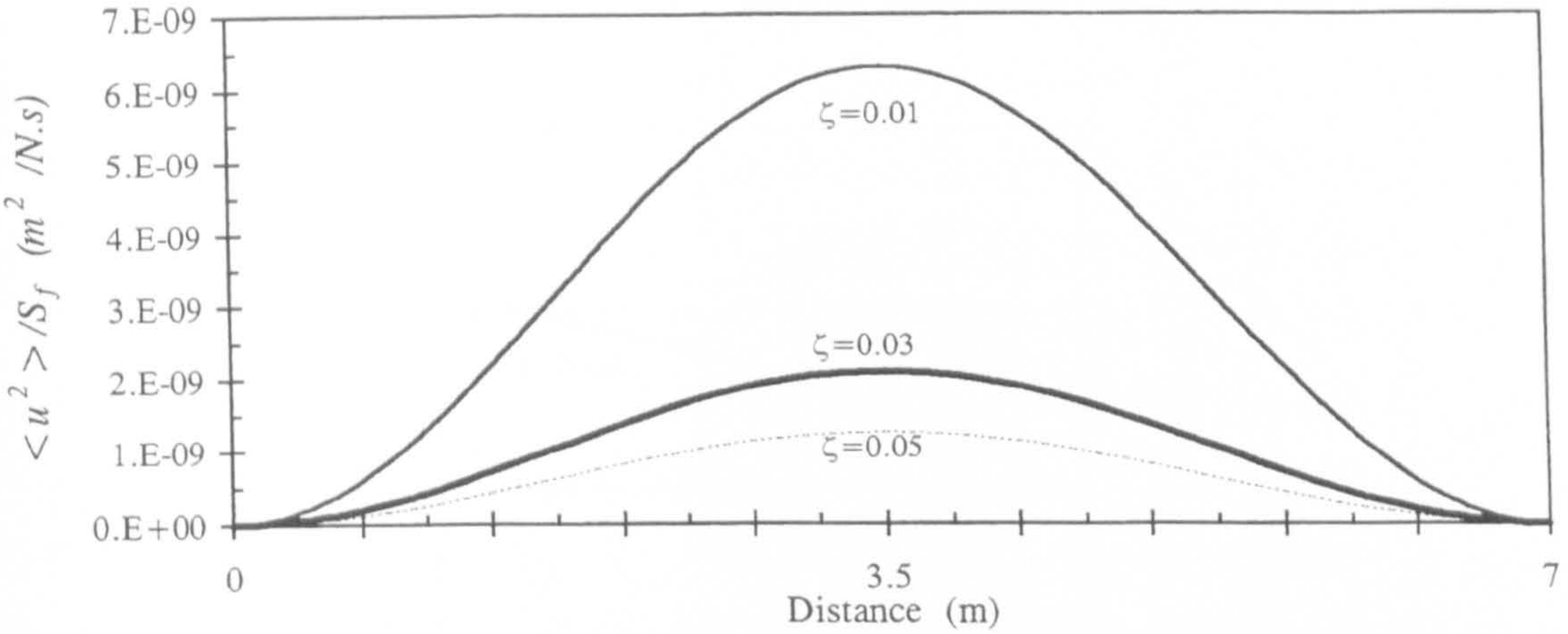

Figure 7-5. Variation of the mean square value of the flexural displacement along the Goland wing with (S-S) end conditions for different damping ratios.

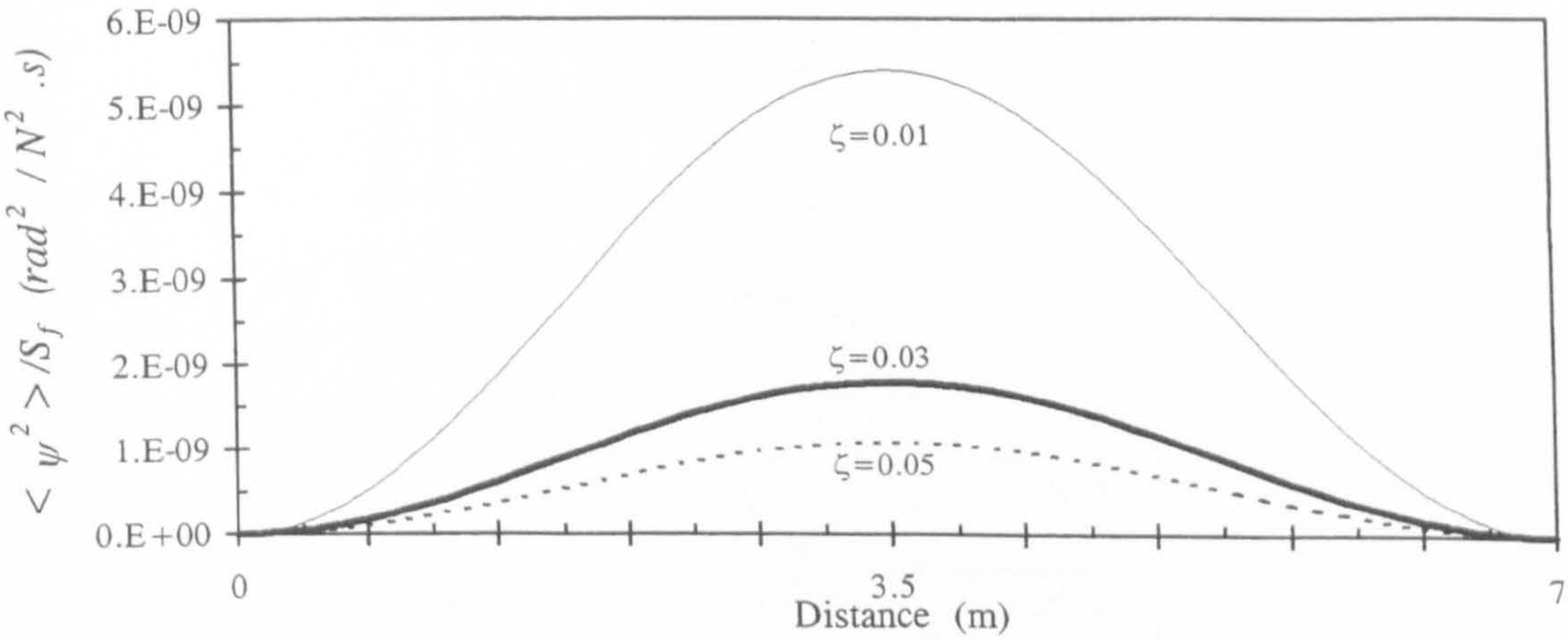

Figure 7-6. Variation of the mean square value of the torsional displacement along the Goland wing with (S-S) end conditions for different damping ratios.

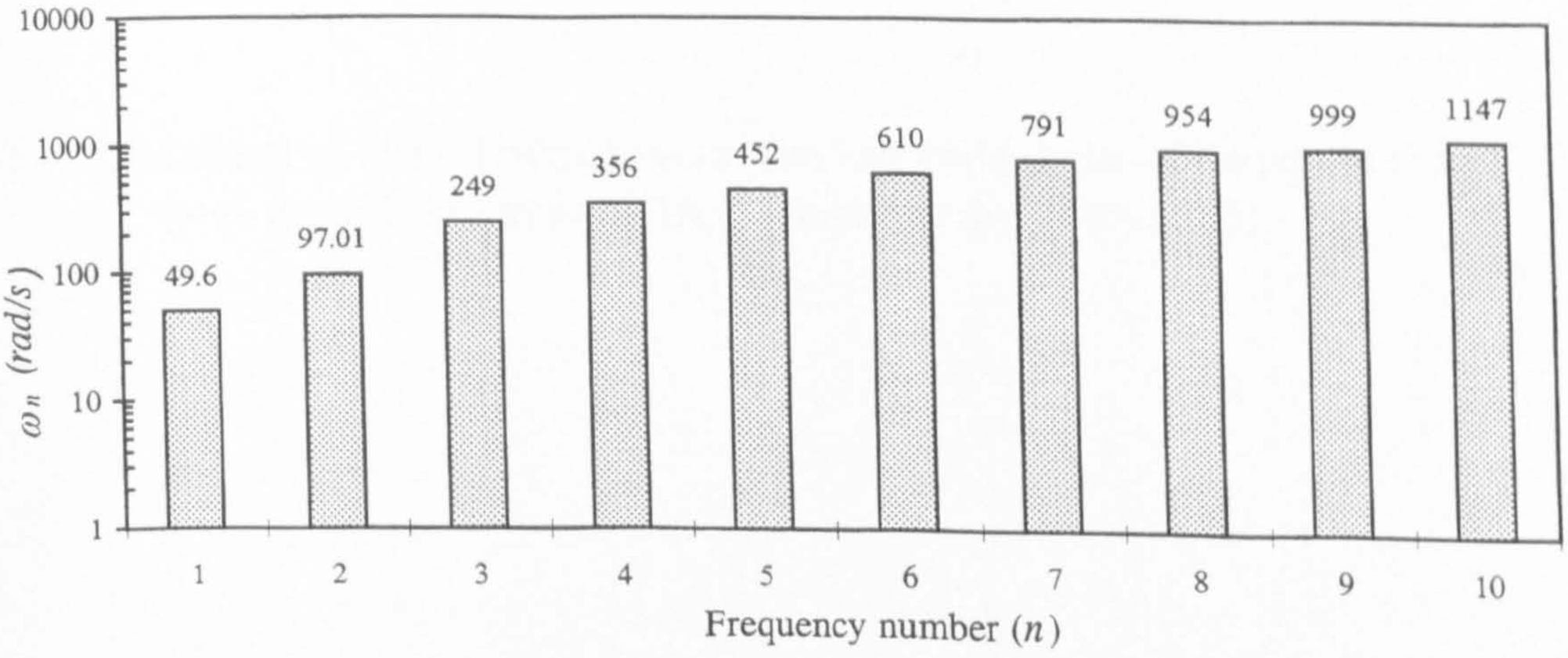

Figure 7-7. Circular natural frequencies (ω_n.) of the Goland wing (C-F).

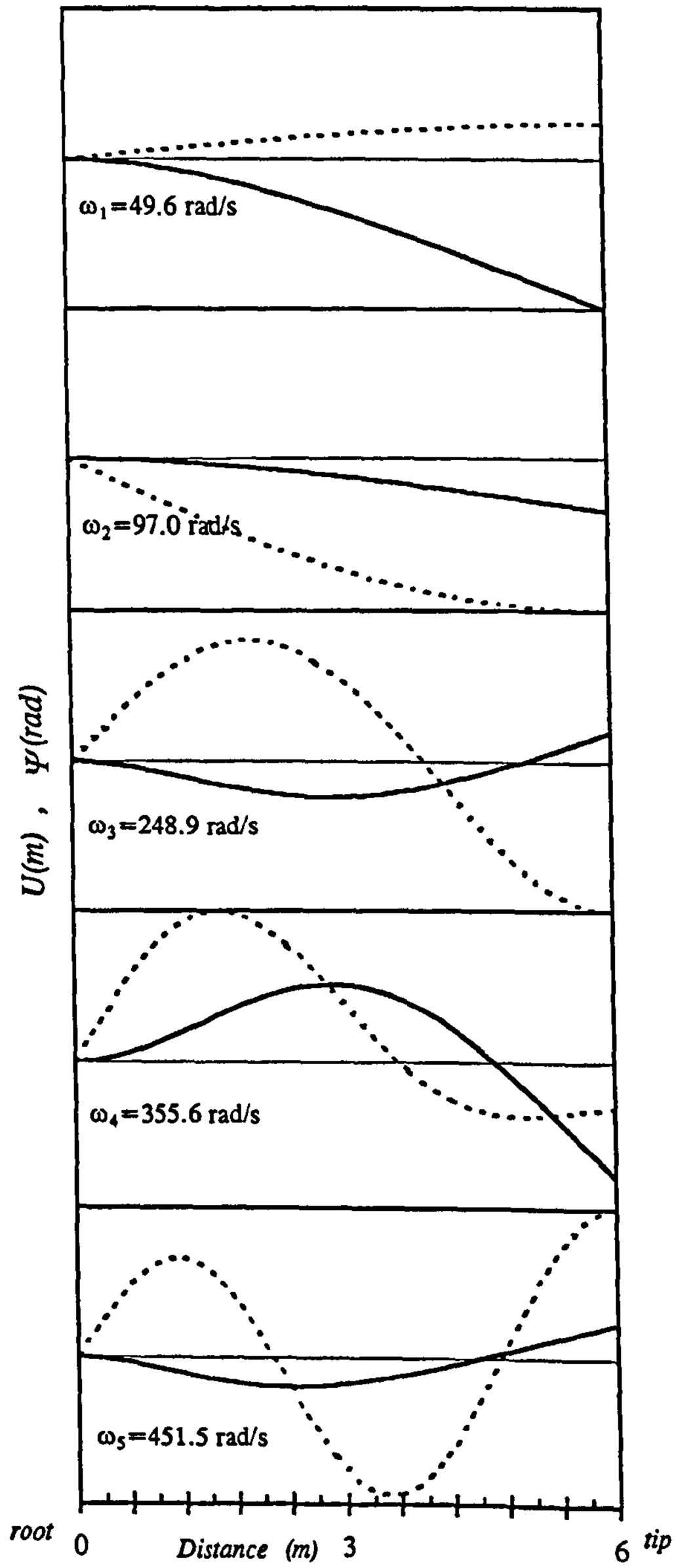

Figure 7-8. Coupled bending-torsioal natural frequencies and mode shapes of the goland wing (C-F);
—— flexural displacement (U),- - - torsional displacement (Ψ).

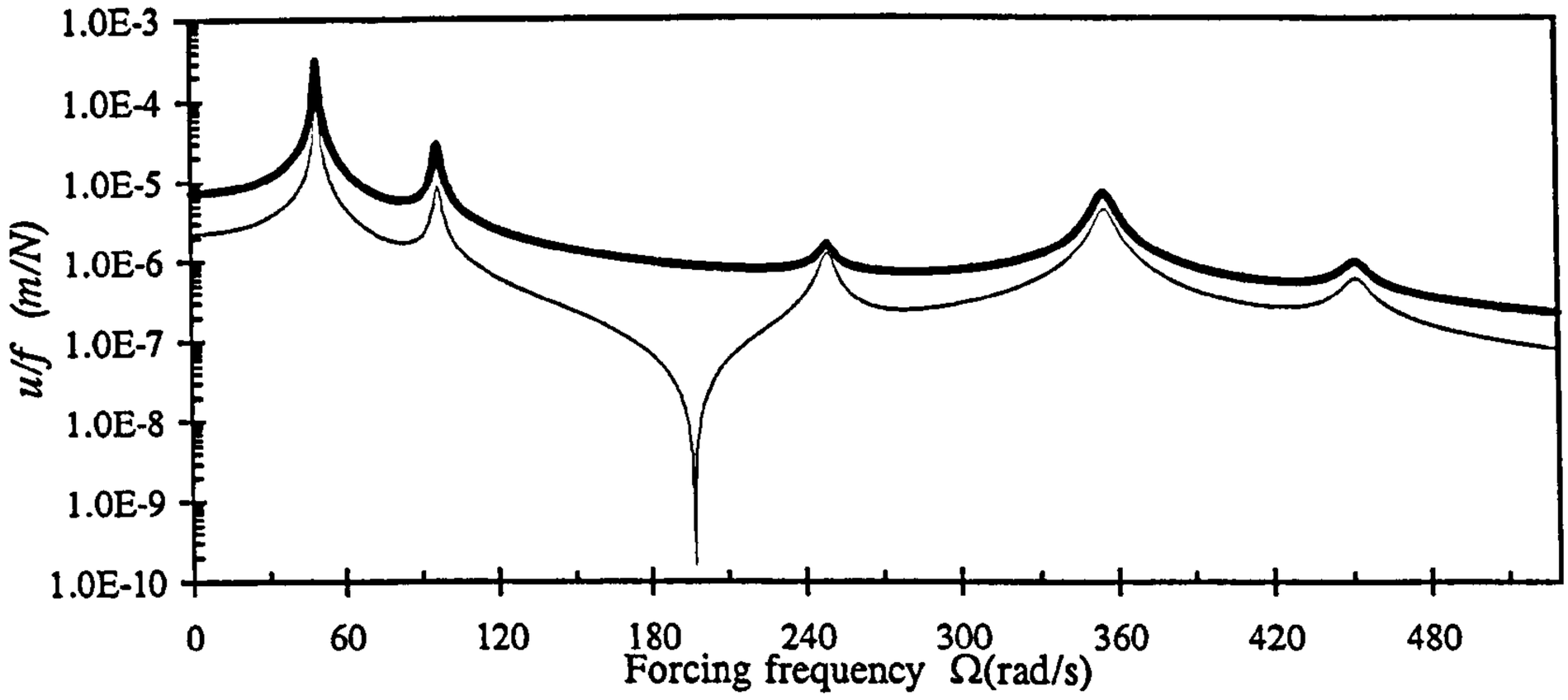

Figure 7-9. Dynamic flexural displacement of the Goland wing (C-F) due to a unit harmonically varying concentrated force at the tip. —— at the mid span, ——— at the tip.

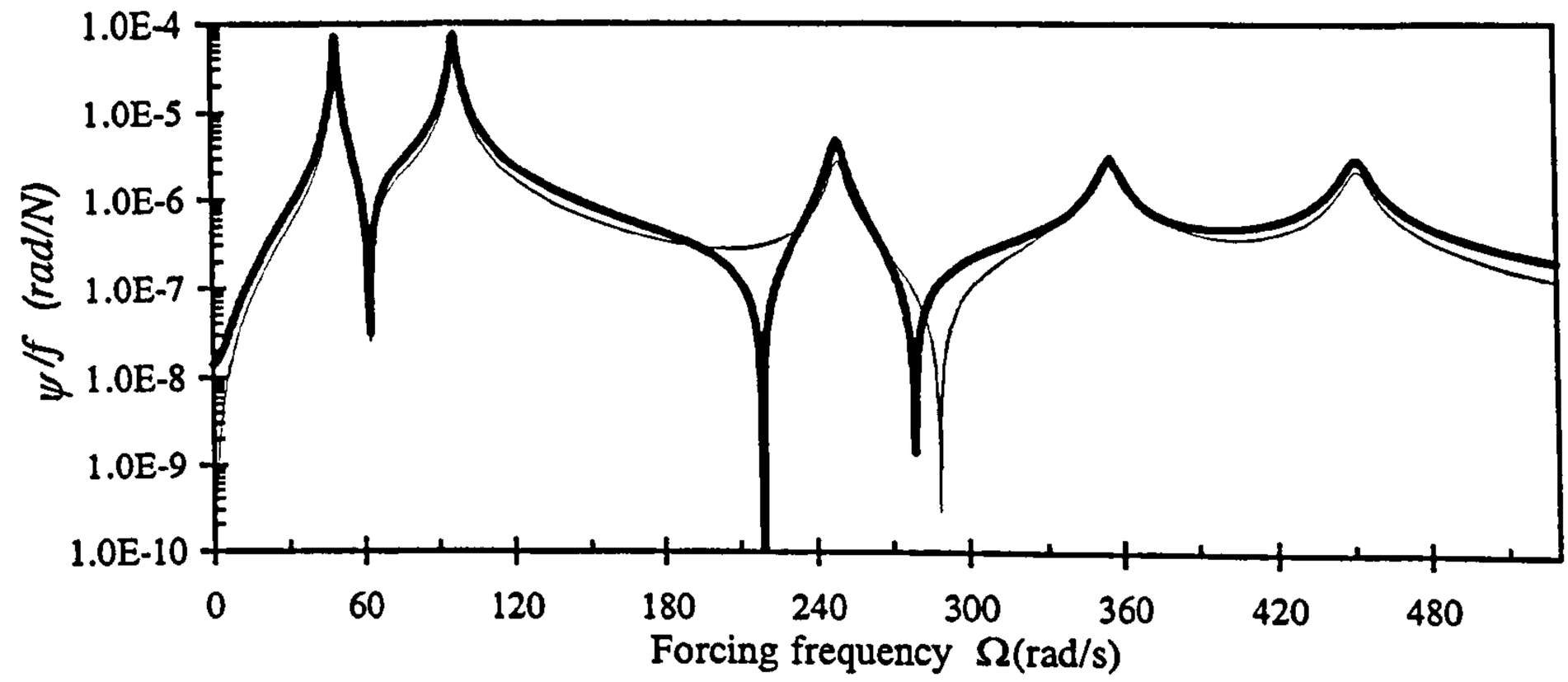

Figure 7-10. Dynamic torsional rotation of the Goland wing (C-F) due to a unit harmonically varying concentrated force at the tip. —— at the mid span, ——— at the tip.

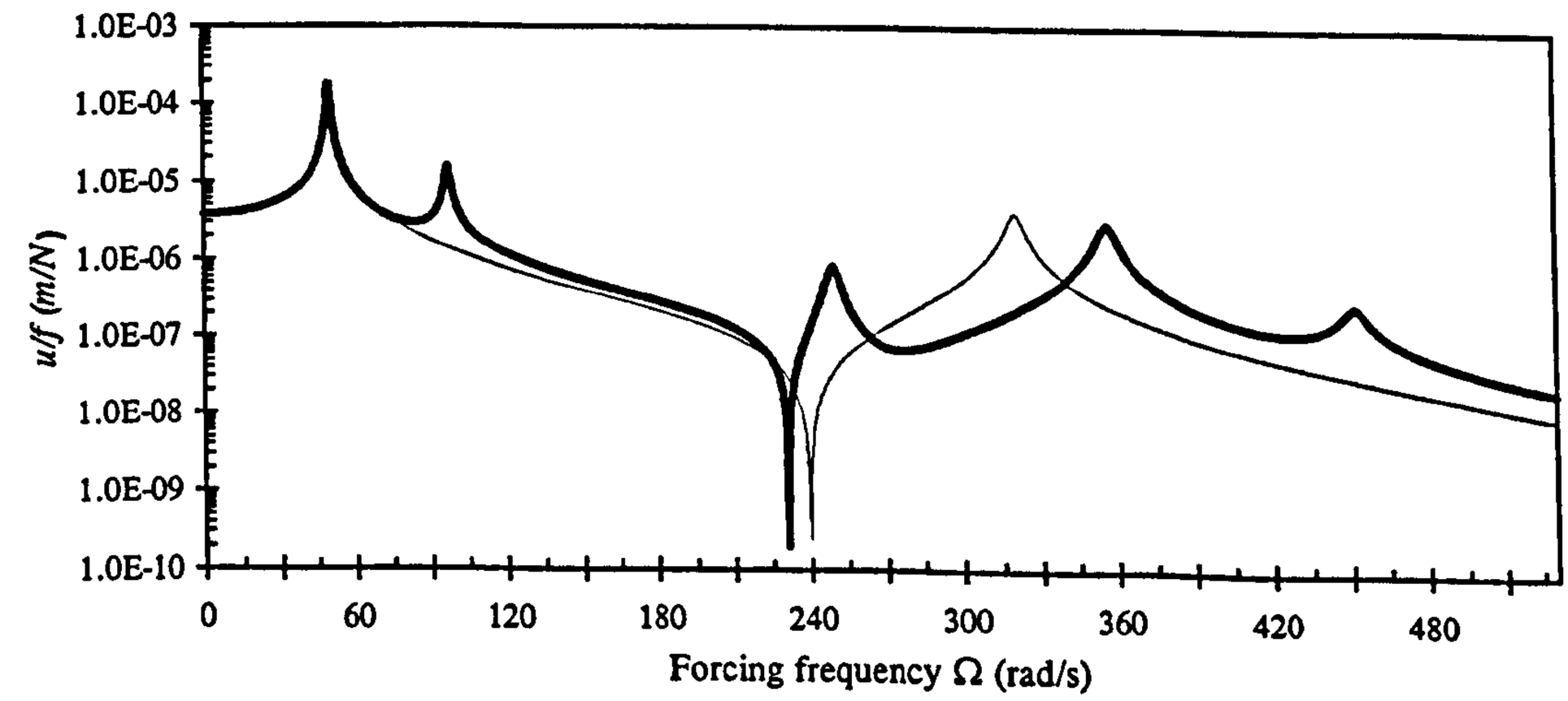

Figure 7-11.Dynamic flexural displacement of the Goland wing (C-F) at a distance of 4 metres from the root due to a unit harmonically varying concentrated force at the tip.

——— Present Theory; — Bernoulli-Euler Theory.

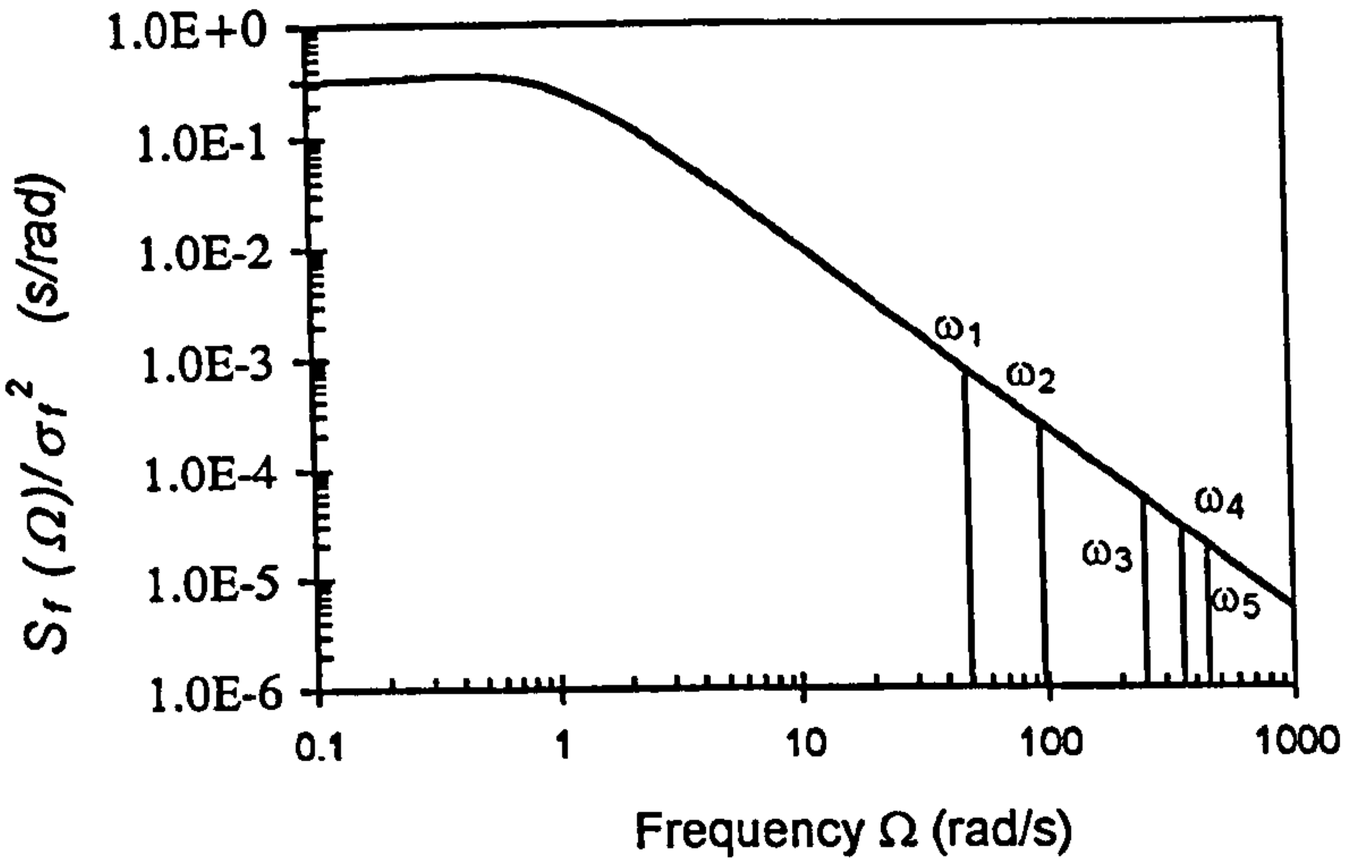

Figure 7-12. The von Karman PSD function ($L_s/V=1$)

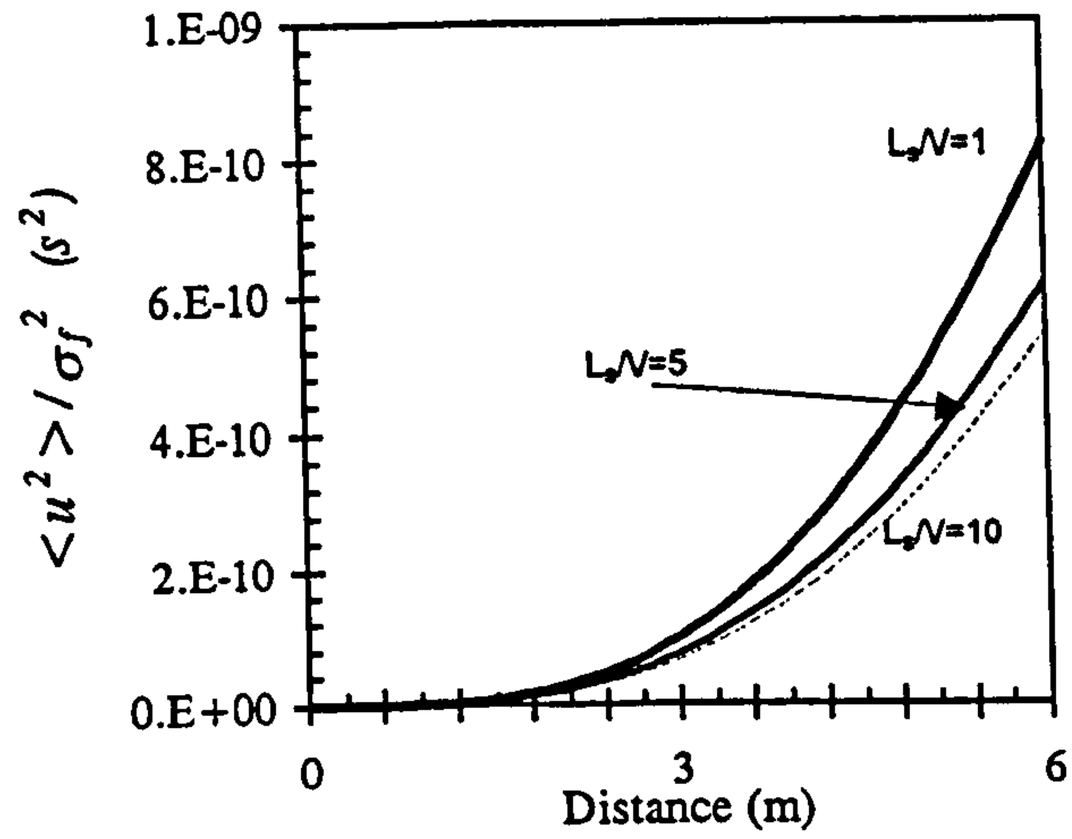

Figure 7-13. Variation of the mean square value of the flexural displacement along the Goland wing (C-F) for different L_s/V ratios (damping coefficient=0.05).

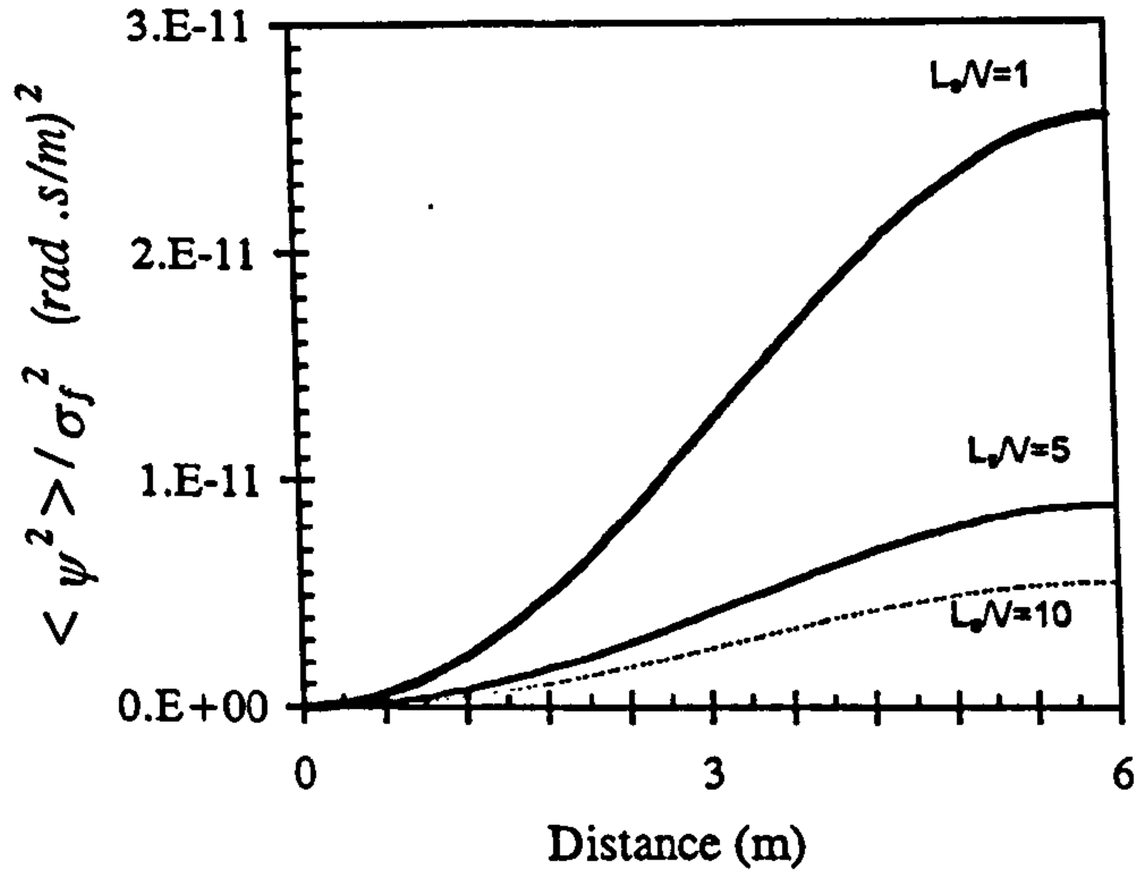

Figure 7-14. Variation of the mean square value of the torsional rotation along the Goland wing (C-F) for different L_s/V ratios (damping coefficient=0.05).

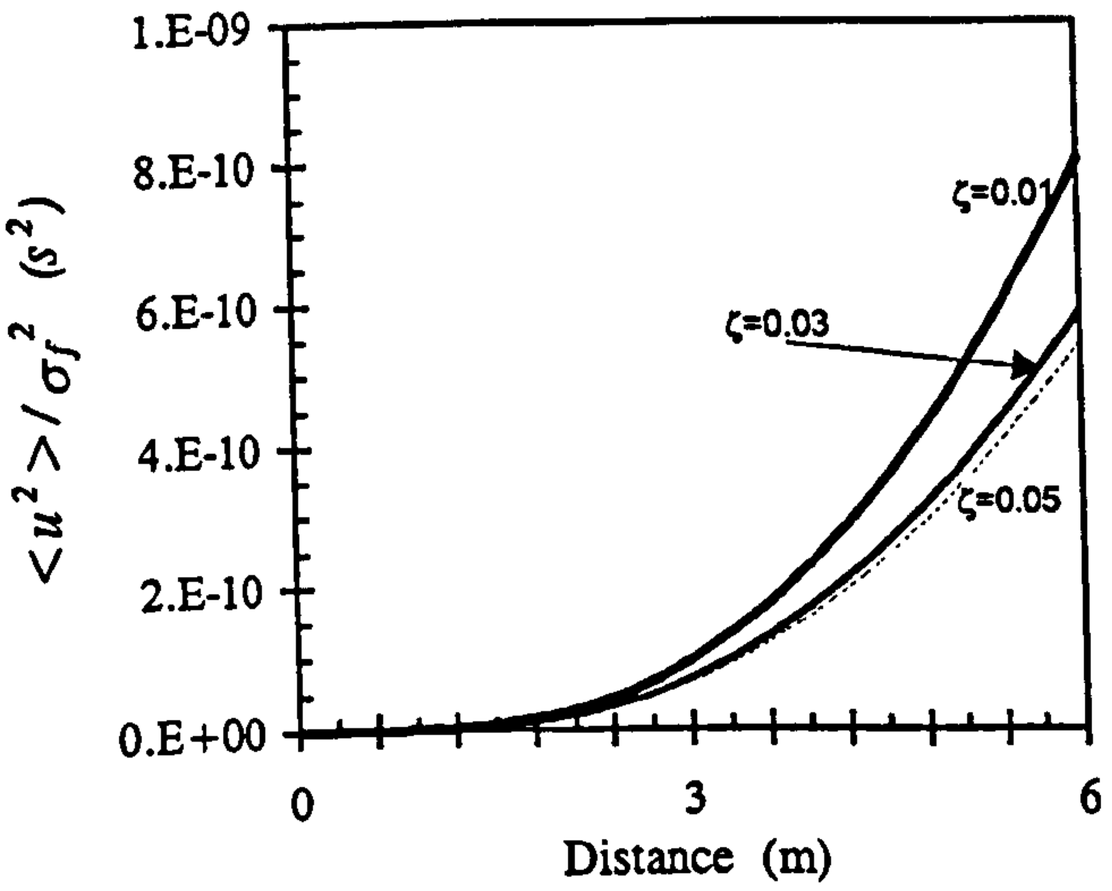

Figure 7-15. Variation of the mean square value of the flexural displacement along the Goland wing (C-F) for different damping coefficients (L_s/V =10).

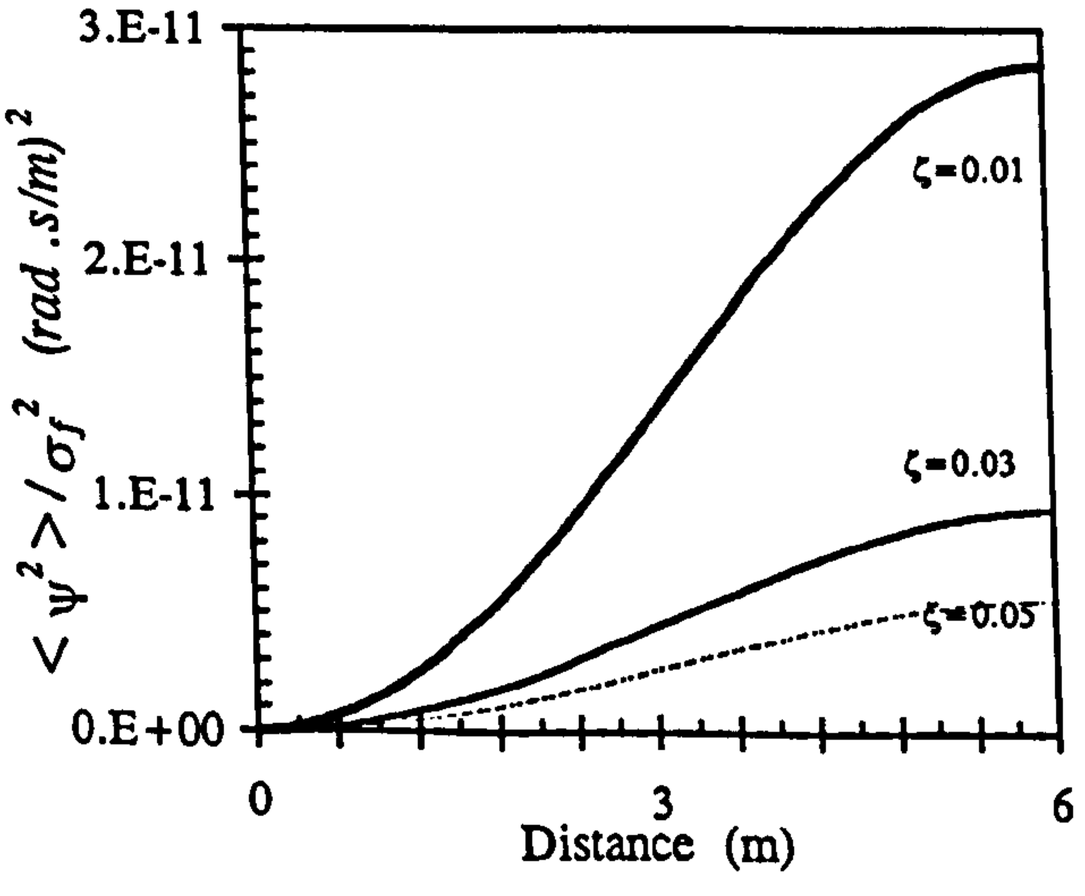

Figure 7-16. Variation of the mean square value of the torsional rotation along the Goland wing (C-F) for different damping coefficients (L_s/V =10).

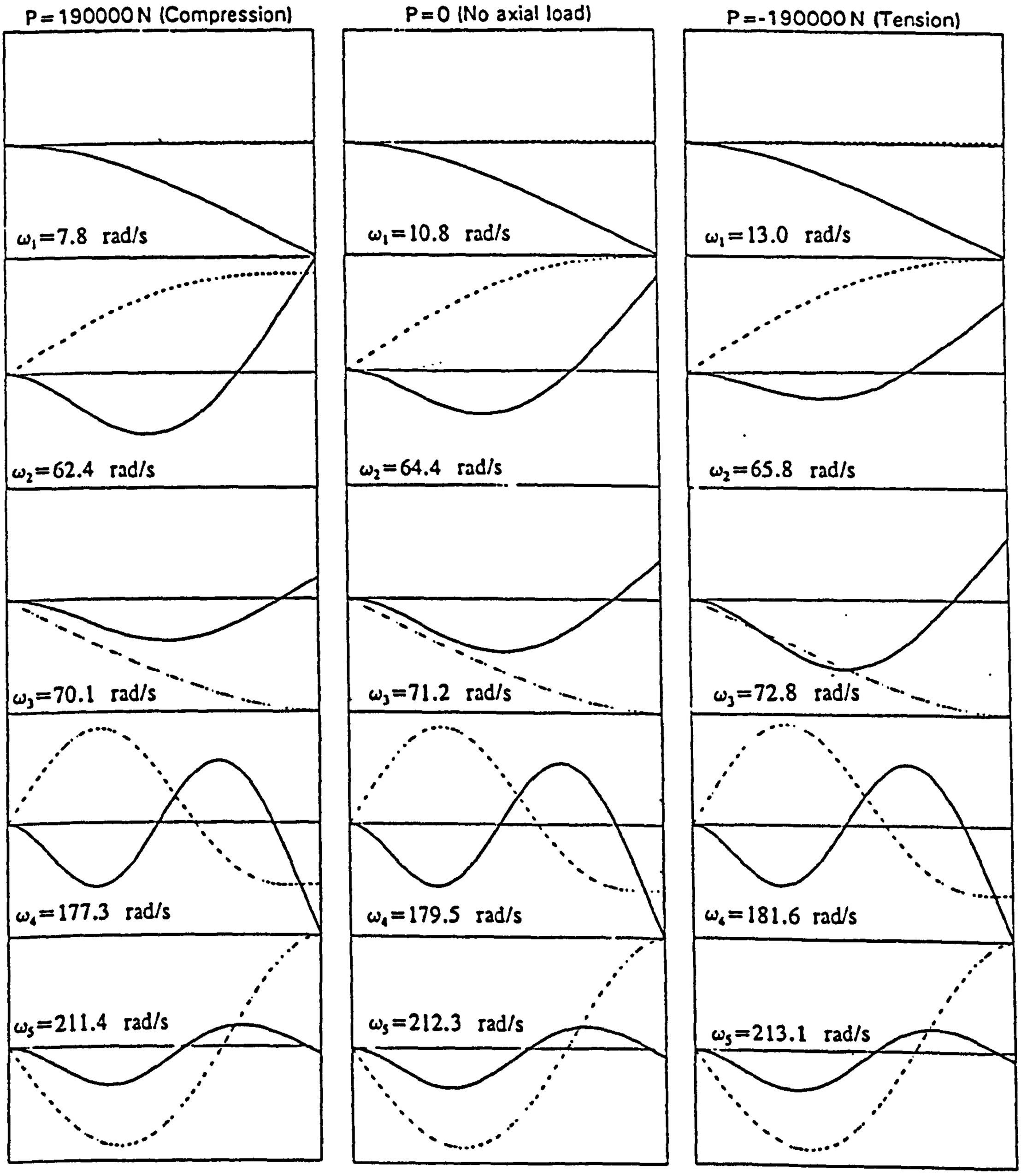

Figure 7-17. Effect of axial load on bending-torsion coupled natural frequencies and mode shapes of a wind turbine blade (Petersen, 1979),

——— Flexural displacement (U), ····· torsional rotation (Ψ).

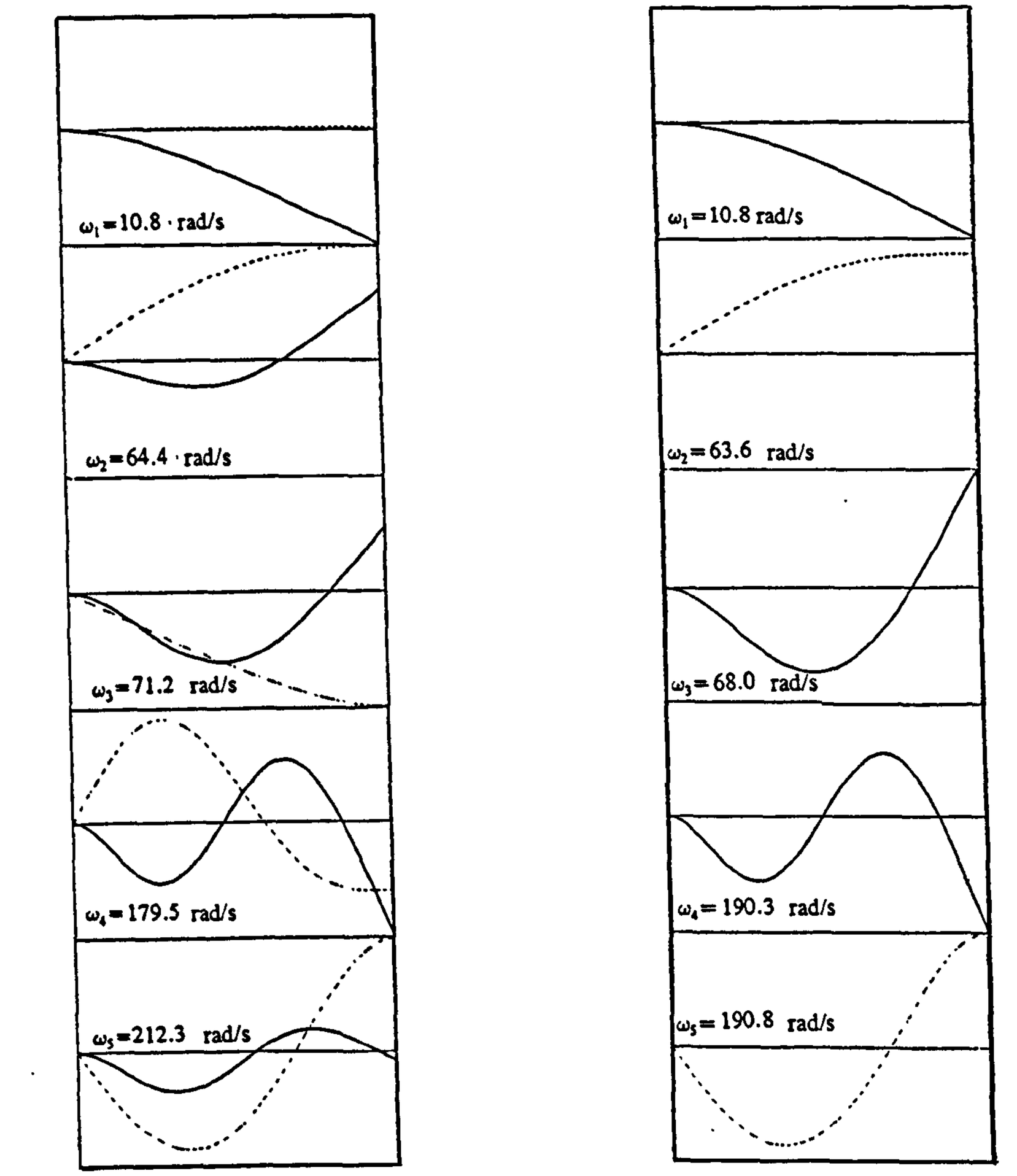

(a) Bending-Torsion Coupled Beam Theory ($x_\alpha \neq 0$);

(b) Bernoulli-Euler Beam Theory ($x_\alpha = 0$).

Figure 7-18. Effect of bending-torsion coupling on natural frequencies and mode shapes of a wind turbine blade (Petersen, 1979).

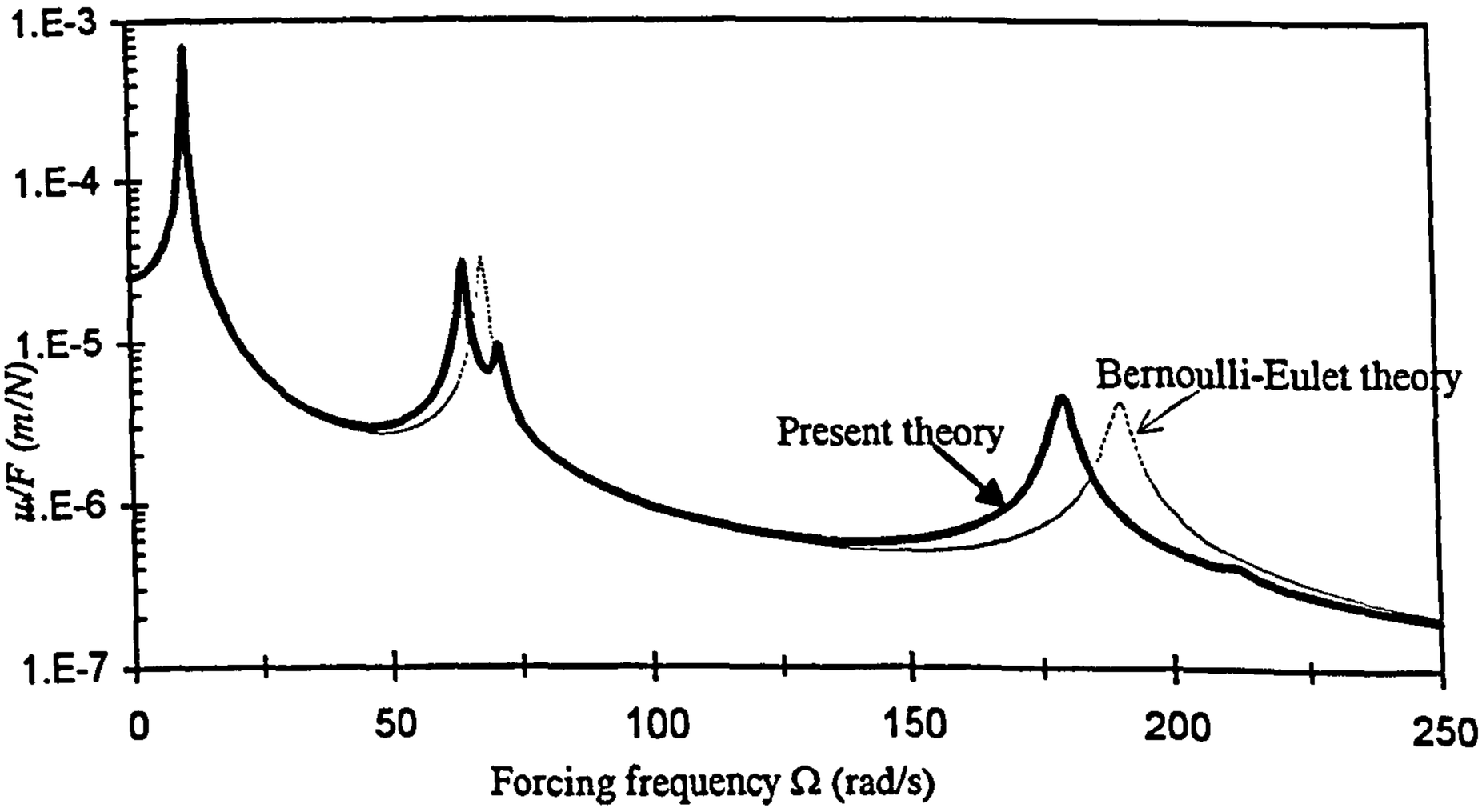

Figure 7-19. Effect of bending-torsion coupling on dynamic flexural response at the tip of a wind turbine blade (Petersen, 1979) due to a unit harmonically varying concentrated force at the tip.

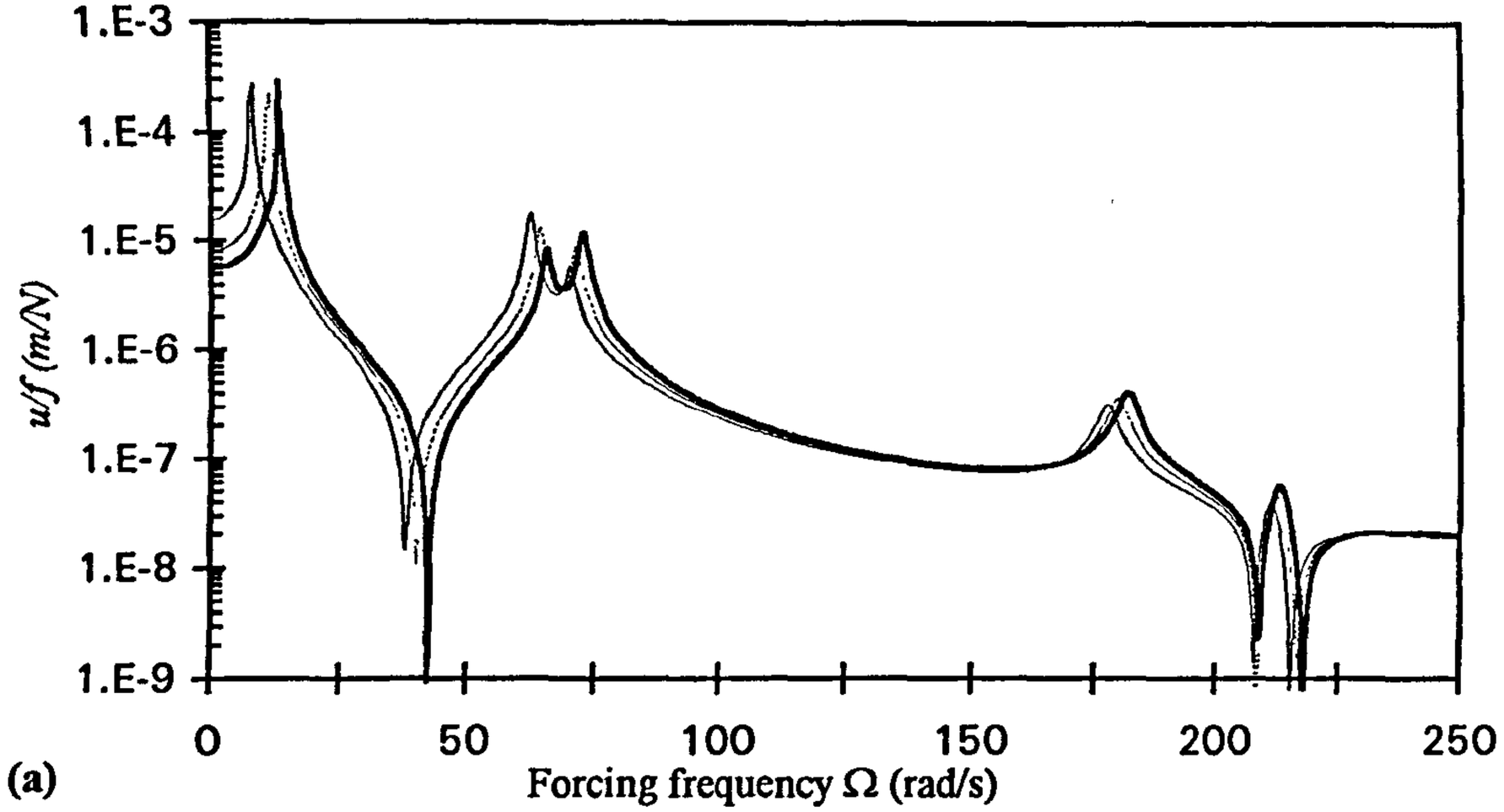

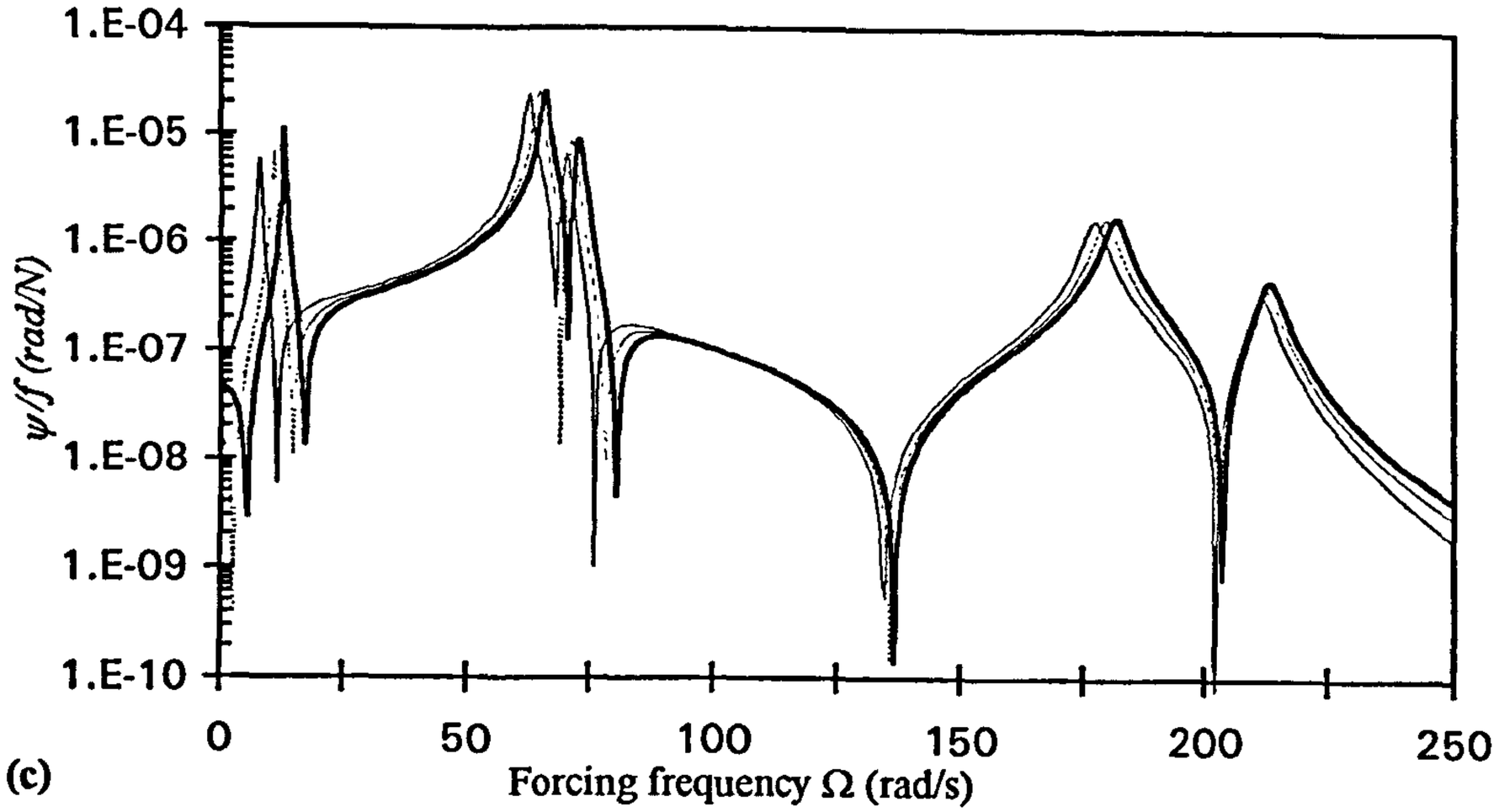

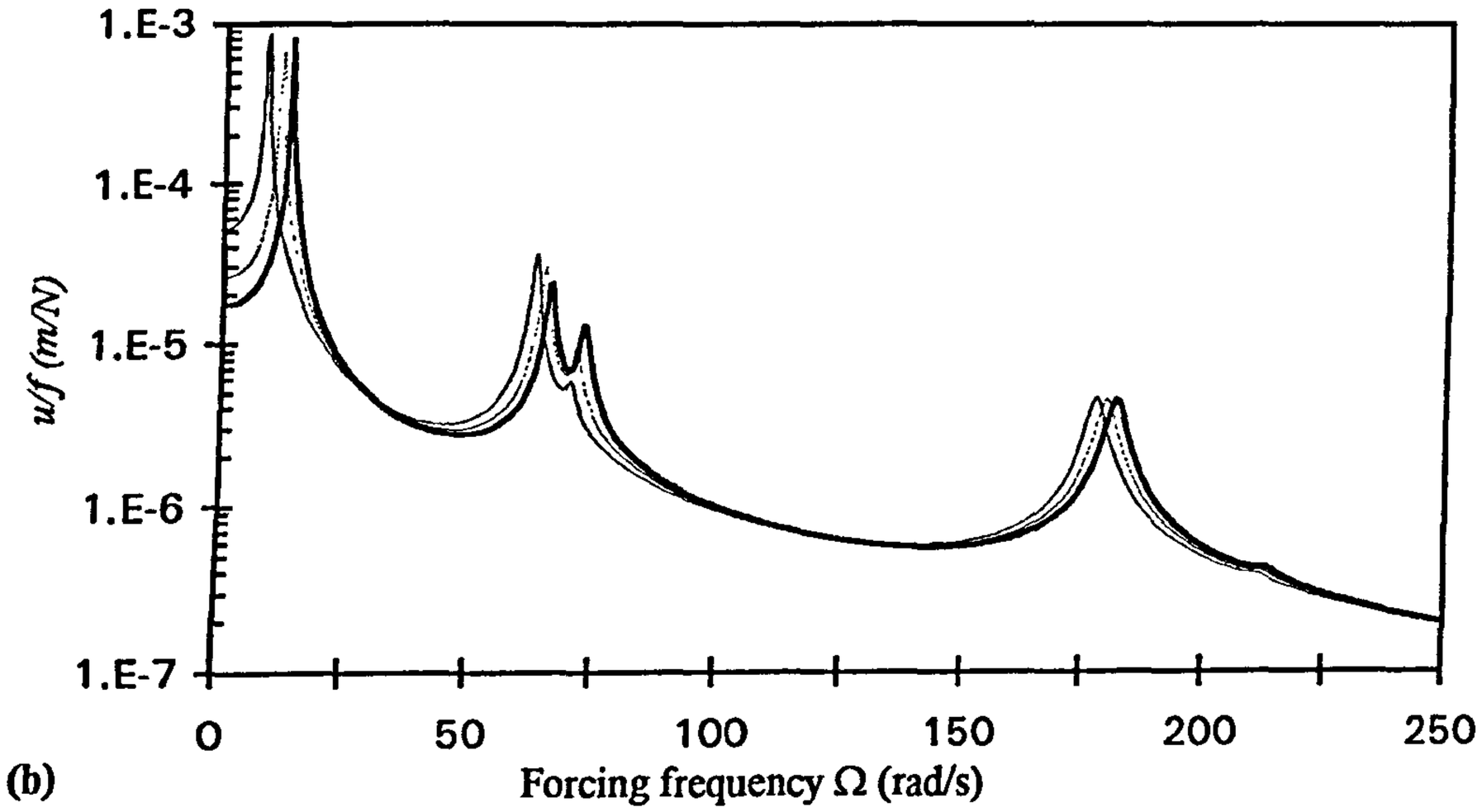

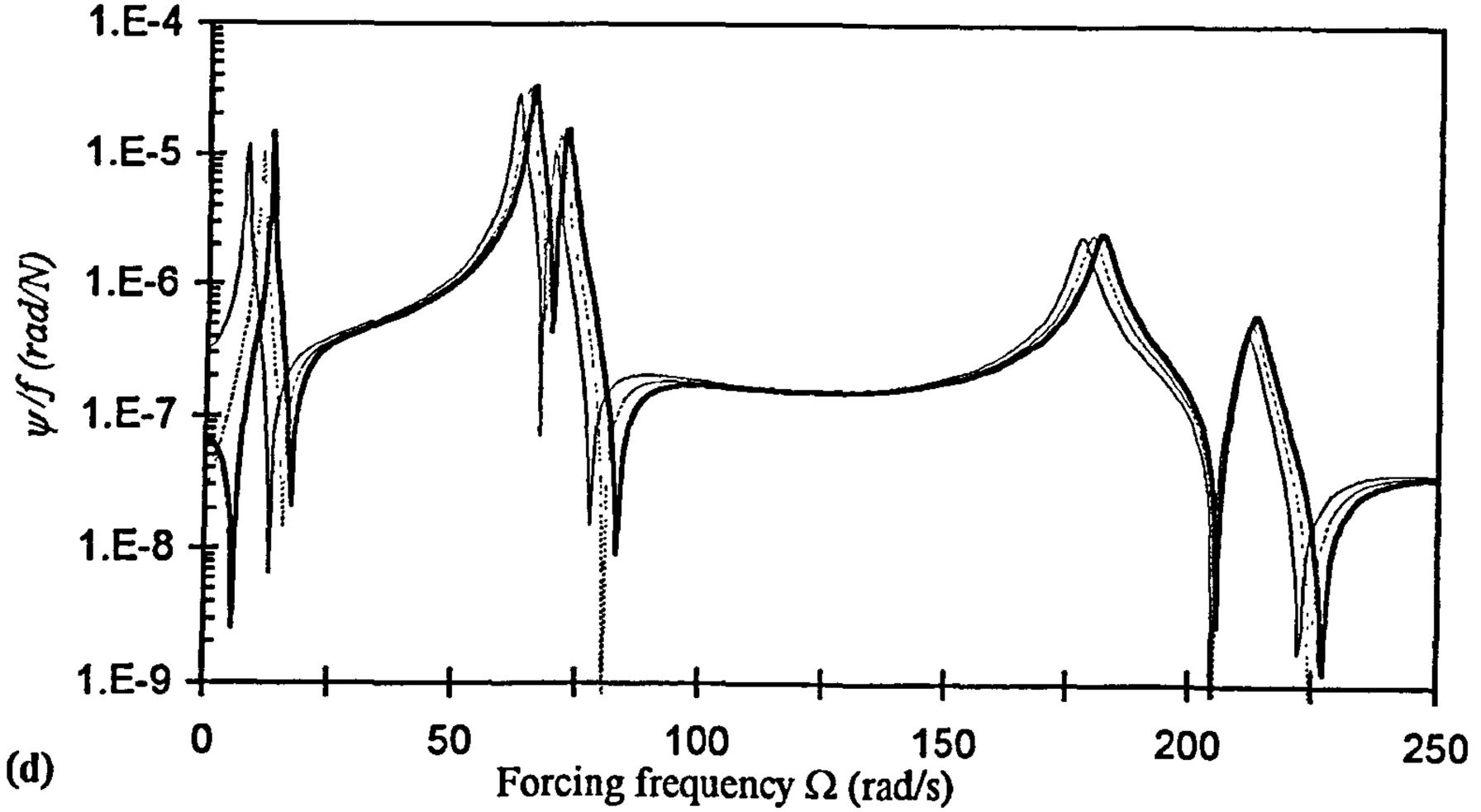

Figure 7-20. Dynamic response of a wind turbine blade (Petersen, 1979) due to a unit harmonically varying concentrated force at the tip.

—— Compresive; - - - - unloaded; ——— tensile.

(a) flexural displacement at mid-span
(b) flexural displacement at the tip
(c) torsional rotation at mid-span
(d) torsional rotation at the tip

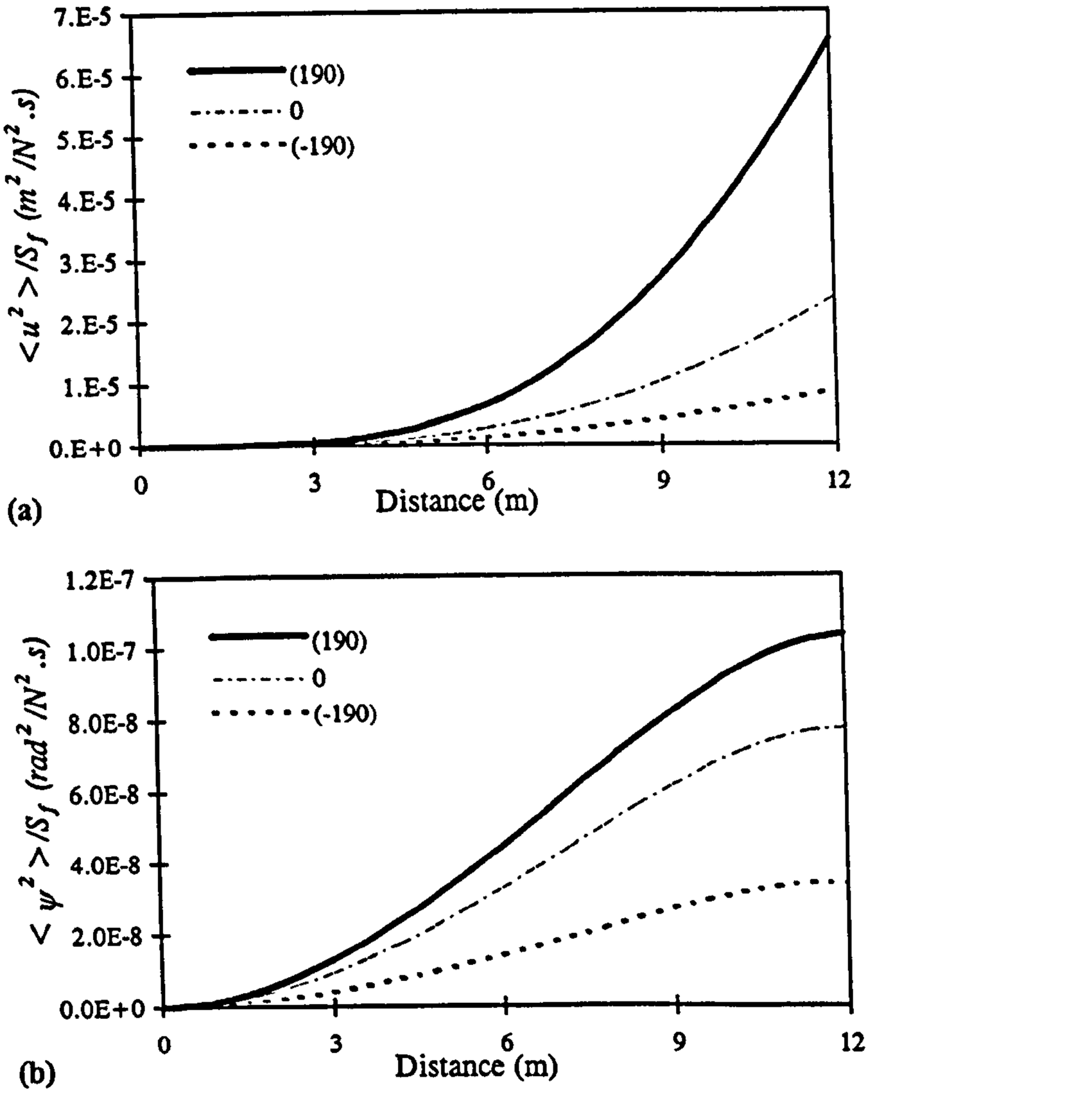

Figure 7-21. Variation of mean square value of a) flexural and b) torsional displacements along a wind turbine blade (Petersen, 1979) for different levels of axial load.

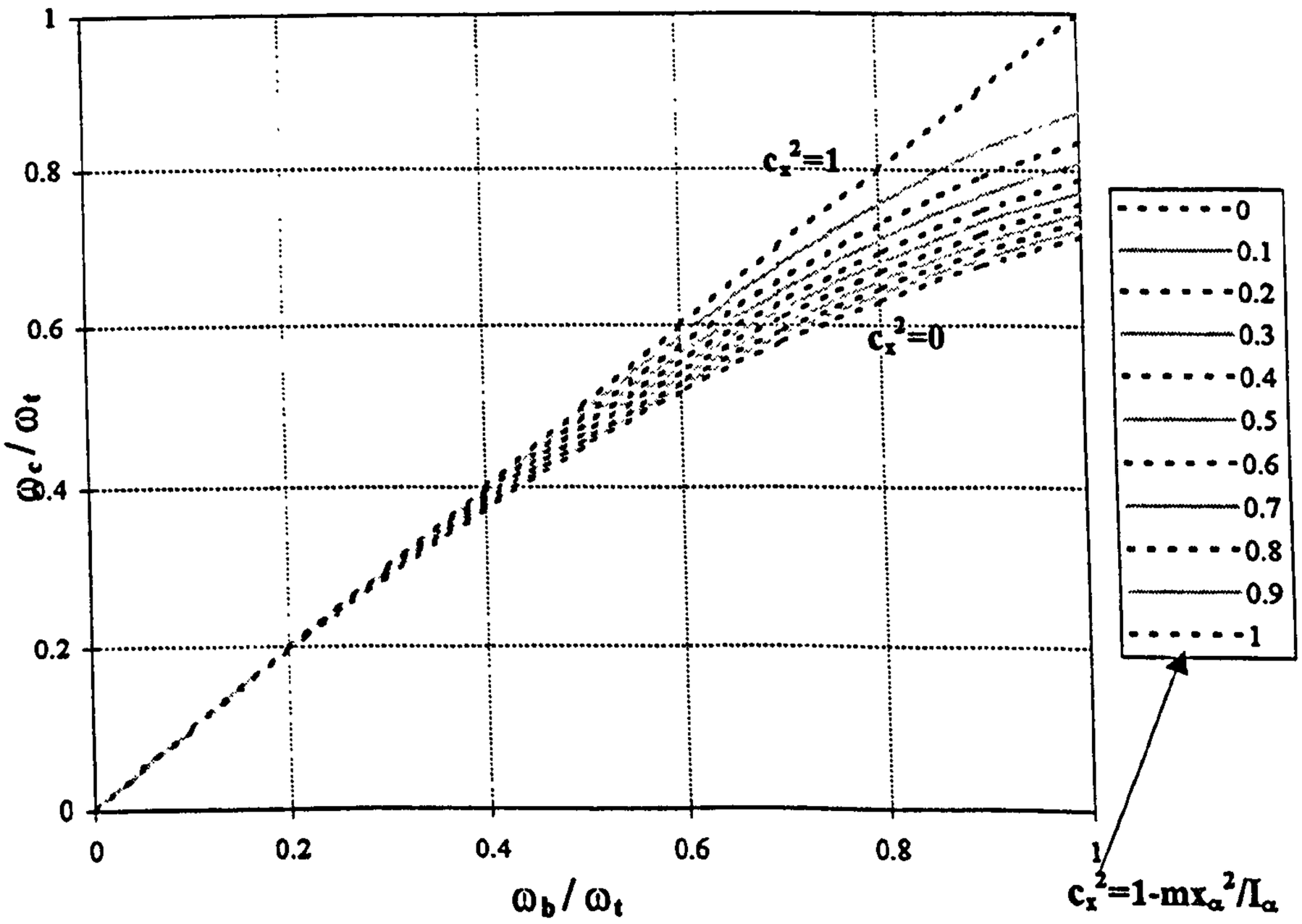

Figure 7-22. Non-dimensional bending-torsion coupled natural frequency graph.

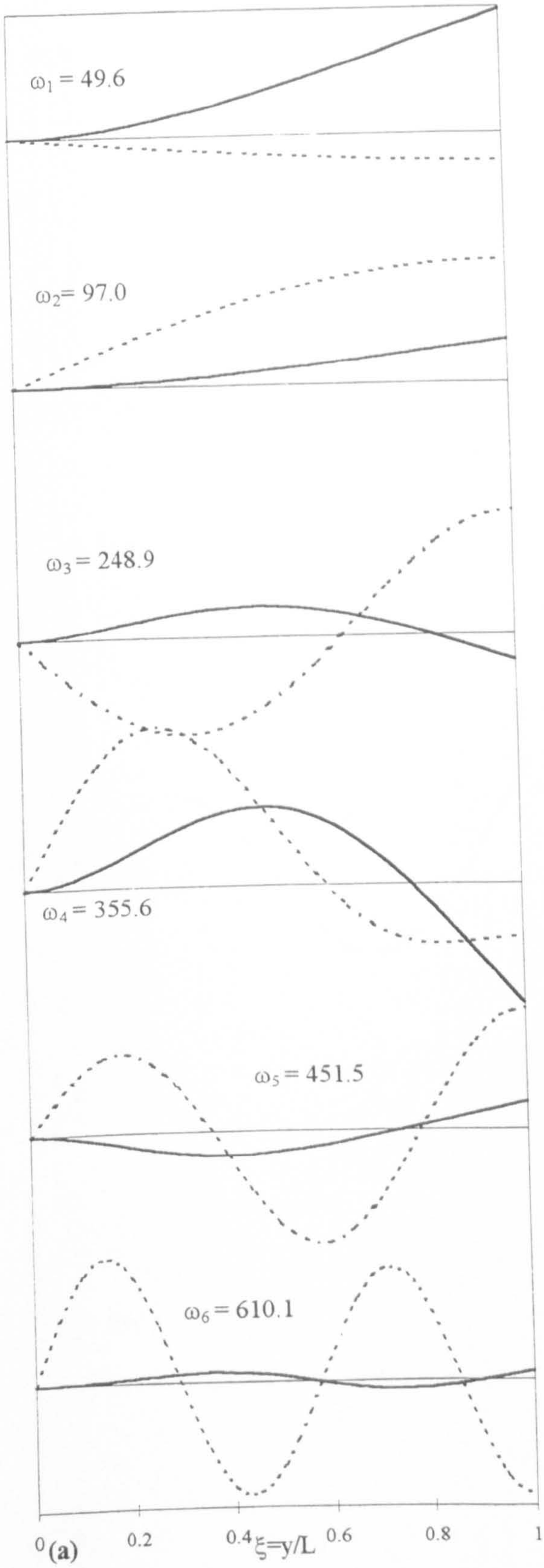

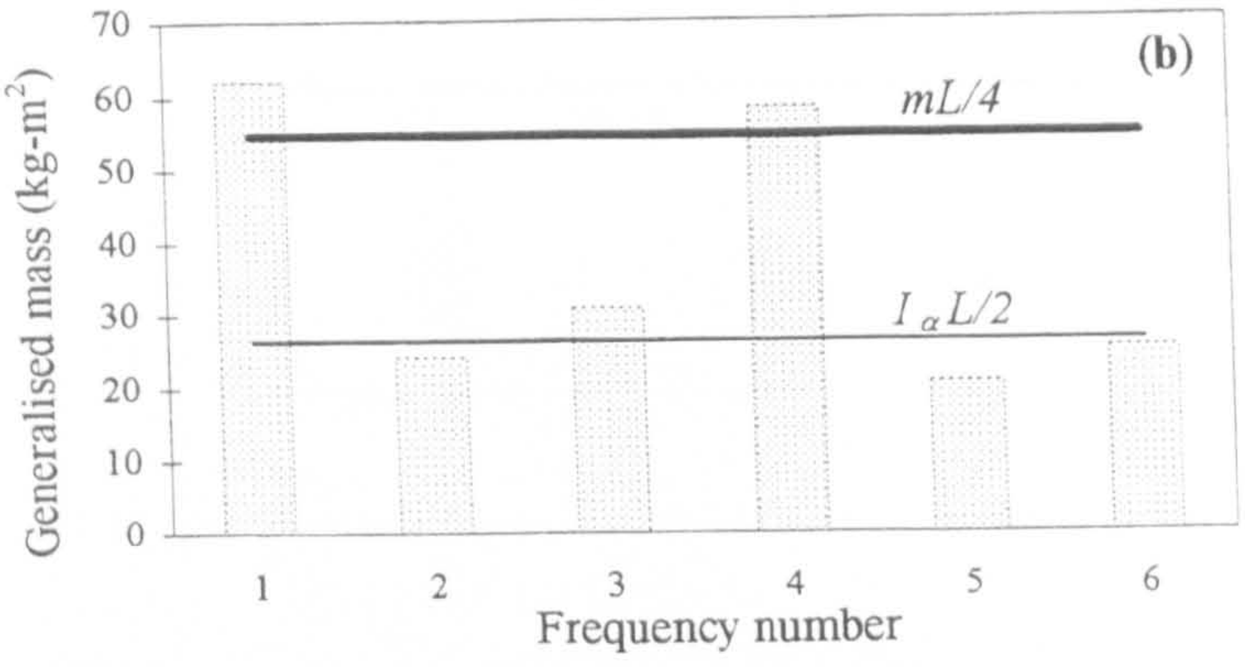

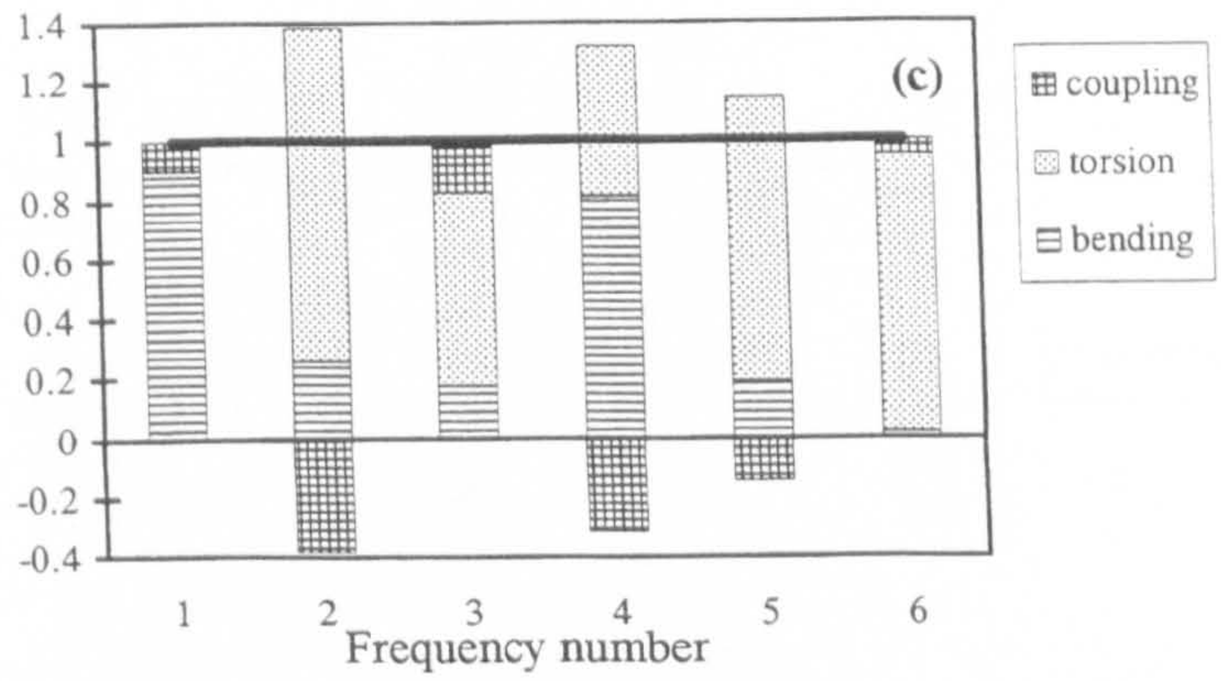

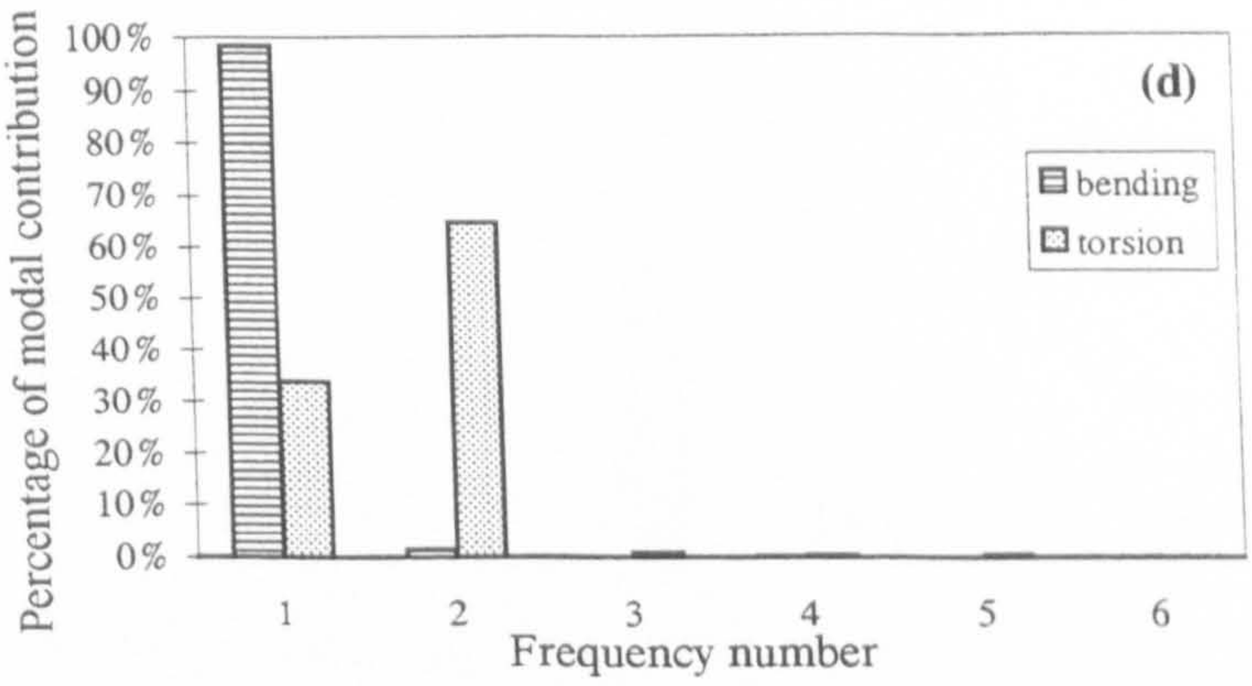

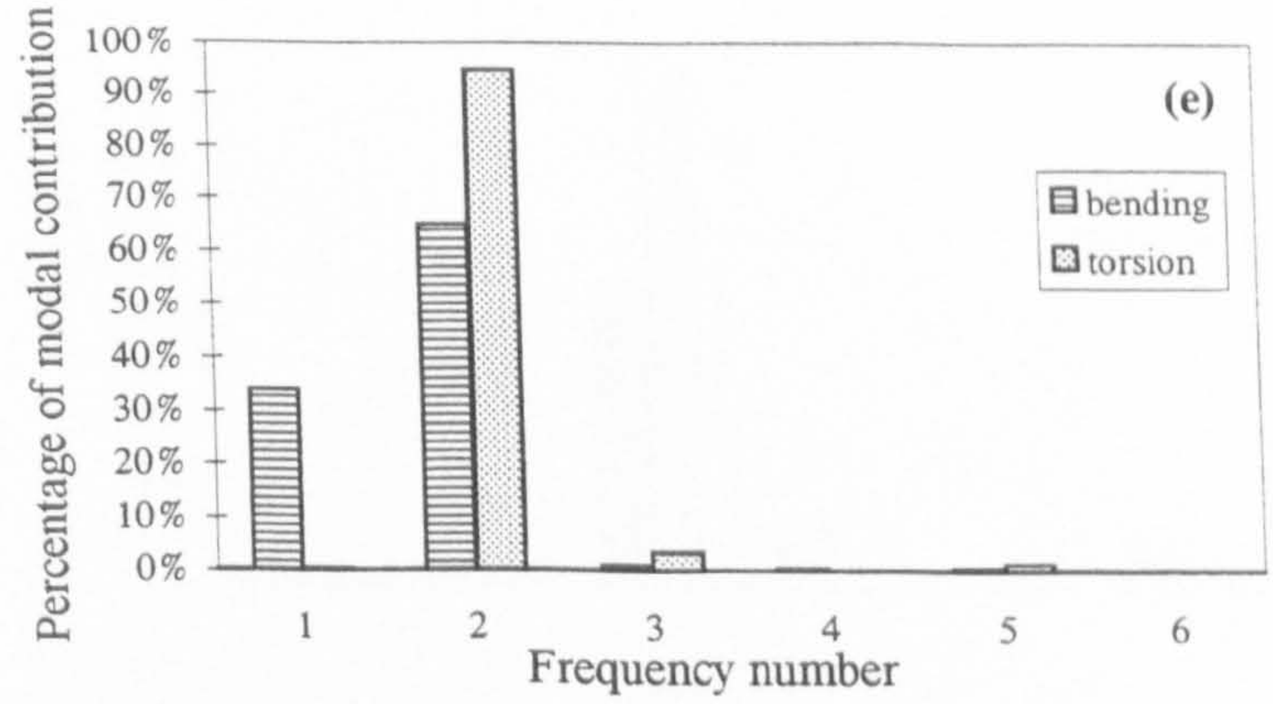

Figure 7-23. Significance of generalised mass in the dynamic response characteristics of a bending-torsion coupled beam. Using the example of Goland wing (Goland, 1945).

(a) the first six frequencies (rad/s) and mode shapes; (b) comparison of generalised mass in each bending-torsion coupled mode with generalised mass in purely flexural or torsional modes; (c) contribution of each term (bending, torsion and coupling) to the generalised mass in different modes; (d) percentage of modal contribution in the dynamic flexural and torsional response of the beam at the tip due to the flexural load at the tip; (e) percentage of modal contribution in the dynamic flexural and torsional response of the beam at the tip due to the torque at the tip.

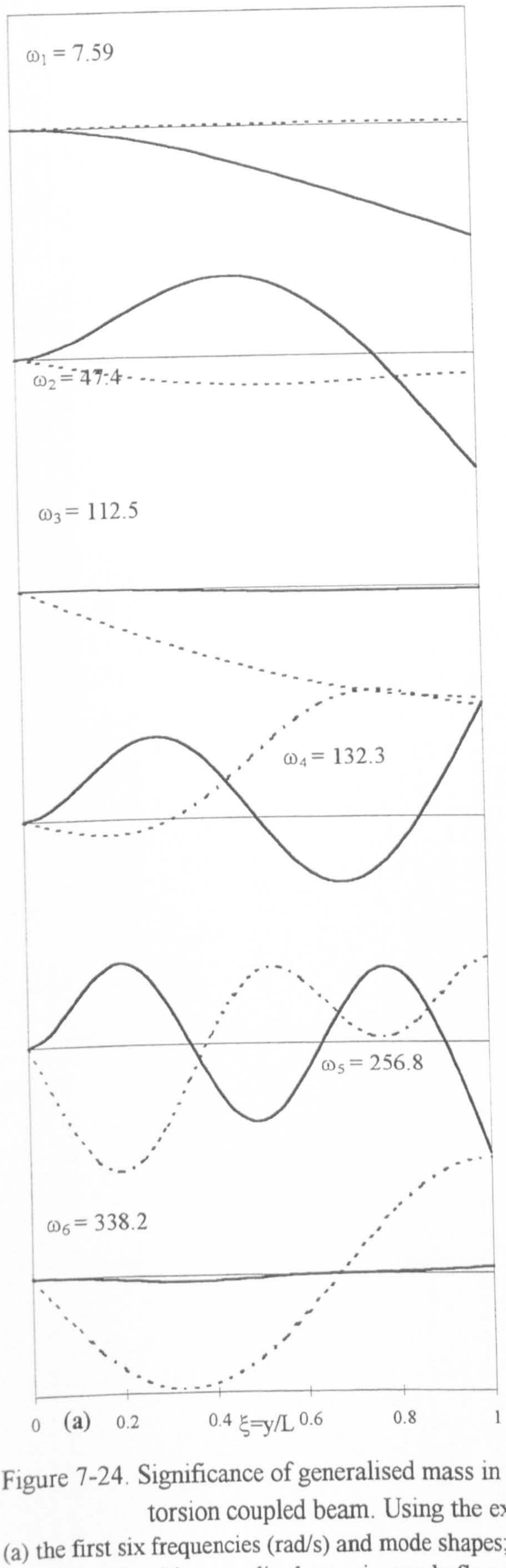

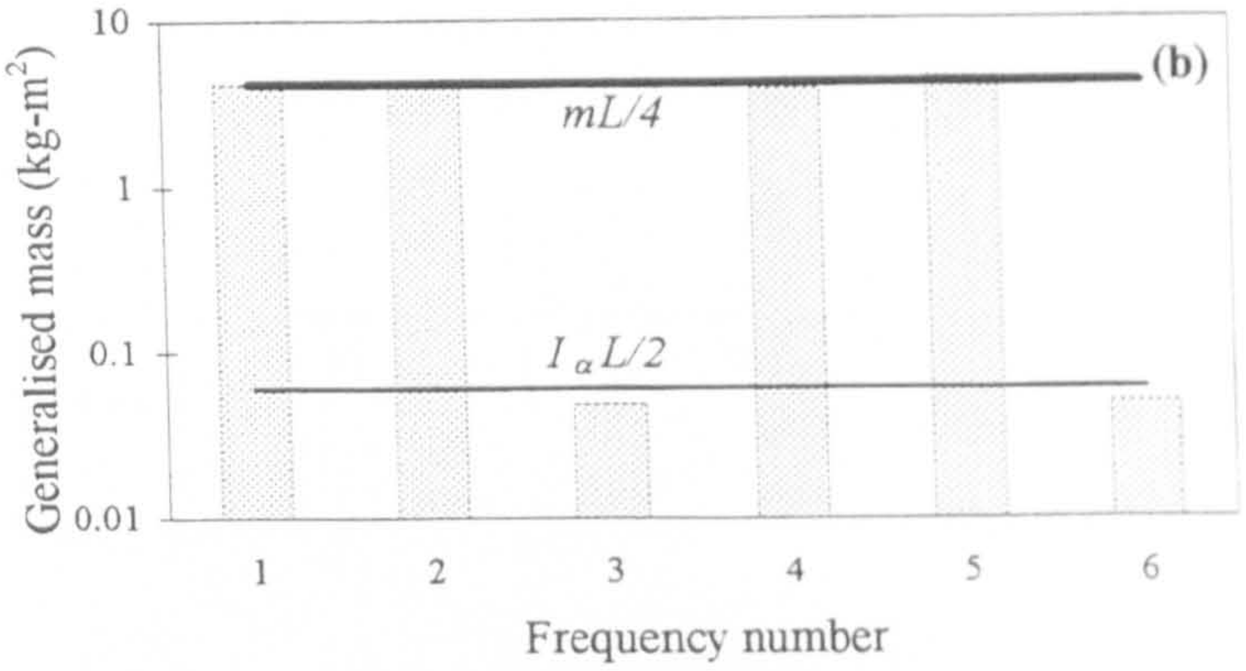

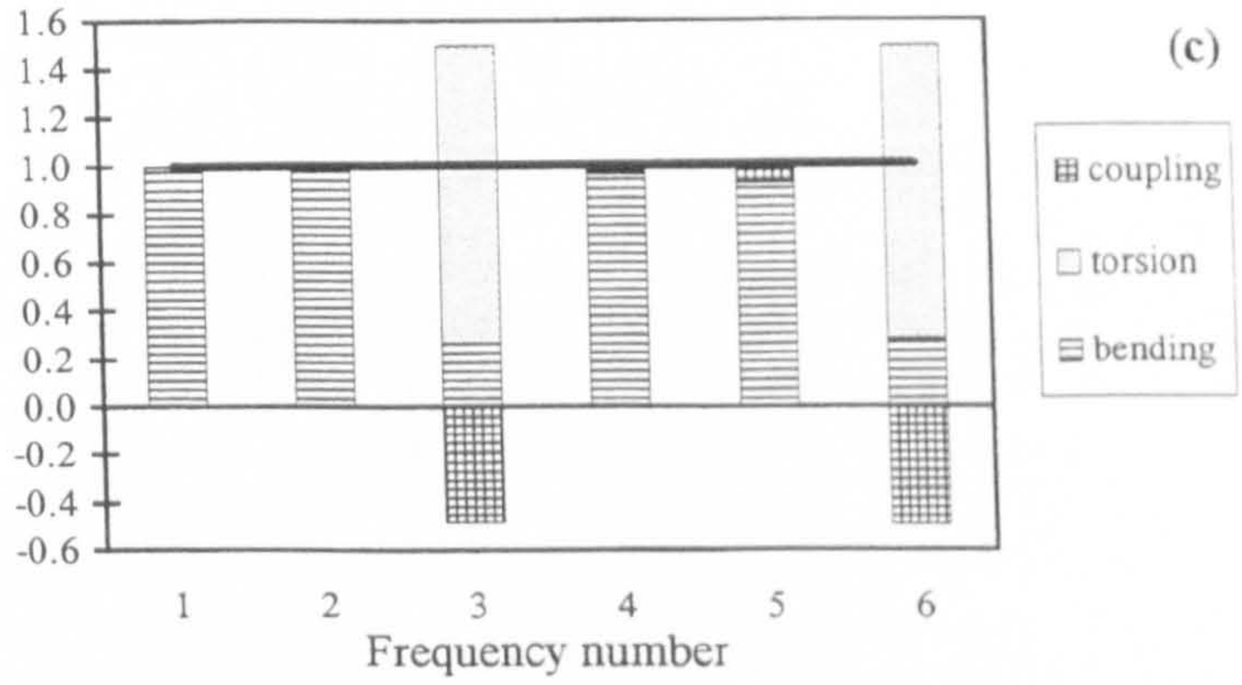

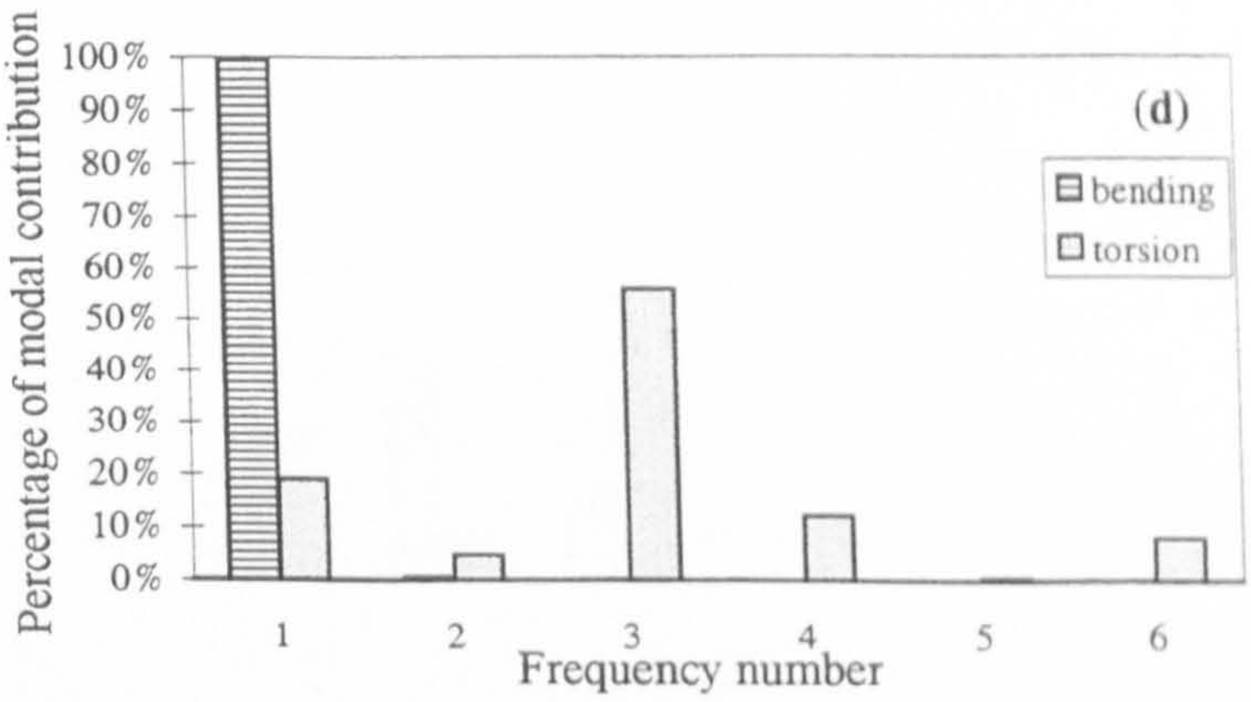

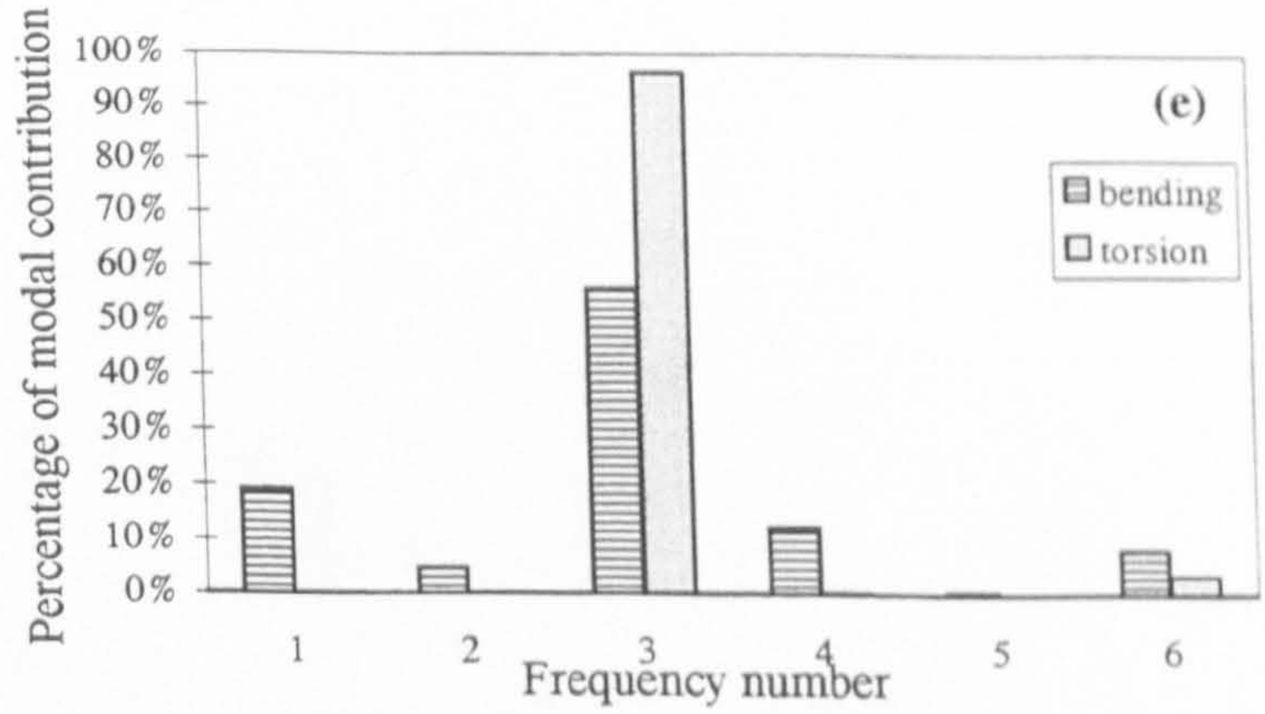

Figure 7-24. Significance of generalised mass in the dynamic response characteristics of a bending-torsion coupled beam. Using the example of Loaring wing (Loaring, 1944).

(a) the first six frequencies (rad/s) and mode shapes; (b) comparison of generalised mass in each bending-torsion coupled mode with generalised mass in purely flexural or torsional modes; (c) contribution of each term (bending, torsion and coupling) to the generalised mass in different modes; (d) percentage of modal contribution in the dynamic flexural and torsional response of the beam at the tip due to the flexural load at the tip; (e) percentage of modal contribution in the dynamic flexural and torsional response of the beam at the tip due to the torque at the tip.

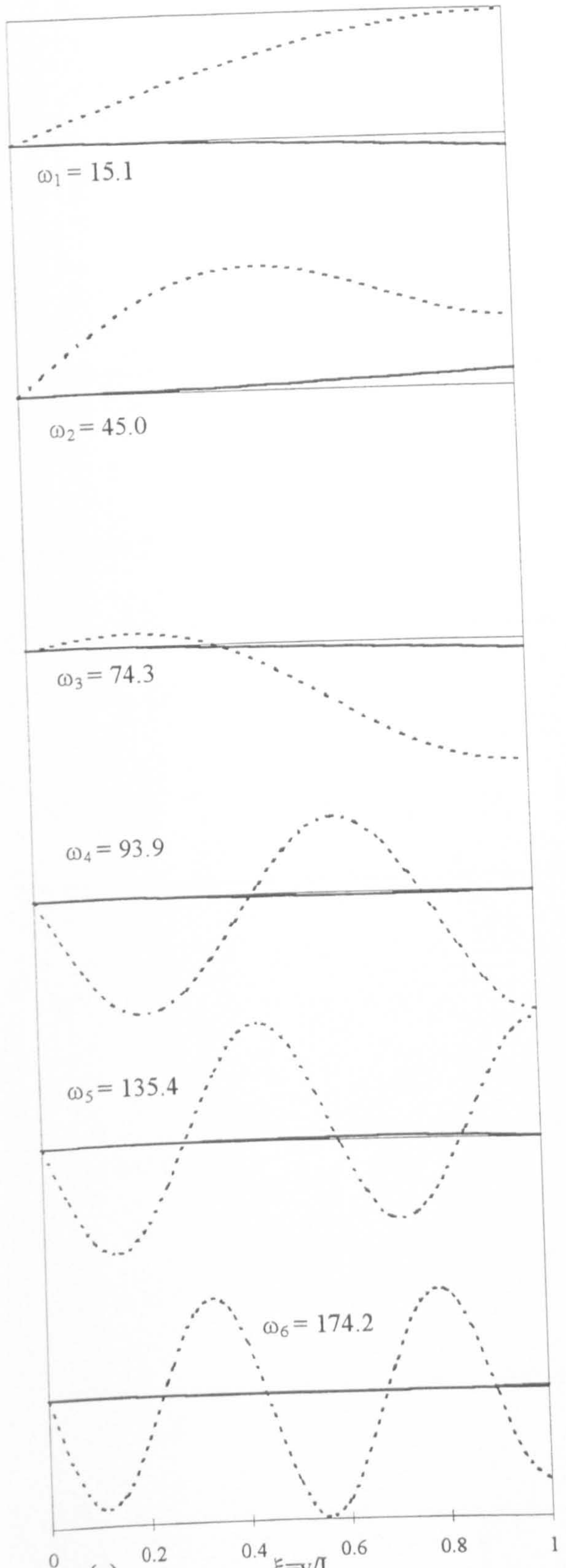

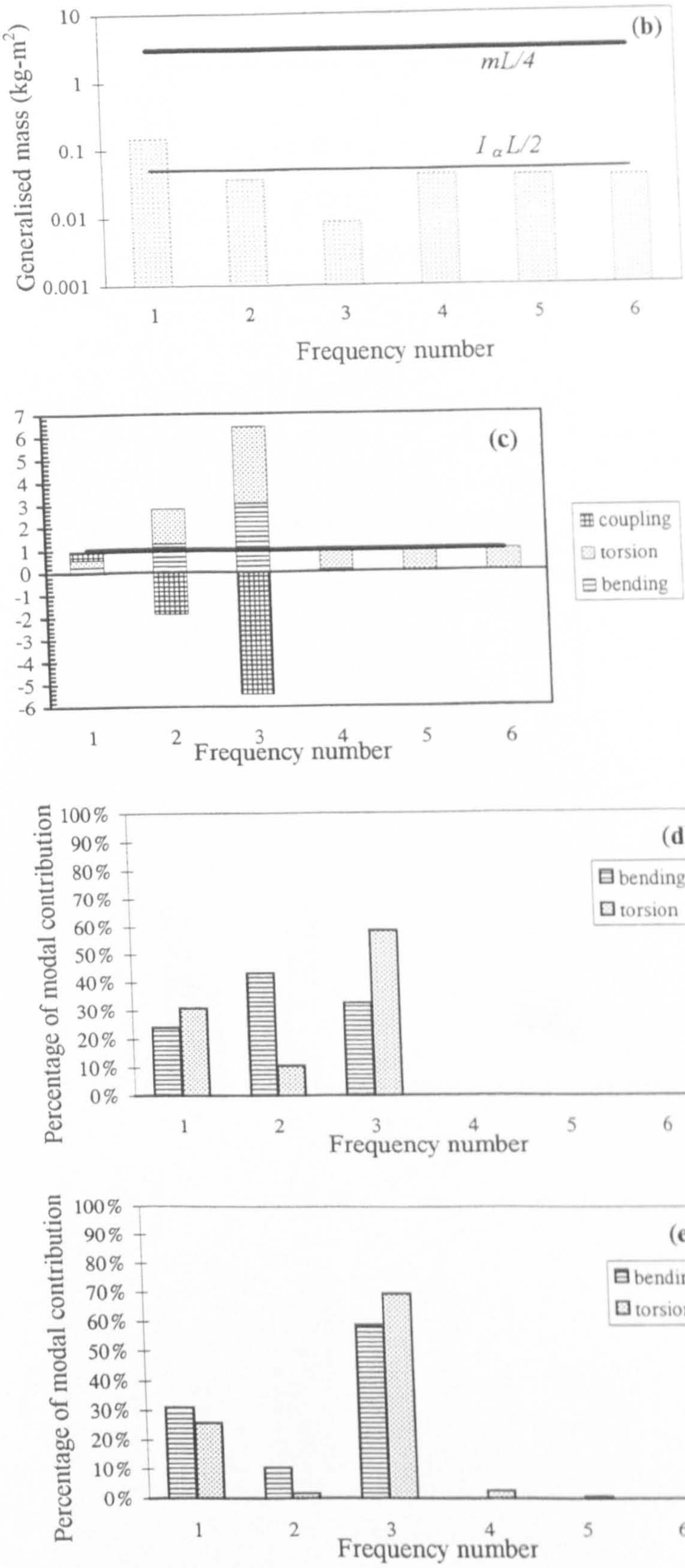

Figure 7-25. Significance of generalised mass in the dynamic response characteristics of a bending-torsion coupled beam. Using the example of a box beam with an axial slit (Banerjee, 1989).

(a) the first six frequencies (rad/s) and mode shapes; (b) comparison of generalised mass in each bending-torsion coupled mode with generalised mass in purely flexural or torsional modes; (c) contribution of each term (bending, torsion and coupling) to the generalised mass in different modes; (d) percentage of modal contribution in the dynamic flexural and torsional response of the beam at the tip due to the flexural load at the tip; (e) percentage of modal contribution in the dynamic flexural and torsional response of the beam at the tip due to the torque at the tip.

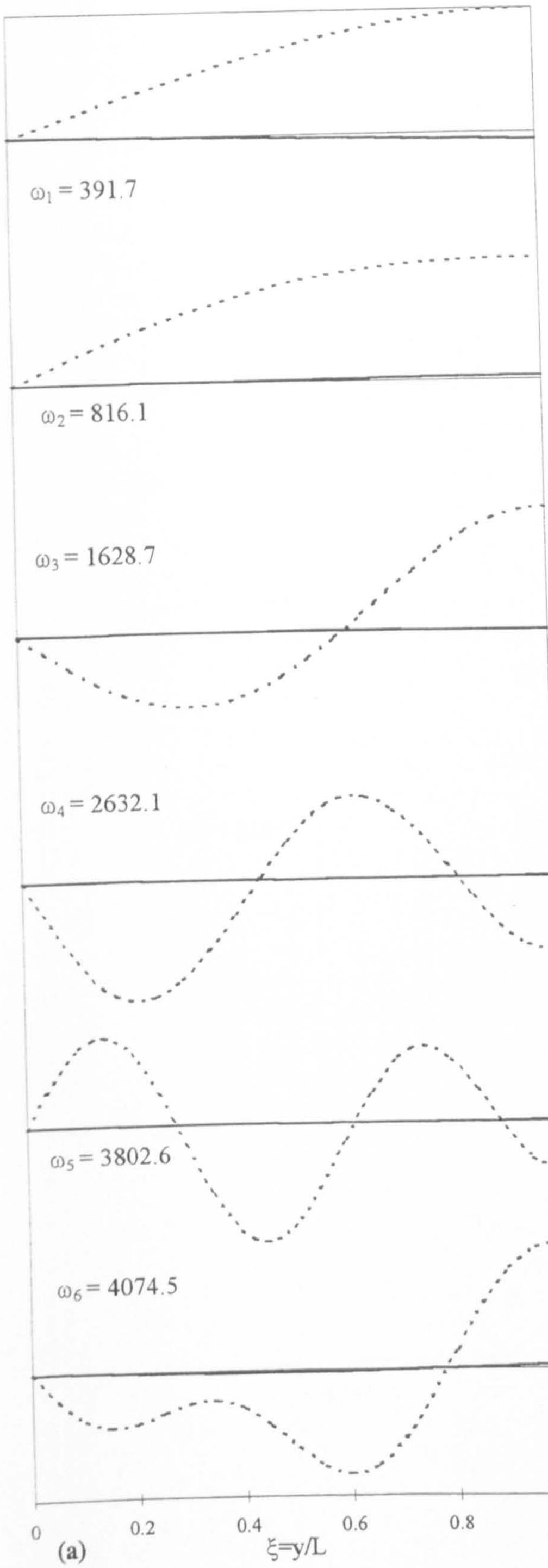

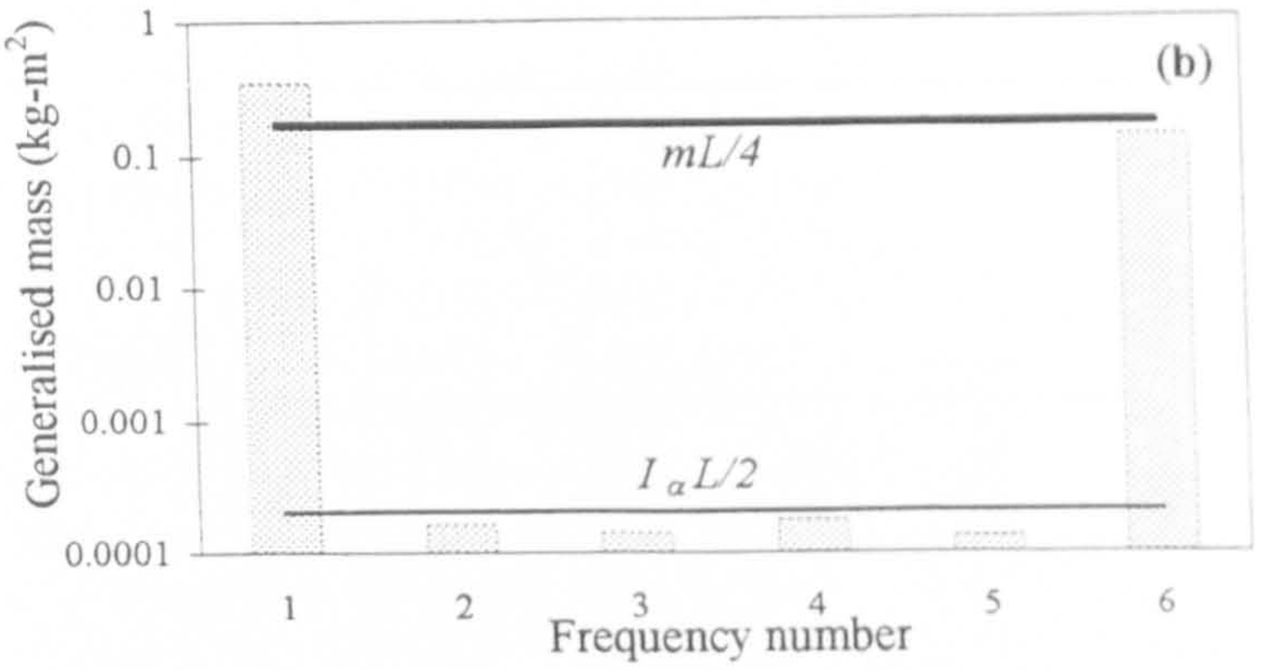

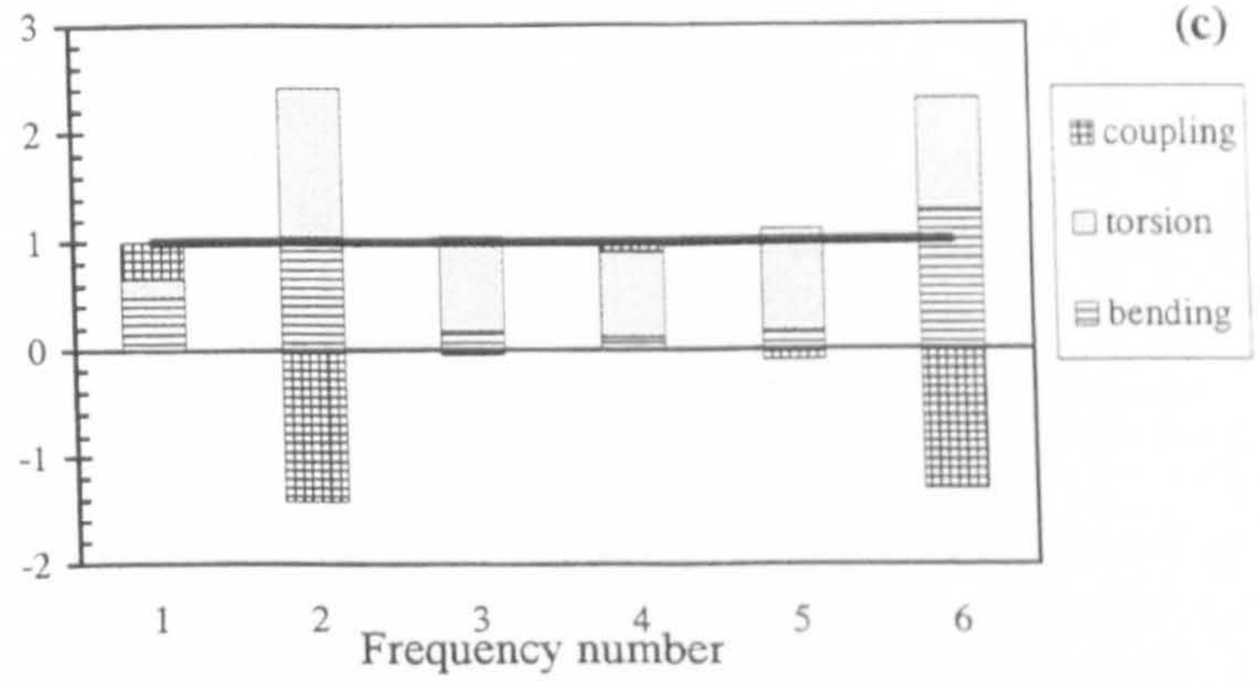

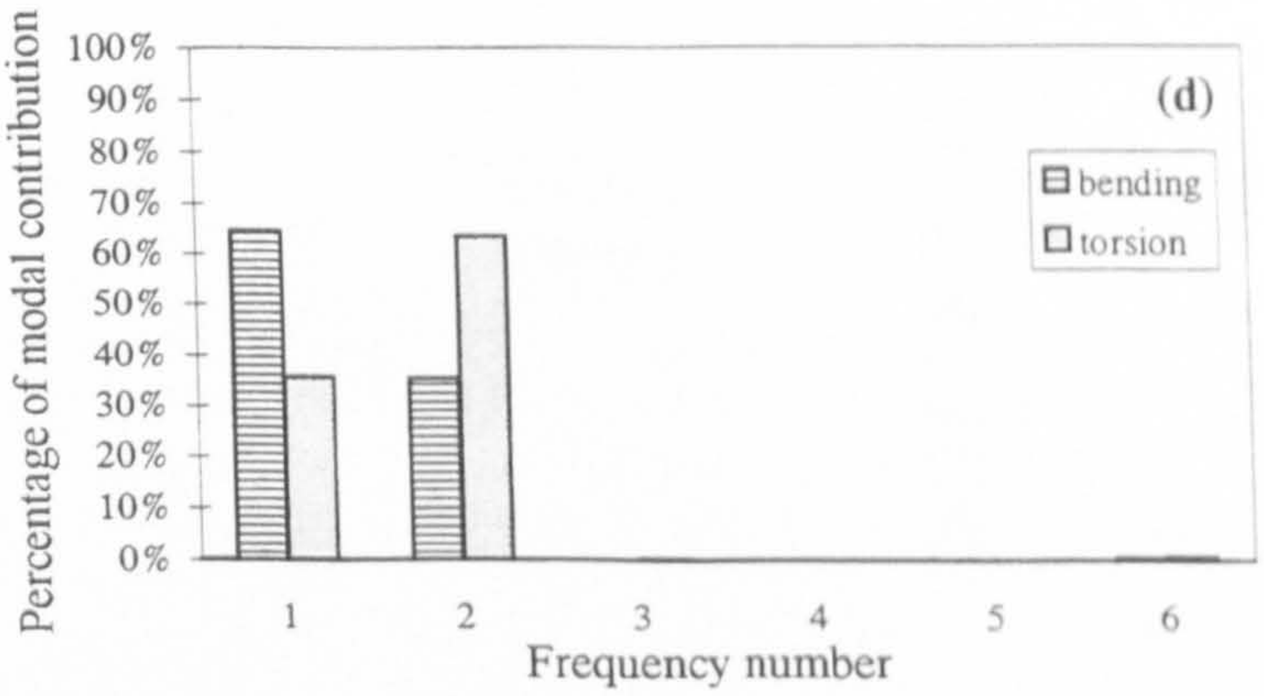

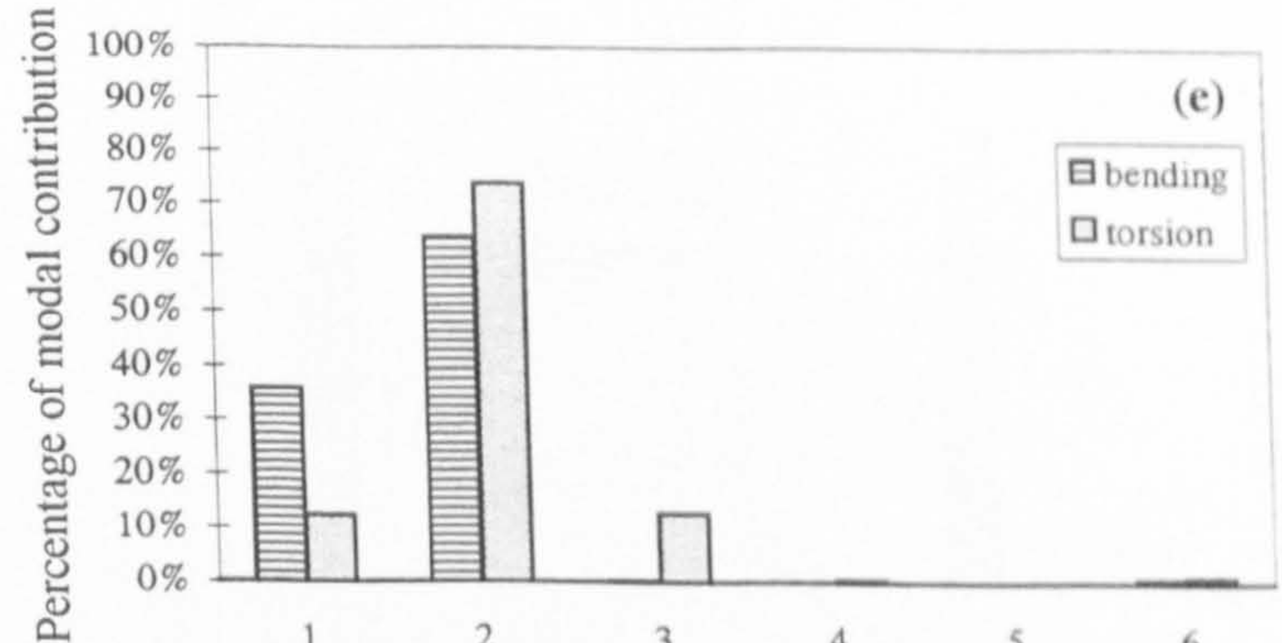

Figure 7-26. Significance of generalised mass in the dynamic response characteristics of a bending-torsion coupled beam with a thin-walled semi-circular cross-section (Friberg, 1985).

(a) the first six frequencies (rad/s) and mode shapes; (b) comparison of generalised mass in each bending-torsion coupled mode with generalised mass in purely flexural or torsional modes; (c) contribution of each term (bending, torsion and coupling) to the generalised mass in different modes; (d) percentage of modal contribution in the dynamic flexural and torsional response of the beam at the tip due to the flexural load at the tip; (e) percentage of modal contribution in the dynamic flexural and torsional response of the beam at the tip due to the torque at the tip.

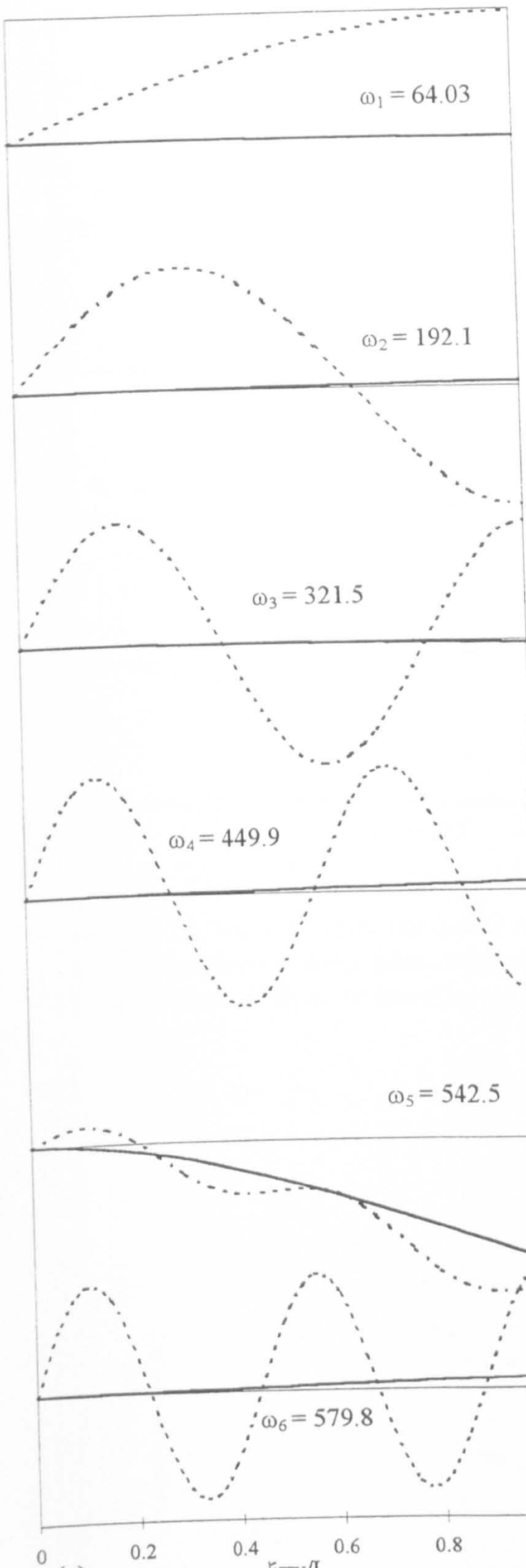

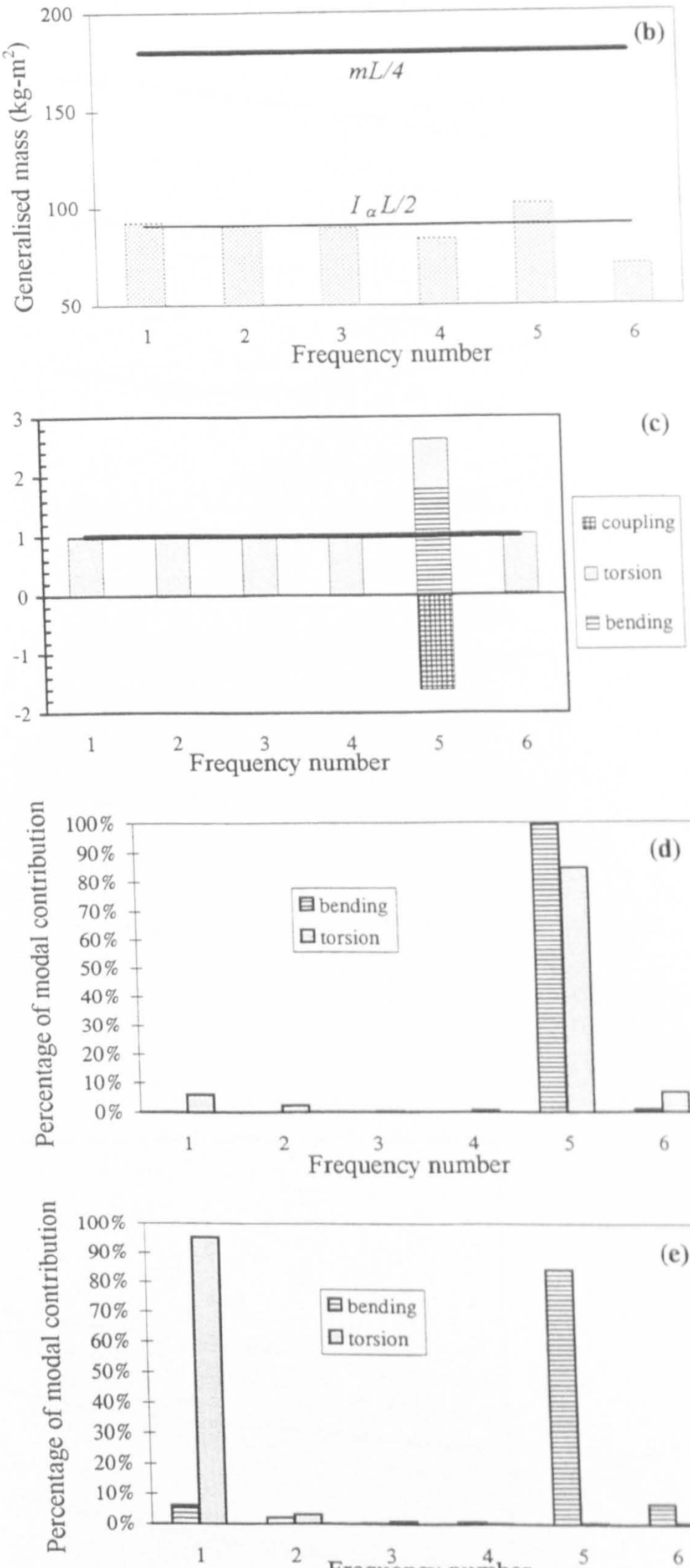

Figure 7-27. Significance of generalised mass in the dynamic response characteristics of a bending-torsion coupled concrete beam with a channel cross-section (Bercin and Tanaka, 1997).

(a) the first six frequencies (rad/s) and mode shapes; (b) comparison of generalised mass in each bending-torsion coupled mode with generalised mass in purely flexural or torsional modes; (c) contribution of each term (bending, torsion and coupling) to the generalised mass in different modes; (d) percentage of modal contribution in the dynamic flexural and torsional response of the beam at the tip due to the flexural load at the tip; (e) percentage of modal contribution in the dynamic flexural and torsional response of the beam at the tip due to the torque at the tip.

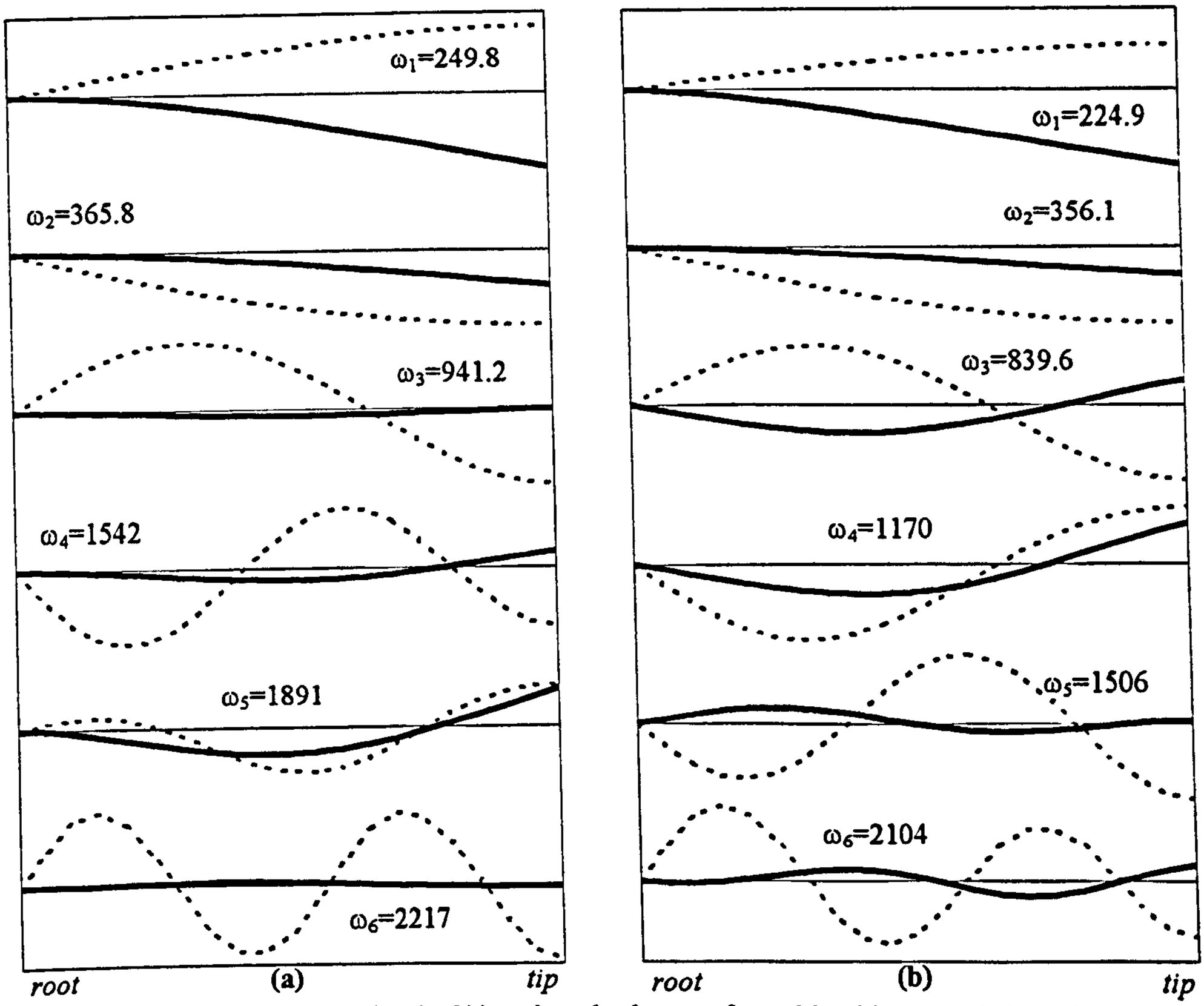

Figure 7-28. Natural frequencies (rad/s) and mode shapes of a turbine blade [L=2.6 m] (Petersen, 1979)
(a) without effects of shear deformation and rotatory inertia
(b) with effects of shear deformation and rotatory inertia

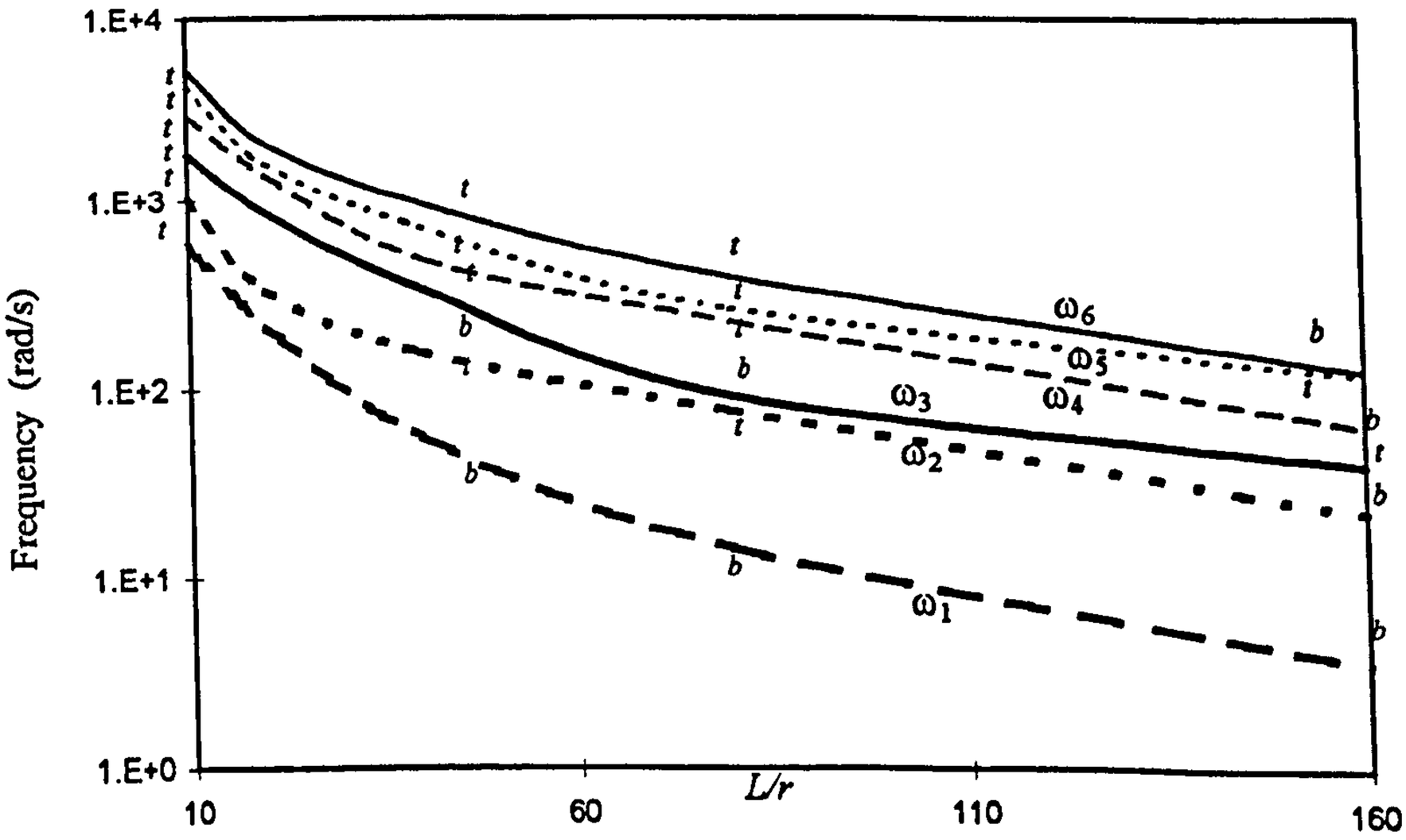

Figure 7-29. Variation of natural frequencies of a turbine blade (Petersen, 1979)
in each mode against slenderness ratio (L/r) t: torsion; b: bending.

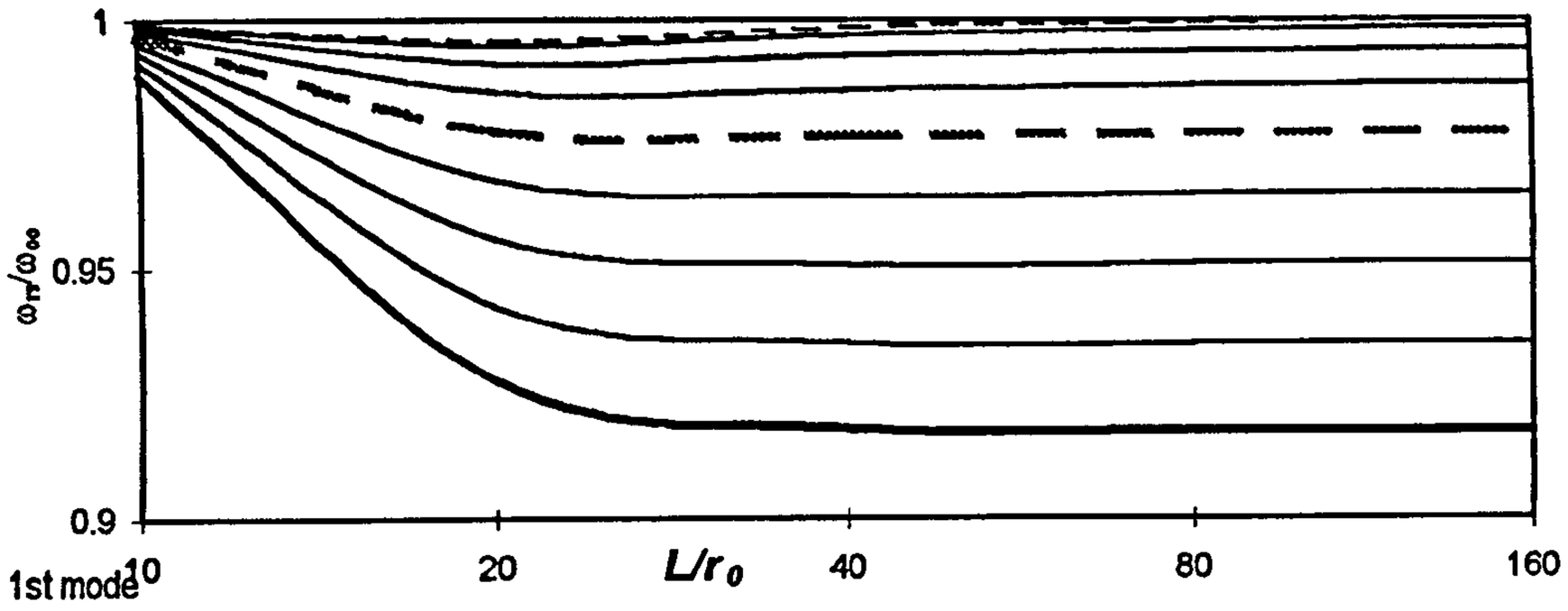

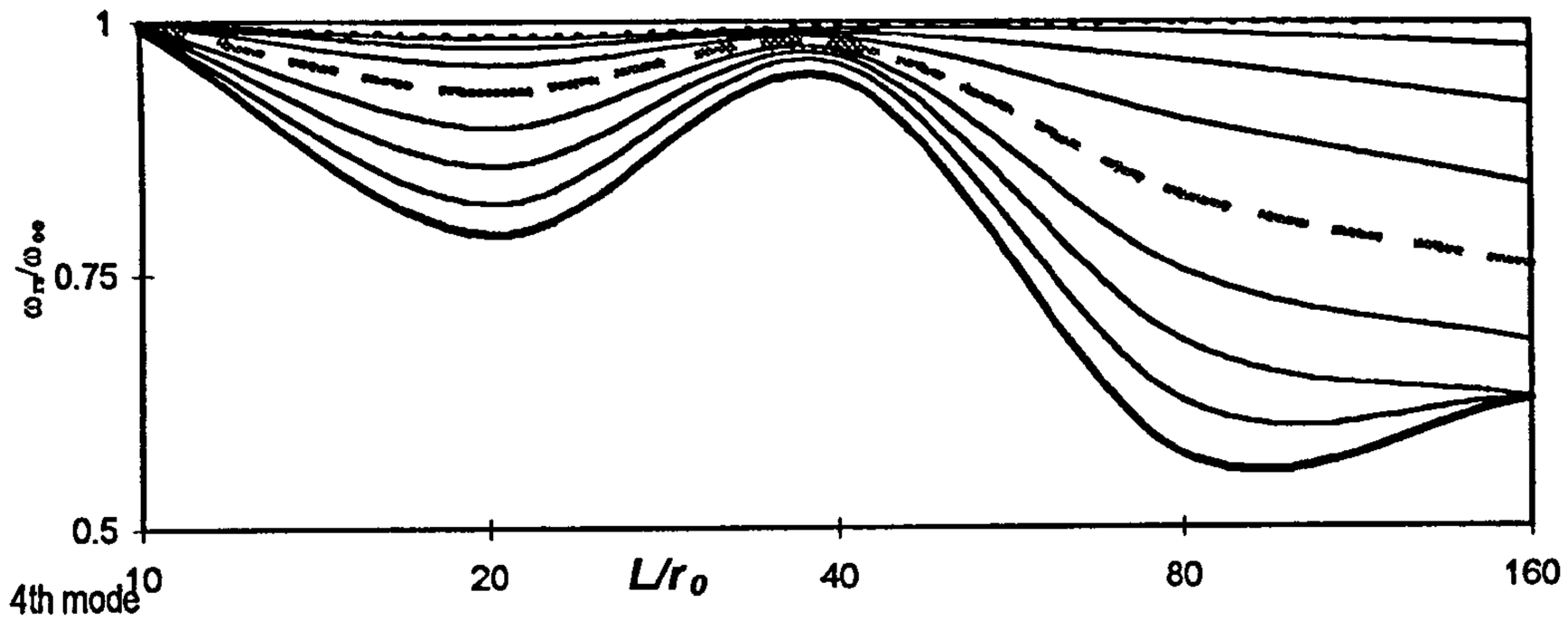

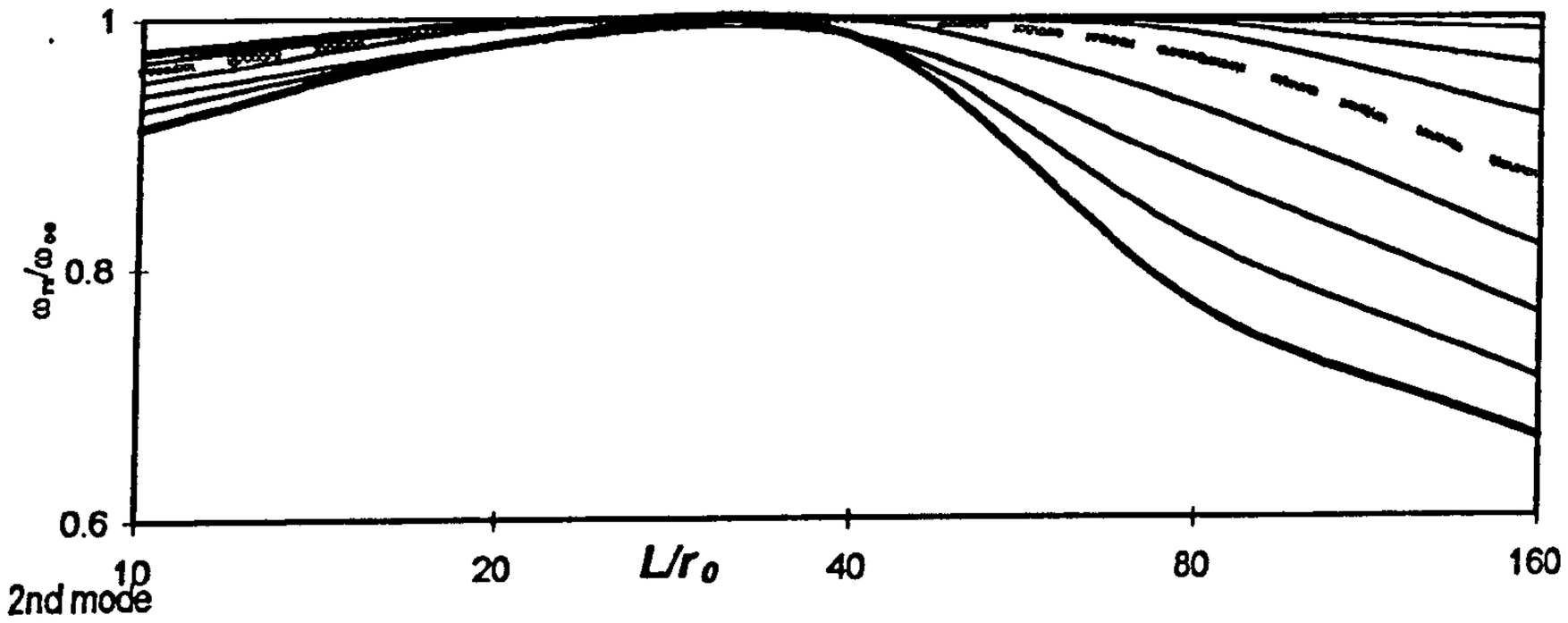

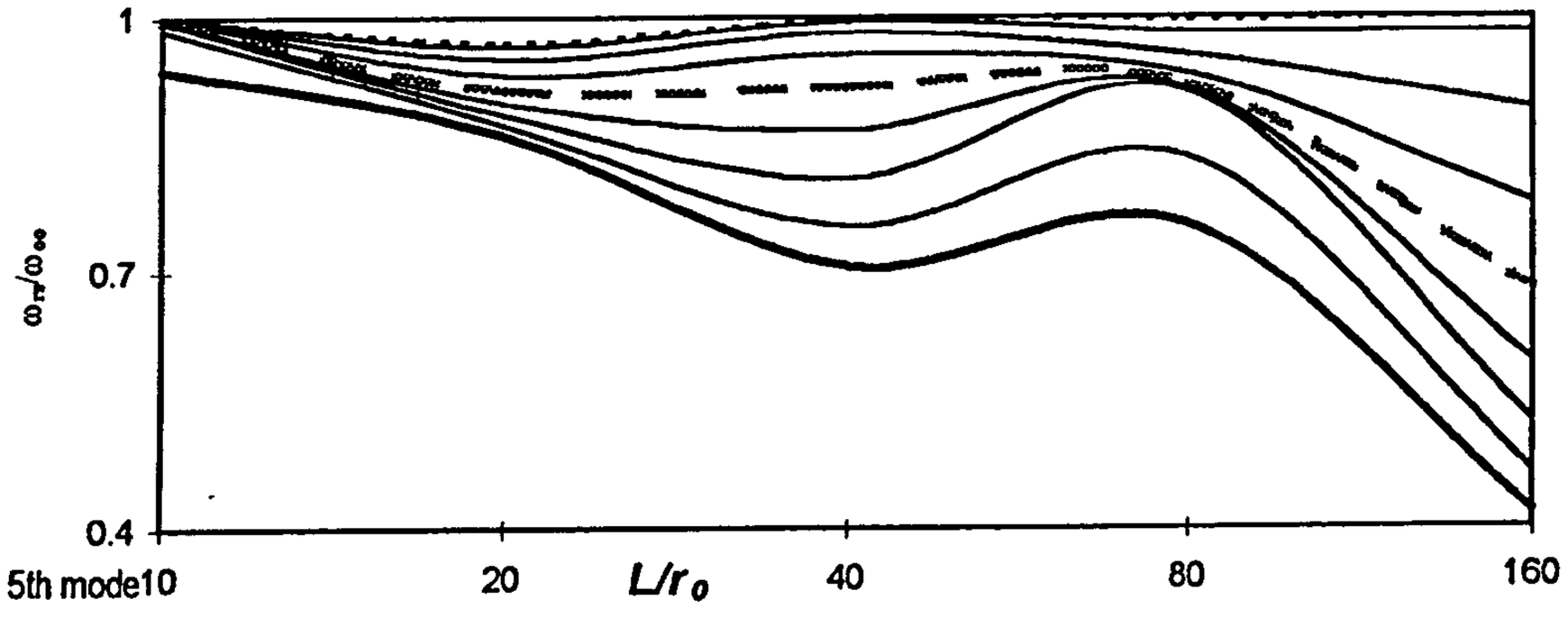

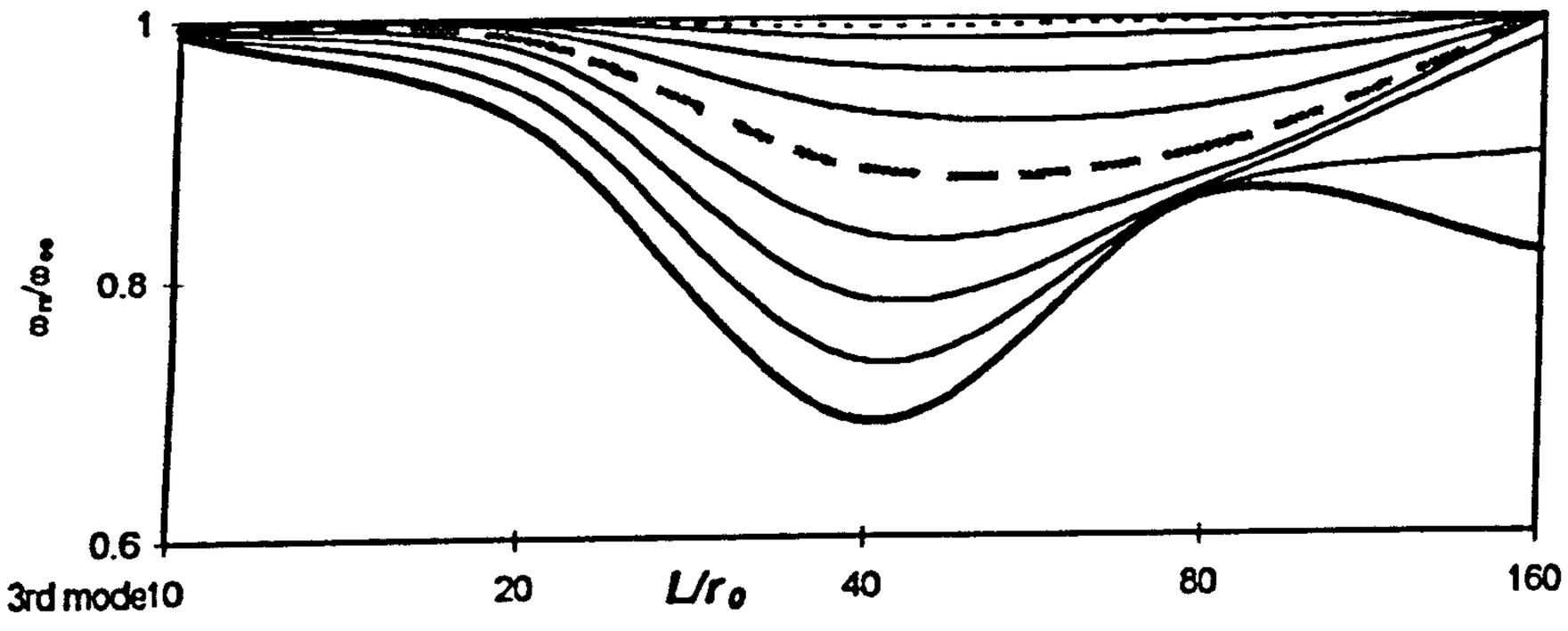

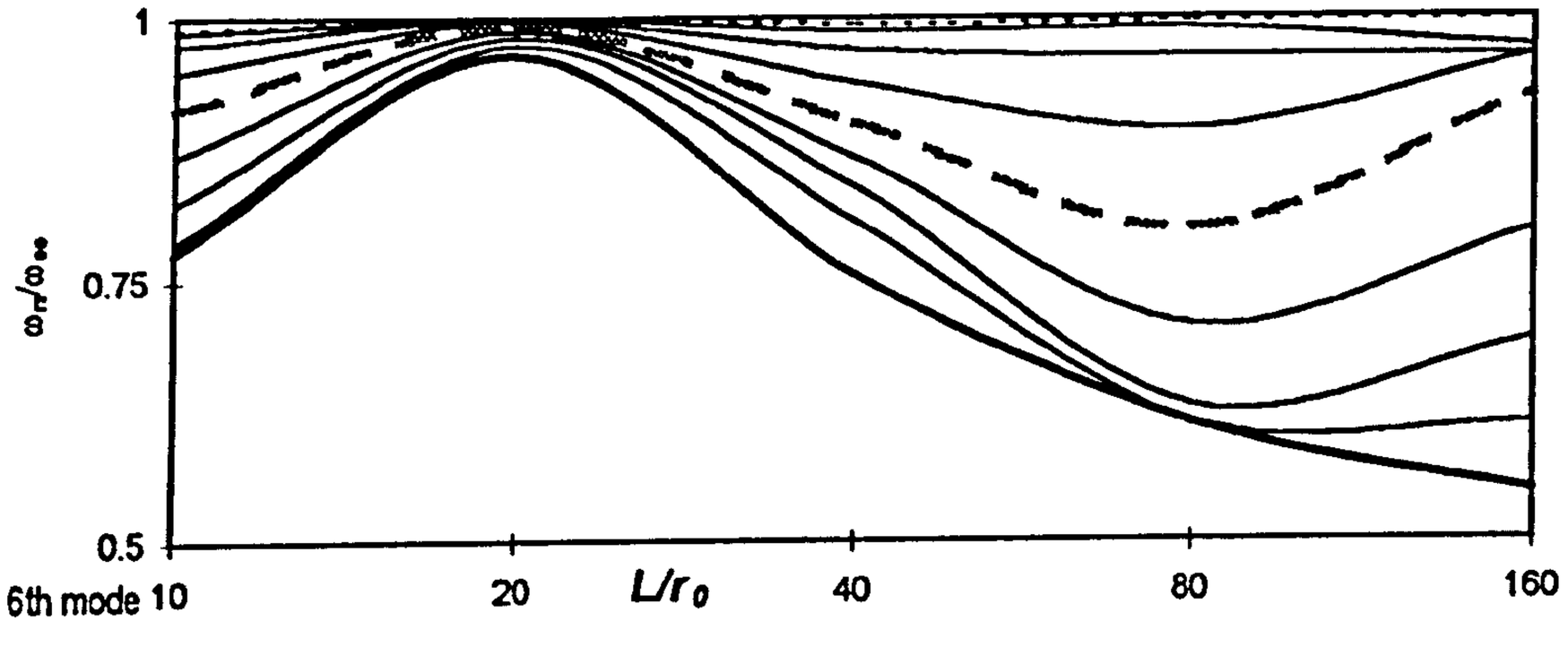

Figure 7-30. Variation of non-dimensional frequencies for different values of $0<s^2<0.2$ against slenderness ratio (L/r) [a turbine blade (Petersen, 1979)].

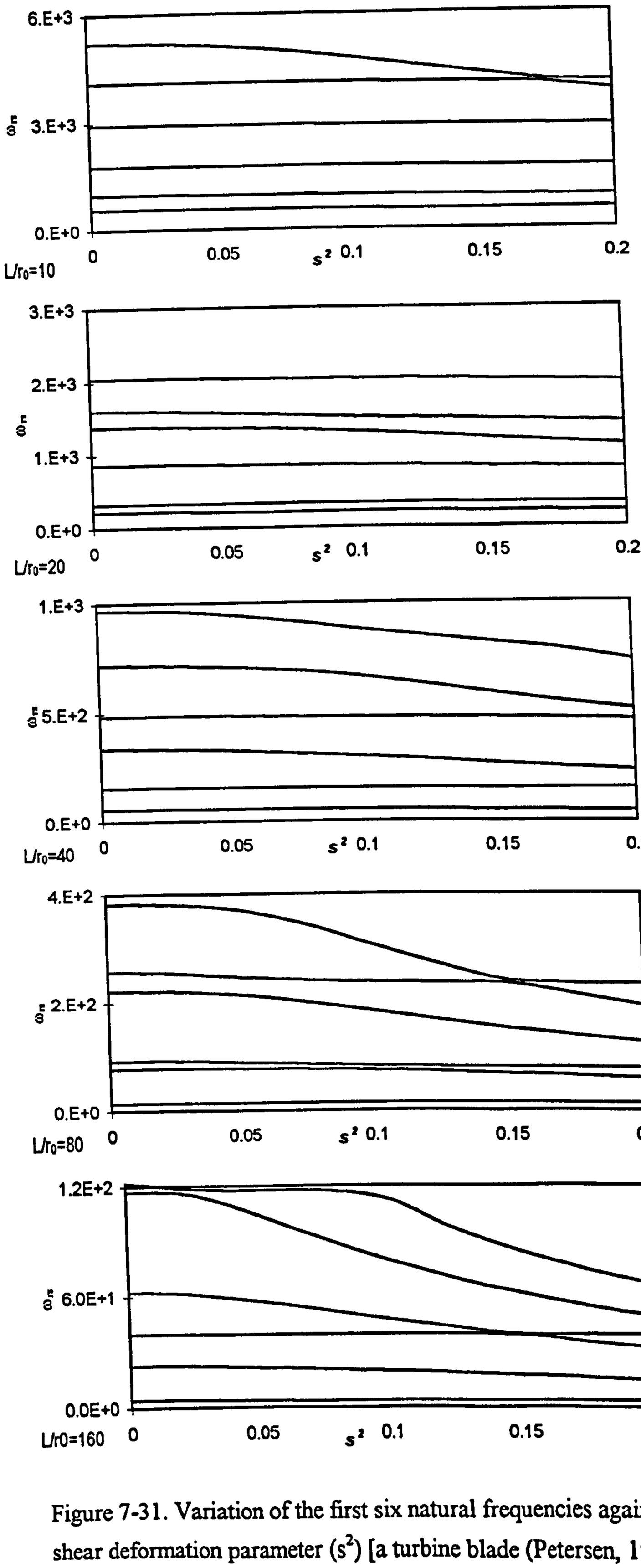

Figure 7-31. Variation of the first six natural frequencies against the shear deformation parameter (s^2) [a turbine blade (Petersen, 1979)].

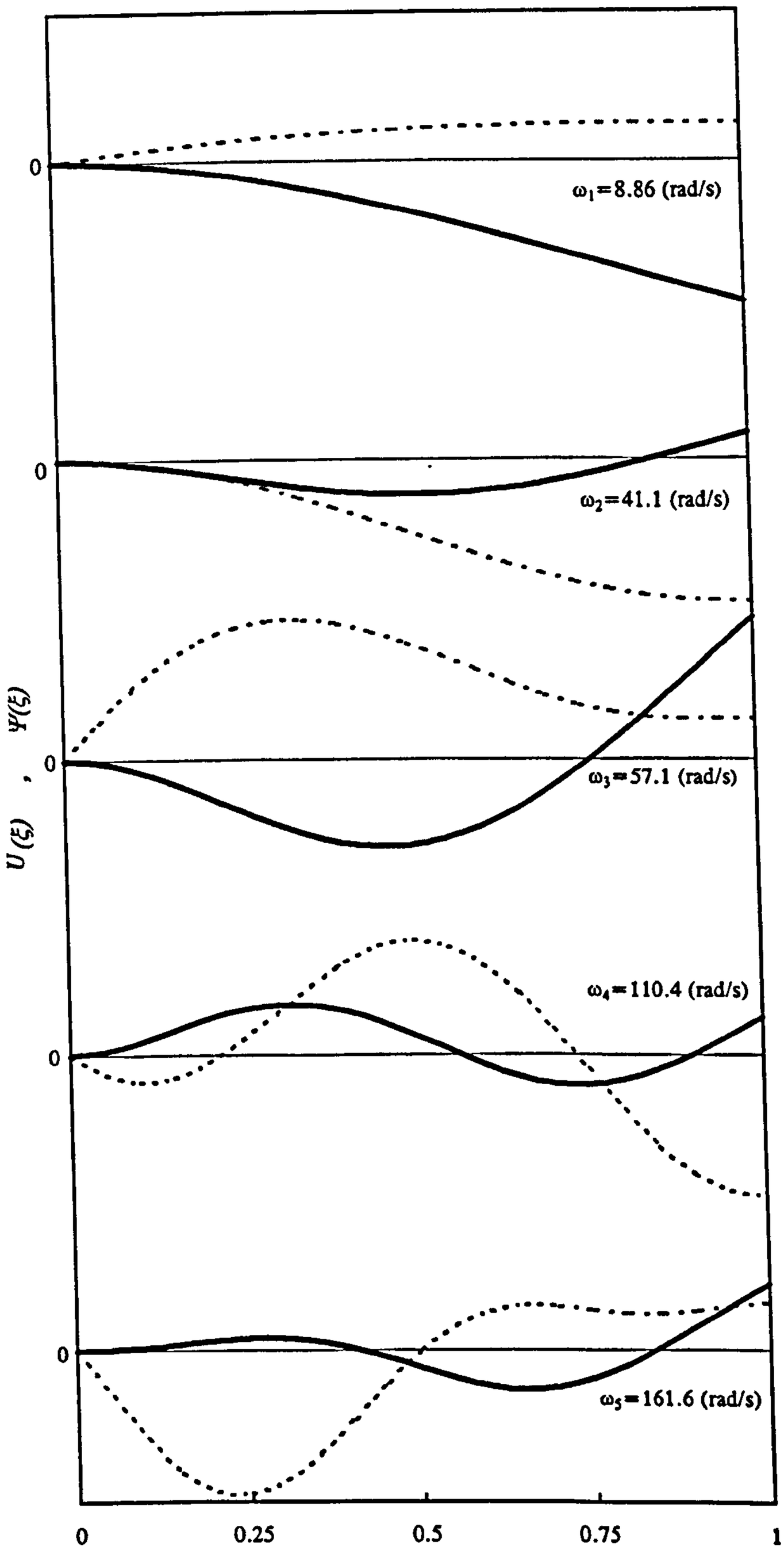

Figure 7-32. Natural frequencies and mode shapes of a bending-torsion coupled composite beam (Eslimy-Isfahany et al.,1996).
—— flexural displacement(U); - - - torsional rotation(Ψ).

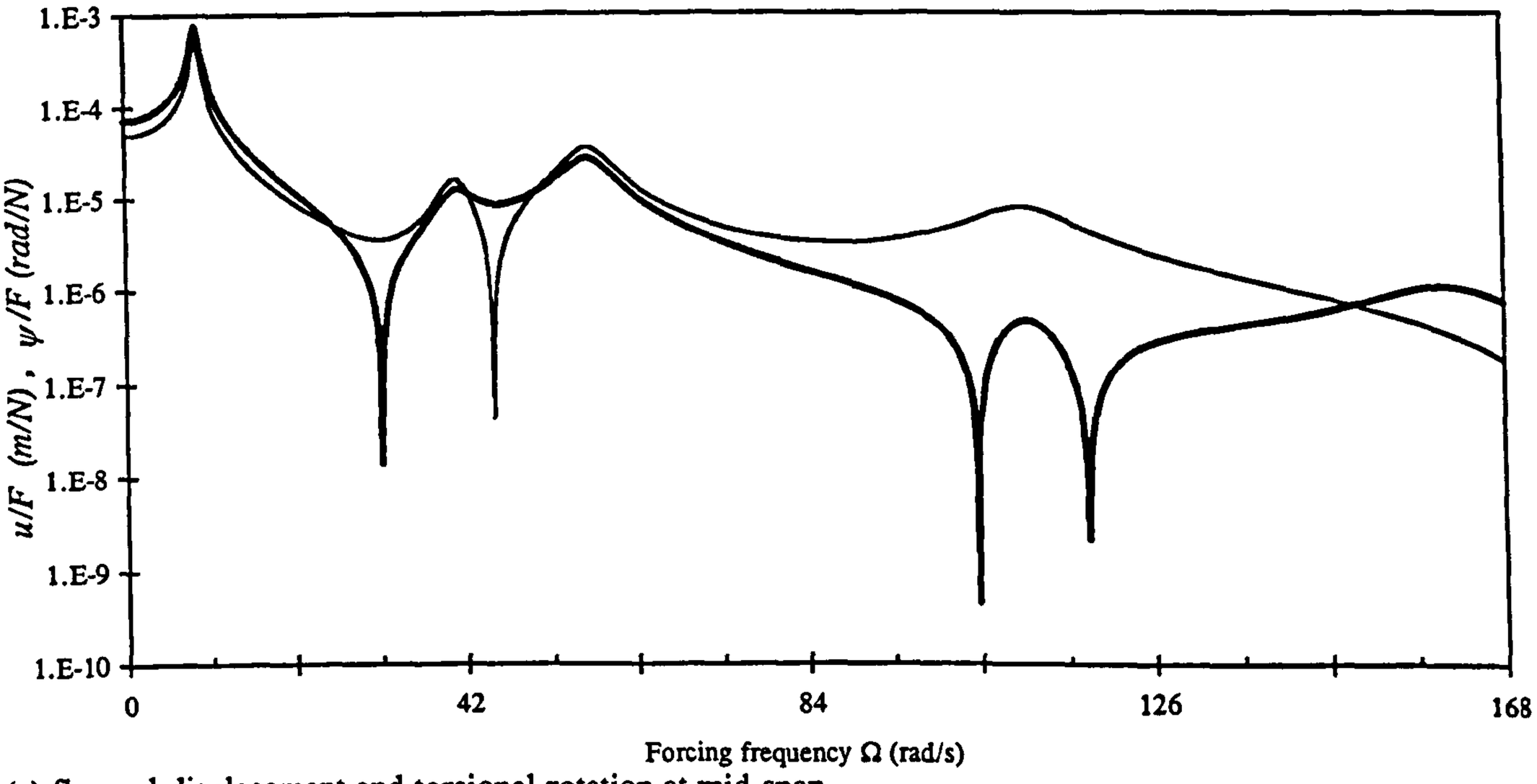

(a) flexural displacement and torsional rotation at mid-span

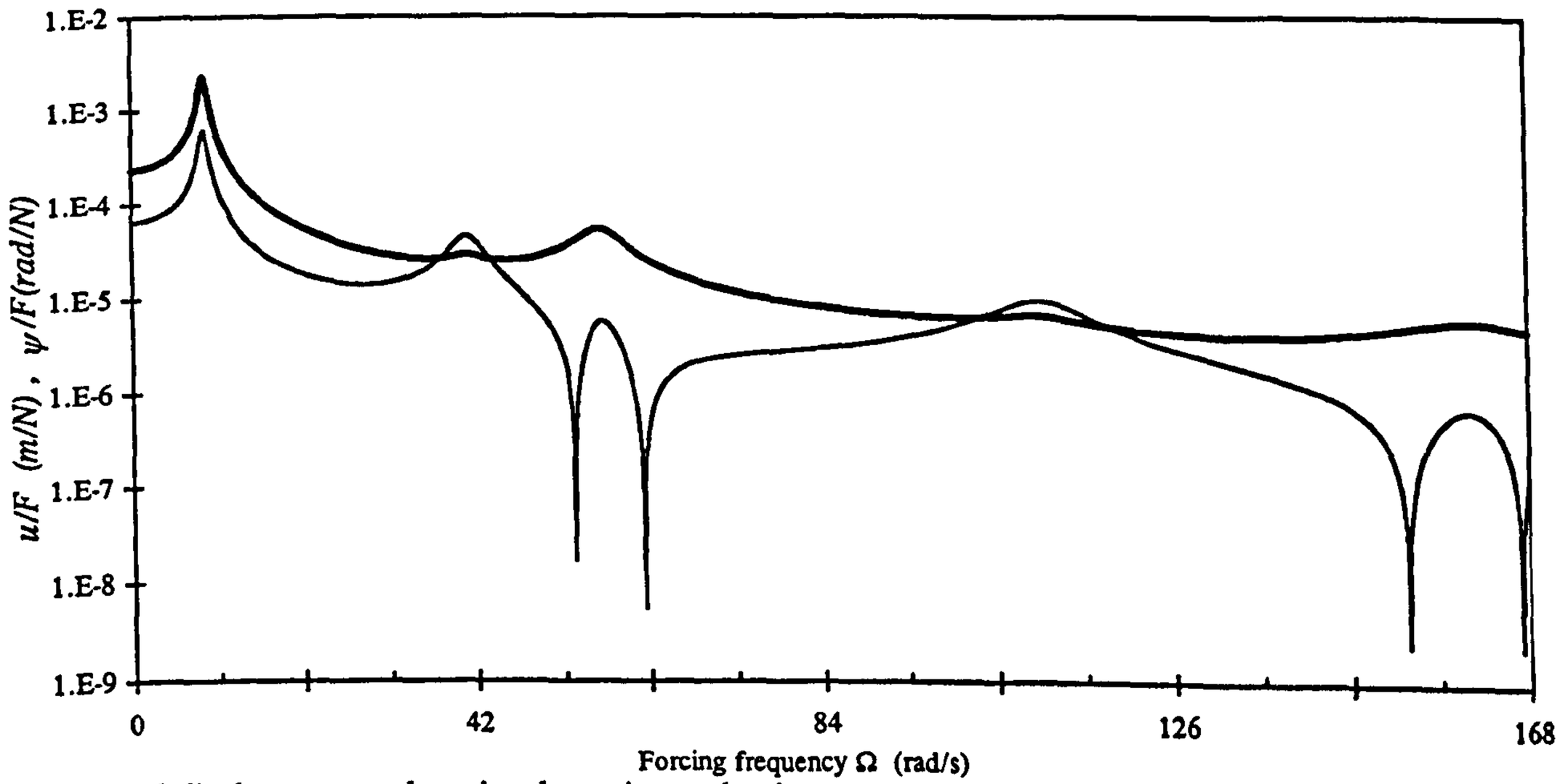

(b) flexural displacement and torsional rotation at the tip

Figure 7-33. Dynamic response of a composite beam (Eslimy-Isfahany et al., 1996) due to a harmonically varying concentrated force at the tip.

——— flexural displacement; —— torsional rotation.

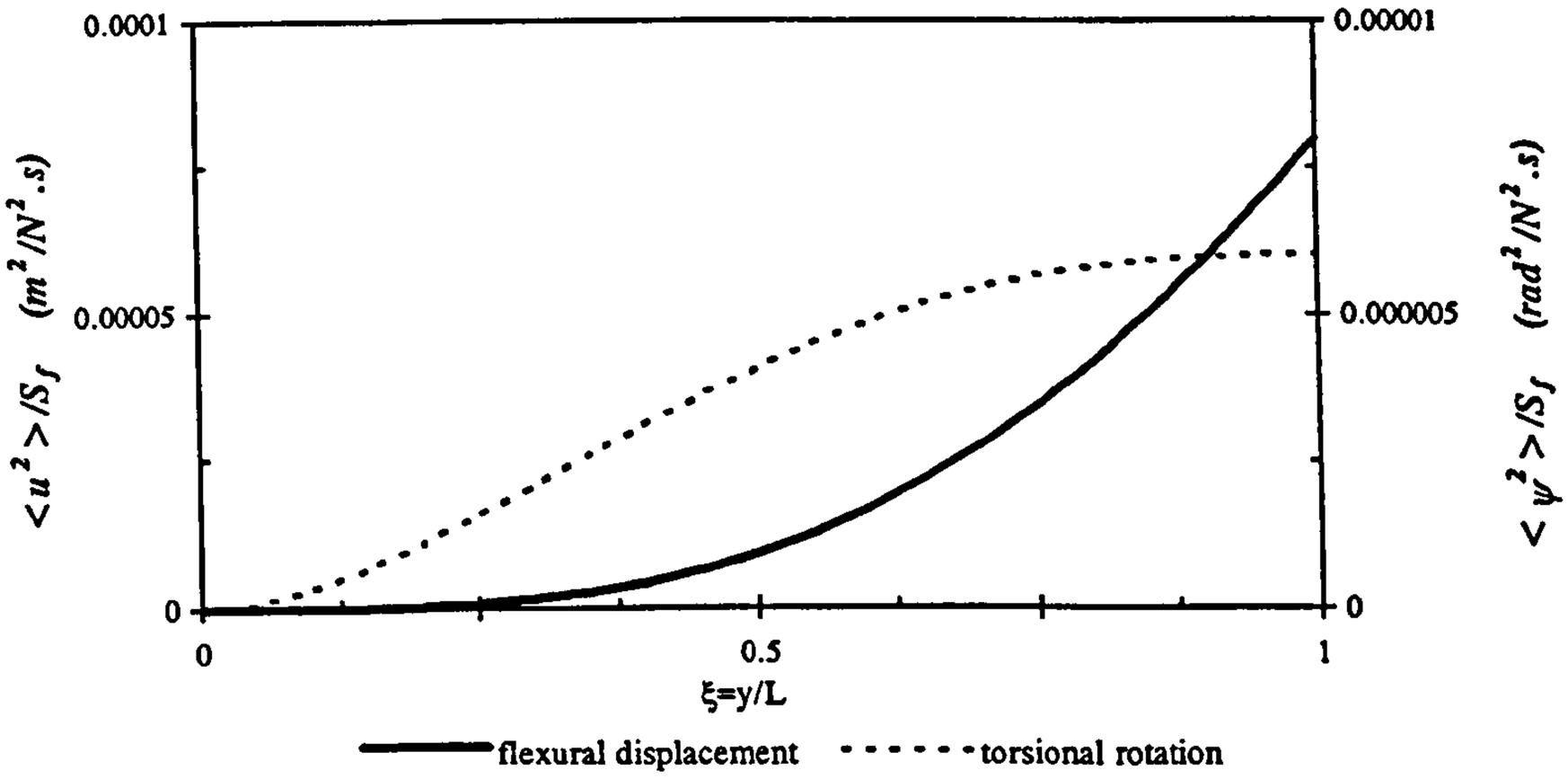

Figure 7-34. Variation of the mean square value of dynamic response along a composite beam (Eslimy-Isfahany et al., 1996).

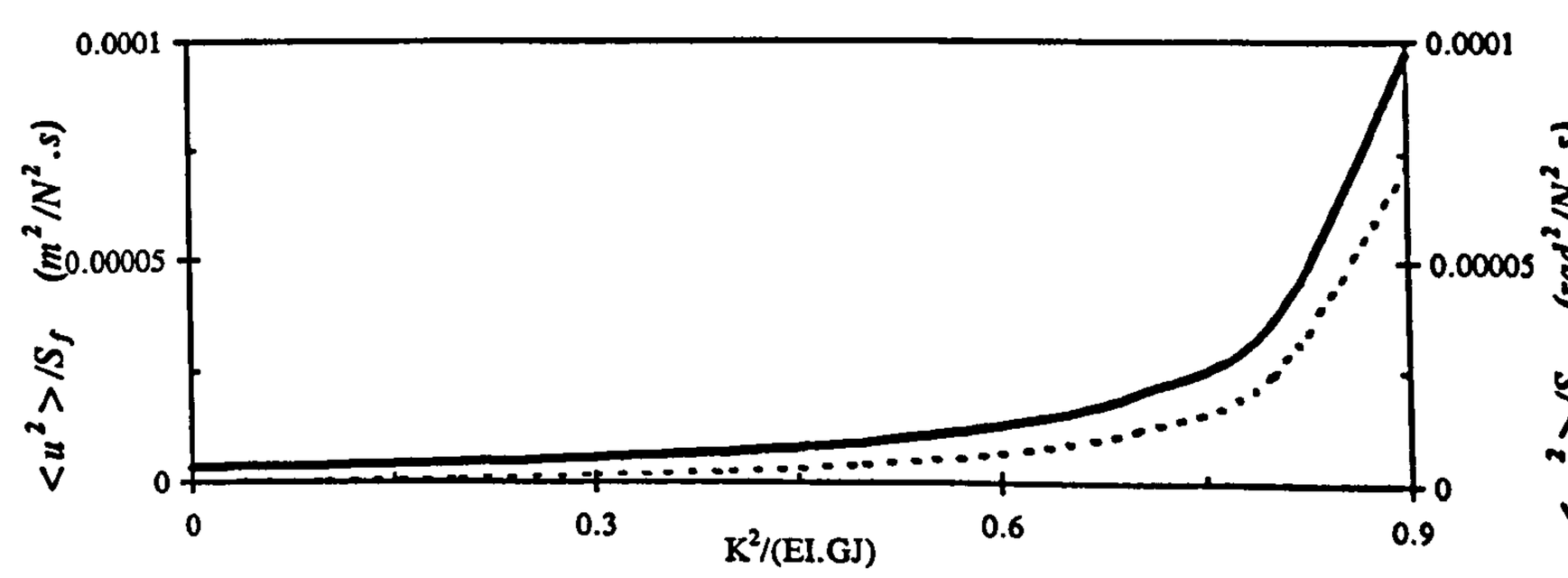

(a) flexural displacement and torsional rotation at mid-span

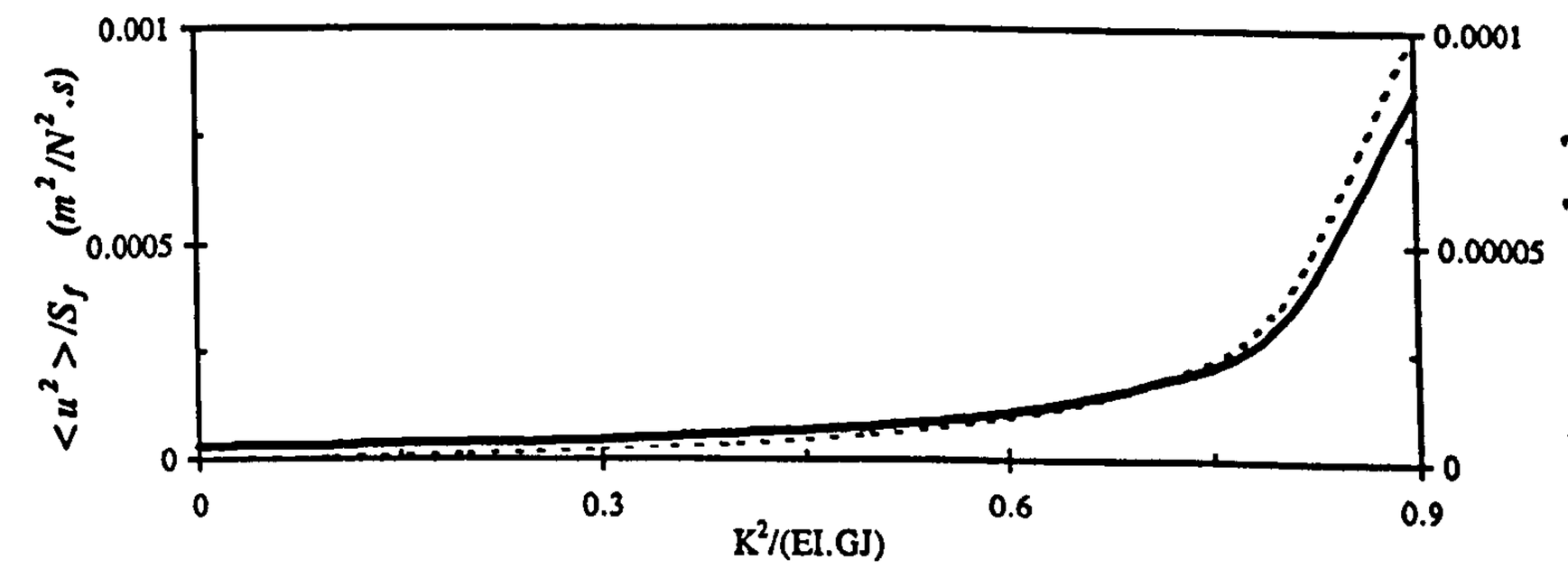

(b) flexural displacement and torsional rotation at the tip

Figure 7-35. The effect of bending-torsion coupling parameter on the mean square value of dynamic response.

——— flexural displacement; - - - - torsional rotation.

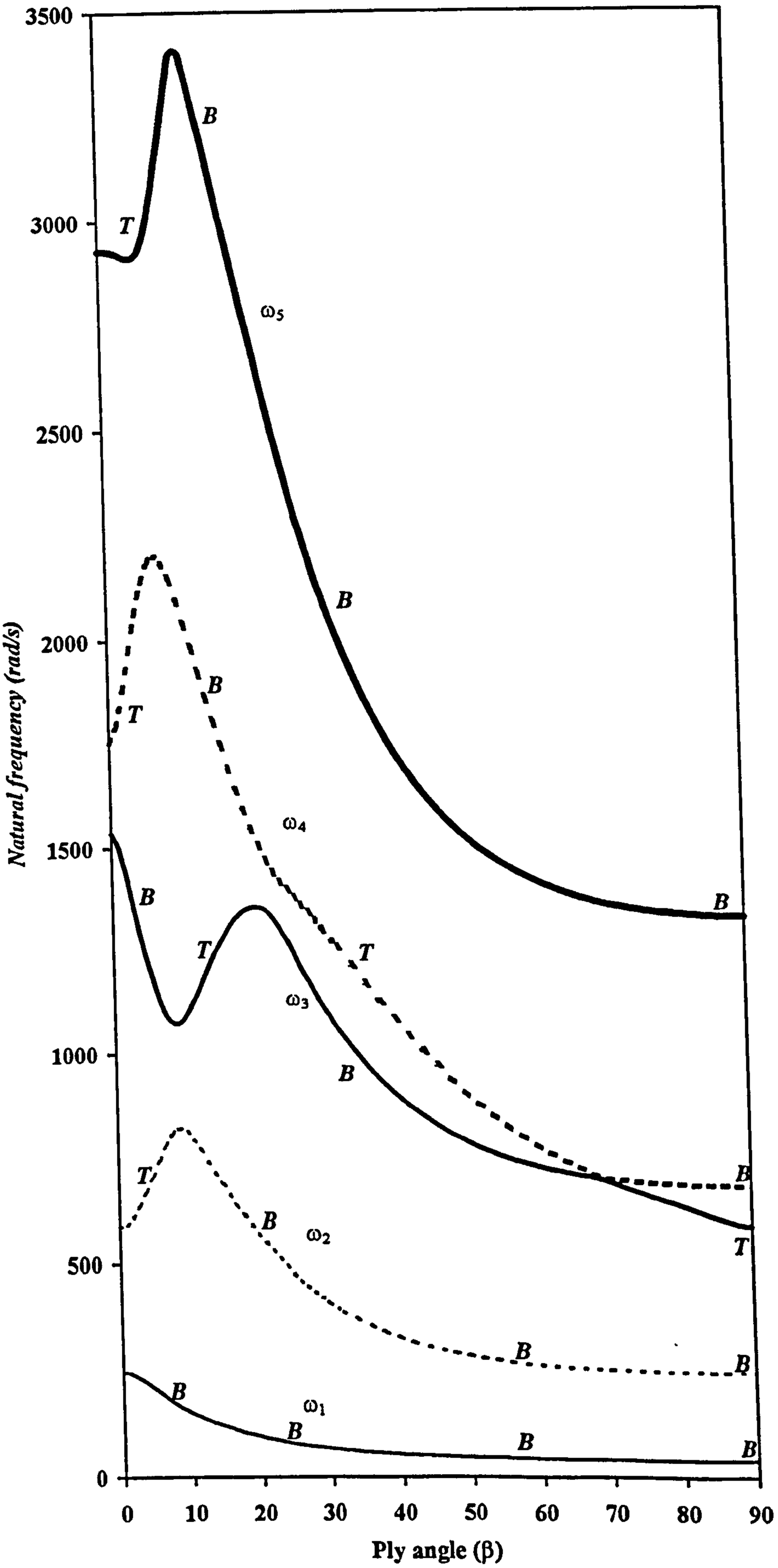

Figure 7-36. Variation of the first five natural frequencies of the box wing against ply angle.
B : bending; T : torsional.

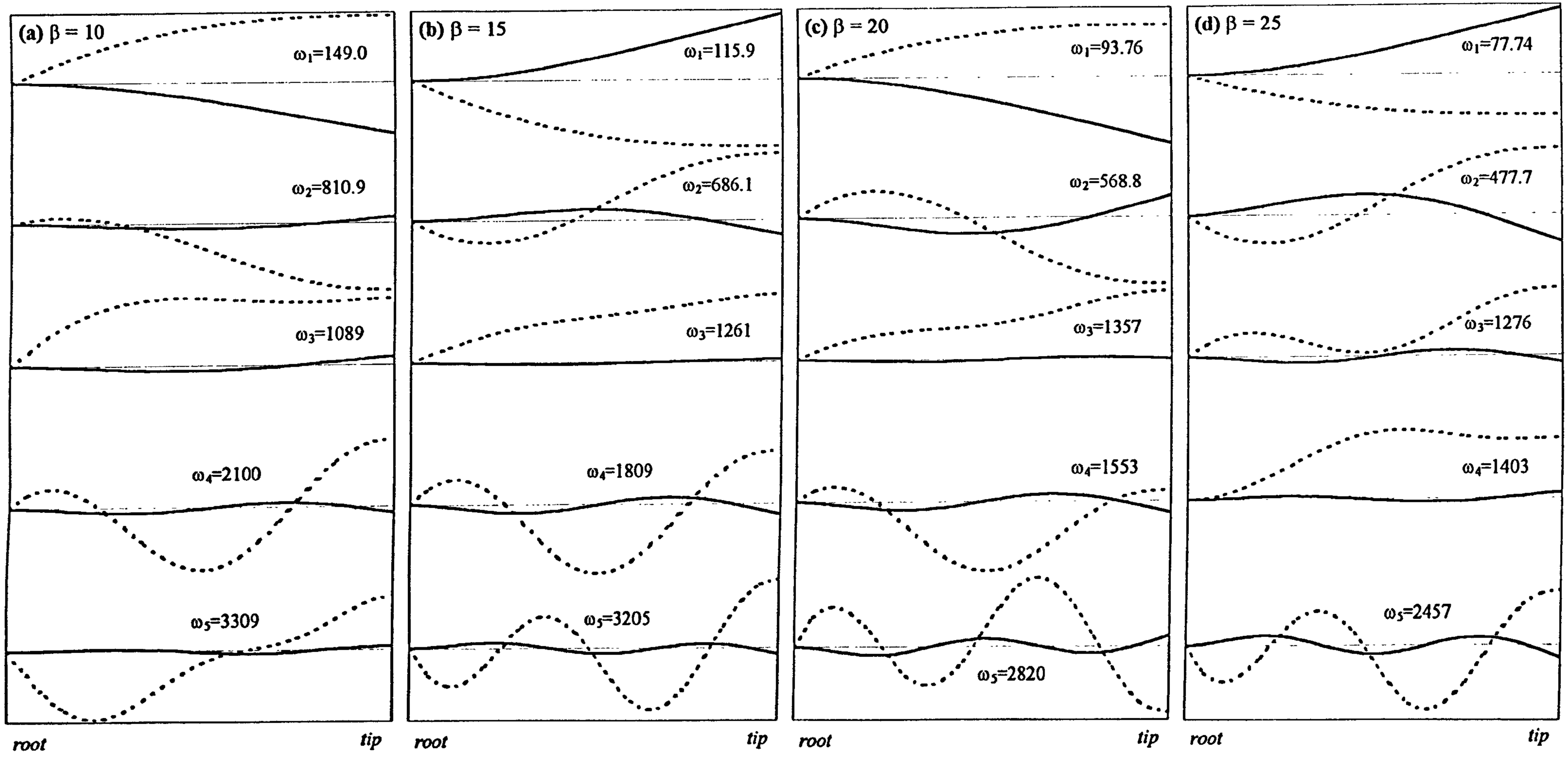

Figure 7-37. Bending-torsion coupled natural frequencies (rad/s) and mode shapes of the box wing.
(a) β=10; (b) β=15; (c) β=20; (d) β=25.

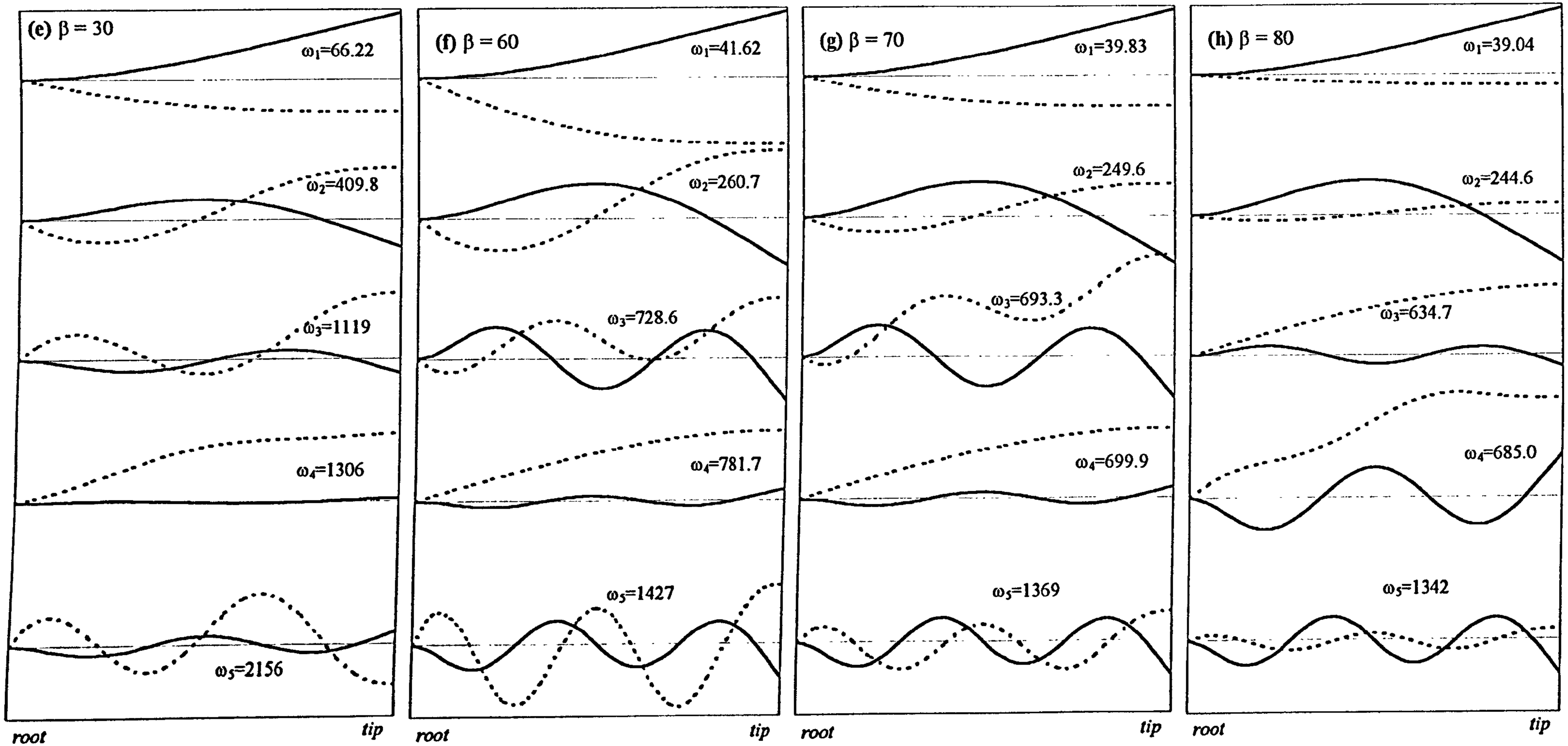

Figure 7-37. Cont. (e) β=30; (f) β=60; (g) β=70; (h) β=80.

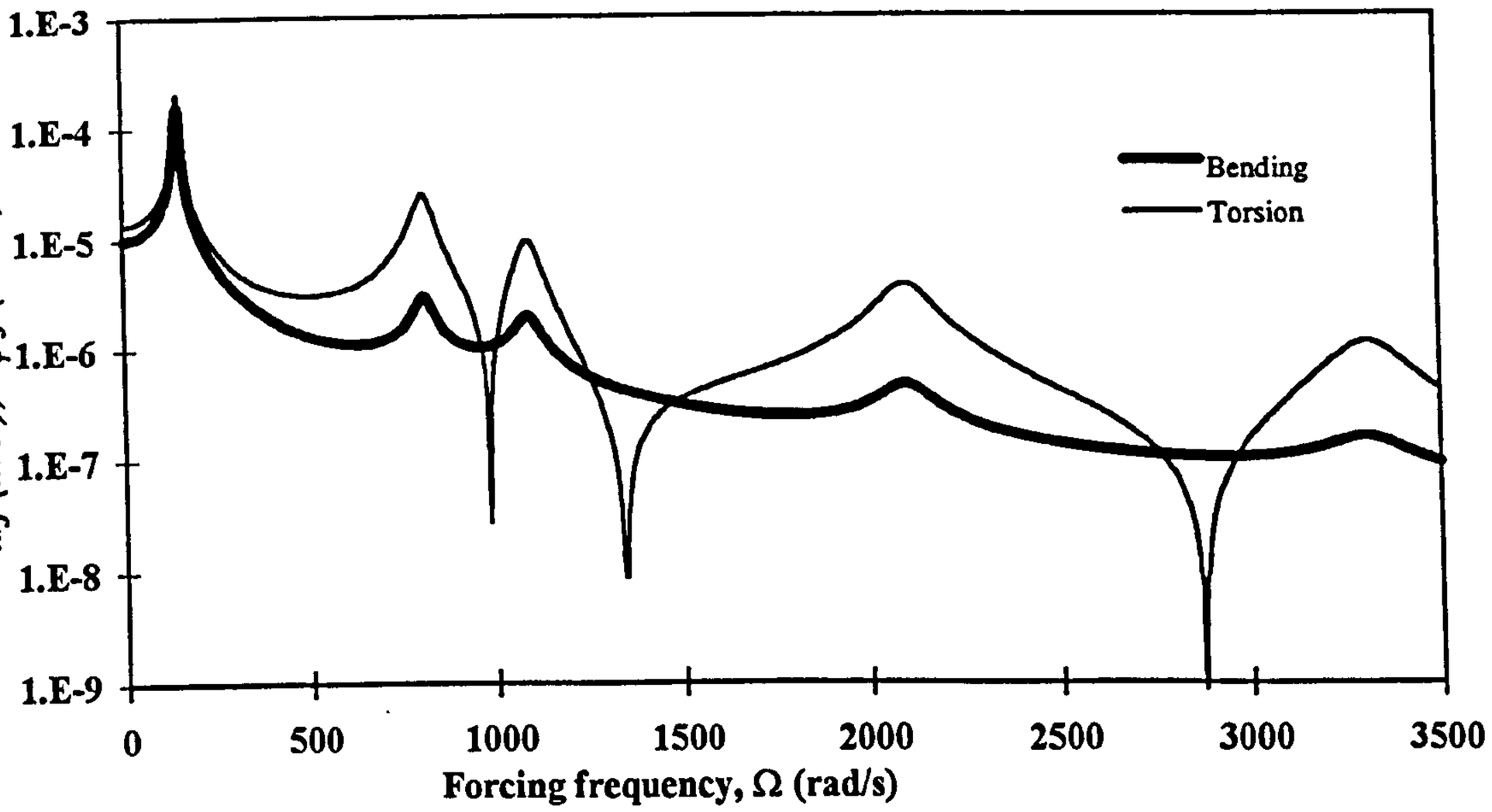

Figure 7-38. The dynamic flexural and torsional response of a box wing (Cesnik, et al. 1996) due to a unit harmonically varying concentrated force at the tip (β=10).

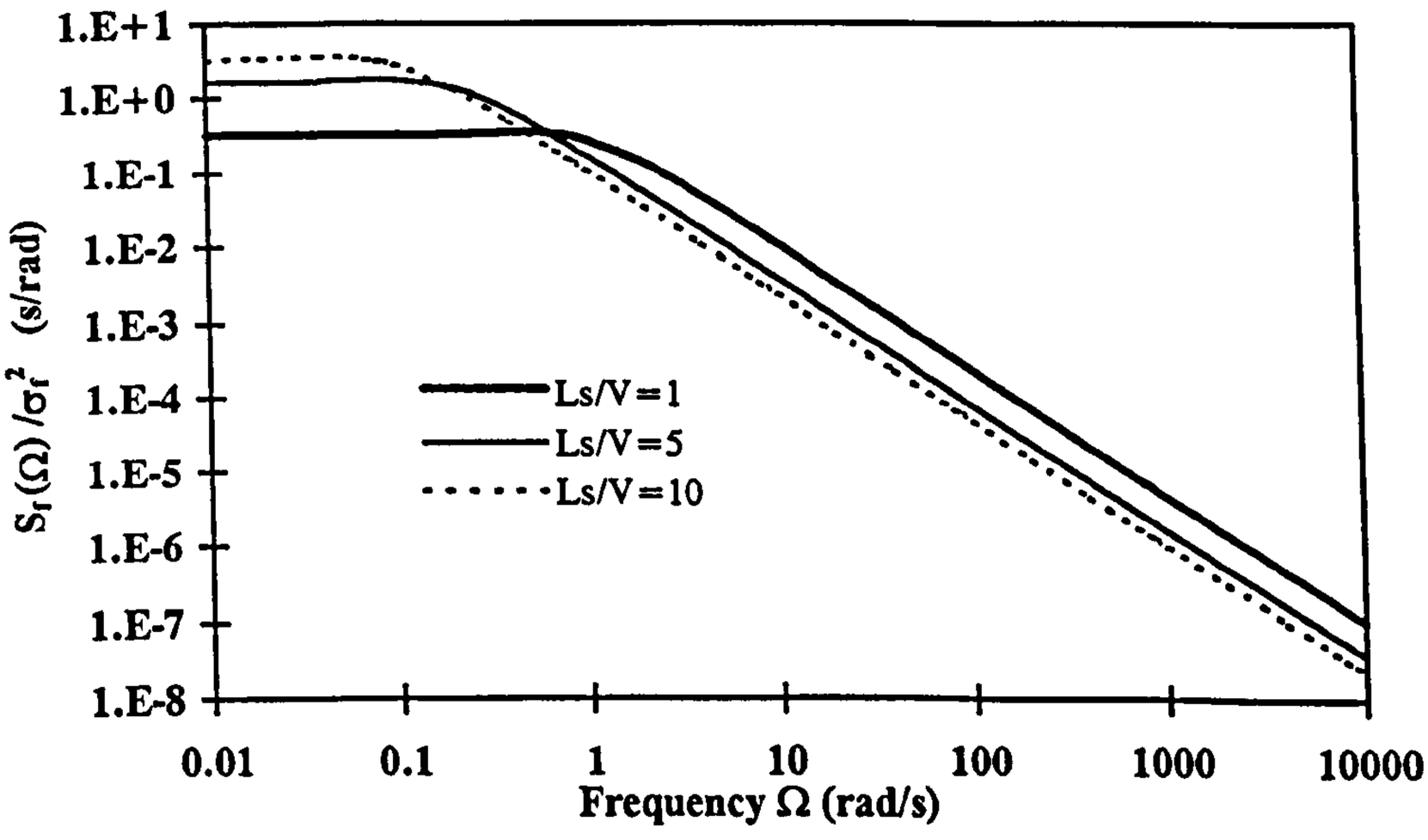

Figure 7-39 The von Karman PSD function for different values of L_s/V.

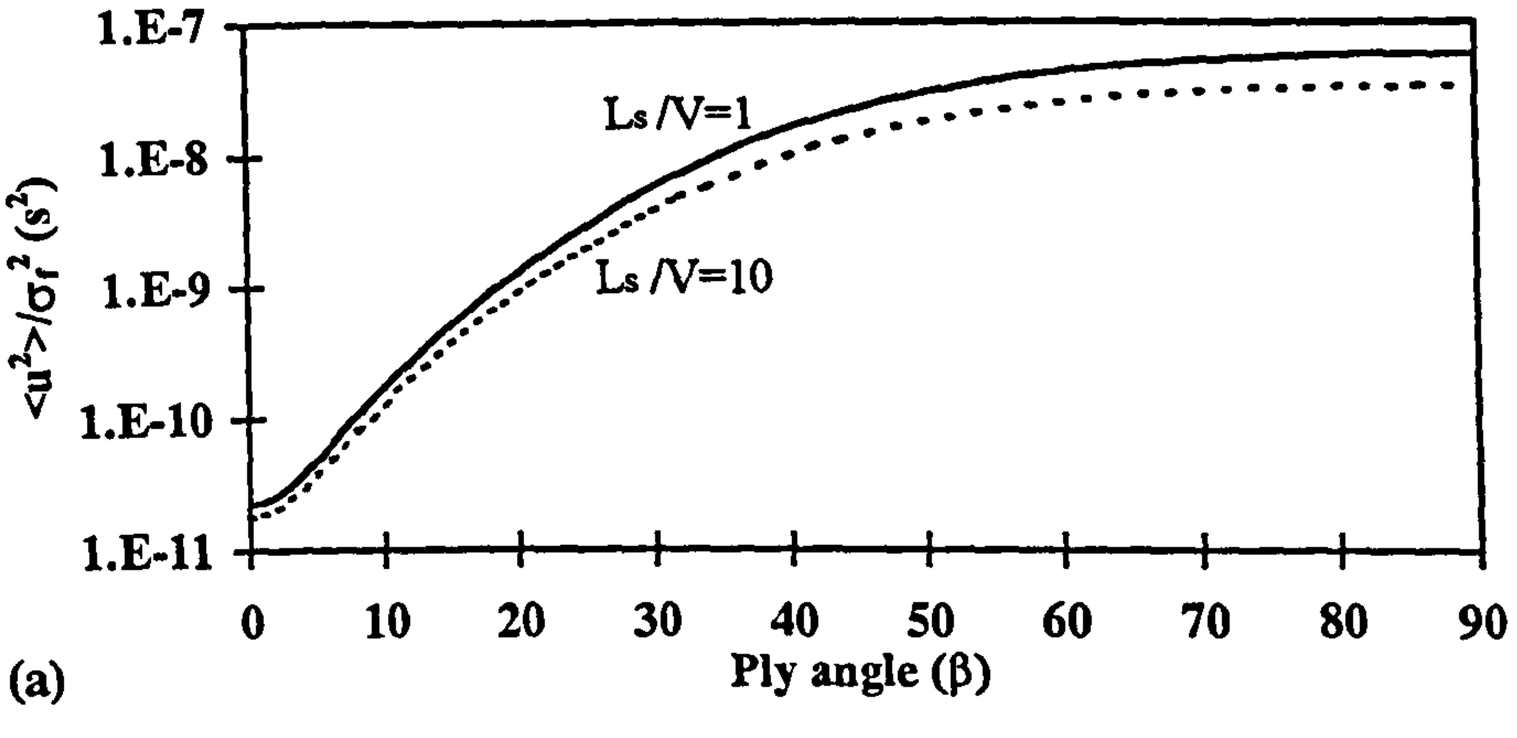

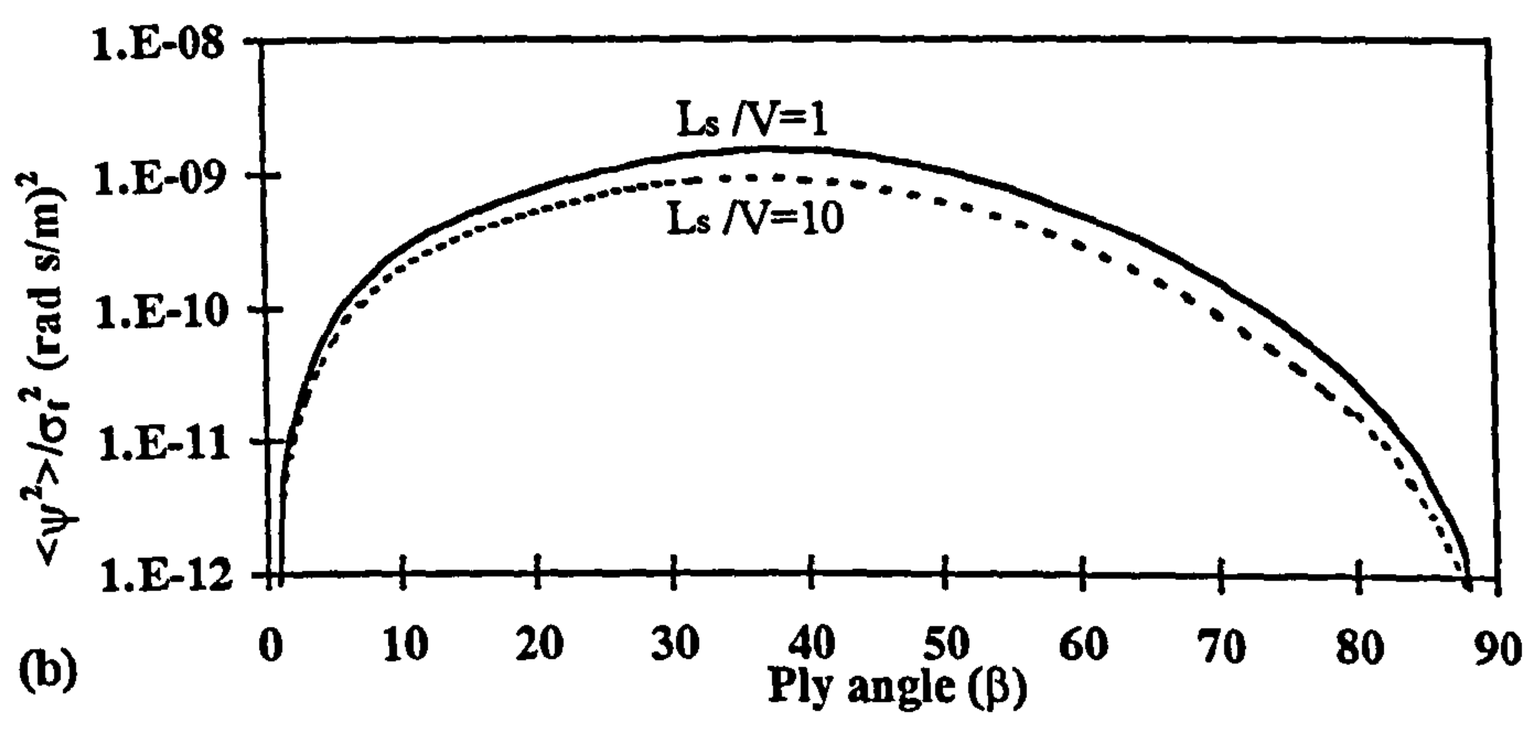

Figure 7-40. Variation of the mean-square value of (a) flexural and (b) torsional response of a box wing (Cesnik et al., 1996) at the tip against ply angle for different L_s/V ratios with ζ=0.03.

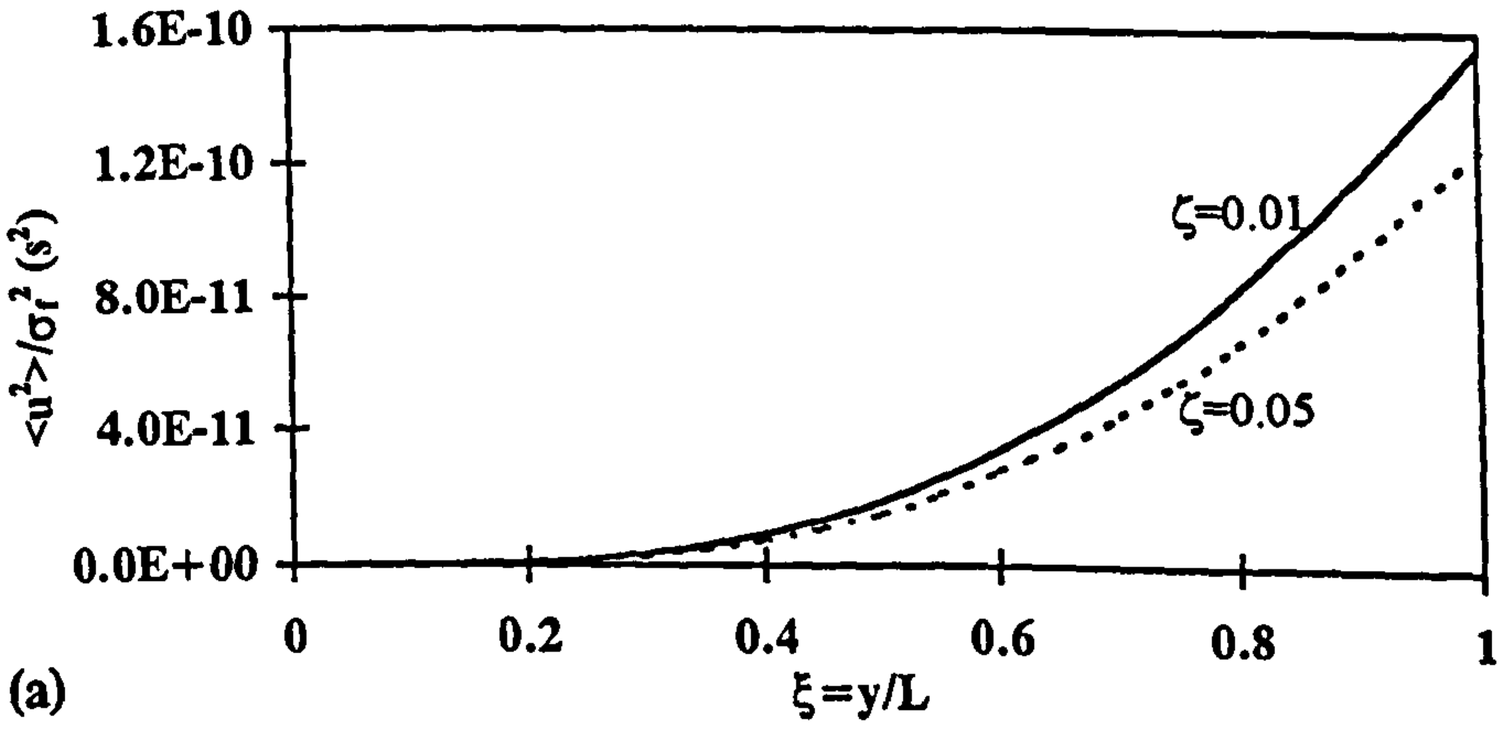

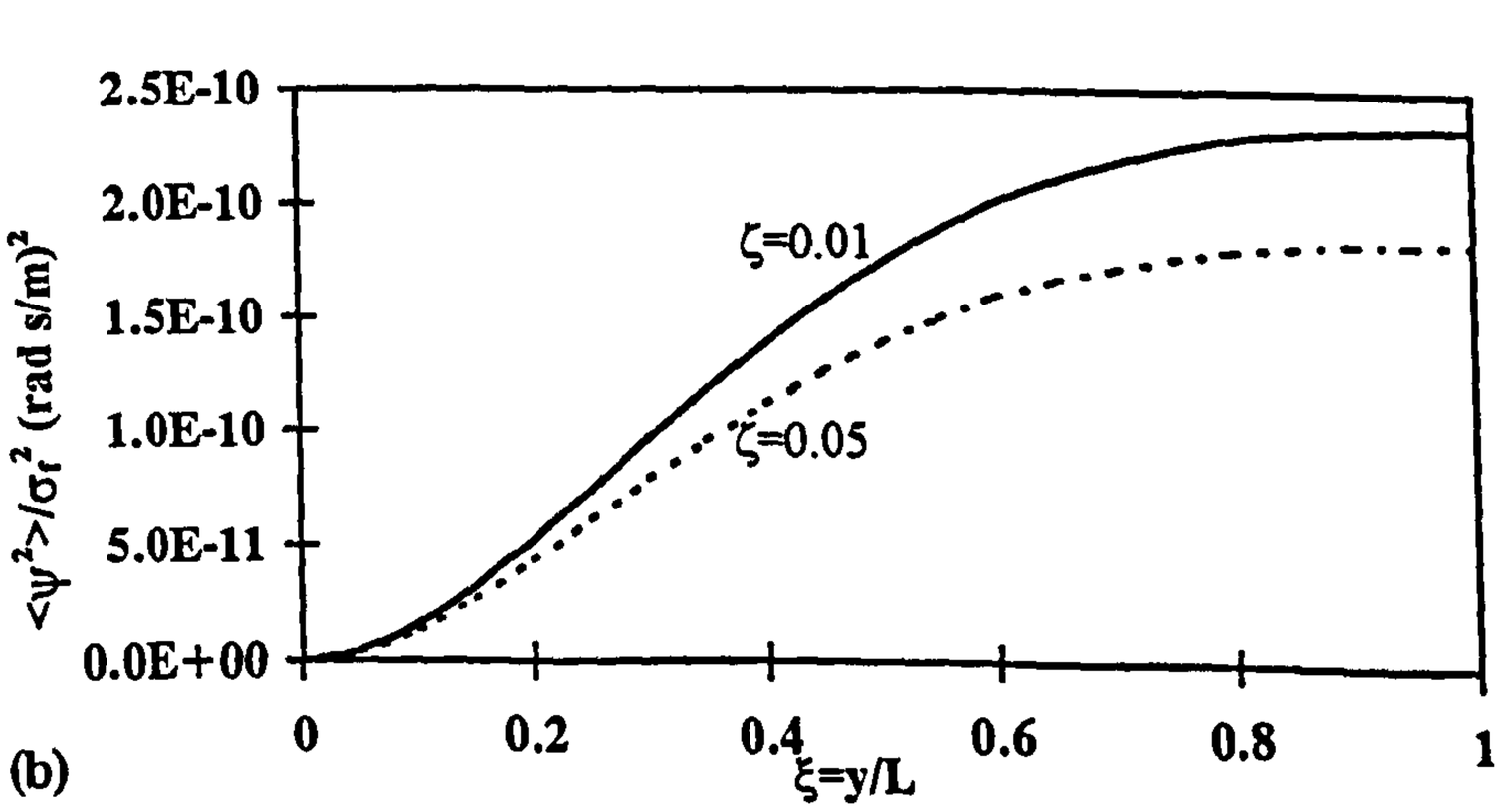

Figure 7-41 Variation of the mean-square value of (a) flexural and (b) torsional response along a box wing (Cesnik et al., 1996) for different damping coefficients (Ls/V=10).

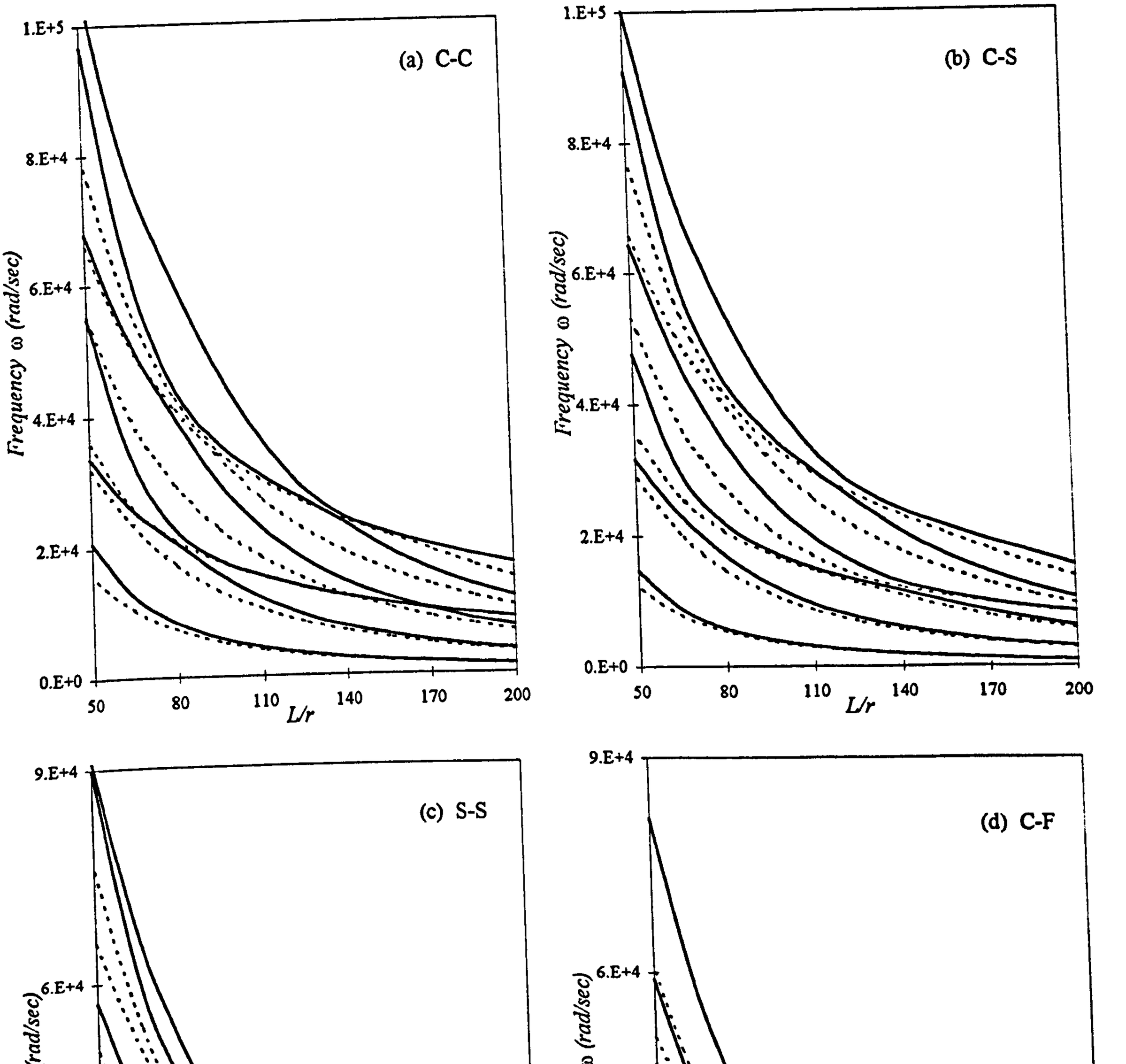

Figure 7-42. The variation of the first six natural frequencies of the composite beam (Teoh and Huang, 1977) with L/r for various boundary conditions with (dashed line) and without (solid line) the effects of shear deformation and rotatory inertia.

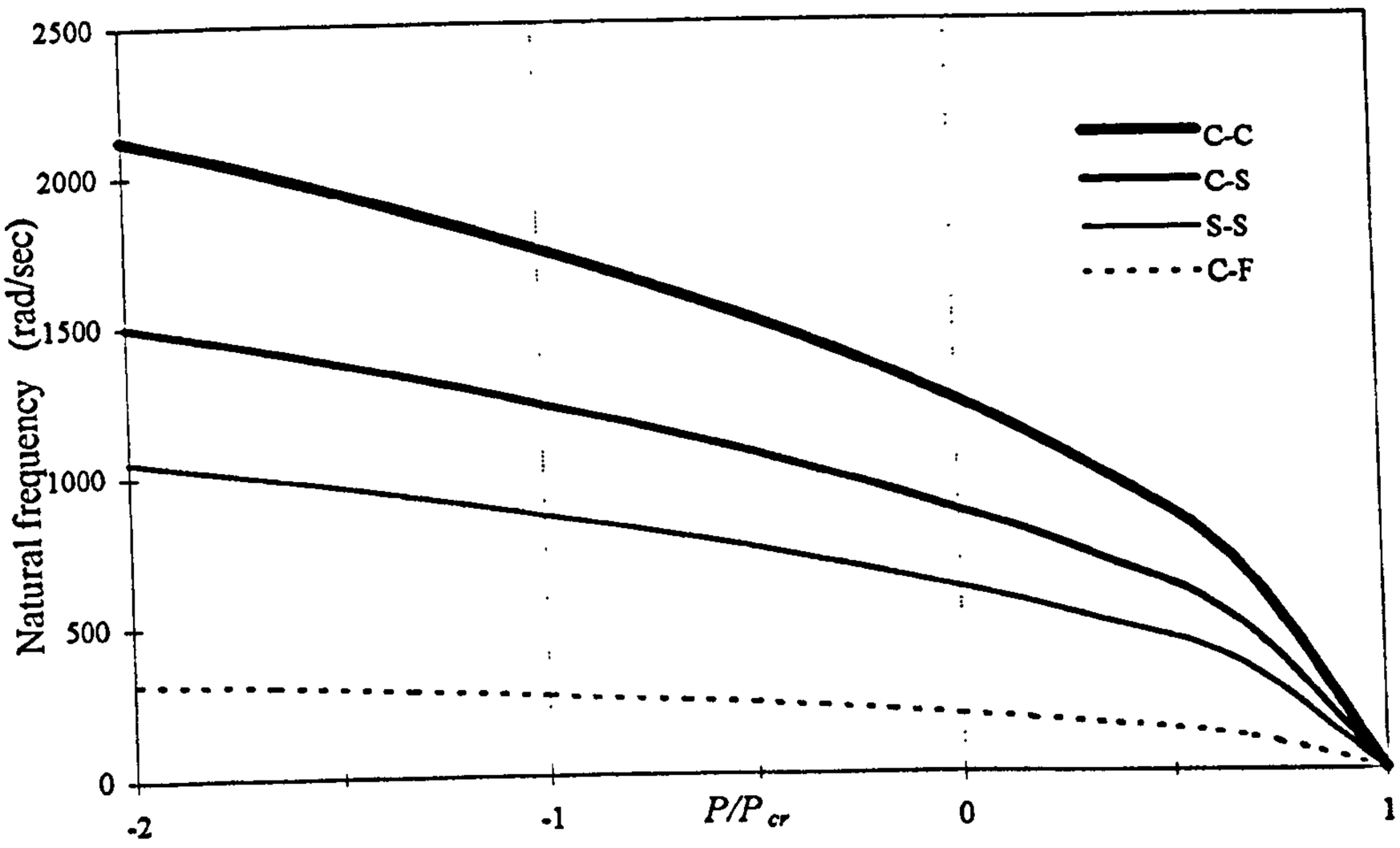

Figure 7-43. The variation of the first natural frequency of the composite beam (Teoh and Huang, 1977) with P/P_{cr} for various boundary conditions.

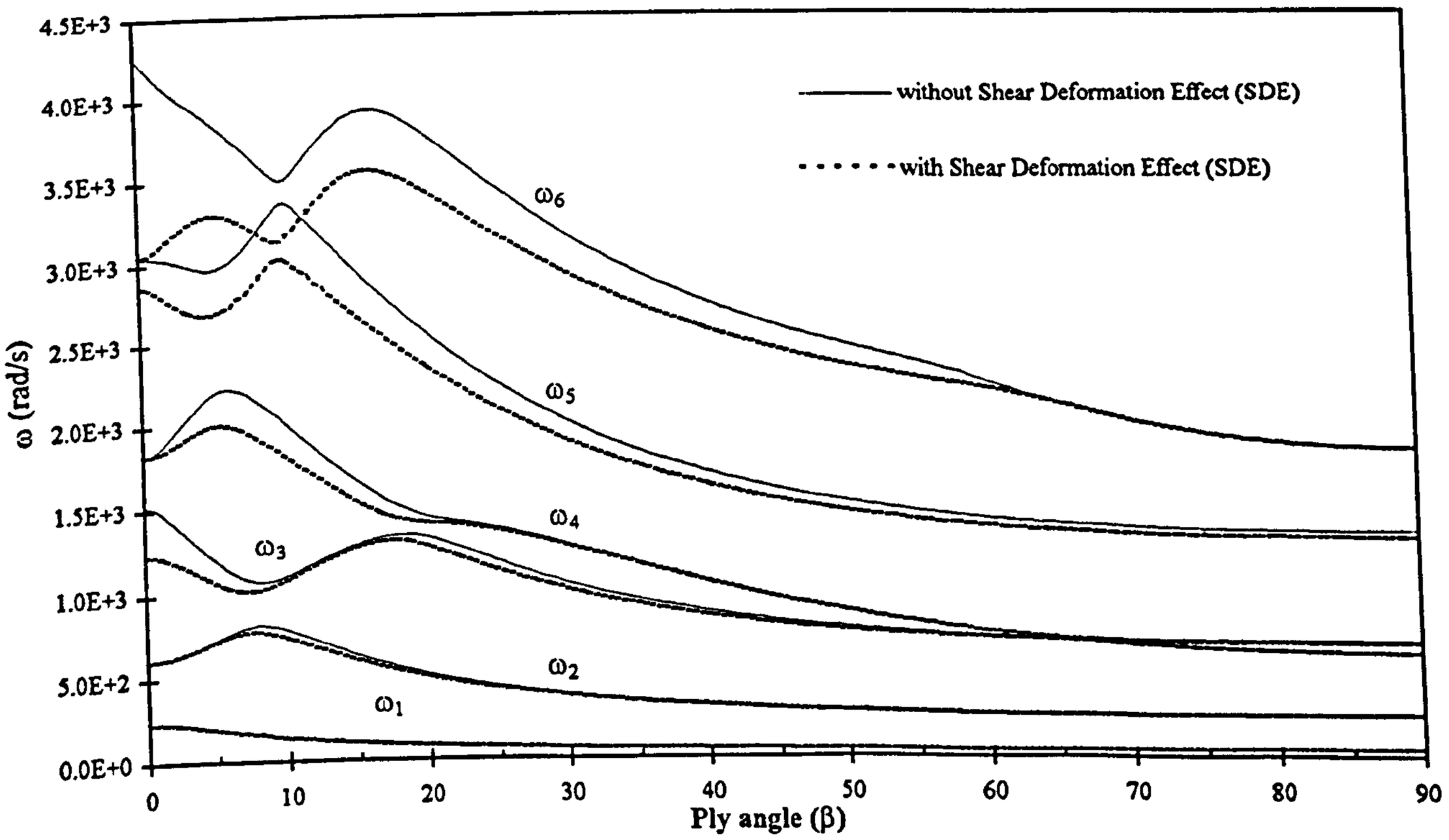

Figure 7-44. Variation of the first six natural frequencies of the bi-convex composite beam against ply angle.

(a) with shear deformation effect

(b) without shear deformation effect

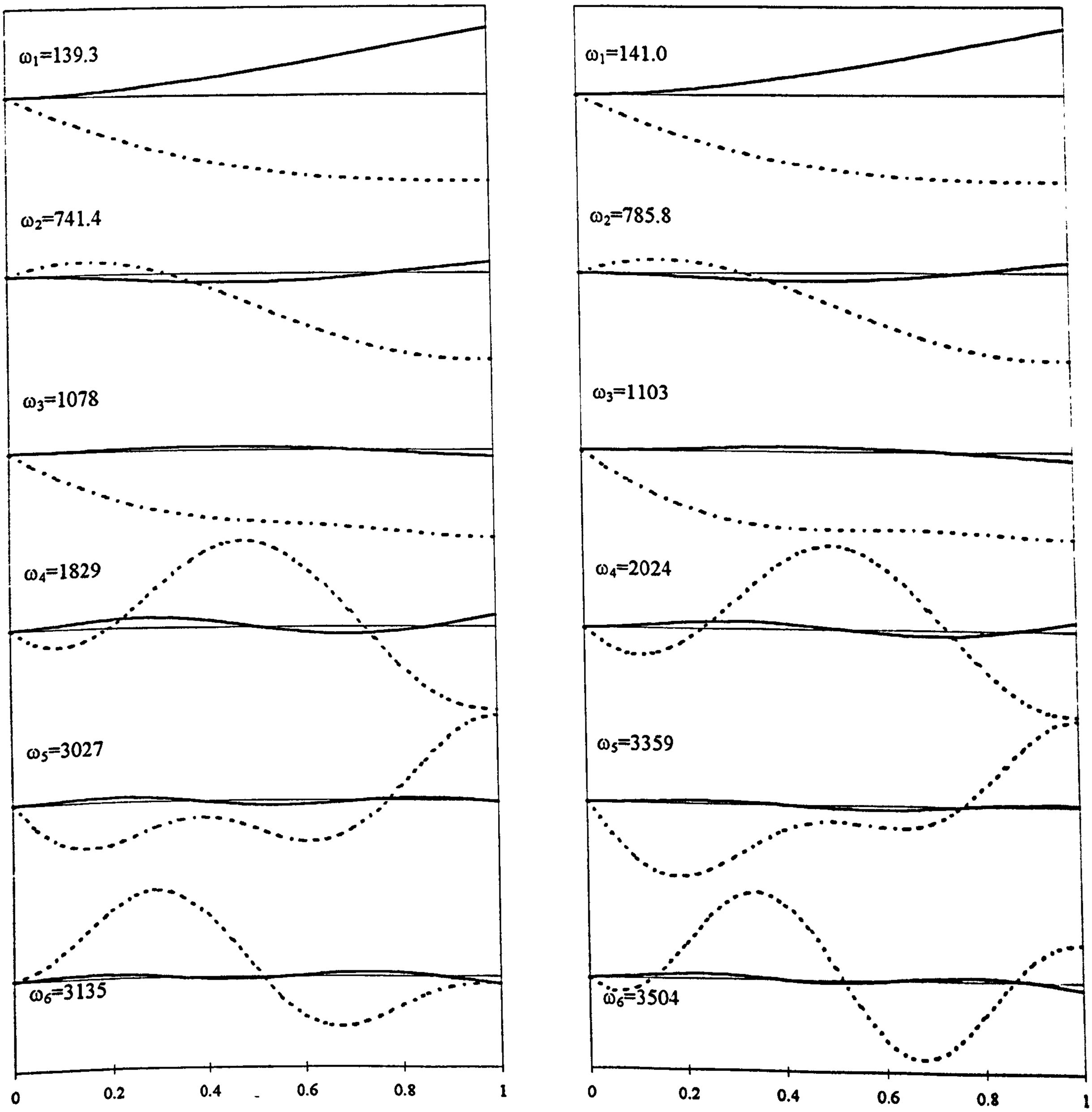

Figure 7-45. Natural frequencies (rad/s) and mode shapes of the bi-convex composite beam when β=10 deg; ----- bending displacement u; - - - torsional rotation ψ.

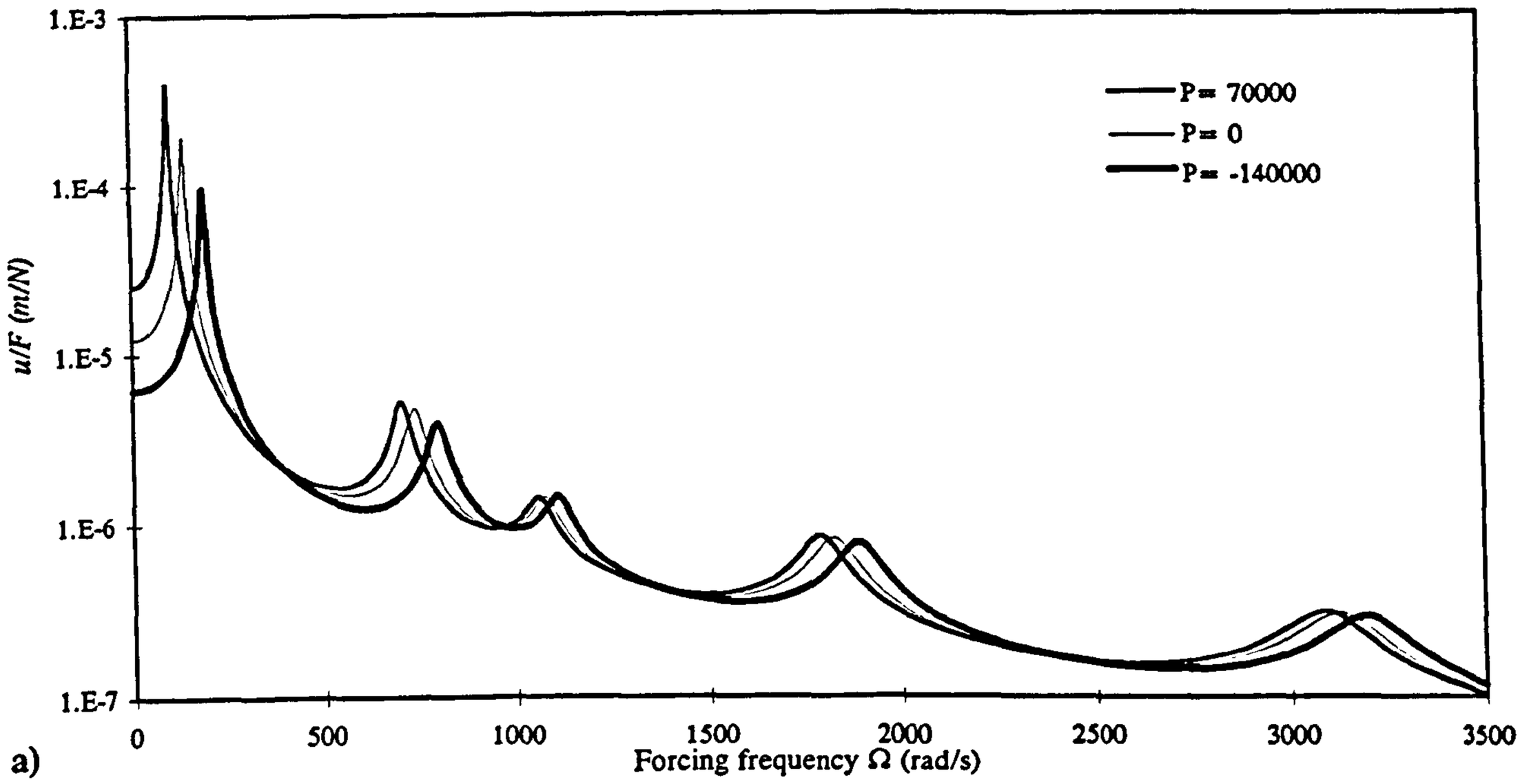

a)

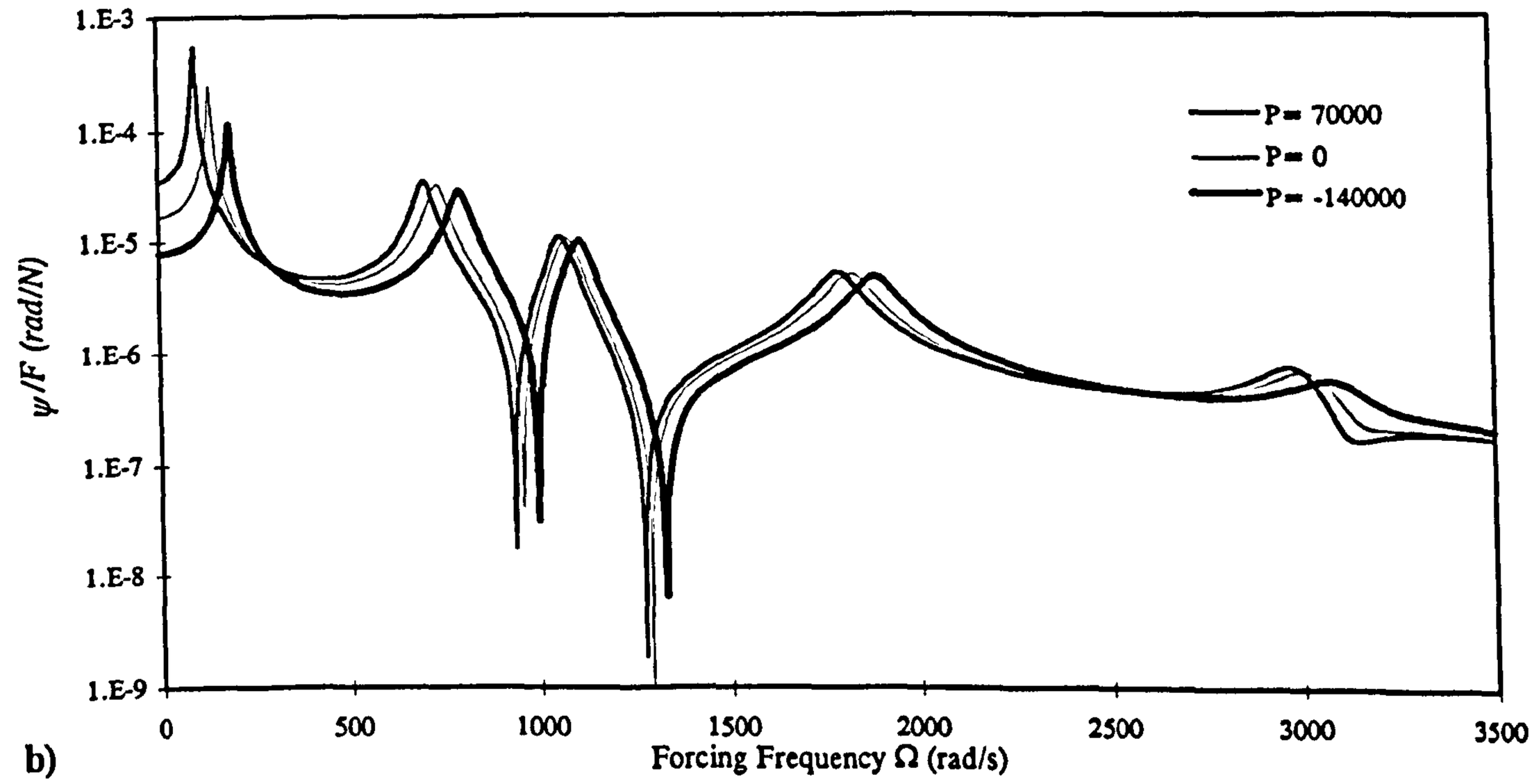

b)

Figure 7-46. Dynamic (a) flexural and (b) torsional displacements of the bi-convex composite beam at the tip due to a unit harmonically varying concentrated force at the tip (axial load in *N*).

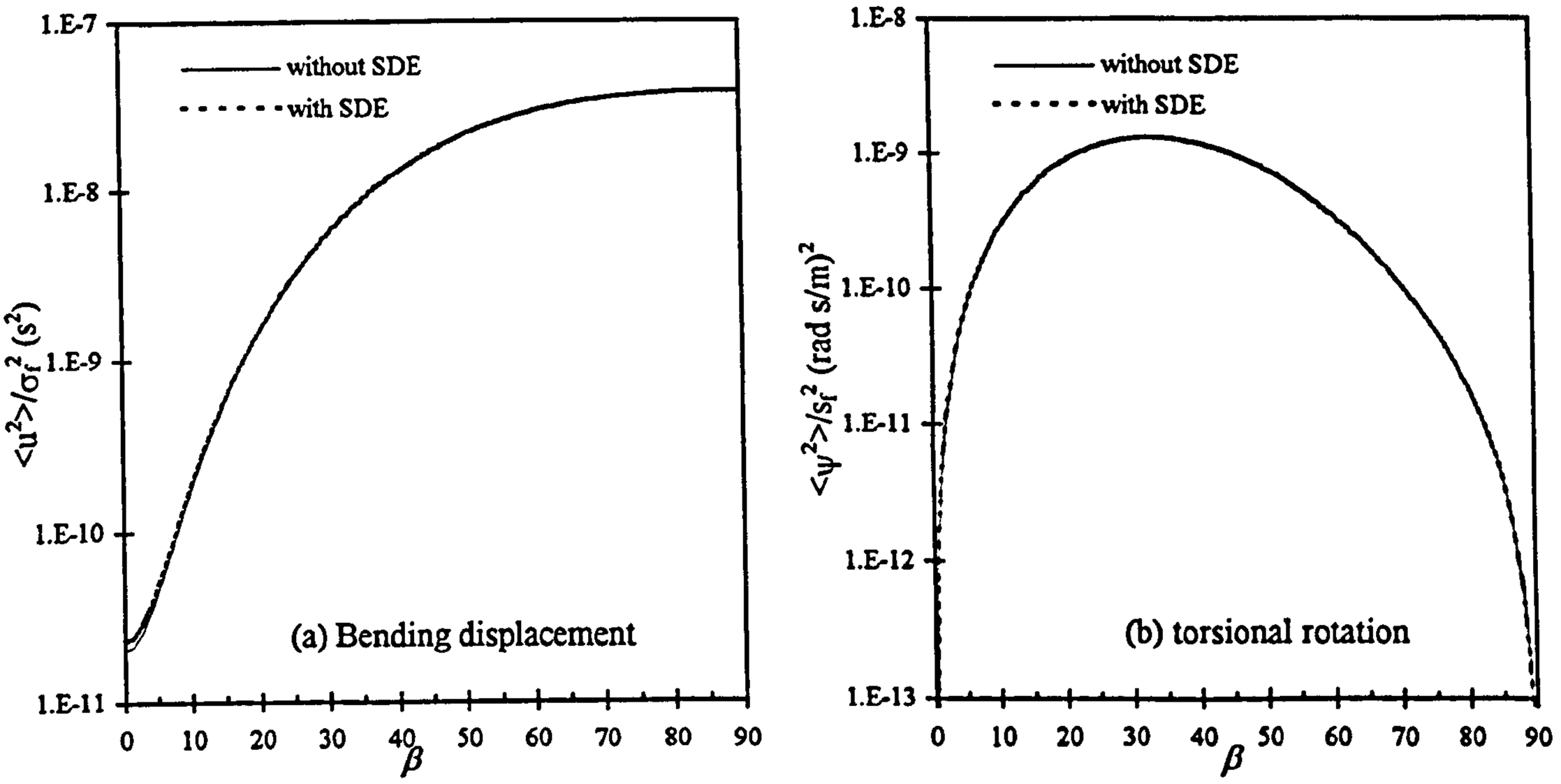

Figure 7-47. Variation of the mean square value of (a) bending displacement and (b) torsional rotation of the bi-convex composite beam against ply angle.

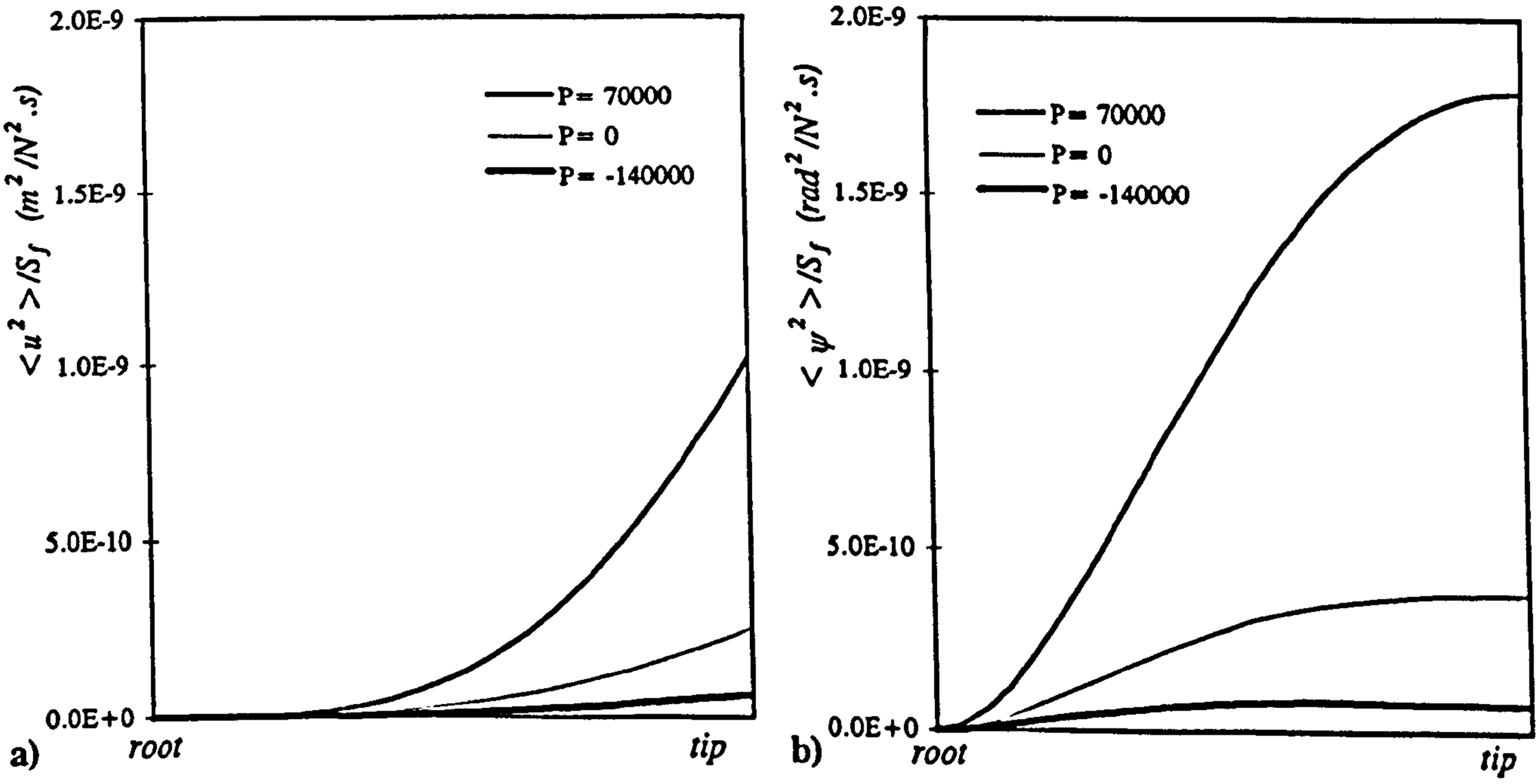

Figure 7-48. Variation of the mean square value of a) flexural b) torsional displacement along the bi-convex beam for different levels of axial load.

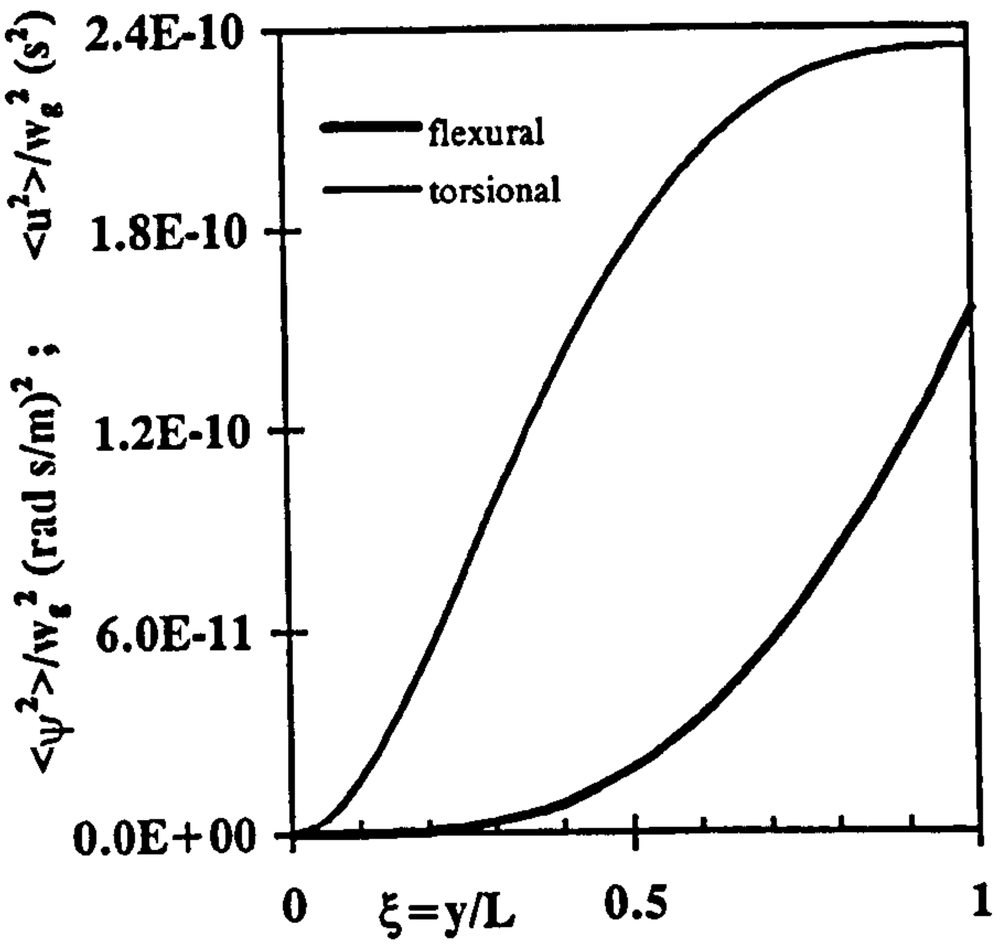

Figure 7-49 Variation of the mean square values of flexural and torsional displacements along the box wing.

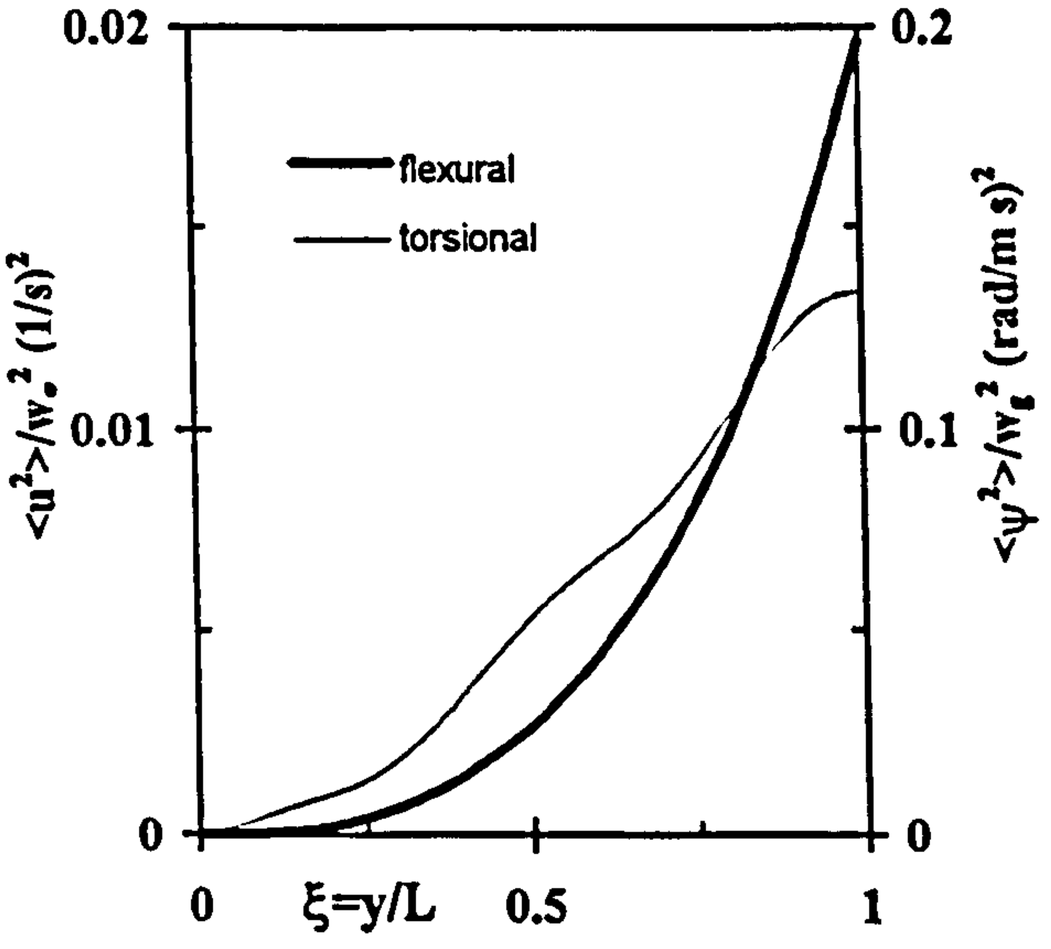

Figure 7-50 Variation of the mean square values of flexural and torsional accelerations along the box wing

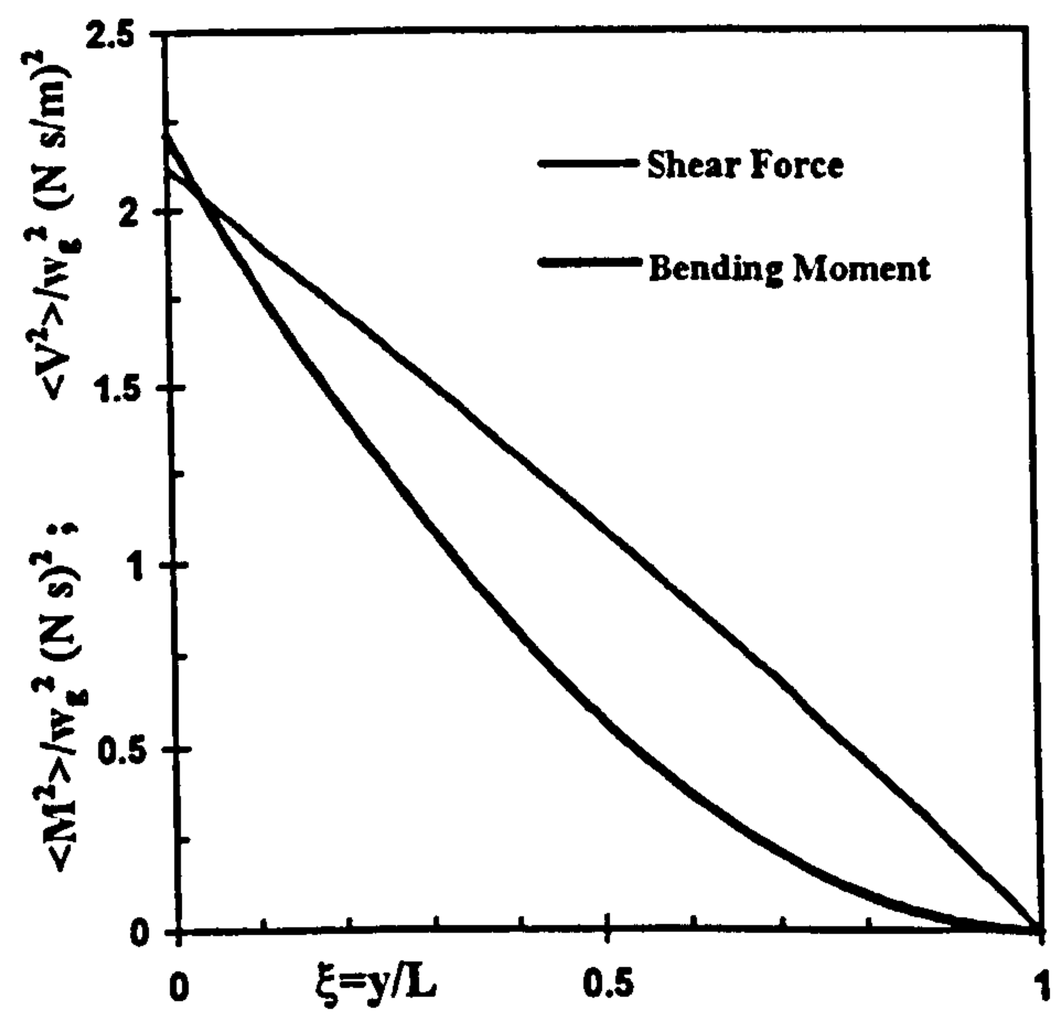

Figure 7-51(a) Variation of the mean square values of shear force and bending moment along the box wing.

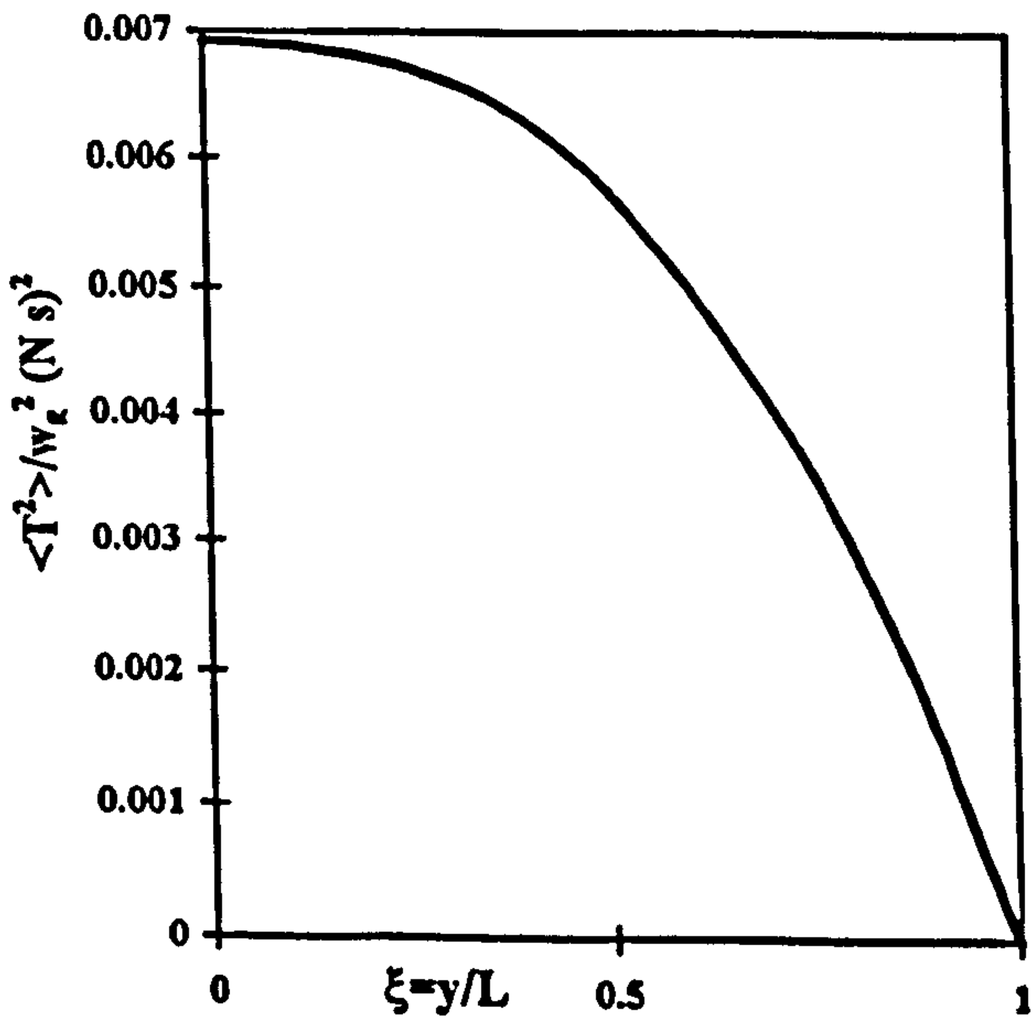

Figure 7-51(b) Variation of the mean square value of torque along the box wing.

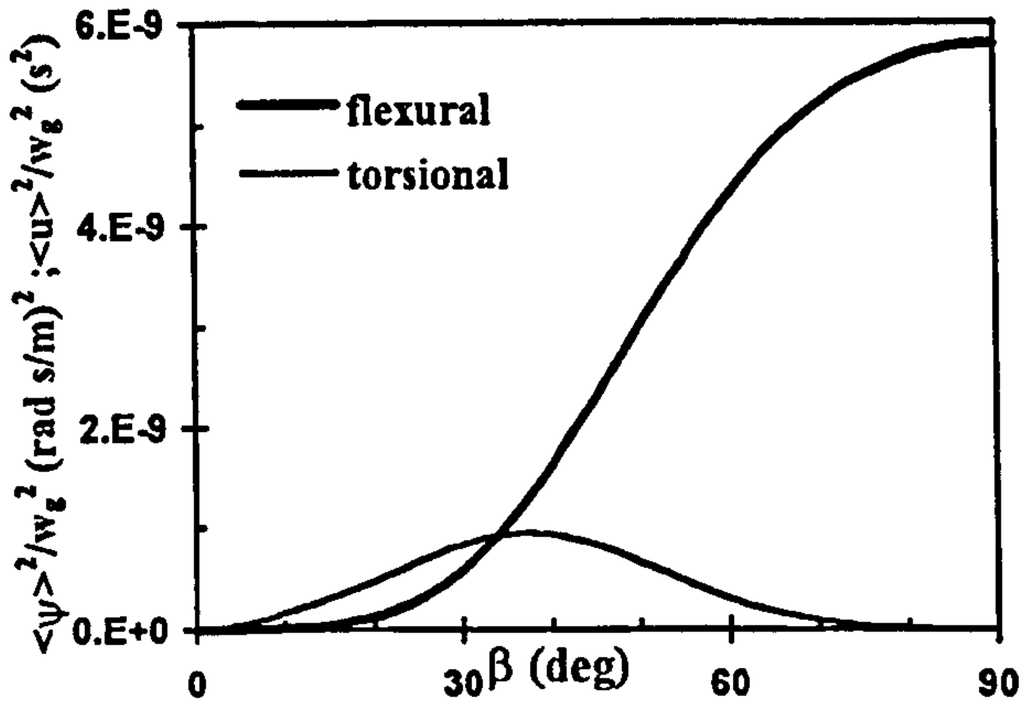

Figure 7-52. Variation of mean square values of the flexural and torsional displacements at the mid-span of the box wing against ply angle.

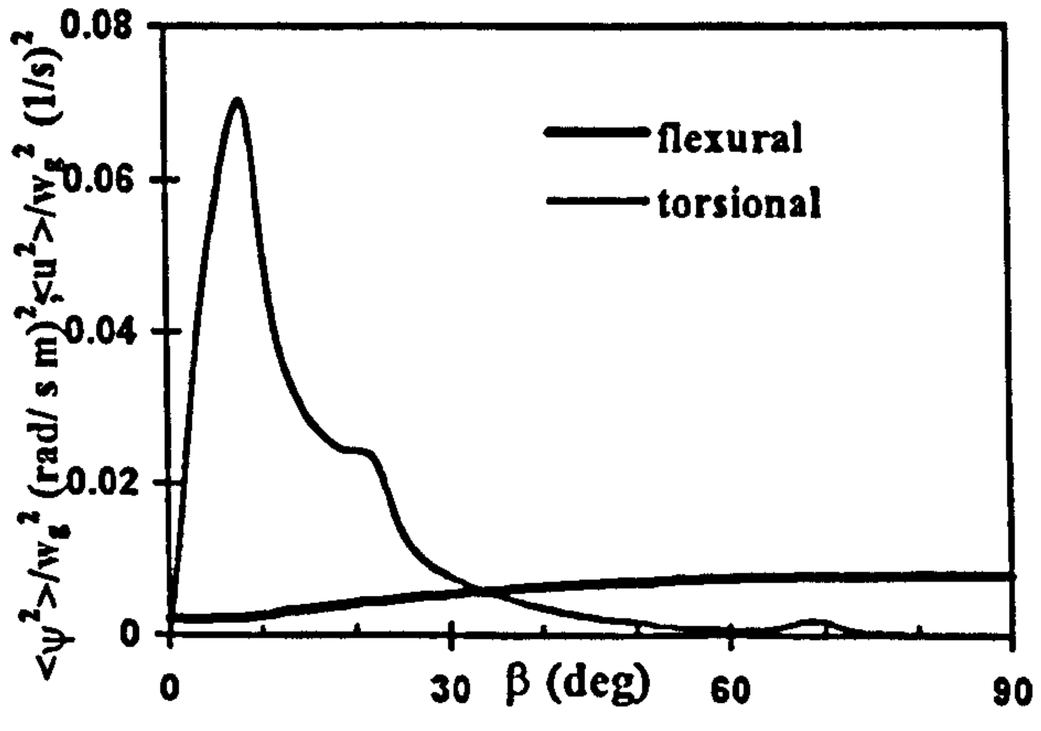

Figure 7-53 Variation of mean square values of the flexural and torsional accelerations at the mid-span of the box wing against ply angle.

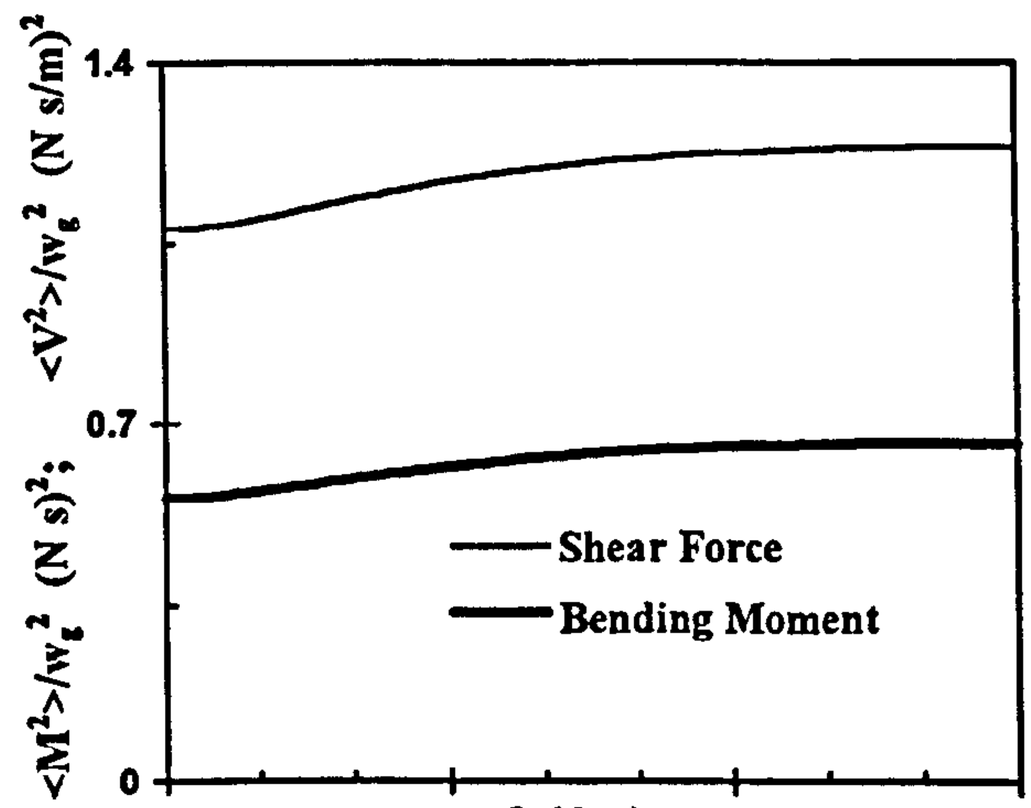

Figure 7-54(a) Variation of mean square values of the shear force and the bending moment at the mid-span of the box wing against ply angle.

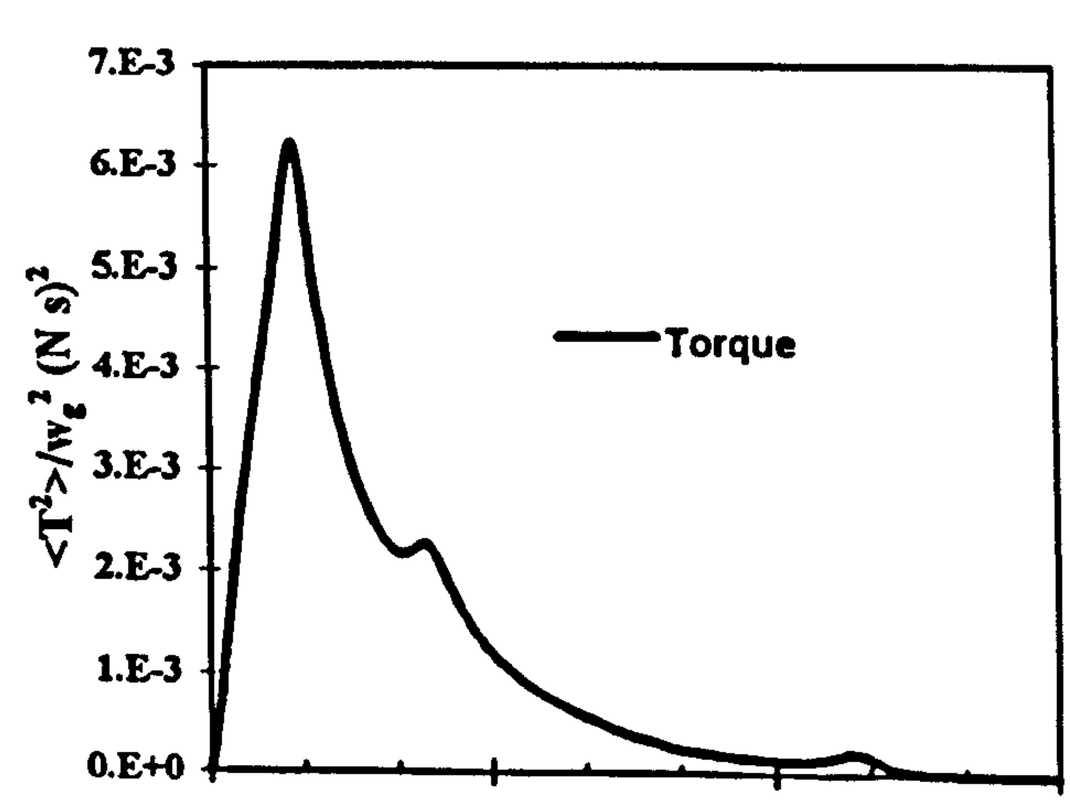

Figure 7-54 (b) Variation of mean square value of the torque at the mid-span of the box wing against ply angle.

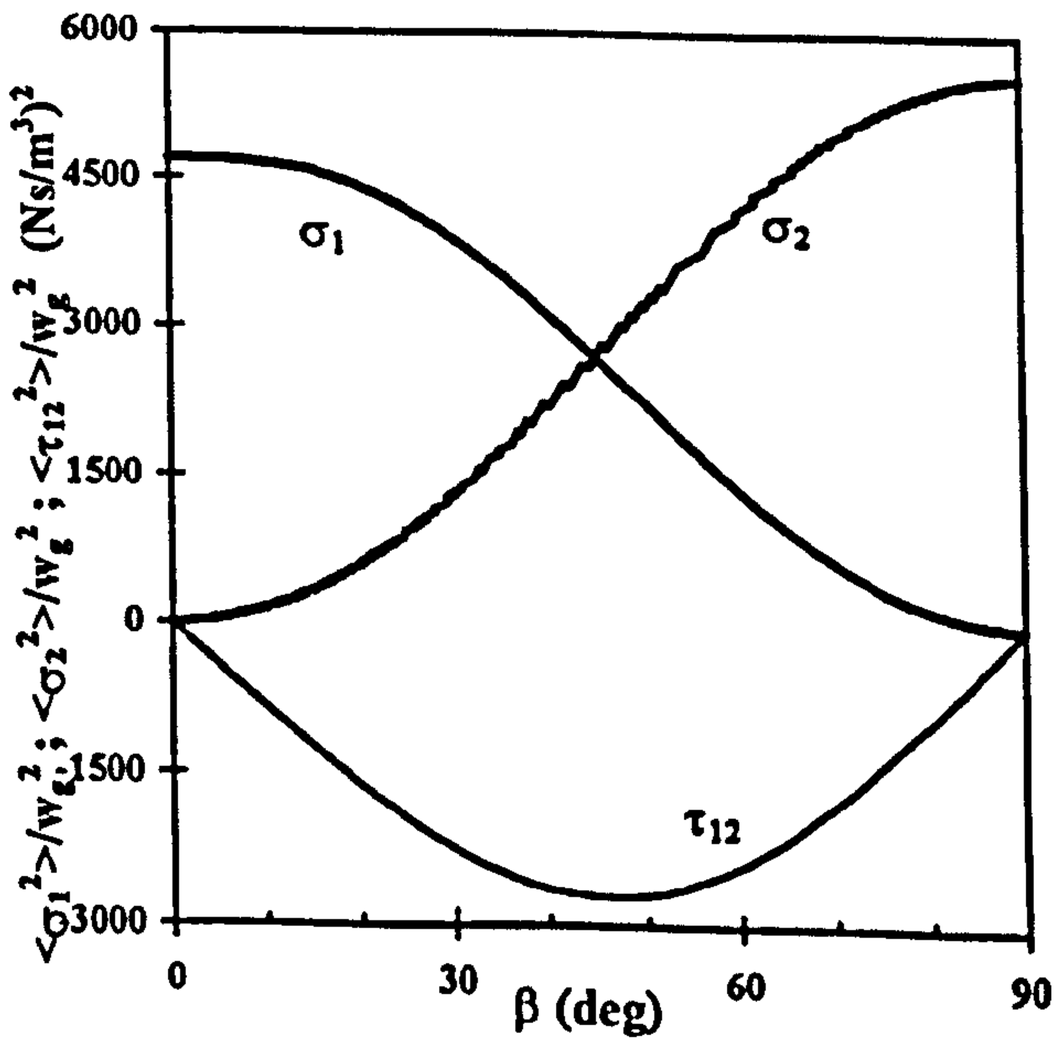

Figure 7-55 Variation of mean square values of principal stresses at the mid-span of the box wing against ply angle.

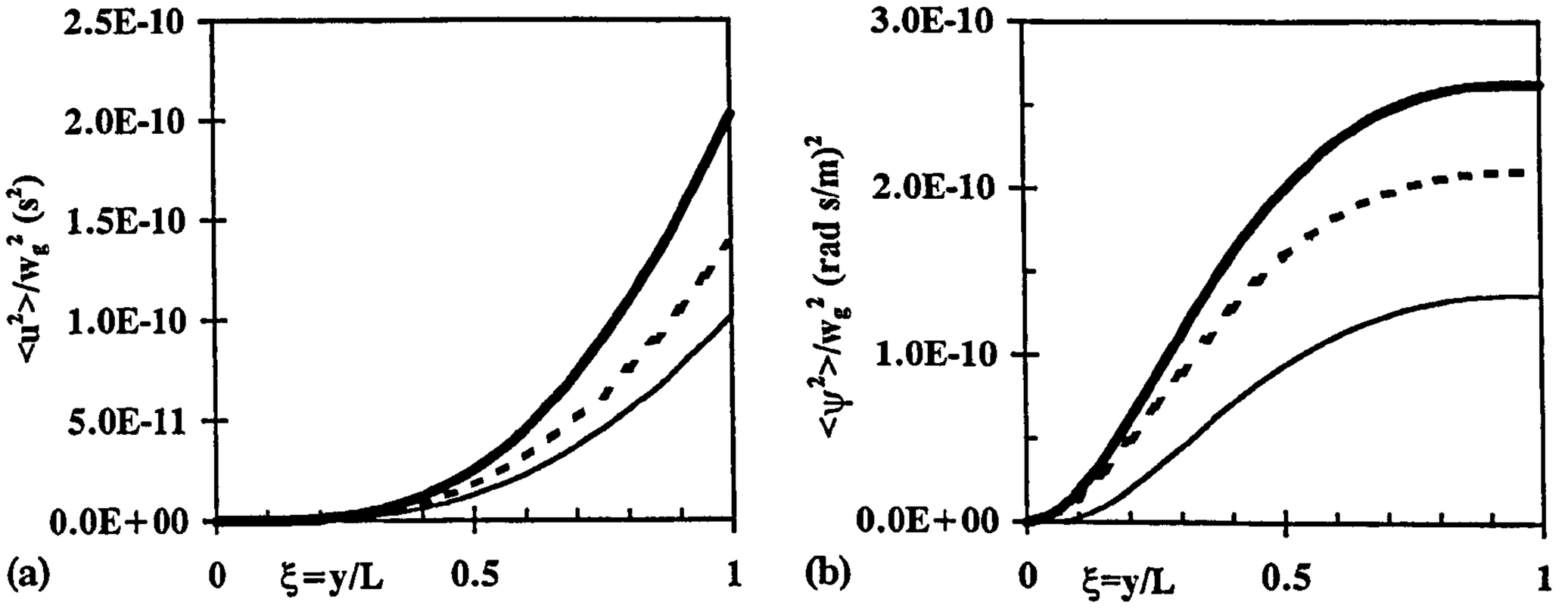

Figure 7-56. Variation of the mean square values of (a) flexural (b) torsional displacements along the box wing for different levels of axial load; _____ compresive, - - - - unloaded, —— tensile.

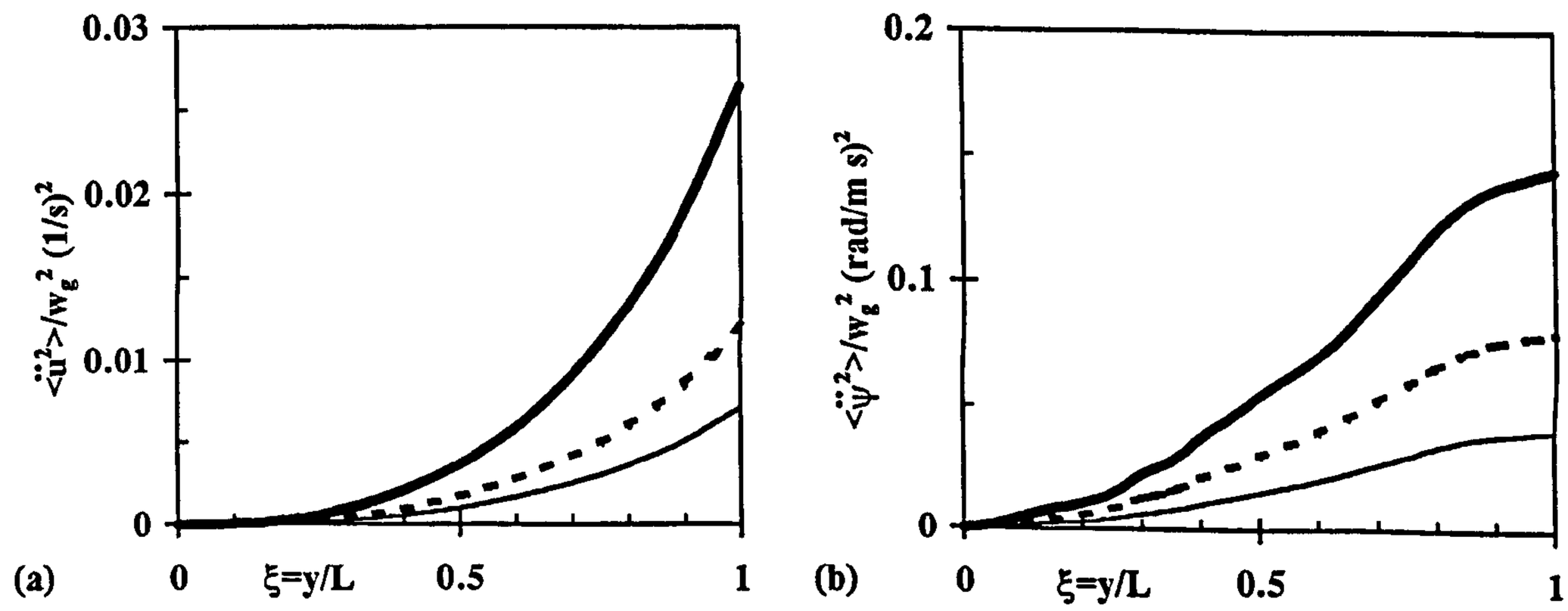

Figure 7-57 Variation of the mean square values of (a) flexural (b) torsional acceleration along the box wing for different levels of axial load; _____ compresive, - - - - unloaded, —— tensile.

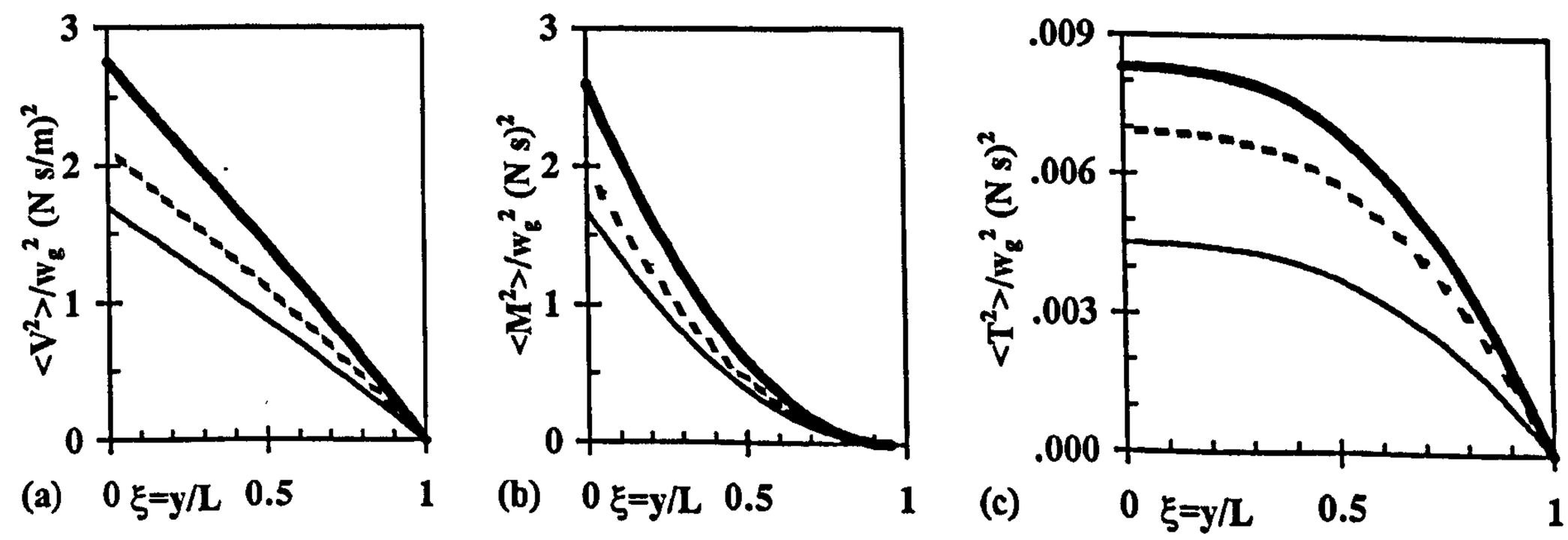

Figure 7-58 Variation of the mean square values of (a) shear force, (b) bending moment and (c) torque along the box wing for different levels of axial load; _____ compresive, - - - - unloaded, ——tensile.

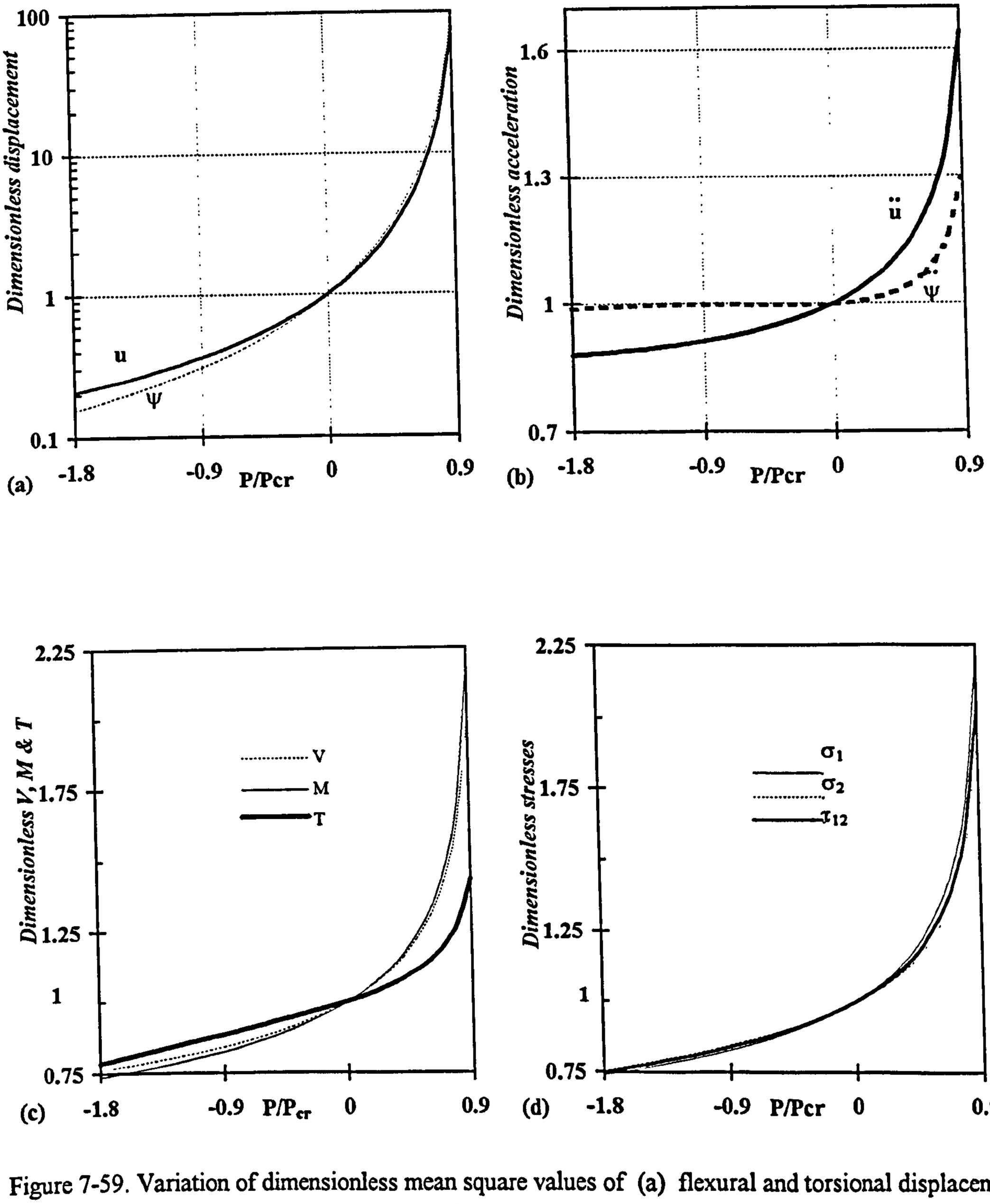

Figure 7-59. Variation of dimensionless mean square values of (a) flexural and torsional displacement; (b) flexural and torsional acceleration; (c) shear force, bending moment and torque; (d) stresses in principal material direction, in the mid span of the box wing against axial load (P/P_{cr}).

Chapter Eight

Concluding remarks and recommendations for future work

8 Concluding remarks and recommendations for future work

8.1. Concluding remarks

A theory has been developed to perform the response analysis of a bending-torsion coupled beam when subjected to deterministic or random loads. The equations of motion are derived using Hamilton's principle. This solution procedure is applied both to metallic and composite beams.

The investigation and examples presented are focused on the potential for enhancing the dynamic characteristics of thin-walled composite structures. Bending-torsion coupling effects arising both from the anisotropic nature of fibrous composites as well as non-coincident mass and geometric shear centres, are taken into account when developing the theory. Applications include aircraft wings, ship hulls, wind turbine and helicopter blades, for which bending and torsional modes of deformation are usually coupled as a result of either non-coincident mass and shear centres or as a result of the intrinsic nature of laminated fibrous composites.

The free vibration characteristics of composite beams have been examined in detail using the dynamic stiffness method. The study has shown that the anisotropic property of composite materials can be used as a modal coupler or decoupler, and can be applied to decouple modes which are geometrically (inertially) coupled in the same way as with mass balancing, but without a weight penalty. It can also be used to reverse completely the unfavourable coupling introduced by sweep angle (backward or forward).

Numerical results are given for all standard classical boundary conditions, showing the effects of shear deformation, rotatory inertia, axial load and slenderness ratio on natural frequencies. The investigation has shown that significant changes in natural frequencies can occur as a result of changing these parameters. It has also been revealed that due recognition to modal coupling must be given when studying the free and forced vibration characteristics of composite beams.

In general, the responses of beams with a greater degree of end constraints (such as clamped-clamped and clamped-simply supported beams) are seen to be more affected by the shear deformation than beams with a lesser end degree of constraints (such as simply supported-simply supported and cantilever beams). The results indicate that thicker and stiffer stocky beams are more susceptible to the effect of shear deformation, which accords with earlier studies. In response analyses and reliability studies of such beams, it is therefore important to consider the effect of shear deformations.

The effects of ply orientation on rigidity properties and their subsequent effects on the response characteristics and dynamic stresses are demonstrated. The variation of stresses along the length of a wing (for a given ply orientation and stacking sequence) is also demonstrated. The investigation has shown that dynamic stresses in composite wings are heavily influenced by fibre angle, shear deformation, rotatory inertia and axial load.

Two important concepts have been discussed. One is the interpretation of normal modes using the concept of generalised mass in each of the modes of vibration. The other one is the significance of modal interchanges between flexural and torsional modes of vibration, which may occur due to the effects of axial load, shear deformation and/or rotatory inertia and additionally in the case of composite beams, the variation in ply angles.

The effect of simultaneous bending and torsion in a composite column, caused by both geometric and material couplings, on the elastic buckling load of composite columns has also been investigated. The effect of shear deformation on the buckling characteristics of the composite column is included in the theory. Bending-torsion coupling reduces the elastic critical buckling load of composite columns.

The importance of experimental procedures in understanding the structural behaviour of composites is emphasised. Experiments have been carried out to establish the elastic critical buckling load of laminated composite flat columns made of carbon-epoxy material. Other objectives are to gain further insights into the rigidity properties and the buckling characteristics of bending-torsion coupled composite columns.

8.2. Recommendations for future work

As with any investigation, a great number of new ideas suggest themselves. The generalised modal approach presented can be used with different models of beams and plates with virtually the same level of ease. Here, some suggestions for future extensions of this work are as follows

In many cases of real life applications, beams are usually non-uniform. Examples of such beams are aircraft wings, turbine and fan propellers, and helicopter rotors. So one extension of the present work is to study non-uniform composite beams. Although the method presented in this study is applied to uniform beams, it may be used in the free and forced vibration analysis of bending-torsion coupled beams with varying cross sections. As is shown in ***Appendix E***, the free vibration solution of non-uniform beams can be obtained by idealising the beam as an assembly of many different uniform beams, i.e. a stepped beam.

Further improvements in the beam model can also be achieved by the inclusion of deformation in the chordwise direction. Chordwise bending has been shown to be of considerable importance, especially for beams of low aspect ratio. Thus the solution of beam problems with these secondary effects included in their equations of motion may sometimes be necessary.

The theory given in this thesis does not include time-dependent oscillatory unsteady aerodynamic forces on the wing that occur because of the forward motion of the aircraft. Consideration of all of the aeroelastic forces is a subject for further investigations and an important improvement to this work.

Throughout this work, the energy dissipation during vibration and response analysis was included in the form of modal damping after the equations of motion were uncoupled. However, it is possible to include more refined forms of energy dissipation by modelling the composite laminate as a viscoelastic material and also by including aeroelastic damping forces.

Further investigation will be required, particularly for thick composite beams (wings) to make an objective assessment of the effects of different theories (first order or other higher order) for the inclusion of shear deformation to complement this study.

In the present investigation, a series of experiments on the elastic buckling behaviour of composite structures was conducted to throw some light on the rigidity properties of composites. However, at the end of the buckling tests, it would have been preferred to have carried out dynamic tests. An alternative type of experiment should be designed to investigate this matter using dynamic means. At the same time experiments should be carried out on the free and forced vibration of composite beams to validate the results and conclusions of the present study.

Effects of the warping stiffness and the warping inertia are considered to be small for beams with closed cross-section. However, the inclusion of warping stiffness and warping inertia in the equations of motion for composite beams, especially when beams with open cross-section are under investigation, is recommended for future works.

Despite the extensive research that has been carried out in the field of dynamic characteristics of composite beams, formal strategies and design goals for efficient utilisation of advanced composite materials have yet to be fully developed. Such design strategies require consideration of issues such as durability, damage tolerance, automatic control and their interaction with structural response, and overall aircraft performance. The literature cited in this report, together with the examples presented, have shown that new approaches and further insights will be required for the new era of structural design.

Finally, a major component of an important procedure that should encompass for further studies is the subject of structural optimisation. The present methodology can be effectively used as a tool in a multidisciplinary structural design and optimisation procedure.

Appendices

Appendix A Derivation of the governing differential equations of motion

In this appendix, the damped forced vibration equations of motion of an axially loaded composite Timoshenko beam are developed in two stages. Firstly, the undamped equations of motion are developed using Lagrangian methods, and then the damping loads are introduced as external loads, together with any other external loads such as those of aerodynamic origin.

The governing differential equations of motion for the coupled bending-torsion undamped free vibration of an axially loaded composite Timoshenko beam can be derived using Hamilton's principle as follows :

The total potential energy V_{pe} of an axially loaded composite Timoshenko beam is given by

$$V_{pe} = \frac{1}{2}\int_0^L \left[EI(\theta')^2 - P\left\{(u')^2 + I_\alpha / m(\psi')^2\right\} + 2K\theta'\psi' + kAG(u' - \theta)^2 + GJ(\psi')^2 \right] dy \quad \text{(A-1)}$$

and the total kinetic energy T_{ke} is given by

$$T_{ke} = \frac{1}{2}\int_0^L \left[m(\dot{u})^2 + I_\alpha(\dot{\psi})^2 + \rho I\left(\dot{\theta}\right)^2 \right] dy \quad \text{(A-2)}$$

where all the terms and symbols are defined in ***Chapter Six***.

Hamilton's principle states that if $\mathcal{L}=T_{ke}-V_{pe}$, where $\mathcal{L}$ is defined as the Lagrangian (kinetic potential), then $\int_{t_1}^{t_2} \mathcal{L}\, dt$ taken between any arbitrary intervals of time (t_1 , t_2), is stationary for a dynamic trajectory. Therefore,

$$\delta\int_{t_1}^{t_2} (T_{ke} - V_{pe})dt = 0 \quad \text{(A-3)}$$

Substituting equations (A-1) and (A-2) into equation (A-3) gives

$$\delta\int_{t_1}^{t_2}\int_0^L \frac{1}{2}\{\left[m(\dot{u})^2 + I_\alpha(\dot{\psi})^2 + \rho I\left(\dot{\theta}\right)^2 \right] - \left[EI(\theta')^2 - P\left\{(u')^2 + I_\alpha / m(\psi')^2\right\} + 2K\theta'\psi' + kAG(u' - \theta)^2 + GJ(\psi')^2 \right]\} dydt = 0 \quad \text{(A-4)}$$

from which follow the governing differential equations of motion

$$kAG(u'' - \theta') - Pu'' - m\ddot{u} = 0 \quad \text{(A-5)}$$

$$GJ\psi'' + K\theta'' - P(I_\alpha / m)\psi'' - I_\alpha \ddot{\psi} = 0 \tag{A-6}$$

$$EI\theta'' + kAG(u' - \theta) + K\psi'' - \rho I\ddot{\theta} = 0 \tag{A-7}$$

and the expression for the shear force (V), bending moment (M) and torque (T)

$$V = EI\theta'' + K\psi'' + Pu' - \rho I\ddot{\theta} \tag{A-8}$$

$$M = -EI\theta' - K\psi' \tag{A-9}$$

$$T = GJ\psi' + K\theta' - P\frac{I_\alpha}{m}\psi' \tag{A-10}$$

Equations (A-5) to (A-10) together with appropriate end conditions completely define the coupled bending-torsional free vibration of an axially loaded composite Timoshenko beam.

In order to account for externally applied loads, firstly, the time dependent forces and torques are introduced on the right had side of the equations (A-5) and (A-6), respectively. Next, the following steps are taken to introduce the damping in equations (A-5) to (A-7). As mentioned in ***Section 6.2***, it is assumed that each point of the cross section moves with a different local velocity, so that the local damping force sums over the section to the given expression containing the c_1 term. Similarly, the expression containing the c_2 term is a torque about the elastic axis brought about by elemental damping forces. The expression containing c_3 is associated with the bending moment about the X-axis. No other sources of damping are taken into account.

Introduction of all the external loads in to equations (A-5) to (A-7) leads to the differential equations of motion of an axially loaded composite Timoshenko beam.

$$kAG(u'' - \theta') - P\ u'' - c_1\dot{u} - m\ddot{u} = f(y,t) \tag{A-11}$$

$$K\theta'' + GJ\psi'' - P(I_\alpha / m)\psi'' - c_2\dot{\psi} - I_\alpha\ddot{\psi} = g(y,t) \tag{A-12}$$

$$EI\theta'' + kAG(u' - \theta) + K\psi'' - c_3\dot{\theta} - \rho I\ddot{\theta} = 0 \tag{A-13}$$

Appendix B Solution of the undamped free vibration

The solutions for free natural vibration of the beam can be assumed in the form

$$u(y,t) = U(y)e^{i\omega t}$$

$$\psi(y,t) = \Psi(y)e^{i\omega t} \qquad \text{(B-1)}$$

$$\theta(y,t) = \Theta(y)e^{i\omega t}$$

Substituting equations (B-1) into equations (A-5) to (A-7) gives the following three ordinary differential equations in U_n , Θ_n and Ψ_n :

$$kAG(U'' - \Theta') - PU'' + m\omega^2 U = 0 \qquad \text{(B-2)}$$

$$GJ\Psi'' + K\Theta'' - P(I_\alpha / m)\Psi'' + I_\alpha \omega^2 \Psi = 0 \qquad \text{(B-3)}$$

$$EI\Theta'' + kAG(U' - \Theta) + K\Psi'' + \rho I\omega^2 \Theta = 0 \qquad \text{(B-4)}$$

By extensive algebraic manipulation, equations(B-2) to (B-4) can be combined into one equation by eliminating all but one of the three variables U, Θ and Ψ, to give :

$$(D^6 + \bar{a}D^4 - \bar{b}D^2 - \bar{c})W = 0 \qquad \text{(B-5)}$$

where

$$W = U, \Theta \text{ or } \Psi \;\; ; \;\; D = d/d\xi \;\; ; \;\; \xi = y/L \qquad \text{(B-6)}$$

and $\bar{a}$, $\bar{b}$ and $\bar{c}$ are given below

$$\bar{a} = \frac{b^2 s^2 (b^2 c_k^2 - a^2 p^2) + (b^2 - a^2 p^2)\{p^2 + b^2 r^2 (1 - p^2 s^2)\} + a^2 b^2 (1 - p^2 s^2)}{(1 - p^2 s^2)(b^2 c_k^2 - a^2 p^2)}$$

$$\bar{b} = \frac{b^2 \{(1 - b^2 r^2 s^2)(b^2 - 2a^2 p^2) - a^2 b^2 (r^2 + s^2)\}}{(1 - p^2 s^2)(b^2 c_k^2 - a^2 p^2)} \qquad \text{(B-7)}$$

$$\bar{c} = \frac{a^2 b^4 (1 - b^2 r^2 s^2)}{(1 - p^2 s^2)(b^2 c_k^2 - a^2 p^2)}$$

with a^2, b^2, p^2, r^2 , s^2 and c_k^2, defined as

$$
\begin{aligned}
a^2 &= I_\alpha \omega^2 L^2 / GJ \\
b^2 &= m\omega^2 L^4 / EI \\
p^2 &= PL^2 / EI \\
r^2 &= I / AL^2 \\
s^2 &= EI / kAGL^2 \\
c_k^2 &= 1 - K^2 / EI.GJ
\end{aligned}
\qquad \text{(B-8)}
$$

The solution of the differential equation (B-5) is

$$W(\xi) = C_1^* \cosh\alpha\xi + C_2^* \sinh\alpha\xi + C_3^* \cos\beta\xi + C_4^* \sin\beta\xi + C_5^* \cos\gamma\xi + C_6^* \sin\gamma\xi \quad \text{(B-9)}$$

where C_1^*-C_6^* are constants and

$$\alpha = [2(q/3)^{0.5}\cos(\phi/3) - \bar{a}/3]^{0.5} \quad \text{(B-10)}$$

$$\beta = [2(q/3)^{0.5}\cos\{(\pi-\phi)/3\} + \bar{a}/3]^{0.5} \quad \text{(B-11)}$$

$$\gamma = [2(q/3)^{0.5}\cos\{(\pi+\phi)/3\} + \bar{a}/3]^{0.5} \quad \text{(B-12)}$$

with

$$q = \bar{b} + \bar{a}^2/3 \quad \text{(B-13)}$$

$$\phi = \cos^{-1}[(27\bar{c} - 9\bar{a}\bar{b} - 2\bar{a}^3)/\{2(\bar{a}^2 + 3\bar{b})^{1.5}\}] \quad \text{(B-14)}$$

Equation (B-9) represent the solution for the bending displacement $U(\xi)$, bending rotation $\Theta(\xi)$, and torsional rotation $\Psi(\xi)$. Thus

$$U(\xi) = A_1 \cosh\alpha\xi + A_2 \sinh\alpha\xi + A_3 \cos\beta\xi + A_4 \sin\beta\xi + A_5 \cos\gamma\xi + A_6 \sin\gamma\xi \quad \text{(B-15)}$$

$$\Theta(\xi) = B_1 \cosh\alpha\xi + B_2 \sinh\alpha\xi + B_3 \cos\beta\xi + B_4 \sin\beta\xi + B_5 \cos\gamma\xi + B_6 \sin\gamma\xi \quad \text{(B-16)}$$

$$\Psi(\xi) = C_1 \cosh\alpha\xi + C_2 \sinh\alpha\xi + C_3 \cos\beta\xi + C_4 \sin\beta\xi + C_5 \cos\gamma\xi + C_6 \sin\gamma\xi \quad \text{(B-17)}$$

where A_1 -A_6 , B_1 -B_6 and C_1 -C_6 are the three different sets of constants.

Substituting equations (B-15) and (B-16) into equation (B-2) shows that

$$
\begin{aligned}
B_1 &= (\bar{\alpha}/L)A_1; B_3 = -(\bar{\beta}/L)A_3; B_5 = -(\bar{\gamma}/L)A_5 \\
B_2 &= (\bar{\alpha}/L)A_2; \; B_4 = (\bar{\beta}/L)A_4; \; B_6 = (\bar{\gamma}/L)A_6
\end{aligned}
\qquad \text{(B-18)}
$$

where

$$\bar{\alpha} = \alpha / (1 - b^2 r^2 s^2 - \alpha^2 s^2)$$
$$\bar{\beta} = \beta / (1 - b^2 r^2 s^2 + \beta^2 s^2) \qquad \text{(B-19)}$$
$$\bar{\gamma} = \gamma / (1 - b^2 r^2 s^2 + \gamma^2 s^2)$$

Then substituting equations (B-15) and (B-17) into equation (B-4) gives

$$C_1 = (k_\alpha / x_\alpha) A_1 ; C_3 = (k_\beta / x_\alpha) A_3 ; C_5 = (k_\gamma / x_\alpha) A_5 \qquad \text{(B-20-a)}$$

$$C_2 = (k_\alpha / x_\alpha) A_2 ; C_4 = (k_\beta / x_\alpha) A_4 ; C_6 = (k_\gamma / x_\alpha) A_6 \qquad \text{(B-20-b)}$$

where k_α, k_β and k_γ are functions of a^2, b^2, p^2, r^2 , s^2 and c_k^2, and are given by

$$k_\alpha = -\bar{\alpha}\alpha^2 (K / GJ) / \{(1 - a^2 p^2 / b^2)\alpha^2 + a^2\}$$
$$k_\beta = -\bar{\beta}\beta^2 (K / GJ) / \{(1 - a^2 p^2 / b^2)\beta^2 + a^2\} \qquad \text{(B-21)}$$
$$k_\gamma = -\bar{\gamma}\gamma^2 (K / GJ) / \{(1 - a^2 p^2 / b^2)\gamma^2 + a^2\}$$

The expressions for the bending moment M, Shear force V and torque T are obtained from equations (B-15) to (B-17), after some simplification, as

$$M(\xi) = -(EI / L)\frac{d\Theta}{d\xi} - (K / L)\frac{d\Psi}{d\xi} = -(EI / L^2) \qquad \text{(B-22)}$$

$$\{A_1 g_\alpha \cosh\alpha\xi + A_2 g_\alpha \sinh\alpha\xi - A_3 g_\beta \cos\beta\xi - A_4 g_\beta \sin\beta\xi - A_5 g_\gamma \cos\gamma\xi - A_6 g_\gamma \sin\gamma\xi\}$$

$$V(\xi) = (EI / L^2)\left[\frac{d^2\Theta}{d\xi^2} + (K / EI)\frac{d^2\Psi}{d\xi^2} + (PL / EI)\frac{dU}{d\xi} + b^2 r^2 \Theta\right] = (EI / L^3) \qquad \text{(B-23)}$$

$$\{A_1 f_\alpha \cosh\alpha\xi + A_2 f_\alpha \sinh\alpha\xi + A_3 f_\beta \cos\beta\xi - A_4 f_\beta \sin\beta\xi + A_5 f_\gamma \cos\gamma\xi - A_6 f_\gamma \sin\gamma\xi\}$$

$$T(\xi) = (GJ / L)\frac{d\Psi}{d\xi} + (K / L)\frac{d\Theta}{d\xi} - (PI_\alpha / mL)\frac{d\Psi}{d\xi} = (GJ / L^2) \qquad \text{(B-24)}$$

$$\{A_1 e_\alpha \cosh\alpha\xi + A_2 e_\alpha \sinh\alpha\xi - A_3 e_\beta \cos\beta\xi - A_4 e_\beta \sin\beta\xi - A_5 e_\gamma \cos\gamma\xi - A_6 e_\gamma \sin\gamma\xi\}$$

where e_α, e_β, e_γ, f_α, f_β, f_γ, g_α, g_β and g_γ are functions of a^2, b^2, p^2, r^2 , s^2 and c_k^2, as given below

$$e_\alpha = \alpha(k_\alpha + \bar{\alpha}\frac{K}{GJ} - a^2 p^2 / b^2) ; e_\beta = \beta(k_\beta + \bar{\beta}\frac{K}{GJ} - a^2 p^2 / b^2) ; e_\gamma = \gamma(k_\gamma + \bar{\gamma}\frac{K}{GJ} - a^2 p^2 / b^2)$$

$$f_\alpha = \alpha(g_\alpha + p^2) + \bar{\alpha} b^2 r^2 \; ; \; f_\beta = \beta(g_\beta - p^2) - \bar{\beta} b^2 r^2 \; ; \; f_\gamma = \gamma(g_\gamma - p^2) - \bar{\gamma} b^2 r^2 \qquad \text{(B-25)}$$

$$g_\alpha = \alpha(\bar{\alpha} + \frac{K}{EI} k_\alpha) \; ; \; g_\beta = \beta(\bar{\beta} + \frac{K}{EI} k_\beta) \; ; \; g_\gamma = \gamma(\bar{\gamma} + \frac{K}{EI} k_\gamma)$$

Finally, equations (B-15) to (B-17) and equations (B-22) to (B-24) in conjunction with the boundary conditions yield the eigenvalues (natural frequencies) and eigenfunctions (mode shapes) of the bending-torsion coupled composite Timoshenko beam. Table B-1 shows the classical boundary conditions for the clamped-clamped (C-C), clamped-simply supported (C-S), simply supported-simply supported (S-S) and clamped-free (C-F) beams. Note that the torsional rotation is prevented for the simply supported end condition.

Table B-1. Boundary conditions for different end conditions.

End conditions	End 1 $\xi = 0$	End 2 $\xi = 1$
C-C	$U=\Theta=\Psi=0$	$U=\Theta=\Psi=0$
C-S	$U=\Theta=\Psi=0$	$U=\Psi=M=0$
S-S	$U=\Psi=M=0$	$U=\Psi=M=0$
C-F	$U=\Theta=\Psi=0$	$V=M=T=0$

Appendix C Expression of the dynamic stiffness matrix

The dynamic stiffness matrix of an axially loaded composite Timoshenko beam relating harmonically varying forces to harmonically varying displacements can be expressed as

$$\begin{bmatrix} V_1 \\ M_1 \\ T_1 \\ V_2 \\ M_2 \\ T_2 \end{bmatrix} = \begin{bmatrix} K_{1,1} & K_{1,2} & K_{1,3} & K_{1,4} & K_{1,5} & K_{1,6} \\ & K_{2,2} & K_{2,3} & K_{2,4} & K_{2,5} & K_{2,6} \\ & & K_{3,3} & K_{3,4} & K_{3,5} & K_{3,6} \\ & & & K_{4,4} & K_{4,5} & K_{4,6} \\ & Sym. & & & K_{5,5} & K_{5,6} \\ & & & & & K_{6,6} \end{bmatrix} \begin{bmatrix} u_1 \\ \theta_1 \\ \psi_1 \\ u_2 \\ \theta_2 \\ \psi_2 \end{bmatrix} \qquad \text{(C-1)}$$

where V, M, T are the amplitudes of the shear force, bending moment and torque and u, θ, ψ are the amplitudes of the transverse displacement, flexural rotation and torsional rotation. The derived expressions for the twelve independent elements of the dynamic stiffness matrix $[K]$, are presented here in a concise form as follows (Banerjee, 1998)

$$\begin{aligned}
K_{1,1} &= K_{4,4} = (EI/L^3)\ \Phi_1 / \Delta \\
K_{1,2} &= -K_{4,5} = (EI/L^2)\ \Phi_2 / \Delta \\
K_{1,3} &= -K_{4,6} = (EI/L^2)\ \Phi_3 / \Delta \\
K_{1,4} &= (EI/L^3)\ \Phi_4 / \Delta \\
K_{1,5} &= -K_{2,4} = (EI/L^2)\ \Phi_5 / \Delta \\
K_{1,6} &= -K_{3,4} = (EI/L^2)\ \Phi_6 / \Delta \\
K_{2,2} &= K_{5,5} = (EI/L)\ \Phi_7 / \Delta \\
K_{2,3} &= K_{5,6} = (EI/L)\ \Phi_8 / \Delta \\
K_{2,5} &= (EI/L)\ \Phi_9 / \Delta \\
K_{2,6} &= K_{3,5} = (EI/L)\ \Phi_{10} / \Delta \\
K_{3,3} &= K_{6,6} = (GJ/L)\ \Phi_{11} / \Delta \\
K_{3,6} &= (GJ/L)\ \Phi_{12}\ \Delta
\end{aligned} \qquad \text{(C-2)}$$

where

$$\Delta = (\mu_1^2 - \mu_2^2 + \mu_3^2)\, S_\beta S_\gamma S_{h\alpha} - 2\mu_1 \mu_2 S_\beta (1 - C_\gamma C_{h\alpha}) - 2\mu_2 \mu_3 S_\gamma (1 - C_\beta C_{h\alpha}) - 2\mu_1 \mu_3 S_{h\alpha} (1 - C_\beta C_\gamma) \qquad \text{(C-3)}$$

and

$$\Phi_1 = -\tau_1(\mu_1 S_\beta C_\gamma S_{h\alpha} - \mu_2 S_\beta S_\gamma C_{h\alpha} + \mu_3 C_\beta S_\gamma S_{h\alpha}),$$

$$\Phi_2 = \tau_2 S_\beta S_\gamma S_{h\alpha} + \lambda_3 S_{h\alpha}(1 - C_\beta C_\gamma) + \lambda_1 S_\beta(1 - C_\gamma C_{h\alpha}) + \lambda_2 S_\gamma(1 - C_\beta C_{h\alpha}),$$

$$\Phi_3 = -\tau_3 S_\beta S_\gamma S_{h\alpha} - \bar{\lambda}_3 S_{h\alpha}(1 - C_\beta C_\gamma) - \bar{\lambda}_1 S_\beta(1 - C_\gamma C_{h\alpha}) - \bar{\lambda}_2 S_\gamma(1 - C_\beta C_{h\alpha}),$$

$$\Phi_4 = \tau_1(\mu_1 S_\beta S_{h\alpha} - \mu_2 S_\beta S_\gamma + \mu_3 S_\gamma S_{h\alpha}),$$

$$\Phi_5 = -\tau_1[k_\alpha S_{h\alpha}(C_\beta - C_\gamma) - k_\beta S_\beta(C_\gamma - C_{h\alpha}) + k_\gamma S_\gamma(C_\beta - C_{h\alpha})],$$

$$\Phi_6 = \tau_1[\bar{\alpha} S_{h\alpha}(C_\beta - C_\gamma) - \bar{\beta} S_\beta(C_\gamma - C_{h\alpha}) + \bar{\gamma} S_\gamma(C_\beta - C_{h\alpha})],$$

$$\Phi_7 = -\xi_1 S_\beta C_\gamma S_{h\alpha} + \xi_2 S_\beta S_\gamma C_{h\alpha} - \xi_3 C_\beta S_\gamma S_{h\alpha} + \sigma_1 C_\beta C_\gamma C_{h\alpha} - \bar{\xi}_3 C_\beta - \bar{\xi}_1 C_\gamma + \bar{\xi}_2 C_{h\alpha},$$

$$\Phi_8 = \rho_1 S_\beta C_\gamma S_{h\alpha} + \rho_3 C_\beta S_\gamma S_{h\alpha} - \rho_2 S_\beta S_\gamma C_{h\alpha} + \sigma_2 C_\beta C_\gamma C_{h\alpha} + \bar{\rho}_3 C_\beta + \bar{\rho}_1 C_\gamma - \bar{\rho}_2 C_{h\alpha},$$

$$\Phi_9 = \xi_1 S_\beta S_{h\alpha} - \xi_2 S_\beta S_\gamma + \xi_3 S_\gamma S_{h\alpha} - \bar{\xi}_3 C_\gamma C_{h\alpha} + \bar{\xi}_2 C_\beta C_\gamma - \bar{\xi}_1 C_\beta C_{h\alpha} + \sigma_1,$$

$$\Phi_{10} = -\rho_1 S_\beta S_{h\alpha} - \rho_3 S_\gamma S_{h\alpha} + \rho_2 S_\beta S_\gamma + \bar{\rho}_3 C_\gamma C_{h\alpha} - \bar{\rho}_2 C_\beta C_\gamma + \bar{\rho}_1 C_\beta C_{h\alpha} + \sigma_2,$$

$$\Phi_{11} = \nu_1 S_\beta C_\gamma S_{h\alpha} + \nu_3 C_\beta S_\gamma S_{h\alpha} - \nu_2 S_\beta S_\gamma C_{h\alpha} + \sigma_3 C_\beta C_\gamma C_{h\alpha} + \bar{\nu}_3 C_\beta + \bar{\nu}_1 C_\gamma - \bar{\nu}_2 C_{h\alpha},$$

$$\Phi_{12} = -\nu_1 S_\beta S_{h\alpha} - \nu_3 S_\gamma S_{h\alpha} + \nu_2 S_\beta S_\gamma + \bar{\nu}_3 C_\gamma C_{h\alpha} - \bar{\nu}_2 C_\beta C_\gamma + \bar{\nu}_1 C_\beta C_{h\alpha} + \sigma_3 \quad \text{(C-4)}$$

with

$$\mu_1 = \bar{\alpha}k_\beta - \bar{\beta}k_\alpha; \quad \mu_2 = \bar{\beta}k_\gamma - \bar{\gamma}k_\beta; \quad \mu_3 = \bar{\gamma}k_\alpha - \bar{\alpha}k_\gamma;$$

$$\epsilon_1 = f_\alpha k_\beta + f_\beta k_\alpha; \quad \epsilon_2 = f_\beta k_\gamma - f_\gamma k_\beta; \quad \epsilon_3 = f_\gamma k_\alpha + f_\alpha k_\gamma;$$

$$\zeta_1 = f_\alpha \bar{\beta} + f_\beta \bar{\alpha}; \quad \zeta_2 = f_\beta \bar{\gamma} - f_\gamma \bar{\beta}; \quad \zeta_3 = f_\gamma \bar{\alpha} + f_\alpha \bar{\gamma};$$

$$\eta_1 = g_\alpha + g_\beta; \quad \eta_2 = g_\beta - g_\gamma; \quad \eta_3 = g_\gamma + g_\alpha;$$

$$\bar{\eta}_1 = e_\alpha + e_\beta; \quad \bar{\eta}_2 = e_\beta - e_\gamma; \quad \bar{\eta}_3 = e_\gamma + e_\alpha;$$

$$\lambda_1 = \mu_1\epsilon_2 - \mu_2\epsilon_1; \quad \lambda_2 = \mu_2\epsilon_3 + \mu_3\epsilon_2; \quad \lambda_3 = \mu_3\epsilon_1 - \mu_1\epsilon_3; \quad \text{(C-5)}$$

$$\bar{\lambda}_1 = \mu_1\zeta_2 - \mu_2\zeta_1; \quad \bar{\lambda}_2 = \mu_2\zeta_3 + \mu_3\zeta_2; \quad \bar{\lambda}_3 = \mu_3\zeta_1 - \mu_1\zeta_3;$$

$$\tau_1 = f_\alpha\mu_2 - f_\beta\mu_3 - f_\gamma\mu_1; \quad \tau_2 = \mu_1\epsilon_1 + \mu_2\epsilon_2 - \mu_3\epsilon_3; \quad \tau_3 = \mu_1\zeta_1 + \mu_2\zeta_2 - \mu_3\zeta_3;$$

$$\xi_1 = k_\alpha\mu_3\eta_2 - k_\beta\mu_2\eta_3; \quad \xi_2 = k_\beta\mu_1\eta_3 - k_\gamma\mu_3\eta_1; \quad \xi_3 = k_\gamma\mu_2\eta_1 + k_\alpha\mu_1\eta_2;$$

$$\bar{\xi}_1 = k_\alpha\mu_2\eta_3 + k_\beta\mu_3\eta_2; \quad \bar{\xi}_2 = k_\beta\mu_3\eta_1 - k_\gamma\mu_1\eta_3; \quad \bar{\xi}_3 = k_\gamma\mu_1\eta_2 - k_\alpha\mu_2\eta_1;$$

$$\rho_1 = \bar{\alpha}\mu_3\eta_2 - \bar{\beta}\mu_2\eta_3; \quad \rho_2 = \bar{\beta}\mu_1\eta_3 - \bar{\gamma}\mu_3\eta_1; \quad \rho_3 = \bar{\gamma}\mu_2\eta_1 + \bar{\alpha}\mu_1\eta_2;$$

$$\bar{\rho}_1 = \bar{\alpha}\mu_2\eta_3 + \bar{\beta}\mu_3\eta_2; \quad \bar{\rho}_2 = \bar{\beta}\mu_3\eta_1 - \bar{\gamma}\mu_1\eta_3; \quad \bar{\rho}_3 = \bar{\gamma}\mu_1\eta_2 - \bar{\alpha}\mu_2\eta_1;$$

$$\nu_1 = \bar{\alpha}\mu_3\bar{\eta}_2 - \bar{\beta}\mu_2\bar{\eta}_3; \quad \nu_2 = \bar{\beta}\mu_1\bar{\eta}_3 - \bar{\gamma}\mu_3\bar{\eta}_1; \quad \nu_3 = \bar{\gamma}\mu_2\bar{\eta}_1 + \bar{\alpha}\mu_1\bar{\eta}_2;$$

$$\bar{\nu}_1 = \bar{\alpha}\mu_2\bar{\eta}_3 + \bar{\beta}\mu_3\bar{\eta}_2; \quad \bar{\nu}_2 = \bar{\beta}\mu_3\bar{\eta}_1 - \bar{\gamma}\mu_1\bar{\eta}_3; \quad \bar{\nu}_3 = \bar{\gamma}\mu_1\bar{\eta}_2 - \bar{\alpha}\mu_2\bar{\eta}_1;$$

$$\sigma_1 = -k_\alpha\mu_2\eta_2 - k_\beta\mu_3\eta_3 + k_\gamma\mu_1\eta_1; \quad \sigma_2 = \bar{\alpha}\mu_2\eta_2 + \bar{\beta}\mu_3\eta_3 - \bar{\gamma}\mu_1\eta_1; \quad \sigma_3 = \bar{\alpha}\mu_2\bar{\eta}_2 + \bar{\beta}\mu_3\bar{\eta}_3 - \bar{\gamma}\mu_1\bar{\eta}_1.$$

in which a^2, b^2, p^2, r^2, s^2, c_k^2, $\bar{a}$, $\bar{b}$, $\bar{c}$, α, β, γ, $\bar{\alpha}$, $\bar{\beta}$, $\bar{\gamma}$, q, ϕ, k_α, k_β, k_γ, e_α, e_β, e_γ, f_α, f_β, f_γ, g_α, g_β, g_γ have all been defined in ***Appendix B***, with $k_t = K/GJ$ and $k_b = K/EI$.

Appendix D Orthogonality condition and modal damping

D.1. Derivation of the orthogonality condition

The free vibrational mode shapes, derived for bending-torsion coupled beams, have orthogonality relationships equivalent to those defined for uncoupled Bernoulli-Euler beams but the derivation is comparatively more difficult. This can be demonstrated in a similar manner by applying Betti's law (Clough and Penzien, 1975). Orthogonality conditions together with the expressions for generalised damping have earlier been given in equations (6-35) to (6-40) for different types of bending-torsion coupled beams (both metallic and composite). The procedure for derivation of the orthogonality condition for the most complicated case is given below.

An axially loaded bending-torsion coupled composite Timoshenko beam is assumed to be vibrating in two different modes, say ***m*** and ***n***. It is also assumed that the displaced shape of the ***nth*** mode is subjected to inertia forces of the ***mth*** mode and the displaced shape of the ***mth*** mode is subjected to inertia forces of the ***nth*** mode. The beam can have any classical boundary conditions and the same procedure is applicable when the beam has arbitrarily varying stiffness and mass along its length. When Betti's law is applied to these two deflection patterns, it means that the work done by the inertia forces of mode ***n*** acting on the deflection of mode ***m*** is equal to the work of the forces of mode ***m*** acting on the displacement of mode ***n*** (Clough and Penzien, 1975), that is,

$$\int_0^1 \left(U_m f_n^u + \Psi_m f_n^\Psi + \Theta_m f_n^\theta \right) d\xi = \int_0^1 \left(U_n f_m^u + \Psi_n f_m^\Psi + \Theta_n f_m^\theta \right) d\xi \qquad \text{(D-1)}$$

where f_n^u, f_n^θ, f_n^Ψ, f_m^u, f_m^θ and f_m^Ψ are the inertia force, moment and torque of mode ***nth*** and ***mth*** and given below

$$f_n^u = m\,[\ddot{U}_n - x_\alpha \ddot{\Psi}_n]\;;\; f_m^u = m\,[\ddot{U}_m - x_\alpha \ddot{\Psi}_m]$$

$$f_n^\Psi = I_\alpha \ddot{\Psi}_n - m x_\alpha \ddot{U}_n\;;\; f_m^\Psi = I_\alpha \ddot{\Psi}_m - m x_\alpha \ddot{U}_m \qquad \text{(D-2)}$$

$$f_n^\theta = \rho I \ddot{\Theta}_n\;;\; f_m^\theta = \rho I \ddot{\Theta}_m$$

Substituting equations (D-2) and (B-1) in (D-1) gives

$$\omega_n^2\int_0^1[mU_mU_n+I_\alpha\Psi_m\Psi_n+\rho I\Theta_m\Theta_n-mx_\alpha(U_m\Psi_n+U_n\Psi_m)]d\xi$$
$$=\omega_m^2\int_0^1[mU_mU_n+I_\alpha\Psi_m\Psi_n+\rho I\Theta_m\Theta_n-mx_\alpha(U_m\Psi_n+U_n\Psi_m)]d\xi \qquad \text{(D-3)}$$

or

$$(\omega_n^2-\omega_m^2)\int_0^1[mU_mU_n+I_\alpha\Psi_m\Psi_n+\rho I\Theta_m\Theta_n-mx_\alpha(U_m\Psi_n+U_n\Psi_m)]d\xi=0 \qquad \text{(D-4)}$$

from which, following the method of Clough and Penzien (1975), the orthogonality condition for an axially loaded bending-torsion coupled composite Timoshenko beam is as follow

$$\int_0^1[mU_mU_n+I_\alpha\Psi_m\Psi_n+\rho I\Theta_m\Theta_n-mx_\alpha(U_m\Psi_n+U_n\Psi_m)]d\xi=\mu_n\delta_{mn} \qquad \text{(D-5)}$$

where μ_n is the generalised mass in the ***nth*** mode.

This leads to the physical meaning of the orthogonality condition which is; work done by the inertia forces of the ***nth*** mode over the displacements of the ***mth*** mode is zero.

D.2. Derivation of damping ratio in each mode

Governing differential equations of motion for the undamped free vibration of an axially loaded bending-torsion coupled composite Timoshenko beam is obtained from equations (6-28) to (6-30) by setting damping coefficients and externally applied loads to zero

$$kAG(u''-\theta')-P(u''-x_\alpha\psi'')-m(\ddot{u}-x_\alpha\ddot{\psi})=0 \qquad \text{(D-6)}$$

$$K\theta''+GJ\psi''-P\{(I_\alpha/m)\psi''-x_\alpha u''\}-I_\alpha\ddot{\psi}+mx_\alpha\ddot{u}=0 \qquad \text{(D-7)}$$

$$EI\theta''+kAG(u'-\theta)+K\psi''-\rho I\ddot{\theta}=0 \qquad \text{(D-8)}$$

Substituting equation (6-31) into equations (D-6) to (D-8) leads to

$$kAG(U_n'' - \Theta_n') - P(U_n'' - x_\alpha \Psi_n'') = -m\omega_n^2(U_n - x_\alpha \Psi_n) \tag{D-9}$$

$$K\Theta_n'' + GJ\Psi_n'' - P\{(I_\alpha / m)\Psi_n'' - x_\alpha U_n''\} = \omega_n^2(-I_\alpha \Psi_n + mx_\alpha U_n) \tag{D-10}$$

$$EI\Theta_n'' + kAG(U_n' - \Theta_n) + K\Psi_n'' = -\omega_n^2(\rho I\Theta_n) \tag{D-11}$$

Substituting equation (6-41) into equations (6-28) to (6-30) follows

$$\sum_{n=1}^{\infty}\begin{bmatrix} kAG(U_n'' - \Theta_n')\ q_n - P(U_n'' - x_\alpha \Psi_n'')\ q_n \\ -c_1(U_n - x_\alpha \Psi_n)\ \dot{q}_n - m(U_n - x_\alpha \Psi_n)\ \ddot{q}_n \end{bmatrix} = f(\xi, t) \tag{D-12}$$

$$\sum_{n=1}^{\infty}\begin{bmatrix} K\Theta_n''\, q_n + GJ\Psi_n''\, q_n - P\{(I_\alpha / m)\Psi_n'' - x_\alpha U_n''\}\ q_n \\ -c_2\Psi_n\ \dot{q}_n + c_1 x_\alpha U_n\ \dot{q}_n - I_\alpha \Psi_n\ \ddot{q}_n + mx_\alpha U_n\ \ddot{q}_n \end{bmatrix} = g(\xi, t) \tag{D-13}$$

$$\sum_{n=1}^{\infty}\begin{bmatrix} EI\Theta_n''\, q_n + kAG(U_n' - \Theta_n)\ q_n + K\Psi_n''\, q_n \\ -c_3\Theta_n\ \dot{q}_n - \rho I\Theta_n\ \ddot{q}_n \end{bmatrix} = 0 \tag{D-14}$$

and substituting equations (D-9) to (D-11) into equations (D-12) to (D-14) leads to

$$\sum_{n=1}^{\infty}\left[-m\omega_n^2(U_n - x_\alpha \Psi_n)q_n - c_1(U_n - x_\alpha \Psi_n)\dot{q}_n - m(U_n - x_\alpha \Psi_n)\ddot{q}_n\right] = f(\xi, t) \tag{D-15}$$

$$\sum_{n=1}^{\infty}\left[\omega_n^2(-I_\alpha \Psi_n + mx_\alpha U_n)q_n - c_2\Psi_n\dot{q}_n + c_1 x_\alpha U_n\dot{q}_n - I_\alpha \Psi_n\ddot{q}_n + mx_\alpha U_n\ddot{q}_n\right] = g(\xi, t) \tag{D-16}$$

$$\sum_{n=1}^{\infty}\left[-\omega_n^2(\rho I\Theta_n)q_n - c_3\Theta_n\dot{q}_n - \rho I\Theta_n\ddot{q}_n\right] = 0 \tag{D-17}$$

Multiplying equations (D-15) to (D-17) by $-U_m$, $-\Psi_m$ and $-\Theta_m$, respectively, adding them together, integrating them with respect to ξ from $\xi=0$ to $\xi=1$, using the orthogonality condition and following method of Bishop and Price (1977), then equations (6-42) and (6-43) are obtained only if

$$\int_0^1 [c_1 U_m U_n + c_2 \Psi_m \Psi_n + c_3 \Theta_m \Theta_n - c_1 x_\alpha (U_m \Psi_n + U_n \Psi_m)]d\xi = 2\zeta_n \omega_n \mu_n \delta_{mn} \tag{D-18}$$

where

$$\zeta_n = \frac{1}{2\omega_n \mu_n}\int_0^1 [c_1 U_n^2 + c_2 \Psi_n^2 + c_3 \Theta_n^2 - 2c_1 x_\alpha U_n \Psi_n]d\xi \tag{D-19}$$

and ζ_n is the damping ratio in the *nth* mode.

Appendix E Free vibration of non-uniform beams with bending-torsion coupling

In many cases of real life applications, beam structures are usually non-uniform. Examples of such structures are aircraft wings, turbine and fan propellers, and helicopter blades. The method developed in this thesis has been applied mainly to uniform beams, however, it may be easily extended to the free and forced vibration analysis of bending-torsion coupled beams with varying cross-sections. A non-uniform beam can be idealised as an assembly of many different uniform beams, i.e. a stepped beam. In this appendix the free vibration characteristics of three non-uniform beams (two metallic and one composite) with different end conditions, is investigated using the present method and the results are compared with those available in the literature.

E.1. A tapered Timoshenko beam

The first chosen example is a metallic beam that is linearly tapered in depth along the length of the beam. The beam has the following mechanical properties (Cleghorn and Tabarrok, 1992) : $E = 210\ GPa$, $G = 80\ GPa$, $k = 0.667$, $L = 25.4\ cm$, height of the beam at the left end = $2.54\ cm$ and height of the beam at the right end = $1.27\ cm$. Boundary conditions are considered to be clamped-clamped and clamped-simply supported.

The first five natural frequencies of tapered beams are calculated using the present method and compared with those of previously published by To (1979, 1981) and Cleghorn and Tabarrok (1992). The natural frequencies are given in Table E-1. Results of the present method show very good agreement with those of To and Cleghorn et al.

To (1979, 1981) and Cleghorn and Tabarrok (1992) used finite element methods, but based on two different formulations. To (1979, 1981) formulated the element matrices for a tapered Timoshenko beam. A cubic polynomial was assumed for the deflected shape, and a linear distribution for the shearing strain. On the other hand, Cleghorn and Tabarrok (1992) developed a finite element model for free lateral vibration analyses of linearly

tapered Timoshenko beams. The shape functions were obtained by them from homogeneous solutions of the governing equations for static deflections.

E.2. A tapered swept back wing

The second example is a non-uniform swept back wing (Hallauer, 1982) and is shown in Figure E-1. Mechanical properties of the wing are given in Table E-2. The first four natural frequencies of wing are calculated using the present method and compared with those of Hallauer (1982) using respectively exact and finite element methods. The natural frequencies are given in Table E-3. Results of the present method show very good agreement with those of Hallauer (1982).

E.3. A tapered composite beam

The third illustrative example is a tapered composite beam (Rao and Ganesan, 1997) and the beam is shown in Figure E-2 for different configurations. The following AS4/3051-6 graphite-epoxy material properties (in the usual notation) are used : $E_1 = 144.8\ GPa$; $E_2 = 9.65\ GPa$; $G_{12} = G_{13} = 4.14\ GPa$; $G_{23} = 3.45\ GPa$; $\nu = 0.3$; $\rho = 1389.23\ kg/m^3$; $L = 25.4\ cm$; $h_1/h_2 = 0.5$; $L/h_2 = 40$ and width of the beam = $2.54\ cm$. The stacking sequence used is [*0/90/90/0*]. The end condition considered is simply supported-simply supported. Three different types of tapered beams as shown in Figure E-2 are considered. The first one is of increasing type, the second one is of decreasing-increasing type and the third one is of increasing-decreasing type (see Figure E-2).

The first three natural frequencies of these beams are calculated using the present method and compared with those published by Rao and Ganesan (1997) who calculated the natural frequencies using two different theories, namely first order shear deformation theory (FSDT) and higher order shear deformation theory (HSDT). Natural frequencies are given in Tables E-4 to E-6, receptively, for increasing type, decreasing-increasing type and increasing-decreasing type. Results obtained from the present method show quite good agreement with those of Rao and Ganesan (1997).

Table E-1. Natural frequencies of a tapered Timoshenko beam

	ω_n (Hz) × 10^4					
	(C-C)			(C-S)		
mode	To (1981)	Cleghorn/Tabarrok (1992)	Present theory (20 elements)	To (1981)	Cleghorn/Tabarrok (1992)	Present theory (20 elements)
1	0.91718	0.91707	0.91721	0.22174	0.22174	0.21983
2	2.4112	2.4118	2.4110	1.0334	1.0336	1.0295
3	4.4775	4.4834	4.4768	2.5588	2.5614	2.5502
4	6.9910	7.0094	6.9875	4.6532	4.6656	4.5978
5	9.8992	9.9152	9.8898	7.2155	7.2448	7.1864

Table E-2. Mechanical properties of a stepped swept back wing (Hallauer, 1982)

element no.	EI (MNm^2)	GJ (MNm^2)	m/L (kg/m)	$\rho I_p/L$ (kg-m)	x_α (m)	L (m)
AB	9.773	0.9877	35.72	8.643	-0.1826	2.438
BC	6.515	0.6584	23.81	5.762	-0.1826	2.134
CD	3.258	0.3292	11.91	2.881	-0.1826	1.829

Table E-3. Natural frequencies of a stepped swept back wing (Hallauer, 1982)

Frequency No.	Present method	Hallauer (1982)	FEM (Hallauer, 1982)
1	57.67	57.68	57.69
2	118.4	118.4	119.0
3	218.1	218.1	220.8
4	368.8	368.8	388.6

Table E-4. Natural frequencies of the increasing type tapered composite beam (kHz).

		Rao and Ganesan (1997)	
mode no.	present theory (20 elements)	FSDT	HSDT
1	2.4056	2.4054	2.4065
2	8.3527	8.3514	8.3671
3	15.574	15.558	15.617

Table E-5. Natural frequencies of the decreasing-increasing type tapered composite beam (kHz).

		Rao and Ganesan (1997)	
mode no.	present theory (20 elements)	FSDT	HSDT
1	2.0898	2.0897	2.0902
2	8.1773	8.1728	8.1885
3	15.727	15.705	15.762

Table E-6. Natural frequencies of the increasing-decreasing type tapered composite beam (kHz).

		Rao and Ganesan (1997)	
mode no.	present theory (20 elements)	FSDT	HSDT
1	2.6171	2.6170	2.6175
2	8.2053	8.1986	8.2148
3	15.651	15.638	15.700

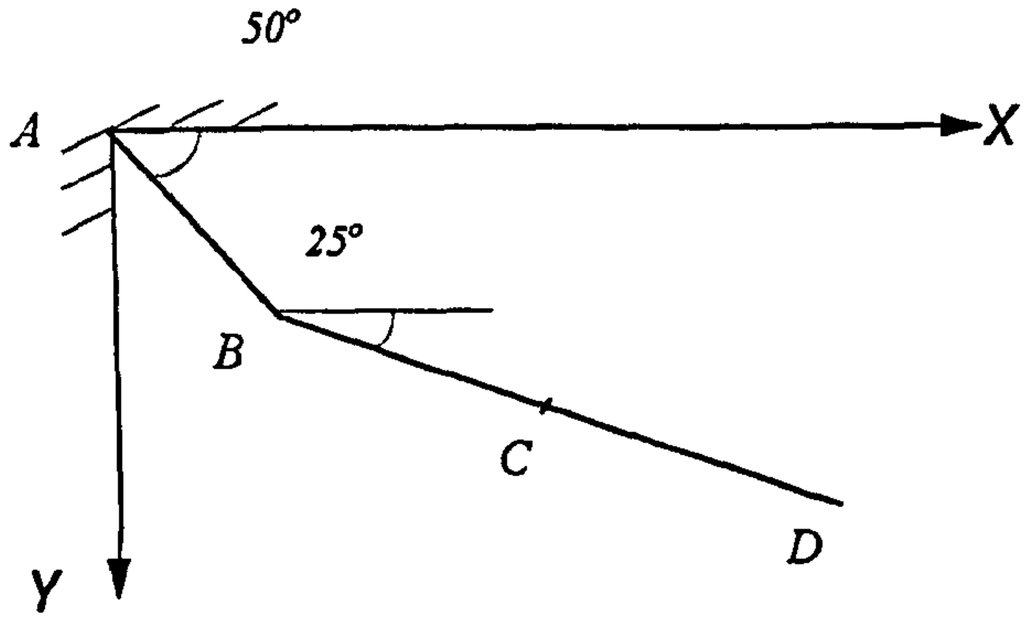

Figure E-1. Elastic axis of cantilevered swept back wing (Hallauer, 1982), planform view.

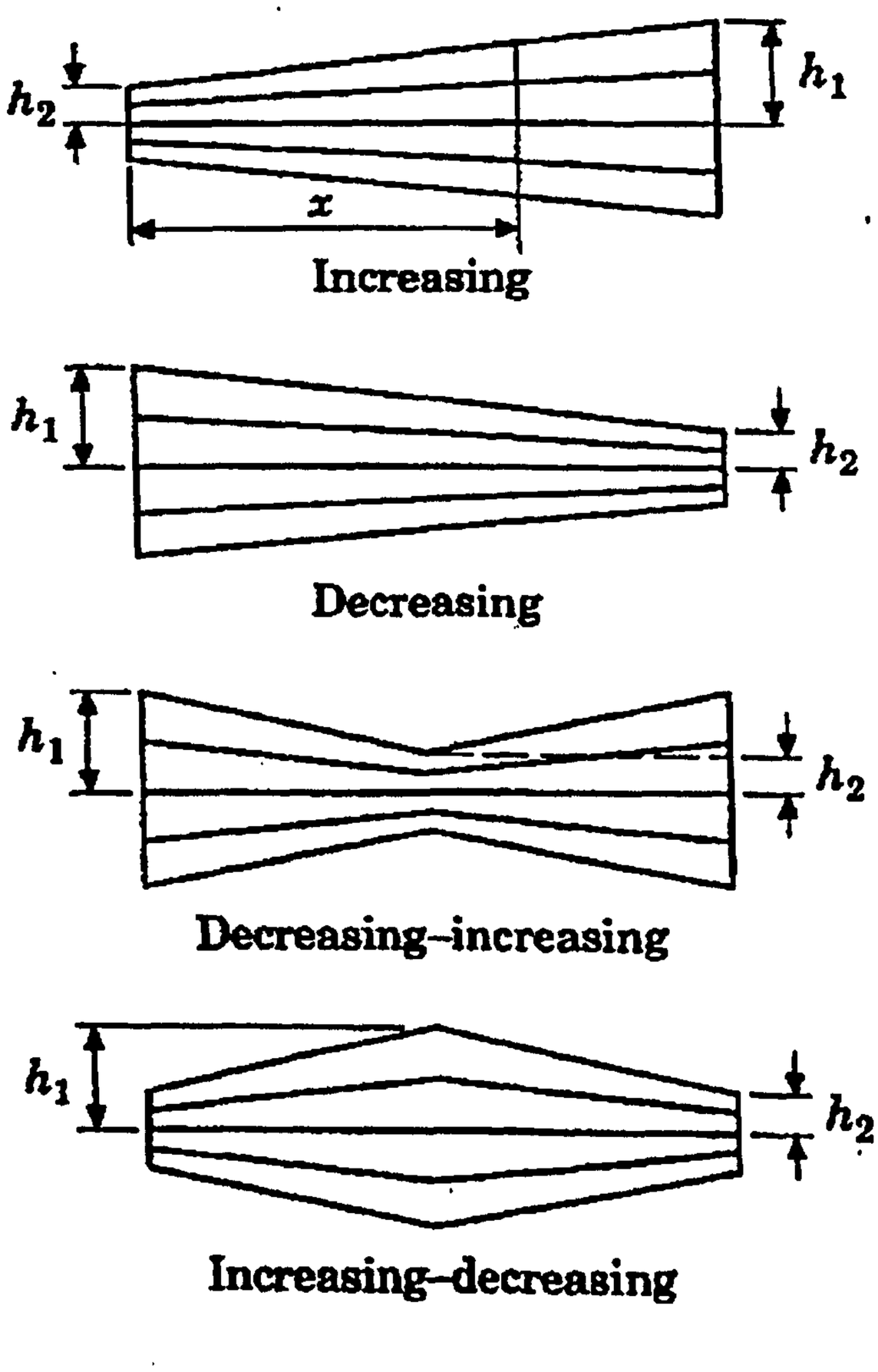

Figure E-2. Different types of taper profile (Rao and Ganesan, 1997).

Appendix F List of computer programs

A suite of computer programs in FORTRAN has been developed during the course of this investigation, (i) to determine the rigidity properties, (ii) to perform the buckling analysis and (iii) to predict the free and forced vibration characteristics of the bending-torsion coupled metallic or composite beams, considered in this research. These programs have been validated using published literature and a series of carefully selected tests. A list of all the main computer programs developed, with a description of their application is given below.

Program	Command lines	Routine	Description
abdmx.f	277	*main*	To calculate the rigidity properties of a composite beam with flat rectangular cross-section.
boxmxe.f	694	*main*	To calculate the rigidity properties of a composite beam with thin-walled cross-section.
psd6.f	978	*main*	To calculate the dynamic response of bending-torsion coupled beams to deterministic and random loads. This program can calculate dynamic displacements or accelerations.
		axitim	To calculate the natural frequencies and mode shapes of a bending-torsion coupled metallic beam.
		subcmp	To calculate the natural frequencies and mode shapes of a bending-torsion coupled composite beam with both geometric and material coupling.
force.f	329	*main*	To calculate the dynamic shear force, bending moment and torque in any cross-section of a bending-torsion coupled beam.
		tw-stress	To calculate the stresses in principal material direction in a thin-walled laminated composite beam.
		fp-stress	To calculate the stresses in principal material direction in a flat rectangular laminated composite beam.
tpcmcomp.f	258	*main*	To calculate the elastic critical buckling load of bending-torsion composite columns with both geometric and material coupling.

Appendix G List of published papers extracted from the present work

A list of published papers extracted from the present work is given here. The papers were published either in refereed journals or presented in refereed established international conferences and appeared in their proceedings.

Journal publications

1. S.H.R. Eslimy-Isfahany and J.R. Banerjee, 1997; *Dynamic Response of Composite Beams with Application to Aircraft Wings*, AIAA Journal of Aircraft, Vol. 34, November-December, No. 6, pp. 785-791.

2. S.H.R. Eslimy-Isfahany, J.R. Banerjee and A.J. Sobey, 1996; *Response of a Bending-Torsion Coupled Beam to Deterministic and Random Loads*, Journal of Sound and Vibration, Vol. 195, No. 2, pp. 267-283.

3. S.H.R. Eslimy-Isfahany and J.R. Banerjee, 1996; *Dynamic Response of an Axially Loaded Bending-Torsion Coupled Beam*, AIAA Journal of Aircraft, Vol. 33, May-June, No. 3, pp. 601-607.

Presented papers and conference proceedings

4. S.H.R. Eslimy-Isfahany and J.R. Banerjee, 1998; *Effects of Axial Load on Dynamic Stresses in Composite Wings Subjected to Random Excitation*, Proceedings of Annual Conference of Aeronautical Engineers, Shahinshahr, Isfahan, Iran, October, Vol. 2, pp. 684-692.

5. S.H.R. Eslimy-Isfahany and J.R. Banerjee, 1998; *Dynamic Stresses in Composite Timoshenko Beams with Application to Aircraft Wings*, Proceedings of AIAA/ASME/ASCE/AHS/ASC 39th Structures, Structural Dynamics and Materials Conference, Long Beach, CA, USA, April, pp. 3201-3211.

6. S.H.R. Eslimy-Isfahany and J.R. Banerjee, 1997; *Deterministic and Random Response of an Axially Loaded Composite Timoshenko Beam*, Proceedings of AIAA/ASME/ASCE/AHS/ASC 38th Structures, Structural Dynamics and Materials Conference, Kissimmee, CA, USA, April, pp. 511-520.

7. S.H.R. Eslimy-Isfahany and J.R. Banerjee, 1997; *Effects of Shear Deformation and Rotatory Inertia on the Response of a Composite Aircraft Wing to Random Atmospheric Turbulence*, Proceedings of Annual Conference of Aeronautical Engineers, Tehran, Iran, January, pp. 620-632.

8. S.H.R. Eslimy-Isfahany and J.R. Banerjee, 1996; *Response of Composite Beams to Deterministic and Random Loads*, Proceedings of AIAA/ASME/ASCE/AHS/ASC 37th Structures, Structural Dynamics and Materials Conference, Salt Lake City, USA, April, pp 813-821.

9. S.H.R. Eslimy-Isfahany and J.R. Banerjee, 1995; *Response of an Axially Loaded Bending-Torsion Coupled Beam to Deterministic and Random Loads*, Proceedings of AIAA/ASME/ASCE/AHS/ASC 36th Structures, Structural Dynamics and Materials Conference, New Orleans, LA, USA, April, pp 2523-2533.

Papers submitted for presentation in international conferences

10. S.H.R. Eslimy-Isfahany and J.R. Banerjee, 1999; *Theoretical and Experimental Investigations into Buckling of Composite Columns*, Proceedings of AIAA/ASME/ASCE/AHS/ASC 40th Structures, Structural Dynamics and Materials Conference, St. Louis, MO , USA, April.

11. J.R. Banerjee and S.H.R. Eslimy-Isfahany, 1998; *Free Vibration of Laminated Composite Beams with Effects of Shear Deformation, Rotatory Inertia and Axial Load*, Proceedings of International Conference on Theoretical, Applied, Computational and Experimental Mechanics, Indian Institute of Technology, Kharagpur, India, December.

Publications in preparation

12. S.H.R. Eslimy-Isfahany and J.R. Banerjee; *Closed Form Solution for the Response of a Simply Supported Bending-Torsion Coupled Beam to Deterministic and Random Loads*, Engineering Structures.

13. S.H.R. Eslimy-Isfahany and J.R. Banerjee; *Response of an Axially Loaded Bending-Torsion Coupled Timoshenko Beam to Deterministic and Random Loads*, International Journal of Solids and Structures.

14. J.R. Banerjee, S.H.R. Eslimy-Isfahany, and F.W. Williams; *Coupled Flexural-Torsional Static Stiffness Matrix of Composite or Metallic Columns*, Composite Structures.

15. S.H.R. Eslimy-Isfahany and J.R. Banerjee; *Significance of Modal Interchange and Generalised Mass in Each Mode of Vibration on Response Characteristics of a Vibrating Bending-Torsion Coupled Beam*, Composites Part B : Engineering.

16. S.H.R. Eslimy-Isfahany and J.R. Banerjee; *Review of the development of free and forced vibration of beams*, The shock and Vibration Digest.

References and bibliography

References and bibliography

1. Abarcar, R.B., and Cunniff, 1972, P.F., "The vibration of cantilever beams of fibre reinforced material", *Journal of Composite Materials*, Vol. 6, pp. 504-517.

2. Abdelnaser, A.S., 1993, "Random vibrations of composite beams and plates", *PhD thesis*, Virginia Polytechnic Institute and State University, Blacksburg, USA.

3. Abdelnaser, A.S., and Singh, M.P., 1993, "Random vibration of cantilevered composite beams with torsion-bending coupling", *Probabilistic Engineering Mechanics*, Vol. 8, pp. 143-151.

4. Abramovich, H., 1994, "Thermal buckling of cross-ply composite laminates using a first-order shear deformation theory", *Composite Structures*, Vol. 28, pp. 201-213.

5. Abramovich, H., Eisenberger, M., and Shulepov, O., 1995, "Vibration and buckling of non-symmetrical laminated composite beams via the exact element method", *Proceedings of the 36th AIAA/ASME/ASCE/AHS/ASC Structures, Structural Dynamics and Materials Conference*, New Orleans, LA, USA, April, 1995, pp. 2672-2680.

6. Adali, S., and Duffy, K.J, 1990, "Design of antisymmetric hybrid laminates for maximum buckling load: I. Optimal fibre orientation, II. Optimal layer thickness", *Composite Structures*, Vol. 14, No. 1, [I] pp. 49-60, and No. 2, [II] pp.113-124.

7. Akesson, B., 1980, "Overall buckling in bending and torsion of rack structures", *Thin-walled Structures* edited by J. Rhodes and A.C. Walkers, Granada, London.

8. Al-Shareedah, E.M., and Seireg, A.A., 1986, "Use of undetermined multipliers in the design of stiffened plates", *Computers in Mechanical Engineering*, Vol. 4, No. 5., pp. 57-64.

9. Anderson, M.S., Williams, F.W., Banerjee, J.R., Durling, B.J., Herstrom, C.L., Kennedy, D., and Warnaar, D.B., 1986, "User manual for BUNVIS RG: An exact buckling and vibration program for lattice structures with repetitive geometry and substructuring option", *NASA Technical Memo 87669*.

10. Anderson, M.S., Williams, F.W., and Wright, C.J., 1983, "Buckling and vibration of

any prismatic assembly of shear and compression loaded anisotropic plates with an arbitrary supporting structure", *International Journal of Mechanical Science*, Vol. 25, No. 8, pp. 585-596.

11. Armanios, E.A. and Badir, A.M., 1995, "Free vibration analysis of anisotropic thin-walled closed-section beams", *AIAA Journal*, Vol. 33, No. 10, pp. 1905-1910.

12. Ardic, E.S., Bolcan, C., and Kayran, A., 1995, "A method of strain and stress analysis for failure prediction in laminated composites", *Proceedings of Institute of Mechanical Engineers-Part G: Journal of Aerospace Engineering*, Vol. 209, pp. 43-51.

13. Ashton, J.E., and Whitney, J.M., 1970, "Theory of laminated plates", *Technomic*, Stamford.

14. Banerjee, J.R., 1984, "Use and capability of CALFUN a program for CALculation of Flutter speed Using Normal modes", *Proceedings of International Athens Summer Conference on Modelling and Simulation*, June 27-29, 1984, Athens, Greece.

15. Banerjee, J.R., 1987, "Effect of axial force on the flutter of high aspect ratio aerofoil blades", *Thirteenth European Rotorcraft Forum*, paper no. 6.13.

16. Banerjee, J.R., 1988, "Flutter modes of high aspect ratio tailless aircraft", *AIAA Journal of Aircraft*, Vol. 25, pp. 473-476.

17. Banerjee, J.R., 1989, "Coupled-bending-torsional dynamic stiffness matrix for beam elements", *International Journal for Numerical Methods in Engineering*, Vol. 28, pp. 1283-1298.

18. Banerjee, J.R., 1991, "A FORTRAN routine for computation of coupled bending-torsional dynamic stiffness matrix of beam elements," *Advances in Engineering Software*, Vol. 13, No. 1, pp. 17-24.

19. Banerjee, J.R., 1997, "Dynamic stiffness formulation for structural elements: A general approach", *Computers and Structures*, Vol. 63, No. 1, pp. 101-103.

20. Banerjee, J.R., 1998, "Free vibration of axially loaded composite Timoshenko beams using the dynamic stiffness matrix method", *Computers and Structures*, Vol. 69, pp.

197-208.

21. Banerjee, J.R., and Butler, R., 1994, "Coupled extensional-torsional vibration of composite beams an exact method", *Proceedings of the 35th AMA/ASME/ASCE/AHS /ASC Structures, Structural Dynamics and Materials Conference*, Paper-94-1325, pp. 147-154.

22. Banerjee, J.R., and Eslimy-Isfahany, S.H.R., 1998, "Free vibration of laminated composite beams with effects of shear deformation, rotatory inertia and axial load", *Proceedings of International Conference on Theoretical, Applied, Computational and Experimental Mechanics*, Indian Institute of Technology, Kharagpur, India, December 1988, accepted for presentation in the conference and publication in the proceedings.

23. Banerjee, J.R., Eslimy-Isfahany, S.H.R., and Williams, F.W., 1998, "Coupled flexural-torsional static stiffness matrix of composite or metallic columns", *in progress*.

24. Banerjee, J.R., and Fisher, S.A., 1992, "Coupled bending-torsional dynamic stiffness matrix for axially loaded beam elements," *International Journal for Numerical Method in Engineering*, Vol. 33, pp. 739-751.

25. Banerjee J.R., Guo, S., and Howson, W.P., 1996, "Exact dynamic stiffness matrix of a bending torsion coupled beam including warping", *Computers and Structures*, Vol. 59, pp. 613-621.

26. Banerjee, J.R., and Kennedy, D., 1985, "Response on an axially loaded Timoshenko beam to random loads," *Journal of Sound and Vibration*, Vol. 101, pp. 481-487.

27. Banerjee, J.R., and Williams, F.W., 1982, "User's guide to the computer program BUNVIS (Buckling or Natural Vibration of Space frames)", *Report no. 5*, Department of Civil Engineering and Building Technology, Institute of Science and Technology, University of Wales.

28. Banerjee, J.R., and Williams, F.W., 1983, "Vibration characteristics of self expanding stayed columns for use in space", *Journal of Sound and Vibration*, Vol. 90, pp. 245-261.

29. Banerjee, J.R., and Williams, F.W., 1984, "Evaluation of efficiently computed exact vibration characteristics of space platforms assembled from stayed columns", *Journal of Sound and Vibration*, Vol. 95, pp. 405-414.

30. Banerjee, J.R., and Williams, F.W., 1985, "Exact Bernoulli-Euler dynamic stiffness matrix for a range of tapered beams", *International Journal for Numerical Method in Engineering*, Vol. 21, pp. 2289-2302.

31. Banerjee, J.R., and Williams, F.W., 1992, "Coupled bending torsional dynamic stiffness matrix for Timoshenko beam elements", *Computers and Structures*, Vol. 42, pp. 301-310.

32. Banerjee, J.R., and Williams, F.W., 1994(a), "An exact dynamic stiffness matrix for coupled extensional-torsional vibration of structural members", *Computers and Structures*, Vol. 50, pp. 161-166.

33. Banerjee, J.R., and Williams, F.W., 1994(b), "Clamped-clamped natural frequencies of a bending torsion coupled beam", *Journal of Sound and Vibration*, Vol. 176, No. 3, pp. 301-306.

34. Banerjee, J.R., and Williams, F.W., 1994(c), "Coupled bending-torsional dynamic stiffness matrix of an axially loaded Timoshenko beam element," *International Journal of Solids Structures*, Vol. 31, No. 6, pp. 749-762.

35. Banerjee, J.R., and Williams, F.W., 1995, "Free vibration of composite beams- an exact method using symbolic computation," *AIAA Journal of Aircraft*, Vol. 32, No. 3, pp. 636-642.

36. Banerjee, J.R., and Williams, F.W., 1996, "Exact dynamic stiffness matrix for composite Timoshenko beams with applications", *Journal of Sound and Vibration*, Vol. 194, No.4, pp. 573-585.

37. Barbero, E., and Tomblin, J., 1993, "Euler Buckling of Thin-Walled Composite Columns", Thin-Walled Structures, Vol. 17, No. 4, pp. 237-258.

38. Barsoum, R.S. and Gallagher, R.H., 1970, "Finite element analysis of torsional and torsional-flexural stability problems", *International Journal for Numerical Methods in Engineering*, Vol. 2, pp. 335 352.

39. Bauchau, O.A., 1985, "A Beam Theory for Anisotropic Materials," *Journal of Applied Mechanics*, Vol. 52, pp. 416-422.

40. Bercin, A.N., and Tanaka, M., 1997, "Coupled flexural-torsional vibrations of Timoshenko beams", *Journal of Sound and Vibration*, Vol. 207, No. 1, pp. 47-89.

41. Berdichevsky, V., Armanios, E., and Badir, A., 1992, "Theory of anisotropic thin-walled closed-cross-section beams," *Composite Engineering*, Vol. 2, No. 5-7, pp. 411-432.

42. Bhaskar, K., and Librescu, L., 1995, "Buckling under axial compression of thin-walled composite beams exhibiting extension-twist coupling", *Composite Structures*, Vol. 31, pp. 203-212.

43. Bhimaraddi, A., 1987, "Static and transient response of rectangular plates", *Thin-Walled Structures*, Vol. 5, pp. 125-143.

44. Bhimaraddi, A., Carr, A.J., and Moss, P.J., 1989, "A shear deformable finite element for the analysis of general shells of revolution", *Computers and Structures*, Vol. 31, pp. 299-308.

45. Bhimaraddi, A., and Chadrashekhara, K., 1991, "Some observation on the modelling of laminated beams with general layups", *Composite Structures*, Vol. 19, pp. 371-380.

46. Bhimaraddi, A., and Stevens, L.K., 1984, "A higher order theory for free vibration for orthotropic, homogeneous and laminated rectangular plates", *ASME Journal of Applied Mechanics*, Vol. 51, pp. 185-198.

47. Bishop, R.E.D., and Price, W.G., 1977, "Coupled bending and twisting of a Timoshenko beam", *Journal of Sound and Vibration*, Vol. 50, pp. 469-477.

48. Bishop, R.E.D., Cannon, S.M., and Miao, S., 1989, "On coupled bending and torsional vibration of uniform beams", *Journal of Sound and Vibration*, Vol. 131, pp. 457-464.

49. Bisplinghoff, R.L., Ashley, H., and Halfman, R.L., 1955, "Aeroelasticity", *Addison Wesley*, Reading, Massachusetts.

50. Blevins, R.D., 1979, "Formulas for natural frequency and mode shape", *Van Nostrand Reinhold*, New York.

51. Bogdanoff, J.L,. and Goldberg, J.E., 1960, "On the Bernoulli-Euler beam theory with random excitation", *Journal of Aerospace Science*, Vol. 27, pp. 371-376.

52. Bolding, G., 1993, "The application of composites in aerospace", Makromolekulare Chemie-Macromolecular Symposia, Vol. 75, pp. 35-43.

53. Cederbaum, G., Librescu, L., and Elishakoff, I., 1988, "Random vibrations of Laminated plates modelled within higher-order shear deformation theory", *Journal of The Acoustic Society of America*, Vol. 84, No. 2, pp. 660-666.

54. Cederbaum, G., Elishakoff, I., Aboudi, J., and Librescu, L., 1992, "Random vibration and reliability of composite structures, *Technicom Publishing Company*, Lancaster, PA.

55. Cederkvist, J., 1982, "Design of beams subjected to random loads", *Journal of Structural Mechanics*, Vol. 10, pp. 49-65.

56. Cesnik, C.E.S., Hodges, D.H., and Patil, M.J., 1996, "Aeroelastic analysis of composite wings", *Proceedings of AIAA/ASME/ASCE/AHS/ASC 37th Structures, Structural Dynamics and Materials Conference*, Salt Lake City, USA, April, 1996, pp. 1113-1123.

57. Chamis, C.C., 1969, "Buckling of anisotropic plates", *Proceedings of ASCE, Engineering Mechanics Division*, Vol. 95, pp. 2119-2139.

58. Chandra, R., Stemple, A.D., and Chopra, I., 1990, "Thin-walled composite beams under bending, torsional and extensional loads", *AIAA Journal of Aircraft*, Vol. 27, No. 7, pp. 619-626.

59. Chandrashekhara, K., and Bangera, K.M., 1992, "Free vibration of composite beams using a refined shear flexible beam element", *Computer and Structures*, Vol. 43, No. 4, pp. 719-727.

60. Chandrashekhara, K., Krishnamurthy, K., and Roy, S., 1990, "Free vibration of composite beams including rotatory inertia and shear deformation", *Composite*

Structures, Vol. 14, pp. 269-279.

61. Chang, T.P., 1994, "Deterministic and random vibration of an axially loaded Timoshenko beam resting on an elastic foundation", *Journal of Sound and Vibration*, Vol. 178, pp. 55-66.

62. Cleghorn, W.L., Tabarrok, B., 1992, "Finite-element formulation of a tapered Timoshenko beam for free lateral vibration analysis", *Journal of Sound and Vibration*, Vol. 152, No. 3, pp. 461-470.

63. Clough, R.W., and Penzien, J., 1975, "Dynamics of Structures", *McGraw-Hill*, New York.

64. Crandall, S.H., and Zhu, W.Q., 1983 "Random vibration : a survey of recent developments", *Transactions of the American Society of Mechanical Engineers*, Vol. 50, pp. 953-962.

65. Crandall, S.H.(editor), 1958, "Random Vibration, Vol. 1", *The MIT Press*, Cambridge, MA.

66. Crandall, S.H.(editor), 1963, "Random Vibration, Vol. 2", *The MIT Press*, Cambridge, MA.

67. Crandall, S.H. and Mark, W.D., 1963, "Random Vibration in Mechanical System", *Academic Press*, New York.

68. Crandall, S.H., and Yildiz, A., 1962, "Random Vibration of beams", *Transactions of the American Society of Mechanical Engineers, Journal of Applied Mechanics*, Vol. 29, pp. 267-275.

69. Crawley, E.F., 1979, "The Natural Modes of Graphite/Epoxy Cantilever Plates and Shells", *Journal of Composite Material*, Vol. 13, pp. 195-205.

70. Cutlet, J., 1981, "Understanding of Aircraft Structures", *Collins Professional and Technical Books*, London, UK.

71. Dancila, D.S., and Armanios, E.A., 1995, "The influence of coupling on the free vibration of anisotropic thin-walled closed-section beams", *Proceedings of AIAA/ASME/ASCE/AHS /ASC 36th Structures, Structural Dynamics and Materials*

Conference, New Orleans, LA, USA, April 1995, pp 2106-2115.

72. Datoo, M.H., 1991, "Mechanics of Fibrous Composites", *Elsevier Apllied Sience*, London.

73. Davalos, J.F., Qiao, P.Z., and Salim, H.A., 1997, "Flexural-torsional buckling of pultruded fiber reinforced plastic composite I-beams: experimental and analytical evaluations", *Composite Structures*, Vol. 38, No. 1-4, pp. 241-250.

74. Davies, G.A.O., 1987, "Aircraft Structures--Metal or Composite, Aluminium Structures", *Advances, Design and Construction, edited by R. Narayanan, Elsevier Applied Science*, London, pp. 171-184.

75. Dobyns, A.L., 1981, "Analysis of simply-supported orthotropic plated subject to static and dynamic loads", *A1AA Journal*, Vol. 19, No. 5, pp. 642-650.

76. Dokumaci, E., 1987, "An exact solution for coupled bending and torsion vibrations of uniform beams having single cross sectional symmetry", *Journal of Sound and Vibration* Vol. 119, pp. 443 449.

77. Dudek, T.J., 1970, "Young and shear moduli of unidirectional composites by a resonant method", *Journal of Composite Materials*, Vol. 4, pp. 232-241.

78. Echaabi, J., and Trochu, F., 1996, "A methodology to drive the implicit equation of failure criteria for fibrous composite laminates", *Journal of Composite Materials*, Vol. 30, No. 10, pp. 1088-1114.

79. Eggenschwyler, A., and Maillart, R.S., 1926, "Bauzeitung", *Proceedings of the 2nd International Congress Applied Mechanics*, Zurich, p. 434.

80. Elishakoff, I., 1983, "Probabilistic methods in the theory of structures", *Wiley-Interscience*, New York.

81. Elishakoff, I., 1977, "Random vibrations of orthotropic plats clamped or simply-supported all round", *Acta Mechanica*, Vol. 28, pp. 165-176.

82. Elishakoff, I. and D. Livshits, 1984, "Some closed form solutions in random vibration of Bernoulli-Euler beams," *Journal of Engineering Science*, Vol. 22, pp. 1291-1302.

83. Elishakoff, I., and Livshits, D., 1989, "Some closed form solutions in random vibration of Bresse-Timoshenko beams", *Probabilistic Engineering Mechanics*, Vol. 4, pp. 49-54.

84. Engelbrecht, A.E., 1951, "Coupled free vibration of a swept wing", *Journal of Aeronautical Science*, Vol. 18, pp. 329-338.

85. Eringen, A.C., 1957, "Response of beams and plates to random loads", *Transactions of the American Society of Mechanical Engineers, Journal of Applied Mechanics*, Vol. 24, pp. 46-52.

86. Eslimy-Isfahany, S.H.R., and Banerjee, J.R., 1995, "Response of an Axially Loaded Bending-Torsion Coupled Beam to Deterministic and Random Loads", *Proceedings of AIAA/ASME/ASCE/AHS/ASC 36th Structures, Structural Dynamics and Materials Conference*, New Orleans, LA, USA, April 1995, pp 2523-2533.

87. Eslimy-Isfahany, S.H.R., and Banerjee, J.R., 1996(a), "Response of Composite Beams to Deterministic and Random Loads, *Proceedings of AIAA/ASME/ASCE/AHS/ASC 37th Structures, Structural Dynamics and Materials Conference*, Salt Lake City, USA, April, 1996, pp. 813-821.

88. Eslimy-Isfahany, S.H.R., and Banerjee, J.R., 1996(b), "Dynamic response of an axially loaded bending-torsion coupled beam", *AIAA Journal of Aircraft*, May-June 1996, Vol. 33, No. 3, pp. 601-607.

89. Eslimy-Isfahany, S.H.R., and Banerjee, J.R., 1997(a), "Effects of shear deformation and rotatory inertia on the response of a composite aircraft wing to random atmospheric turbulence", *Proceedings of the First Annual Conference of Aeronautical Engineers*, Tehran, Iran, January, 1997, pp. 620-632.

90. Eslimy-Isfahany, S.H.R., and Banerjee, J.R., 1997(b), "Deterministic and random response of an axially loaded composite Timoshenko beam", *Proceedings of AIAA/ASME/ASCE/AHS/ ASC 38th Structures, Structural Dynamics, and Materials Conference*, April 1997, Kissimmee, FL, USA, pp. 511-520.

91. Eslimy-Isfahany, S.H.R., and Banerjee, J.R., 1997(c), "Dynamic response of composite beams with application to aircraft wings", *AIAA Journal of Aircraft*,

November-December 1997, Vol. 34, No. 6, pp. 785-791.

92. Eslimy-Isfahany, S.H.R., and Banerjee, J.R., 1998(a), "Dynamic Stresses in Composite Timoshenko Beams with Application to Aircraft Wings", *Proceedings of AIAA/ASME/ ASCE/AHS/ASC 39th Structures, Structural Dynamics and Materials Conference*, Long Beach, CA, USA, April 1998, pp. 3201-3211.

93. Eslimy-Isfahany, S.H.R., and Banerjee, J.R., 1998(b), "Effects of axial load on dynamic stresses in composite wings subjected to random excitation", *Proceedings of the Second Annual Conference of Aeronautical Engineers*, Shahinshahr, Isfahan, Iran, October, 1998.

94. Eslimy-Isfahany, S.H.R., and Banerjee, J.R., 1999, "Theoretical and Experimental Investigations into Buckling of Composite Columns", *Proceedings of AIAA/ASME/ASCE/ AHS/ASC 40th Structures, Structural Dynamics and Materials Conference*, St. Louis, MO , USA, April 1999, accepted for publication.

95. Eslimy-Isfahany, S.H.R., and Banerjee, J.R., "Closed form solution for the response of a simply supported bending-torsion coupled beam to deterministic and random loads", *in progress*.

96. Eslimy-Isfahany, S.H.R., and Banerjee, J.R., "Response of an axially loaded bending-torsion coupled Timoshenko beam to deterministic and random loads", *in progress*.

97. Eslimy-Isfahany, S.H.R., and Banerjee, J.R., "Review of the development of free and forced vibration of beams", *in progress*.

98. Eslimy-Isfahany, S.H.R., and Banerjee, J.R., "Significance of modal interchange and generalised mass in each mode of vibration on response characteristics of a vibrating bending-torsion coupled beam", *in progress*.

99. Eslimy-Isfahany, S.H.R, Banerjee, J.R., and Sobey, A.J., 1996, "Response of a bending-torsion coupled beam to deterministic and random loads," *Journal of Sound and Vibration*, Vol. 195, No. 2, pp. 267-283.

100. Eslimy-Isfahany, S.H.R., Sadatpour, M.M., and Vafaeian, M., 1993, "Application of Winckler theorem in analysis of tunnel supports using finite element method (in Persian), *Esteghlal*, September 1993, No. 13, pp. 113-128.

101. Etkin, B., 1972, "Dynamics of atmospheric flight", *John Wiley & Sons*, New York.

102. Farghaly, S.H., Gadelrab, R.M., 1995, "Free-vibration of a stepped composite Timoshenko cantilever beam", *Journal of Sound and Vibration*, Vol. 187, No. 5, pp. 886-896.

103. Fisher, H.R., 1934, "An extension of Southwell's method of analysing experimental observations in problems of elastic stability", *Proceedings of the Royal Society London* (A), Vol. 144, pp. 609-630.

104. Fitch, J., 1985, "Solving algebraic problems with REDUCE", *Journal of Symbolic Computation*, Vol. 1, pp. 211-227.

105. Friberg, P.O., 1983, "Coupled vibration of beams - An exact dynamic element stiffness matrix", *International Journal for Numerical Methods in Engineering*, Vol. 19, pp. 479-493.

106. Friberg, P.O., 1985, "Beam element matrices derived from Vlasov's theory of open thin-walled elastic beams", *International Journal for Numerical Methods in Engineering*, Vol. 21, pp. 1205-1228.

107. Fukunaga, H., and Vanderplatts, G.N., 1991, "Stiffness optimisation of orthotropic laminated composites using lamination parameters", *AIAA Journal*, Vol. 29, No. 4, pp. 641-646.

108. Fung, Y.C., 1955, "An introduction to the theory of aeroelasticity", *Dover publication*, New York, 1969 revised publication.

109. Georghiades, G.A., 1997, "Aeroelastic behaviour of composite beams", *PhD thesis*, City University, London, UK.

110. Gere, J.M. and Timoshenko, S.P. , 1991, "Mechanics of materials", *Chapman and Hall*, 3rd SI edition, London.

111. Gerhard, C.S., Gurdal, Z., and Kapania, R.K., 1994, "Finite element analysis of geodesically stiffened cylindrical composite shells using a layerwise theory", *CCMS 9408*, Centre for Composite Materials and Structures, Virginia Polytechnic Institute and State University.

112. Goland, M., 1945, "Flutter of a uniform cantilever wing", *Journal of Applied Mechanics*, Vol. 12, pp. 197-208.

113. Goland, M. and Luke, Y.L., 1948, "The flutter of a uniform wing with tip weights," *Journal of Applied Mechanics*, Vol. 15, pp. 13-20.

114. Goodier, J.N., 1942, "Torsional and flexural buckling of thin-walled open section under compressive and bending loads", *Journal of Applied Mechanics*, Vol. 9, pp. A103-A107.

115. Green, J. A., 1987, "Aeroelastic tailoring of swept high aspect ratio composite wings", *Journal of Aircraft*, Vol. 24, pp. 812-819.

116. Gregory, M.S., 1967, "Elastic instability" *E. & F.N. SPON limited*, London, UK.

117. Grenestedt, J.L., 1989(a), "A study on the effect of bending twisting coupling on buckling strength", *Composite Structures*, Vol. 12 , pp. 271-290.

118. Grenestedt, J.L., 1989(b), "Layup optimization and sensitivity analysis of the fundamental eigenfrequency of composite plates", *Composite Structures*, Vol. 12, pp. 193-209.

119. Grenestedt, J.L., 1990, "Composite plate optimization only requires one parameter", *Structural Optimization*, Vol. 2, pp. 29-37.

120. Grenestedt, J.L., 1991, "Layup optimization against buckling of shear panels," *Structural Optimization*, Vol. 3, pp. 115-120.

121. Grenestedt, J.L., 1992, "Layup optimization of composite structures", *PhD thesis*, Royal Institute of Technology, Department of Light Weight Structures, Stockholm, Sweden.

122. Grenestedt, J.L., 1994, "Lamination parameters for reissner - mindlin plates", *AIAA Journal*, Vol. 32, pp. 2328-2331.

123. Haftka, R.T., and Gurdal, Z., 1992, "Elements of structural optimization", 3rd Revised and Expanded Edition, *Kluwer Academic Publishers*, Boston.

124. Hajela, P., and Shih, C. J., 1989, "Optimal design of laminated composites using a

modified mixed integer and discrete programming algorithm", *Computers and Structures*, Vol. 32, No. 1, pp. 213-221.

125. Hallauer, W.L., and Lu, R.Y.L., 1982, "Beam bending torsion dynamic stiffness method for calculation of exact vibration modes", *Journal of Sound and Vibration*, Vol. 85, pp. 105-113.

126. Henrych, J., 1981, "The dynamics of arches and frames", Elsevier Science, New York.

127. Hirano, Y., 1980, "Stability optimisation of laminated composites plates", *NASA-CR-163456*, July.

128. Hodges, D.H., Atilgan, A.R., Fulton, M.V., and Rehfield, L.W., 1991, "Free vibration analysis of composite beams", *Journal of American Helicopter Society*, Vol. 36, No. 3, pp. 23-35.

129. Hodges, D.H. and Dowell, E.H., 1974, "Nonlinear equations of motions for the elastic bending and torsion of twisted nonuniform blades", *NASA-TN-D 7818*, December.

130. Hodges, D.H., Nixon, M.W., and Rehfield, L.W., 1987, "Comparison of composite rotor blade models: A coupled beam analysis and an MSC/NASTRAN finite element model, " *NASA-TM-89024*.

131. Hoff, N.J. and Goodier, J.N., 1943, "Torsional and flexural buckling of thin-walled open section under compressive and bending loads", *Journal of Applied Mechanics*, Vol. 10, pp. A110-A111.

132. Hong, C.H., and Chopra, I., 1985, "Aeroelastic stability analysis of a composite rotor blade," *Journal of the American Helicopter Society*, Vol. 30, No. 2, pp. 57-67.

133. Hong, C.H., and Chopra, I., 1986, "Aeroelastic stability analysis of a composite bearingless rotor blade," *Journal of the American Helicopter Society*, Vol. 31, No. 4, pp. 29-35.

134. Horgan, C.O., and Simmonds, J.G., 1994, "Saint-Venant end effects in composite structures", *Composites Engineering*, Vol. 4, No. 3, pp. 279-286.

135. Houbolt, J.C., Steiner, R., and Pratt, K.G., 1964, "Dynamic response of airplanes to

atmospheric turbulence including flight data on input response", *NASA-TR-R-199.*

136. Housner, J.M. and Stein, *M., 1974, "Flutter analysis* of swept-wing subsonic aircraft with parameters studies of composite wings", *NASA TN D-7539*, September *1979.*

137. Howson, W.P., Banerjee, J.R., and Williams, F.W., 1983, "Concise equations and program for exact eigensolutions of plane frames including member shear", Advance Engineering Software, Vol. 5, No. 3, pp. 137-141.

138. *Humar, J.L., 1990,* "Dynamics of structures", *Prentice Hall*, New Jersey.

139. Hurty, W.C. and Rubinstein, M.E. , 1964, "Dynamics of structures", *Prentice Hall,* Englewood Cliffs, New Jersey.

140. Ishikawa, T., Matsushima, M., and Hayashi, Y., 1993, "Improved correlation of predicted and experimental initial buckling stresses of composite stiffened panels", *Composite Structures*, Vol. 26, No. 1-2, pp. 25-38.

141. Jaunky, N., Knight, N.F., and Ambur, D., 1995(a), "Buckling analysis of general triangular anisotropic plates using polynomials", *AIAA Journal*, Vol. 33, No. 12, pp. 2414-2417.

142. Jaunky, N., Knight, N.F., and Ambur, D., 1995(b), "Buckling of arbitrary quadrilateral anisotropic plates", *AIAA Journal*, Vol. 33, No. 5 , pp. 938-944.

143. Jaunky, N., 1997, Private Communication.

144. Jensen, D.W., and Crawley, E.F., 1984, "Frequency determination techniques for cantilevered plates with bending torsion coupling", *AIAA Journal*, Vol. 22, pp. 415-420.

145. Jensen, D.W., Crawley, E.F., and Dugundji, J., 1982, "Vibration of cantilevered graphite/epoxy plates with bending-torsion coupling", *Journal of Reinforced Plastics and Composites*, Vol. 1, July 1982, pp. 254-269.

146. Johnson, D.C., and Bishop, R.E.D., 1960, "The mechanics of vibrations", *Cambridge University Press*, Cambridge, UK.

147. Jones, R.M., 1975, "Mechanics of composite materials", *McGraw-Hill*, New York.

148. Kant, T., and Manjunatha, B.S., 1992, "On accurate estimation of transverse stresses in multi-layer laminates", *Computers and Structures*, Vol. 50, No. 3, pp. 351-365.

149. Kapania, R. K., and Raciti, 1989, "Recent Advances in Analysis of Laminated Beams and Plates Part I: Shear Effects and Buckling", *AIAA Journal*, Vol. 27, No. 7, pp. *923-934.*

150. Khadeir, A.A., and Reddy, J.N., 1988, "Dynamic. response *of antisymmetric angle-*ply laminated plates subjected to arbitrary loading", *Journal of Sound and Vibration*, Vol. 126, No. 3, pp. 347-445.

151. Khadeir, A.A., and Reddy, J.N., 1989, "Exact solutions for the transient response of symmetric cross-ply laminates using a higher-order plate theory", *Composite Science and Technology*, Vol. 36, pp. 205-224.

152. Khadeir, A.A. and Reddy, J.N., 1997, "Buckling of cross-ply laminated beams with arbitrary boundary conditions", *Composite Structures*, Vol. 37, No. 1, pp. 1-3.

153. Khan, J.Z., 1993, "Static, dynamic and aeroelastic behaviour of thin-walled composite structures with application to aircraft wings", *PhD thesis*, City University, London, UK.

154. Kolousek, V., 1973, "Dynamics in Engineering Structures", *Butter worths*, London, UK.

155. Kosmatka, J. B., 1986, "Structural dynamic modelling of advanced composite propellers by the finite element method", *Ph.D. Dissertation*, University of California, Los Angeles.

156. Kosmatka, J.B., 1991, "Extension bend twist coupling behaviour of thin walled advanced composite beams with initial twist," *Proceedings of the 32nd AIAA/ASME/ASCE/ AHS/ ASC Structures, Structural Dynamics and Materials Conference*, AIM Paper 91-1023, pp.1037-1049.

157. Krishna Murty, A.V., 1970, "Vibration of short beams", *A1AA Journal*, Vol. 8, pp. 34-38.

158. Krishna Murty, A.V., 1977, "Higher order theory for vibration of thick plates", *A1AA*

Journal, Vol. 15, pp. 1823-1824.

159. Krishna Murty, A.V., and Shimpi, R.P., 1974, "Vibrations of laminated beams", *Journal of Sound and Vibration*, Vol. 36, No. 2, pp. 273-284.

160. Kulkarni, A.M., Banerjee, J.R. and Sinha, P.K., 1975, "Response of excited orthotropic sandwich plates", *Journal of Sound and Vibration*, Vol. 41, No. 2., pp. 197-205.

161. Lee, S.Y., Lin, S.M., 1992, "Free vibrations of elastically restrained non-uniform plates", *Journal of Sound and Vibration*, Vol. 158, No. 1, pp. 121-131

162. Lenoe, E.M., Oplinger, D.W., and Burke, J.J., 1980, "Fibrous composites in structural design", *Plenum Press*, New York.

163. Leung, A.Y.T., 1985, "Dynamic stiffness method for exponentially varying harmonic excitation of continuous systems", *Journal of Sound and Vibration*, Vol. 98, No. 3, pp. 337-347.

164. Leung, A.Y.T., 1988, "Direct method for the steady-state response of structures", *Journal of Sound and Vibration*, Vol. 124, No. 1, pp. 135-139.

165. Leung, A.Y.T., 1992(a), "Dynamic stiffness analysis of thin-walled structures", *Thin-Walled Structures*, Vol. 14, No. 3, pp. 209-222.

166. Leung, A.Y.T., 1992(b), "Dynamic stiffness for lateral buckling", *Computers and Structures*, Vol. 42, No. 3, pp. 321-325.

167. Leung, A.Y.T., 1993(a), "Non-conservative dynamic stiffness analysis of axial lateral buckling", *Journal of Sound and Vibration*, Vol. 165, No. 3, pp. 553-561.

168. Leung, A.Y.T., 1993(b), "Non-conservative dynamic stiffness analysis of thin-walled structures", *Computers and Structures*, Vol. 48, No. 4, pp. 703-709.

169. Leung, A.Y.T., and Zeng, S.P., 1994, "Analytical formulation of dynamic stiffness", *Journal of Sound and Vibration*, Vol. 177, No. 4, pp. 555-564.

170. Leung, A.Y.T., and Zhou, W.E., 1995(a), "Dynamic stiffness analysis of axially loaded non-uniform Timoshenko columns", *Computers and Structures*, Vol. 56, No.

4, pp. 577-588.

171. Leung, A.Y.T., and Zhou, W.E., 1995(b), "Dynamic stiffness analysis of non-uniform Timoshenko beams", *Journal of Sound and Vibration*, Vol. 181, No. 3, pp. 447-456.

172. Levinson, M., 1980, "An accurate simple theory of the statics and dynamics of elastic plates", *Mechanics Research Communications*, Vol. 7, pp. 343-350.

173. Levinson, M., 1981, "A new rectangular beam theory", *Journal of Sound and Vibration*, Vol. 74, pp. 81-87.

174. Libove, C., 1988, "Stresses and Rate of Twist in Single cell Thin walled Beams with Anisotropic Walls", *AIAA Journal*, Vol. 26, No. 9, September, 1988.

175. Librescu, L., Khdeir, A.A., and Reddy, J.N., 1987, "A comprehensive analysis of state of stress of elastic anisotropic flat plates using refined theories", Acta Mechanica, Vol. 70, pp. 57-81.

176. Librescu, L., Meirovitch, L., and Song, O., 1996, "Refined structural modelling for enhancing vibrational and aeroelastic characteristics of composite aircraft wings", *La Recherche Aerospatiale*, No. 1, pp. 23-35.

177. Lin, K, 1967, "Probabilistic theory of structural dynamics", *McGraw-Hill*, New York.

178. Loaring, S.J., 1944, "Use of generalised coordinates in flutter analysis", *SAE Journal*, Vol. 52, No. 4, pp. 113-132.

179. Lunden, R., and B., Akesson, 1983, "Damped second-order Rayleigh-Timoshenko beam vibration in space-an exact complex dynamic member stiffness matrix", *International Journal for Numerical Methods in Engineering*, Vol. 19, pp. 431-499.

180. Maiti, D.K., and Sinha, P.K., 1995, "Impact behavior of thick laminated composite beams", *Journal of Reinforced Plastics and Composites*, Vol. 14, No. 3, pp. 255-279.

181. Mallikarjuna, A., and Kant, T., 1988, "Dynamics of laminated composite plates with a higher order theory and finite element discretization", *Journal of Sound and Vibration*, Vol. 126, No. 3, pp. 463-475.

182. Mallows, C.L., 1987, "Design, data and analysis", *John Wiley and Sons*, New York.

183. Manevich, A.I., 1990, "Weight optimisation of a longitudinally compressed panel with T-shape stiffeners", *Prikladnaya Mekhanika*, Vol. 26, No. 2, pp. 82-88.

184. Manjunatha, B.S., and Kant, T., 1993, "Different numerical techniques for the estimation of multi-axial stresses in symmetric/unsymmetric composite and sandwich beams with refined theories", *Journal of Reinforced Plastic and Composites*, Vol. 12, 2-37.

185. Mansfield, E. H., 1981, "The Stiffness of a Two Cell Anisotropic Tube", *Aeronautical Quarterly*, Vol. 32, pp. 338-353.

186. Mansfield, E.H. and Sobey, A.J., 1979, "The fibre composite helicopter blade, Part 1: Stiffness properties, Part 2: Prospects for aeroelastic tailoring," *Aeronautical Quarterly*, May 1979, pp. 413-449.

187. Mei, C., 1970, "Coupled torsion vibrations of thin walled beams of open section using the finite element method international", *Journal of Mechanical Science*, Vol. 12, pp.883-891.

188. Mei, C., and Wentz, K.R., 1982, "Large-amplitude random response of angle ply laminated composite plates", *AIAA Journal*, Vol. 20, No. 10, pp. 1450-1458.

189. Miki, M., 1986, "Optimum design of fibrous laminated composite plates subject to axial compression", *Proceedings, 3rd Japan US Composite Materials Conference*, Tokyo, Technomic Publishing Co., Lancaster, pp. 673-680.

190. Miller, A.K., and Adams, D.F., 1975, "An analytic means of determining the flexural and torsional resonant frequencies of generally orthotropic beams", *Journal of Sound and Vibration*, Vol. 41, No. 2, pp. 433-449.

191. Mindlin, R.D, 1951, "Influence of rotatory inertia and shear deformation on flexural motions of isotropic elastic plates", *ASME Journal of Applied Mechanics*, Vol. 18, pp. A31-A38.

192. Minguet, P., and Dugundji, J., 1990, "Experiments and analysis for composite blades under large deflection, Part I: Static behaviour, Part II: Dynamic behaviour", *AIAA*

Journal, Vol. 28, No. 9, pp. 1573-1588.

193. Miravete, A., 1990, "Strain and stress analysis in tapered laminated composite structures", *Composite Structures*, Vol. 16, No. 1-3, pp. 65-84.

194. Morey, T.A., Johnson, E., and Shield, C.K., 1998, "A simple beam theory for the buckling of symmetric composite beams including interaction of in-plane stresses", *Composite Science and Technology*, Vol. 58, No. 8, pp. 1321-1333.

195. Nagem, R., 1991, "Random vibration of point driven beams", *Journal of Sound and Vibration*, Vol. 151, pp. 168-174.

196. Nagendra, S., Haftka, R.T., and Gurdal, Z., 1992, "Stacking sequence optimisation of simply supported laminates with stability and strain constraints", *AIAA Journal*, Vol.30, No.8, pp. 2132-2137.

197. Nagendra, S., and Kapania, R.K., 1995, "Recent advances in stability analysis of stiffened and laminated structures", International Conference on Stability of Structures-ICSS 95, June 7-9, PSG College of Technology, Coimbatore, India, pp.151-166.

198. Nemeth, M.P., 1986, "Importance of anisotropy on buckling of compression loaded symmetric composite plates", *AIAA Journal*, Vol. 24, pp. 1831-1835.

199. Newland, D.E., 1984, "An introduction to random vibration and spectral analysis", *Longmans*, London.

200. Nixon, M. W., 1987, "Extension twist coupling of composite circular tubes and application to tilt rotor blade design", *Proceedings of the 28th AIAA/ASME/ASCE/AHS/ ASC Structures, Structural Dynamics and Materials Conference*, AIM Paper 87-0772, pp. 295-303.

201. Noor, A.K., Mathers, M.D., 1976, "Anisotropy and shear deformation in laminated composite plates", *AIAA Journal*, Vol. 14, pp. 282-285.

202. Noor, A.K., Mathers, M.D., Anderson, M.S., 1977, "Exploiting symmetries for efficient postbuckling analysis of composite plates", *AIAA Journal*, Vol. 15, pp. 24-32.

203. Pearson, D., Wittrick, W.H., 1986, "An exact solution for the vibration of helical springs using a Bernoulli-Euler model", *International Journal of Mechanical Sciences*, Vol. 28, No. 2, pp. 83-96.

204. Pedersen, P.T., 1991, "Beam theories for torsional-bending response of ship hulls", *Journal of Ship Research*, Vol. 35, No. 3, September 1991, pp. 254-265.

205. Pekoz, T.B. and Winter, G., 1969, "Torsional-flexural buckling of thin-walled sections under eccentric load", *Journal of Structural Division*, ASCE, Vol. 95, pp. 941-963.

206. Penny, R.K., 1974, "The experimental method", *Introductory Engineering series*, Longman Group Limited, London.

207. Perry, B., Pototzky, A.S. and Woods, J.S., 1990, "NASA Investigation of a claimed overlap between two gust *response* analysis methods", *AIAA Journal of Aircraft*, Vol. 27, pp. 605-611.

208. Petersen, H., 1979, "Some data for the 12-m long wind turbine blade manufactured by VØLUND A/S and O.L. Boats, Denmark", *RISØ-M-2194*, National library, Denmark.

209. Piszczek, K. and J. Niziol, 1986, "Random vibration of mechanical systems", *John Wiley and Sons*, New York.

210. Popov, E.P., 1976, "Mechanics of materials", 2nd edition, *Prentice-Hall*, Englewood Cliffs, London.

211. Qian, G.L., Hoa, S.V., and Xiao, X.R., 1997, "A vibration method for measuring mechanical properties of composite, theory and experiment", *Composite Structures*, Vol. 39, No. 1-2, pp. 31-38.

212. Rao, J.S. and Carnegie, W., 1970, "Solution of the equations of motion of coupled bending of turbine blades by the method of Ritz-Galerkin", *International Journal of Mechanical Sciences*, Vol. 12, pp. 875-882.

213. Rao., S.R., Ganesan, N., 1995, "Dynamic response of tapered composite beams using higher-order shear deformation-theory", *Journal of Sound and Vibration*, Vol. 187,

No. 5, pp.737-756.

214. Rao., S.R., Ganesan, N., 1997, "Dynamic response of non-uniform composite beams", *Journal of Sound and Vibration*, Vol. 200, No. 5, pp. 563-577.

215. Rayna, G., 1986, "REDUCE Software for algebric computation", *Springer*, New York.

216. Rayleigh (Lord), 1977, "Theory of sound (2 vols.)", Second edition, 1945 re-issue, *Dover Publications*, New York.

217. Reddy, J.N, 1982, "On the solutions of forced. motions of rectangular composite plates", *ASME Journal of Applied Mechanics*, Vol. 49, pp. 403-408.

218. Reddy, J.N, 1984, "A simple higher-order theory for laminated composite plates", *ASME Journal of Applied Mechanics*, Vol. 51, pp. 745-752.

219. Rehfield, L. W., 1985, "Design analysis methodology for composite rotor blades", *AFWAL-TR-85-3094*, June 1985, pp. 1-15.

220. Rehfield, L.W., and Atilgan, A.R., 1987, "A structural theory for composite rotor blades and lifting surfaces", *Proceedings of the 28th AIAA/ASME/ASCE/AHS/ ASC Structures, Structural Dynamics and Materials Conference*, AIAA paper 87-0769.

221. Rehfield, L.W., and Atilgan, A.R., 1988, "Structural modelling for multicell composite rotor blades", *Proceedings of the 29th AIAA/ASME/ASCE/AHS/ASC Structures, Structural Dynamics and Materials Conference*, AIAA paper 88-2250.

222. Rehfield, L.W., and Atilgan, A.R., 1989, "On the buckling behaviour of thin-walled laminated composite open section beams", *Proceedings of the 30th AIAA/ASME/ASCE/ AHS/ASC Structures, Structural Dynamics and Materials Conference*, AIAA paper 89-1171.

223. Rehfield, L.W., Atilgan, A.R., and Hodges, D.H., 1990, "Non-classical behaviour of thin-walled composite beams with closed cross-sections", *Journal of the American Helicopter Society*, Vol. 35, No. 2, pp. 42-50.

224. Reissner, E., and Tsai, W.T., 1972, "Pure bending, stretching, and twisting of anisotropic cylindrical shells," *Journal of Applied Mechanics*, Vol. 39, pp.148 154.

225. Renton, J.D., 1960, "A direct solution of the torsional-flexural buckling of axially loaded thin-walled bars", *The Structural Engineer*, Vol. 38, pp. 273-276.

226. Renton, J.D., 1962, "Stability of space frames by computer analysis", *Journal of Structural Division*, ASCE, Vol. 88, pp. 81-103.

227. Roberts, J.B., and Bishop, R.E.D., 1965, "A simple illustration of spectral density analysis", *Journal of Sound and Vibration*, Vol. 2, No. 1, pp. 37-41.

228. Robson, J.D., 1963, "An introduction to random vibration", *The University Press*, Edinburgh.

229. Rossi, R.E., Laura, P.A.A., Maurizi, M.J., 1992, "Numerical experiments on the effect of the value of the shear coefficient upon the natural frequencies of a Timoshenko beam", *Journal of Sound and Vibration*, Vol. 154, No. 2, pp. 374-379

230. Salkind, M.J., and Holister, G.S., 1973, "Applications of composite materials", *ASTM Publication-524*, Philadelphia, USA.

231. Samuels, J.C. and A.C. Eringen, 1958, "Response of simply supported Timoshenko beam to a purely random Gaussian process," *Transactions of the American Society of Mechanical Engineers, Journal of Applied Mechanics*, Vol. 25, pp. 496-500.

232. Savoia, M., and Reddy, J.N., 1994, "Post-buckling behaviour of stiffened cross-ply cylindrical shells", *Journal of Applied Mechanics*, ASMÆ, Vol. 61, pp. 998-1000.

233. Sheinman, I., 1987, "Non-linear equations of laminated panels with laminated stiffeners", *Composite Structures*, Vol. 8, pp. 287-292.

234. Sheinman, I., 1989, "Cylindrical buckling load of laminated columns", *Journal of Engineering Mechanics*, Vol. 115, pp. 659-661.

235. Shen, H.S., and Williams, F.W., 1993, "Post-buckling analysis of laminated stiffeners", *Computers and Structures*, Vol. 48, pp. 1117-1123.

236. Sherbourne, A.N., and Pande, M.D., 1991, "Differential quadrature method in buckling analysis of beams and composite plates", *Computers and Structures*, Vol. 40, pp.903-913.

237. Shield, C.K., and Morey, T.A., 1997, "Kinematic theory for buckling of open and closed section thin-walled composite beams", Journal of Engineering Mechanics-ASCE, Vol. 123, No. 10, pp. 1070-1081.

238. Shin, D.K, Gurdal, Z., and Griffin, O.H., 1990, "A penalty approach for nonlinear optimisation with discrete design variables", *Engineering Optimisation*, Vol.16, pp.29-42.

239. Shin, P.Y., 1991, "Optimal design of stiffened laminated plates using a homotopy method", *AIAA Paper No. 91-0963, 32nd AIAA/ASME/ASCE/AHS/ASC Structures, Structural Dynamics and Materials Conference*, Baltimore, MD, April 8-10, Vol. 2, pp. 1627-1636.

240. Singh, M.P. and A.S. Abdelnaser, 1990, "Random vibration of Timoshenko beams with generalized boundary conditions", *Second International Conference on Stochastic and Structural Dynamics*, May 10-12, Boba Raton, Florida, USA.

241. Singh, M.P. and A.S. Abdelnaser, 1992, "Random response of symmetric cross-ply composite beams with arbitrary boundary conditions", *AIAA Journal*, Vol. 30, No. 4, pp. 1081-1088.

242. Singh, M.P. and A.S. Abdelnaser, 1993, "Random vibration of externally damped viscoelastic Timoshenko beams with general boundary conditions", *The American Society of Mechanical Engineers, Journal of Applied Mechanics*, Vol. 60, pp. 149-156.

243. Smith, E.C., and Chopra, I., 1991, "Formulation and evaluation of an analytical model for composite box beams," *Journal of the American Helicopter Society*, Vol. 36, pp. 23-35.

244. Song, O., and Librescu, L., 1997, "Structural modelling and free vibration analysis of rotating composite thin-walled beams", *Journal of the American Helicopter Society*, Vol. 42, No. 4, pp.358-369.

245. Song, S.J. and Waas, A.M., 1997, "Effects of shear deformation on buckling and free vibration of laminated composite beams", *Composite Structures*, Vol. 37, No. 1, pp.33-43.

246. Southwell, R.V., 1932, "On the analysis of experimental observations in problem of elastic stability", *Proceedings of the Royal Society*, London (A), Vol. 135, pp. 601-616.

247. Southwell, R. V., 1941, "An introduction to the theory of elasticity", 2nd edition, *Oxford University Press*, New York.

248. Spiegel, M.R., 1968, "Mathematical handbook", Schaum's Outline Series, *McGraw-Hill Book Company*, New York.

249. Sridharan, S., and Peng, M.H., 1989, "Performance of axially compressed stiffened panels", *International Journal of Solids and Structures*, Vol. 25, No. 8, pp. 879-899.

250. Stacey, J.A., 1976, "The development of a finite element aeroelastic calculation package and its application to the cranfield aerobatic aircraft Al", *M.Sc. Thesis*, College of Aeronautics, Cranfield Institute of Technology.

251. Stein, M., and Jegley, D.C., 1985, "Effects of transverse shearing on cylindrical bending, vibration, and buckling of laminated plates", *AIAA Paper* 85-0744, April 1985.

252. Stemple, A.D., and Lee, S.W., 1988, "A finite element model for composite beams with arbitrary cross sectional warping", *AIAA Journal*, Vol. 26, pp. 1512-1520.

253. Stemple, A.D., and Lee, S.W., 1989, "A finite element modelling for composite beams undergoing large deflections with arbitrary cross sectional warping", *International Journal of Numerical Methods in Engineering*, Vol. 28, pp. 2143-2163.

254. Sun, C.T., and Chattopadhyay, S., 1975, "Dynamic response of anisotropic laminated plates under initial stress to impact of a mass", *ASME Journal of Applied Mechanics*, Vol. 42, pp. 693-698.

255. Sun, C.T., and Whitney, J.M., 1976, "Dynamic response of laminated composite plates under initial stress", *AIAA Journal*, Vol. 14, No. 2, pp. 268-270.

256. Sun, C.T., and Whitney, J.M., 1974, "Forced vibrations of laminated composite plates in cylindrical bending", *Journal of The Acoustical Society of America*, Vol. 55, No. 5,

pp. 1003-1008.

257. Sundarajan, C., and Reddy, D.V., 1973, "Response of rectangular orthotropic plates to random excitations", *Earthquake Engineering and Structural Dynamics*, Vol. 2, pp. 161-170.

258. Suresh, J.K., Venkatesan, C., and Ramamurti, V., 1990, "Structural dynamic analysis of composite beams," *Journal of Sound and Vibration*, Vol. 143, No. 3, pp. 503-519.

259. Suresh, R., Malhotra, S.K., 1997, "Some studies on static analysis of composite thin-walled box beam", *Computers and Structures*, Vol. 62, No. 4, pp. 625-634.

260. Tan, D.Y., 1994, "Discrete analysis method for random vibration of structures subjected to temporally and spatially correlated coloured excitations", *Computers and structures*, Vol. 43, pp. 1051-1056.

261. Tan, D.Y., Yang, Q.S., and Zhao, C., 1992, "Discrete analysis method for random vibration of structures subjected to spatially correlated filtered white noises", *Computers and structures*, Vol. 43, pp. 1051-1056.

262. Teboub, Y. and Hajela, P., 1995, "Free vibration of generally layered composite beams using symbolic computations," *Composite structures*, Vol. 33, No. 3, pp. 123-134.

263. Teh, K.K., and Huang, C.C., 1979, "The vibrations of generally orthotropic beams, a finite element approach", *Journal of Sound and Vibration*, Vol. 62, pp. 195-206.

264. Teoh, L.S., and Huang, C.C., 1977, "The vibration of beams of fibre reinforced material", *Journal of Sound and Vibration*, Vol. 51, pp. 467-473.

265. Thangjitham, S., and Librescu, L, 1991, "Vibration characteristics of anisotropic composite wing structures," *Proceedings of the 32nd AIAA/ASME/ASCE/ AHS/ASC Structures, Structural Dynamics and Materials Conference*, AIM Paper 91-1185, pp. 2115-2122.

266. Thomson, W.T., 1988, "Theory of vibration with applications", 3rd edition, *Prentice Hall*, London, UK.

267. Timoshenko, S.P., 1921, "On the correction for shear of the differential equation for

transverse vibration of prismatic bars", London Phil. Mag., Vol. 6, pp. 41-44.

268. Timoshenko, S.P., 1945, "Theory of bending, torsion and buckling of thin-walled members of open cross-sections", *Journal of Franklin Institute*, Vol. 239, pp. 201-219, pp. 249-268, pp.343-361.

269. Timoshenko, S.P. and Gere, J.M., 1961, "Theory of elastic stability", 2nd edition, *McGraw-Hill*, London.

270. Timoshenko, S.P. and Young, D.H., 1955,. "Vibration problems in engineering", *Van Nostrand*, third edition, New York,

271. To, C.W.S., 1979, "Higher order taper beam finite elements for vibration analysis", *Journal of Sound and Vibration*, Vol. 63, pp. 33-50.

272. To, C.W.S., 1981, "A linearly tapered beam finite element incorporating shear deformation and rotatory inertia for vibration analysis ", *Journal of Sound and Vibration*, Vol. 78, pp. 475-484.

273. Tomblin, J. S., 1991, "A universal design equation for pultruded composite columns", *PhD. Thesis*, Mechanical and Aerospace Engineering, West Virginia University, Morgantown, WV.

274. Tripathy, A.K., Patel, H.J., and Pang, S.S., 1994, "Bending analysis of laminated composite box beams", *Journal of Engineering Materials and Technology-Transactions of the ASME*, Vol. 116, No. 1, pp. 121-129.

275. Tsai, S.W. and Hahn, H.T., 1980, "Introduction to composite materials", *Technomic Publishing Co.*, Westport, CT.

276. Tsai, S.W., 1986, "Composite design 1986, think composites", Dayton, Ohio, *Society for the Advancement of Material and Process Engineering*, Covina, CA.

277. Tsai, W.T., 1986, "Note on Southwell's method for buckling tests of struts", *Journal of Applied Mechanics*, Vol. 53, pp. 953-954.

278. Vinson, J.R., and Sierkowsaky, R.L., 1986, "The behavior of structures composed of composite materials", *Martinus Nijhoff Publishers*, Boston, MA.

279. Vlasov, V.Z., 1959, "Thin walled elastic rods", Second Edition, English Translation, Moscow.

280. Wang, X., Bert, C.W., and Striz, A.G., 1993, "Differential quadrature analysis of deflection, buckling, and free vibration of beams with rectangular plates", *Computers and Structures*, Vol. 48, pp. 473-479.

281. Weisshaar, T.A., 1980, "Divergence of forward swept composite wings," *AIAA Journal of Aircraft*, Vol. 17, No. 6, June 1980.

282. Weisshaar, T.A., 1981, "Aeroelastic tailoring of forward swept composite wings", *Journal of Aircraft*, Vol. 18, pp. 669-676.

283. Weisshaar, T.A., 1982, "Structural dynamic tailoring of advanced composite lifting surfaces", *Technical Report AAE-82-1*, Purdue University, June 1982.

284. Weisshaar, T.A. and Foist, B.L., 1985, "Vibration tailoring of advanced composite lifting surface," *AIAA Journal of Aircraft*, Vol. 22, No. 2, February 1985, pp. 141-147.

285. Whitney, J.M, and Sun, C.T., 1977, "Transient response of laminated composite plates subjected to dynamic loading", *Journal of The Acoustical Society of America*, Vol. 61, No. 1, pp. 101-104.

286. Williams, F.W., and Anderson, M.S., 1983, "Incorporation of langrangian multipliers into and algorithm for finding exact natural frequencies of critical buckling loads", *International Journal of Mechanical Science*, Vol. 25, No. 8, pp. 579-584.

287. Williams, F.W., Anderson, M.S., Kennedy, D., Butler, R., and Aston, G., 1990, "User manual for VICONOPT : An exact analysis and optimum design program covering the buckling and vibration of prismatic assemblies of flat inplane loaded, anisotropic plates, with approximates for discrete supports and transverse stiffeners", *NASA CR 181966.*

288. Wittrick, W.H., 1968, "General sinusoidal stiffness matrices for buckling and vibration analysis of thin flat-walled structures", *International Journal of Mechanical Science*, Vol. 10, pp. 949-966.

289. Wittrick, W.H., and Williams, F.W., 1971, "A general algorithm for computing natural frequencies of elastic structures", *Quarterly Journal of Mechanics and Applied Mathematics* , Vol. 24, pp. 263-284.

290. Worndle, R., 1982, "Calculation of the cross section properties and the shear stresses of composite rotor blades", *Vertica*, Vol. 6, pp. 111-129.

291. Wu, X.X. and Sun, C.T., 1991, "Vibration analysis of laminated composite thin-walled beams using finite elements", *AIAA Journal*, Vol. 29, No. 5, pp. 736-742.

292. Yu, S.D., Cleghorn, W.L., and Fenton, R.G., 1994, "Free vibration and buckling of symmetric cross-ply rectangular laminates", *AIAA Journal*, Vol. 32, pp. 2300-2308.

293. Zagainov, G.I., and Lozino-Lozinsky, G.E., 1990, "Composite materials in Aerospace Design", *Chapman and Hall*, London, UK.

294. Zhang, C. and T.L. Zhu, 1996, "On interrelationships of elastic-moduli and strains in cross ply laminated composites", *Composites Science and Technology*, Vol. 56, No. 2, pp. 135-146.